



Alqahtani, Saeed Saad H. (2023) *Characterisation of M2 muscarinic acetylcholine receptor signalling in dental pulp stem cells*. PhD thesis.

<http://theses.gla.ac.uk/83994/>

Copyright and moral rights for this work are retained by the author

A copy can be downloaded for personal non-commercial research or study, without prior permission or charge

This work cannot be reproduced or quoted extensively from without first obtaining permission in writing from the author

The content must not be changed in any way or sold commercially in any format or medium without the formal permission of the author

When referring to this work, full bibliographic details including the author, title, awarding institution and date of the thesis must be given

Enlighten: Theses

<https://theses.gla.ac.uk/>  
[research-enlighten@glasgow.ac.uk](mailto:research-enlighten@glasgow.ac.uk)



# University of Glasgow

## Characterisation of M2 Muscarinic Acetylcholine Receptor Signalling in Dental Pulp Stem Cells

Saeed Saad H Alqahtani BDS, MSc

Submitted in fulfilment of the requirements for the  
Degree of Doctor of Philosophy

School of Medicine, Dentistry and Nursing  
College of Medical, Veterinary and Life Sciences

University of Glasgow

August 2023

## Abstract

Cholinergic signalling is hypothesised to occur in stem cells, and there is evidence that mesenchymal stem cells (MSCs) express a functional cholinergic system. Expression of functional acetylcholine receptors (AChRs) have been reported in several types of MSC, which suggests that MSCs have non-neuronal cholinergic properties that may play a role in their regenerative potential. However, this remains relatively unexplored, particularly, in Dental pulp stem cells (DPSCs). This project commenced by reviewing AChRs in MSCs, highlighting DPSCs characteristics, and then investigated the presence of functional AChRs and their role in modulating DPSCs regenerative potential.

This study commenced by identifying gene expression of both classes of AChRs, the muscarinic (mAChRs) and the nicotinic (nAChRs), in DPSCs. Protein expression of detected AChRs was assessed via western blotting and immunofluorescence. Functionality of expressed AChRs was assessed using an array of AChRs agonists and antagonists and DPSCs viable count was measured via MTT assay. Subtype selective agonist was used to study the role of the targeted AChR and its influence on DPSCs regenerative potential. Proliferation of DPSCs in response to that stimulation was assessed via measuring viable cell count using MTT assay, Cell Counting Kit-8 (CCK-8), and cell cycle analysis. Survival of DPSCs was assessed via detecting proliferation recovery, measuring Lactate dehydrogenase (LDH) levels, and detecting Annexin V/Propidium iodide staining. Stemness potential of DPSCs was assessed via detecting gene expression of MSCs stemness markers and pluripotency markers. Migration of DPSCs was investigated using a wound healing assays. Osteogenic differentiation of DPSCs was assessed via phenotypic mineralisation stains. Gene expression of cell cycle markers, stemness markers, osteogenic markers were assessed via Real-time polymerase chain reaction (q-PCR). Whole RNA sequencing (RNA-seq) was undertaken to measure transcriptome changes and enriched signalling pathways. Follow-up analysis was undertaken via measuring the phosphorylation and transcripts levels of ERK1 and ERK2 of the Mitogen-activated protein kinase (MAPK) pathway.

The results showed transcripts expression for the M2, M3 and M5 mAChRs, and expression of subunits that support the formation of  $\alpha 7$  and  $\alpha 4\beta 2$ -nAChRs. Subtype selective agonists/antagonists results suggest DPSCs to express functional M2

mAChR,  $\alpha 7$  nAChRs, and  $\alpha 4\beta 2$ -nAChRs. This was based on the ability of the agonists to influence DPSCs viable count and the subtype selective antagonist to cancel that effect. The project then focussed on mAChRs and protein expression of M2, M3 and M5 mAChRs were detected. The subsequent work focused on investigating the role of the M2 mAChRs in modulating the function of DPSCs via activating this receptor through its selective agonist Arecaidine propargyl ester (APE). Activation of the M2 mAChR inhibited DPSCs proliferation, in a reversible manner, without affecting DPSCs viability or survival. Further evidence showed that the M2 mAChR inhibits DPSCs proliferation by arresting cell cycle progression. This was further corroborated via expression analysis of key genes involved in the regulating cell cycle. The results also showed that M2 mAChR activation inhibited DPSCs migration and differentiation potential but did not interfere with DPSCs stemness. This was further corroborated via expression analysis of key genes involved in stemness and osteogenesis. The data obtained suggests that M2 mAChR activation induce DPSCs to go into a quiescent state.

The RNA-seq results showed that DPSCs responded differently to M2 mAChR activation 4 and 24 hours post activation, with different sets of differentially expressed genes (DEGs). The analysis of the enriched pathways suggested that M2 mAChR activation regulates cellular processes involved in metabolism, growth, adhesion, and response to stimuli. These processes function in proliferation, migration, and cell cycle through several metabolic pathways associated with response to cellular and oxidative stress. Follow up analysis showed upregulation of ERK1 and ERK2 phosphorylation and transcripts, which are downstream effectors of the MAPK pathway. The data obtained suggests that the transcriptomic data support the observed inhibitory effect of the M2 mAChR on DPSCs functions and highlights the many downstream effectors involved in the M2 mAChR downstream signalling.

In conclusion, this thesis presents evidence for the expression of a functional M2 mAChR in DPSCs, indicating the involvement of ACh signalling in modulating DPSCs behaviour. It also provides a promising route ultimately to pharmacologically control the regenerative output of DPSCs.

# Contents

Abstract .....	i
Tables .....	vi
Figures .....	vii
Supplementary Figures and Tables .....	ix
Acknowledgement .....	x
Author's Declaration .....	xi
Publications .....	xii
List of Accompanying Material.....	xiii
Abbreviations .....	xiv
<b>1 General introduction .....</b>	<b>1</b>
<b>1.1 The non-neuronal cholinergic system .....</b>	<b>2</b>
1.1.1 Acetylcholine synthesis, transportation, and degradation .....	3
1.1.2 Acetylcholine receptors .....	5
1.1.2.1 Nicotinic Acetylcholine Receptor .....	7
1.1.2.2 Muscarinic Acetylcholine Receptors.....	7
1.1.3 Muscarinic receptor's structure, expression and function .....	8
1.1.3.1 Structure .....	8
1.1.3.2 Expression .....	11
1.1.3.3 Function .....	12
<b>1.2 Acetylcholine receptors in mesenchymal stem cells .....</b>	<b>17</b>
1.2.1 Mesenchymal stem cells .....	17
1.2.2 Expression of Muscarinic Receptors in Mesenchymal Stem Cells .....	21
1.2.2.1 Bone marrow MSCs (BM-MSCs).....	21
1.2.2.2 Adipose derived MSCs (AD-MSCs) .....	23
1.2.2.3 Salivary gland derived stem cells (SGDCs) .....	24
1.2.2.4 Reaming debris-derived MSCs (RD-MSCs) .....	24
1.2.2.5 Foetal membrane MSCs (FM-MSCs) .....	25
1.2.2.6 Umbilical cord-derived MSCs (UC-MSCs) .....	25
1.2.2.7 Summary.....	26
1.2.3 Expression of Nicotinic Receptors in Mesenchymal Stem Cells .....	28
1.2.3.1 Bone marrow MSCs (BM-MSCs).....	28
1.2.3.2 Adipose-derived MSCs (AD-MSCs) .....	30
1.2.3.3 Periodontal ligament derived MSCs (PDL-MSCs) .....	30
1.2.3.4 Wharton's Jelly MSCs (WJ-MSCs).....	32
1.2.3.5 Reaming debris-derived MSCs (RD-MSCs) .....	32
1.2.3.6 Summary.....	33
1.2.4 Conclusion .....	35
1.2.4.1 Downstream signalling of Acetylcholine receptors in MSCs .....	36
1.2.4.2 Acetylcholine receptors as a potential target to regulate MSC function.....	39
<b>1.3 Dental pulp stem cells (DPSCs) .....</b>	<b>41</b>
1.3.1 Characteristics and properties of DPSCs .....	41
1.3.2 Isolation and culture of DPSCs.....	46
1.3.3 Differentiation and applications of DPSCs: .....	48
1.3.4 Limitation and barriers in DPSCs utilisations.....	52
<b>1.4 Summary.....</b>	<b>53</b>
<b>1.5 Project hypothesis and aims.....</b>	<b>55</b>
<b>2 Expression Of Acetylcholine Receptors In Dental Pulp Stem Cells And Methodology</b>	
<b>Development.....</b>	<b>56</b>
<b>2.1 Introduction.....</b>	<b>57</b>
<b>2.2 Materials and Methods .....</b>	<b>59</b>

2.2.1	Cells and cell culture .....	59
2.2.1.1	Development of osteogenic differentiation protocol.....	59
2.2.2	Transcript expression .....	61
2.2.2.1	Ribonucleic acid (RNA) Extraction.....	61
2.2.2.2	Ribonucleic acid (RNA) quantification .....	61
2.2.2.3	Reverse Transcription into complementary deoxyribonucleic acid (cDNA) ....	62
2.2.2.4	Polymerase chain reaction (PCR) and quantitative (q-PCR) analysis .....	62
2.2.3	Screening of functional acetylcholine receptors .....	65
2.2.3.1	Proliferation assessment via methylthiazol tetrazolium (MTT) assay.....	65
2.2.3.2	Pharmacological competition assays.....	67
2.2.4	Protein expression.....	67
2.2.4.1	Immunofluorescence .....	67
2.2.4.2	Western blot .....	68
2.2.5	Statistical analysis.....	69
<b>2.3</b>	<b>Results .....</b>	<b>71</b>
2.3.1	Media type did not affect dental pulp stem cells stemness .....	71
2.3.2	Detection of muscarinic and nicotinic transcripts:.....	77
2.3.3	Detection of acetylcholine synthesis, transportation, and degradation transcripts:	81
2.3.4	Expression of functional muscarinic and nicotinic receptors: .....	82
2.3.5	Subtype specific muscarinic and nicotinic agonists .....	85
2.3.6	Expression of muscarinic subtypes 2, 3, and 5 protein .....	88
<b>2.4</b>	<b>Discussion .....</b>	<b>93</b>
<b>2.5</b>	<b>Supplementary .....</b>	<b>104</b>
<b>3</b>	<b>Effect of M2 muscarinic receptor stimulation on DPSCs survival, proliferation, and cell cycle .....</b>	<b>108</b>
3.1	Introduction.....	109
3.2	Materials and Methods .....	110
3.2.1	Cells and cell culture .....	110
3.2.2	M2 muscarinic receptor stimulation .....	110
3.2.3	Proliferation and recovery .....	110
3.2.4	Cytotoxicity and cell survival.....	111
3.2.4.1	Trypan blue analysis .....	111
3.2.4.2	Lactate dehydrogenase measurement .....	111
3.2.4.3	Cell counting Kit-8 analysis.....	112
3.2.4.4	Annexin V and Propidium iodide staining .....	112
3.2.5	Cell cycle analysis .....	113
3.2.6	Quantitative polymerase chain reaction (q-PCR) analysis.....	113
3.2.7	Statistical analysis.....	115
3.3	Results .....	116
3.3.1	Activation of the M2 receptor reversibly inhibits DPSCs proliferation .....	116
3.3.2	Activation of the M2 receptor does not affect DPSCs viability .....	118
3.3.3	Activation of the M2 receptor inhibits cell cycle progression .....	122
3.4	Discussion .....	126
3.5	Supplementary .....	139
<b>4</b>	<b>Effect of M2 muscarinic receptor stimulation on DPSCs stemness, migration and differentiation .....</b>	<b>141</b>
4.1	Introduction.....	142
4.2	Materials and Methods .....	144
4.2.1	Cells and cell culture .....	144
4.2.2	M2 muscarinic receptor stimulation .....	144
4.2.3	Migration.....	144
4.2.4	Stemness.....	145
4.2.5	Osteogenic differentiation .....	145
4.2.6	Quantitative polymerase chain reaction (q-PCR) analysis.....	146
4.2.7	Statistical analysis.....	147
4.3	Results .....	148

4.3.1	M2 receptor activation inhibit DPSCs migration .....	148
4.3.2	M2 receptor activation does not affect DPSCs stemness .....	150
4.3.3	M2 receptor activation modulate DPSCs osteogenic differentiation.....	152
4.4	Discussion .....	156
4.5	Supplementary .....	162
5	Activated pathways in response to M2 muscarinic receptor activation.....	164
5.1	Introduction.....	165
5.2	Materials and Methods .....	167
5.2.1	Cells and cell culture .....	167
5.2.2	M2 muscarinic receptor stimulation .....	167
5.2.3	RNA sequencing.....	167
5.2.3.1	Sample preparation and RNA isolation.....	167
5.2.3.1	RNA sequencing workflow: .....	167
5.2.3.2	Analysis pipeline: .....	168
5.2.3.2.1	Quality control .....	168
5.2.3.2.2	Reads mapping to the reference genome.....	168
5.2.3.2.3	Novel transcripts prediction .....	169
5.2.3.2.4	Quantification of gene expression .....	169
5.2.3.2.5	Differential expression analysis .....	169
5.2.3.2.6	Gene set enrichment analysis.....	169
5.2.3.2.7	Pathways enrichment analysis of differentially expressed genes .....	170
5.2.4	ERK1/2 Enzyme-linked immunosorbent assay.....	171
5.2.5	Quantitative polymerase chain reaction (q-PCR) analysis.....	171
5.2.6	Statistical analysis.....	172
5.3	Results .....	173
5.3.1	Overview of RNA sequencing data .....	173
5.3.2	Differentially expressed genes in response to M2 agonist stimulation .....	177
5.3.3	Gene Ontology (GO) analysis .....	180
5.3.4	KEGG enrichment analysis .....	186
5.3.5	Protein-protein interaction analysis.....	191
5.3.6	Involvement of MAPK/ERK in downstream signalling of the M2 receptor.....	196
5.4	Discussion .....	198
5.4.1	Transcriptomic data.....	200
5.4.2	Protein interaction network .....	210
5.4.3	The MAPK/ERK pathway .....	211
5.4.4	Key summary points.....	211
5.5	Supplementary .....	213
6	General discussion .....	217
6.1	Findings in the context of therapeutic applications.....	223
6.2	Future work.....	224
6.3	Concluding remarks .....	226
	References .....	227

# Tables

Table 1-1 Summary of muscarinic receptors in MSCs.....	26
Table 1-2 Summary of nicotinic receptors in MSCs..	33
Table 1-3 Reported variation of human DPSCs phenotype characteristics.....	45
Table 1-4 Transplantation studies using human DPSCs.....	50
Table 1-5 Non-dental therapeutic applications of DPSCs. ....	52
Table 2-1 Primer sequences for genes investigated in chapter 2.....	63
Table 2-2 Commercially available Acetylcholine receptor agonists and antagonists. ....	66
Table 2-3 Summary of Acetylcholine receptors expression in DPSCs. ....	80
Table 3-1 Primer sequences for genes investigated in chapter 3.....	114
Table 4-1 Primer sequences for genes investigated in chapter 4.....	146
Table 5-1 Primer sequences for genes investigated in chapter 5.....	172
Table 5-2 Functional summary of protein coding DEGs co-expressed in stimulation timepoints. ....	200
Table 5-3 Function summary of DEGs involved in downregulated GO pathways.....	202
Table 5-4 Clusters of the remaining significantly upregulated GO terms in biological category. .....	204
Table 5-5 Clusters of the remaining significantly upregulated GO terms in molecular category. .....	206
Table 5-6 Function summary of DEGs involved in more than 15 upregulated GO pathways.	207

# Figures

Figure 1-1 Schematic presentation of acetylcholine receptors. ....	6
Figure 1-2 Illustration representing general structure of a muscarinic receptor.....	9
Figure 1-3 Overview of the metabotropic downstream signalling phases of muscarinic receptors (mAChRs).....	13
Figure 1-4 The possible origin and differentiation potential of MSCs. ....	19
Figure 1-5 Metabotropic signalling of muscarinic receptors. ....	37
Figure 1-6 Diagram depicting the $\alpha 7$ nAChR signalling pathway. ....	38
Figure 1-7 Sources of adult stem cells in the oral and maxillofacial region. ....	41
Figure 2-1 Stemness properties of DPSCs in different media types. ....	72
Figure 2-2 Mineralisation of differentiated DPSCs. ....	74
Figure 2-3 Alizarin Red stain quantification.....	75
Figure 2-4 Gene expression of seven osteogenic markers. ....	76
Figure 2-5 Gene expression of muscarinic receptors in DPSCs. ....	78
Figure 2-6 Gene expression of nicotinic subunits in DPSCs. ....	79
Figure 2-7 Gene expression of acetylcholine synthesis, transportation, and degradation components in DPSCs. ....	81
Figure 2-8 Proliferation of DPSCs after 72 h treatment with several non-selective agonists. ....	83
Figure 2-9 Proliferation of DPSCs after 72 h treatment with several subtype selective agonists. ....	84
Figure 2-10 Proliferation of DPSCs after 72 h treatment with several acetylcholine receptors antagonist. ....	86
Figure 2-11 Subtype specific acetylcholine receptors agonist selectivity. ....	87
Figure 2-12 Immunofluorescent staining of the M2 receptor in DPSCs. ....	89
Figure 2-13 Immunofluorescent staining of the M3 receptor in DPSCs. ....	90
Figure 2-14 Immunofluorescent staining of the M5 receptor in DPSCs. ....	91
Figure 2-15 Western blot analysis for the M2, M3, and M5 receptors. ....	92
Figure 3-1 Proliferation of DPSCs over a 72 h time course after stimulation with the M2 agonist (APE). ....	117
Figure 3-2 Proliferative recovery of DPSCs after stimulation with M2 agonist (APE). ....	118
Figure 3-3 Proliferative recovery of DPSCs after stimulation with 100 $\mu$ M the M2 agonist (APE). ....	118
Figure 3-4 Viability of DPSCs after stimulation with 100 $\mu$ M of the M2 agonist (APE). ....	120
Figure 3-5 Fluorescent microscopic images of Annexin V/PI stained cells. ....	121
Figure 3-6 Flow cytometry analysis of DPSCs after 72 h of stimulation with the M2 agonist. ....	123
Figure 3-7 Analysis of genes involved in proliferation and cell cycle following stimulation with the M2 agonist for 72 h. ....	125
Figure 3-8 Overview of cell cycle phases. ....	130
Figure 3-9 Effect of M2 activation on cell cycle progression. ....	131
Figure 3-10 Overview of cell cycle progression. ....	138
Figure 4-1 Migration of DPSCs after stimulation with the M2 selective agonist for eight hours. ....	149
Figure 4-2 Stemness properties of DPSCs after stimulation with the M2 selective agonist for 72 h. ....	151
Figure 4-3 Alizarin reds staining of DPSCs osteogenic differentiation with M2 agonist stimulation.....	153
Figure 4-4 Von Kossa staining of DPSCs osteogenic differentiation with M2 agonist stimulation.....	154
Figure 4-5 Gene expression of osteogenic markers following stimulation with the M2 agonist. ....	155
Figure 4-6 Overview of DPSCs stemness markers. ....	157
Figure 5-1 Experimental procedures and sequencing workflow. ....	168
Figure 5-2 Bioinformatic analysis pipeline.....	170
Figure 5-3 Pearson correlation coefficients between samples. ....	174
Figure 5-4 Principal Component Analysis (PCA). ....	174
Figure 5-5 Venn diagrams illustrating gene expression patterns and co-expression in each experimental group. ....	176
Figure 5-6 Volcano plots for differentially expressed genes (DEGs).....	177
Figure 5-7 Heatmaps of the top 50 significantly (DEGs) after stimulation with the M2 agonist. ....	178

Figure 5-8 Heatmap of the 38 significantly differentially expressed genes (DEGs) at both timepoints (4h and 24h). .....	179
Figure 5-9 GO enrichment analysis of significantly enriched GO terms. ....	181
Figure 5-10 Top 30 GO terms (top ten in each category) after stimulation with the M2 agonist (APE). ....	183
Figure 5-11 Top 30 GO terms (top ten in each category) of upregulated and downregulated DEGs. ....	185
Figure 5-12 KEGG enrichment analysis of significant enriched KEGG pathways. ....	186
Figure 5-13 Top 20 KEGG pathways after stimulation with the M2 agonist (APE). ....	188
Figure 5-14 Top 20 downregulated and upregulated KEGG pathways. ....	190
Figure 5-15 Overview of protein-protein interaction analysis. ....	191
Figure 5-16 Main network of protein-protein interaction after 24 h of stimulation with the M2 agonist APE. ....	192
Figure 5-17 Generated modules of the protein-protein interaction (PPI) network. ....	195
Figure 5-18 Analysis of MAPK/ERK pathway. ....	197

Figure 1-1, Figure 1-2, Figure 1-3, Figure 1-4, Figure 1-5, Figure 1-6, Figure 1-7, Figure 3-8, Figure 3-9, Figure 3-10, Figure 4-6, Figure 5-1, and Figure 5-2 were created with BioRender.com.

# Supplementary Figures and Tables

Sup 2-1 Melt curve analysis of muscarinic receptors gene expression. ....	104
Sup 2-2 Melt curve analysis of nicotinic receptors gene expression. ....	105
Sup 2-3 Immunofluorescent staining of the M2, M3 and M5 receptors using Alexa Fluor™ 488 conjugated secondary antibody. ....	106
Sup 2-4 Western blot analysis for the non-specific bands present in TR146 sample. ....	107
Sup 3-1 Structure of DPSCs following 72 h treatment with higher concentrations of the M2 agonist. ....	139
Sup 3-2 Flow cytometry gating strategy. ....	140
Sup 4-1 Higher magnification of fluorescent microscopic images of DPSCs migration. ....	162
Sup 4-2 Expression of the M2 receptor following DPSCs osteogenic differentiation. ....	163
Sup 5-1 Quality control criteria for all sequenced samples. ....	213
Sup 5-2 Quality check and mapping statistics. ....	214
Sup 5-3 Unprocessed protein-protein interaction (PPI) networks. ....	216

## Acknowledgement

I would like to express my deepest appreciation to my supervisors Dr Christopher Nile and Professor William McLean for their support and guidance throughout my PhD. Chris, I am deeply grateful for your commitment to supporting me through my PhD. It was because of you that I was able to overcome challenges and persevere, and ultimately complete my degree. Will, thank you for sticking by me during my MSc and PhD. Your valuable insights and advice shaped my research and the person I became.

I wish to thank all other members of GDH who have helped me along the way. Including Professor Shauna Culshaw, Professor Andrea Sherriff, Professor Marcello Riggio, Professor Gordon Ramage, Dr Andrew Hamilton, Dr Douglas Robertson and Mr Steven Milligan. I would also like to thank all those that supported me from outside of the GDH, who I was able to reach out to for assistance or collaboration for the work that was undertaken. I would like to thank Professor Matthew Dalby for his support and expert advice. I would like to thank Jennifer Cassels for her support with my FACS analysis. I would also like to thank Katerina Miari and Dr Mark Williams (Glasgow Caledonian University) for their support with my FACS analysis.

A big thank you to all my lab colleagues, past and present, who have all helped to make GDH a great place to work: Abdullah Baz, Abeer Alghamdi, Ahmed Bakri, Bryn Short, Christopher Delaney, Emily McCloud, Hafsa Abduljalil, Hui Wang, Jason Brown, Karwan Aljubiar, Khawlah Albashaireh, Krystyna Piela, Laurence Rowan, Mark Butcher, Muhanna Alshehri, Om Alkhir Alshanta, Othman Baradwan, Robert Reilly, Ryan Kean, Sumaya Abrusrewil, Suror Shaban, Tracy Young and William Johnston. Thank you all for making this journey joyful.

I'm extremely grateful to my mum, dad, brothers, and sisters for their continued encouragement and unconditional support during this journey.

To my wife Mona and daughters Alma and Lama, I dedicate this thesis to you. My wife, thanks for being patient and understanding of my prolonged absences. My daughters, thank you for all the hugs, smiles, laughter, and squabbling that gave me the motivation to see this through.

## **Author's Declaration**

I declare that I have carried out the work described in this thesis unless otherwise acknowledged or cited, under the supervision of Dr Christopher Nile, Professor William McLean and Professor Gordon Ramage. I further declare that this thesis has not been submitted for any other degree at the University of Glasgow, or any other institution.

Saeed Alqahtani

## Publications

Alqahtani, S., Butcher, M. C., Ramage, G., Dalby, M. J., McLean, W., & Nile, C. J. (2023). Acetylcholine Receptors in Mesenchymal Stem Cells. *Stem Cells and Development*, 32(3-4), 47-59.

Chapters three, four, and five. **Alqahtani S** (16 09 2022) 'M2 muscarinic receptor modulates dental pulp stem cell behaviour' [conference presentation], PER-IADR Oral Health Research Congress, Marseille, France.

# List of Accompanying Material

## Appendices

- I. Differentially expressed genes from RNA-Sequencing data set of DPSCs.
- II. Enriched pathways from joint GO and KEGG pathway analysis.
- III. STRING protein-protein interaction (PPI) analysis.

## Abbreviations

ACh:	Acetylcholine
AChR:	Acetylcholine receptor
AD-MSCs:	Adipose-derived mesenchymal stem cells
ANOVA:	Analysis of variance
APE:	Arecaidine propargyl ester hydrobromide
BM-MSCs:	Bone marrow mesenchymal stem cells
BP:	Biological process
BrdU:	Bromodeoxyuridine
CC:	Cellular component
cDNA:	Complementary DNA
Ct:	Cycle threshold
Ctrl:	Control
DEGs:	Differentially expressed genes
DMEM:	Dulbecco's modified eagle's medium
DPBS:	Dulbeco's phosphate buffered saline
DPSCs:	Dental pulp stem cells
ELISA:	Enzyme-linked immunosorbent assay

ERK:	Extracellular signal-regulated kinases
FBS:	Foetal bovine serum
FM-MSCs:	Foetal membrane mesenchymal stem cells
G-proteins:	Guanine nucleotide binding proteins
GAPDH:	Glyceraldehyde 3-phosphate dehydrogenase
GO:	Gene ontology
IgG:	immunoglobulin G
IP3:	Inositol triphosphate
iPSC:	Induced pluripotent stem cells
kDa:	Kilodalton
KEGG:	Kyoto Encyclopedia of Genes and Genomes
LDH:	Lactate dehydrogenase
mA:	Milliampere
mAChRs:	Muscarinic acetylcholine receptors
MAPK:	Mitogen-activated protein kinase
MF:	Molecular function
MSCs:	Mesenchymal stem cells
MTT:	Methylthiazol tetrazolium
nAChRs:	Nicotinic acetylcholine receptors

nM:	Nanomolar
padj:	Adjusted p-value
PBS:	Phosphate buffered saline
PCR:	Polymerase chain reaction
PDL-MSCs:	Periodontal ligament derived mesenchymal stem cells
PI:	Propidium iodide
PKC:	Protein kinase C
PPI:	Protein-protein interaction
qPCR:	Quantitative polymerisation chain reaction
RD-MSCs:	Reaming debris-derived mesenchymal stem cells
ROS:	Reactive oxygen species
RT:	Room temperature
SGDCs:	Salivary gland derived stem cells
UC-MSCs:	Umbilical cord-derived mesenchymal stem cells
V:	Voltage
WJ-MSCs:	Wharton's Jelly mesenchymal stem cells
$\mu$ M:	Micromolar

# 1 General introduction

## 1.1 The non-neuronal cholinergic system

The non-neuronal cholinergic system is a term introduced in the late '90s to differentiate between the neuronal cholinergic system and cholinergic systems that exist in cells other than neurons (Wessler, Kirkpatrick and Racké, 1998). This term is now well recognised and undoubtable proof exists that most human cells have the ability to utilise cholinergic mechanisms that once were thought exclusive to neurons. Like the neuronal cholinergic system, the non-neuronal cholinergic system is driven by an ancient signalling molecule, acetylcholine (ACh). In fact, ACh is present in basic life forms long before the evolutionary origin of neurons (Wessler, Kirkpatrick and Racke, 1999). Thus, it could be said that the neuronal signalling tuned an already present signalling system to communicate on a millisecond scale.

Although the non-neuronal cells share similar cholinergic components of the neuronal system, the release mechanism of ACh is different. In neurons, the machinery of its release involves storage vesicles, specialised transporter, and synapses with upregulated ACh receptors and degradation enzymes (Kawashima and Fujii, 2008). This allows for rapid release and breakdown of large amounts of ACh, consummate with its role as a neurotransmitter. In contrast, ACh in non-neuronal cells is not stored in vesicles, but rather released continuously, in smaller quantity, to act in an autocrine and paracrine fashion (Wessler and Kirkpatrick, 2016). Thus, it acts to maintain cellular homeostasis as well as communication with the external environment (Wessler and Kirkpatrick, 2008). Literature that describe the mechanism of syntheses, expression, and function of ACh in human non-neuronal cells is scarce, and most is still focused on neuronal cells (Kawashima and Fujii, 2008; Wessler and Kirkpatrick, 2008).

Acetylcholine (ACh) is a universal molecule synthesised by practically all living cells. The different types of non-neuronal cells utilise a diversity of signalling pathways in response to ACh signalling. This allow ACh signalling to be involved in regulating numerous cellular events that can range from growth to death (Grando *et al.*, 2007). Furthermore, ACh among other cholinergic components were identified in different population of stem cells (Paraoanu *et al.*, 2007; Hoogduijn, Cheng and Genever, 2009; Alessandrini *et al.*, 2015; El-Habta, Kingham and Backman, 2018; Ishizuka *et al.*, 2018). This adds further to the biological

significance of this molecule in regulating the proliferation and differentiation potential of these stem cells. The wide-ranging influence of ACh on different types of non-neuronal cells has made it challenging to evaluate a particular role. Different types of non-neuronal cells express diverse ACh synthesis, transportation, and degradation components. Furthermore, different types of non-neuronal cells express different patterns of the receptors that specialise in binding and translating the effects of ACh. Therefore, non-neuronal cells response to ACh signalling is dependent on the expressed ACh receptors and if the cell is equipped with the components to synthesis, transport, or degrade ACh. Thus, it is worthy to have an insight into the components that govern ACh function.

### **1.1.1 Acetylcholine synthesis, transportation, and degradation**

Non-neuronal ACh and its related components, pathways, and effects are emerging to have a significant part in the cellular function of different types of non-neuronal cells. Expression of components of the non-neuronal cholinergic system has been recognized in almost all mammalian cells. To name a few, it has been detected in epithelial, endothelial, mesothelial, immune and stem cells (Wessler and Kirkpatrick, 2008). Acetylcholine can mediate several actions in relation to the control of basic cell functions such as proliferation, differentiation, migration and communication (Sastry and Sadavongvivad, 1978; Wessler, Kirkpatrick and Racké, 1998; Tracey, 2007; Wessler and Kirkpatrick, 2008). In addition, the non-neuronal cholinergic system can mediate anti-inflammatory mechanisms, thus establishing the involvement of this system in the pathophysiology of disease (Profita *et al.*, 2005; Pahl *et al.*, 2006; Bühling *et al.*, 2007).

The detailed source of choline that make up ACh in non-neuronal cells is yet to be defined. However, it appears that some non-neuronal cells (mainly in the human placenta) are equipped with high affinity choline transporters or organic cation transporters (OCTs) which mediate choline uptake (Haberberger *et al.*, 2002; Hanna-Mitchell *et al.*, 2007; Kawashima and Fujii, 2008). Acetylcholine is synthesised from choline and acetyl coenzyme A mainly by the enzyme choline acetyltransferase (ChAT) (Tuček, 1982; Wessler, Kirkpatrick and Racké, 1998; Wessler *et al.*, 2003). Positive anti-ChAT immunoreactivity, ChAT enzyme activity, and measurement of ACh release provided good evidence of ACh synthesis in non-

neuronal cells (Wessler and Kirkpatrick, 2008). However, it is worthy to mention the specificity of ChAT is very high for the choline substrate. This means it may not only make ACh, but other choline related signalling molecules (Wessler, Kirkpatrick and Racke, 1999). Additionally, carnitine acetyltransferase (CarAT) contributes, to some extent, in the synthesis of ACh (White and Wu, 1973; Tuček, 1982; Lips, Wunsch, *et al.*, 2007). This highlights the importance of specificity in detection methods when identifying non-neuronal cells capable of synthesising ACh.

The exact mechanism by which ACh is released or transported in non-neuronal cells is partially understood at best. What is known is that ACh is liberated into the extracellular space of these cells, when needed and in a small continuous quantity (Kawashima and Fujii, 2000; Wessler, Roth, *et al.*, 2001; Schlereth *et al.*, 2006). Upon its release, it is diffused near the vicinity of its source to influence adjacent cells. As ACh degrading enzymes are lowly expressed in non-neuronal cells, it allows for not only autocrine but also paracrine effects on adjacent cells (Wessler and Kirkpatrick, 2016). Literature driven from using the human placenta (as a model of the non-neuronal cholinergic system) indicates the involvement of organic cation transporters (OCTs) in ACh release and transportation (Wessler and Kirkpatrick, 2012). This comes from the notion that ACh, regardless of pH, represents a permanent cation and that OCTs are widely expressed in almost all cells (Wessler, Roth, *et al.*, 2001). Three OCT subtypes have been identified to be involved in ACh release. The specific subtypes involved in ACh release may differ between different types of cells (Wessler, Roth, *et al.*, 2001; Lips *et al.*, 2005; Kummer *et al.*, 2006; Lips, Lührmann, *et al.*, 2007). Nevertheless, evidence suggests OCT suppression affects ACh release (Schlereth *et al.*, 2006). In addition, nicotine, stimulation of  $\alpha$ -adrenoceptors, and increase in the intracellular calcium concentration may influence the release of ACh (Reinheimer *et al.*, 1998; Wessler, Kirkpatrick and Racke, 1999).

Little is known about ACh transportation in non-neuronal cell compared to neuronal cells. In the later, ACh is transported via the vesicular ACh transporter (VAChT) and stored until its release (Kawashima and Fujii, 2008). Detection of VAChT was only reported in airway epithelial cells (Lips, Lührmann, *et al.*, 2007), while other non-neuronal cells (skin, urothelium, and T cells) do not express this type of transporter (Kawashima and Fujii, 2000; Elwary, Chavan and Schallreuter,

2006; Hanna-Mitchell *et al.*, 2007). Instead, in general, non-neuronal ACh appears to be released when needed without being stored in vesicles. Therefore, non-neuronal ACh exist beyond the neuronal system and can be detected, however, the exact events that leads to its release and transportation need to be further elaborated.

Generally, two types of cholinesterase enzymes are identified to terminate and cleave ACh into choline and acetic acid, these are acetylcholinesterase (AChE) and butyrylcholinesterase (BuChE). Although both enzymes are able to break down ACh, AChE may exert the more prominent role (Adler *et al.*, 1991). They both circulate in bodily fluids as a free form or can be found anchored to the cell membrane (Massoulié *et al.*, 1993; El-Fakahany and Jakubik, 2016). This widespread presence, presumably, prevents ACh from acting as a hormone (i.e., keeping the effect of ACh near the vicinity of its source). In non-neuronal cells, both cholinesterases (AChE and BuChE) are expressed ubiquitously (Grando *et al.*, 2007). Though, presence of one or both is insufficient to postulate a non-neuronal cholinergic system. This is due to the fact that cholinesterases can conduct multiple non-enzymatic functions (i.e. independent from ACh) such as regulation of proliferation, apoptosis, and angiogenesis (Wessler and Kirkpatrick, 2017). Furthermore, the specific means of how these cholinesterases terminate ACh in non-neuronal ACh is still unclear.

### **1.1.2 Acetylcholine receptors**

There are two major classes of receptors that bind ACh and transmit its signal, namely, muscarinic and nicotinic AChRs (Figure 1-1). Apart from ACh, both classes of receptor bind to distinct secondary ligands that aided their identification; muscarinic receptors (mAChRs) bind muscarine and nicotinic receptors (nAChRs) bind nicotine (Albuquerque *et al.*, 2009). Both classes and their constituent subtypes permit communication between non-neuronal cells and activate signal-transduction pathways allowing maintenance of cellular function and ultimately organ homeostasis (Wessler and Kirkpatrick, 2008). Muscarinic and nicotinic receptors have been shown to be expressed and functional in non-neuronal cells (Wessler, Kirkpatrick and Racké, 1998). Both receptor families are membrane bound. However, they are two inherently different classes of receptor, with structural differences, resulting in regulation of different downstream effects

(Wessler and Kirkpatrick, 2008). The mAChRs belong to the G-protein coupled receptor (GPCRs) family and mediate the metabotropic effects of ACh (Eglen, 2005). The nAChRs are ligand-gated ion channel receptors that mediate the ionotropic effects of ACh (Miyazawa, Fujiyoshi and Unwin, 2003; Forsgren *et al.*, 2009). Both families include several subtypes or subunits, which again are expressed in a ubiquitous manner across a variety of non-neuronal cells (Shirvan, Pollard and Heldman, 1991; Grando, 1997; Wessler, Kirkpatrick and Racké, 1998; Albuquerque *et al.*, 2009).

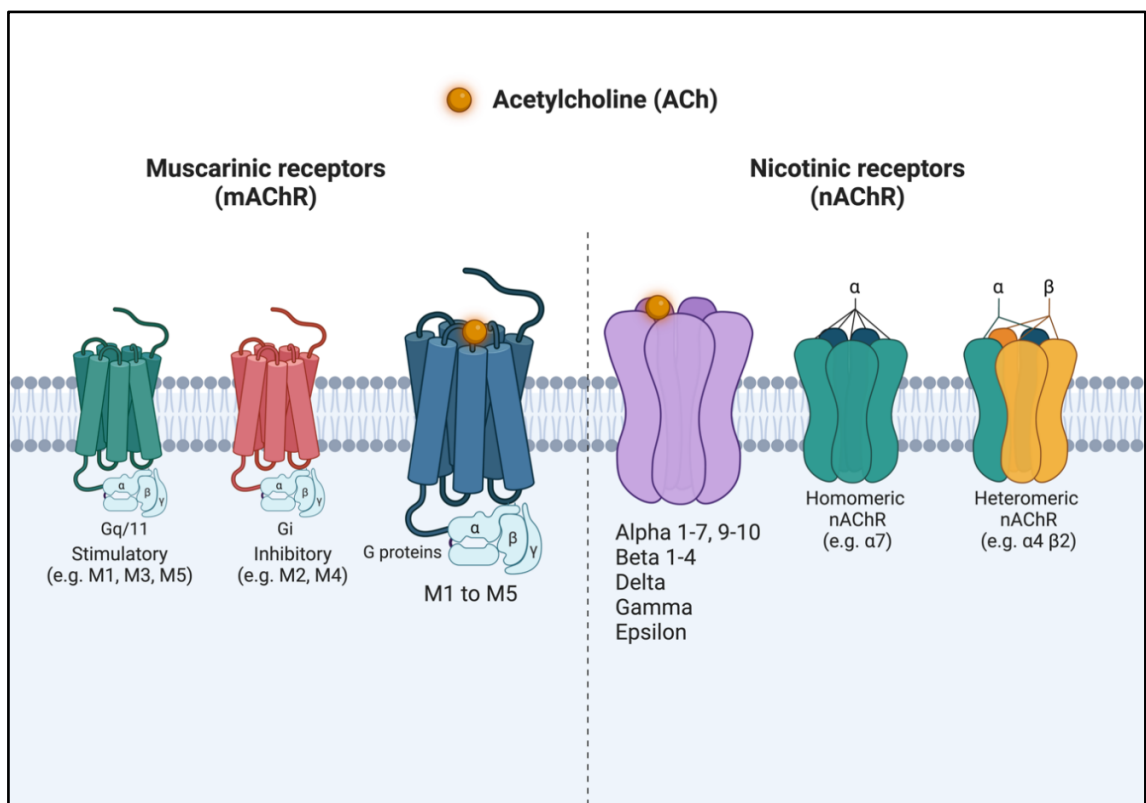


**Figure 1-1 Schematic presentation of acetylcholine receptors. Left: Muscarinic acetylcholine receptors (mAChRs) are G-protein coupled receptors. Based on downstream functionality of the coupled g proteins they are commonly divided into two groups, stimulatory in nature (M1, M3, and M5) or inhibitory (M2 and M4). Right: Nicotinic acetylcholine receptors (nAChRs) are pentamers from 16 possible subunits. They may present as either homopentamers (consisting of five identical subunits) or heteropentamers (consisting of combinations of different subunits).**

The near ubiquitous AChR expression across non-neuronal cell populations have made it challenging to evaluate their role. The expression of receptor classes or subtypes varies across different non-neuronal cell types and is influenced by cell state and environmental factors (Wessler and Kirkpatrick, 2008). Both receptor classes form an auto and paracrine loop of ACh activity in non-neuronal cells. They may coexist in individual cells, with stimulation of one class potentially having a

positive or negative effect on the other (Bencherif and Lukas, 1993; Evinger *et al.*, 1994). Furthermore, the wide ranging influence of ACh on different types of non-neuronal cells adds to the complexity of this system (Wessler, Kirkpatrick and Racké, 1998).

#### **1.1.2.1 Nicotinic Acetylcholine Receptor**

The nAChRs are composed of multi-subunit proteins that form ligand-gated ion channels within the cell membrane (Resende and Adhikari, 2009) (Figure 1-1). A nAChR can be a pentamer based upon 13 possible subunits (in human) which may present as either homopentameric (consisting of 5 identical subunits) or heteropentameric (consisting of combinations of different subunits) (Dani and Bertrand, 2007; Albuquerque *et al.*, 2009). There are nine  $\alpha$ -subunits ( $\alpha 1 - 7, -9,$  and  $-10$ ) and four  $\beta$ -subunits ( $\beta 1 - 4$ ). In addition, other subunits such as delta ( $\delta$ ), epsilon ( $\epsilon$ ), and gamma ( $\gamma$ ) have also been identified in humans (Hoogduijn, Cheng and Genever, 2009; Weist *et al.*, 2018). The different subunit compositions of this receptor class allow for specialised properties and diverse functions, and so they mediate numerous downstream effects (Albuquerque *et al.*, 2009). Multiple nAChR subunits have been identified in non-neuronal cell populations (Thuong Nguyen *et al.*, 2000; Gahring and Rogers, 2005). Generally, these receptors are rapid acting cationic receptors that mediate a temporal opening of ion channels to allow sodium, potassium or calcium passage (Albuquerque *et al.*, 2009). Consequently, an intracellular increase of such ions leads to activation of a series of signal transduction pathways. This in turn, may lead to alterations in cell proliferation, cytoskeletal rearrangement, and differentiation (Dicker *et al.*, 2005).

#### **1.1.2.2 Muscarinic Acetylcholine Receptors**

The mAChRs consist of five distinct subtypes referred to as type 1 - 5 (M1 - M5). These receptors are members of the GPCR family (Eglen, 2005) (Figure 1-1). Once stimulated, muscarinic receptors couple to distinct types of G proteins that in turn activate second messenger signalling pathways as well as activating gated ion channels (Eglen, 2006). Thus, the cellular cascade of events depends on the types of G protein with which a muscarinic receptor interacts. This, arguably, is what makes these receptors relatively slower acting compared to their nicotinic receptor counterpart (Eglen, 2005). The resultant downstream effects of activated muscarinic receptors are immensely complex and have widespread

consequences. At almost all stages of development, mAChRs mediate the effects of ACh in almost all cells; both neuronal and non-neuronal (Eglen, 2012). In fact abnormalities in mAChRs signalling is a sign in many diseases (Resende and Adhikari, 2009). This and the fact that they are GPCRs have made them a focus of studies from a pharmacological perspective. Indeed, there is commercial incentives to develop research into GPCRs as a whole (Leach *et al.*, 2012). To date, GPCRs, including mAChRs, are the most therapeutically targeted family of receptors (Jacoby *et al.*, 2006; Lappano and Maggiolini, 2011; Sriram and Insel, 2018).

### **1.1.3 Muscarinic receptor's structure, expression and function**

Muscarinic receptors are a set of membrane bound structures undoubtedly involved in many biological systems of the body. In fact, they were the second to be identified as a main component of the cholinergic system after ACh. The pioneer work of Otto Löwi in 1921 paved the way for their identification through observing a deacceleration of heartbeats as a sequel to vagal nerve stimulation (Loewi, 1921). That was proven later as an ACh provoking action via the muscarinic receptors (Caulfield, 1993). Since then, research in this field exploded with pharmacological driven studies initially indicating that only three subtypes existed (Michel and Whiting, 1987; Caulfield, 1993; Felder *et al.*, 2000). Indeed, not until the 1990s, were all five muscarinic receptors conclusively identified and suggested that they have a much bigger role beyond neurons (Wessler, Kirkpatrick and Racke, 1999; Eglen, 2005). Since then, the diversity of muscarinic receptors was revisited not only in relation to their activity in the neuronal system but also in other cell types and tissues independent of the classical cholinergic entity.

#### **1.1.3.1 Structure**

The five muscarinic receptor subtypes M1-M5, encoded by genes *CHRM1* to *CHRM5*, belong to the class I ("Rhodopsin-like") GPCRs family (Wess, Eglen and Gautam, 2007). They display high sequence homology with each other and with other GPCRs in their general architecture (Leach *et al.*, 2012). This characteristic feature is the presence of seven transmembrane segments with an extracellular N-terminal region and intracellular C-terminal region (Figure 1-2). This means a receptor crosses the membrane seven times in a shape of helical domains. These domains are connected by three extracellular and three intracellular loops. All five

muscarinic receptors, across several species, share this general structural homology, which have historically made it difficult to identify subtypes (Hulme, Birdsall and Buckley, 1990; Fredriksson *et al.*, 2003; Kruse *et al.*, 2013).

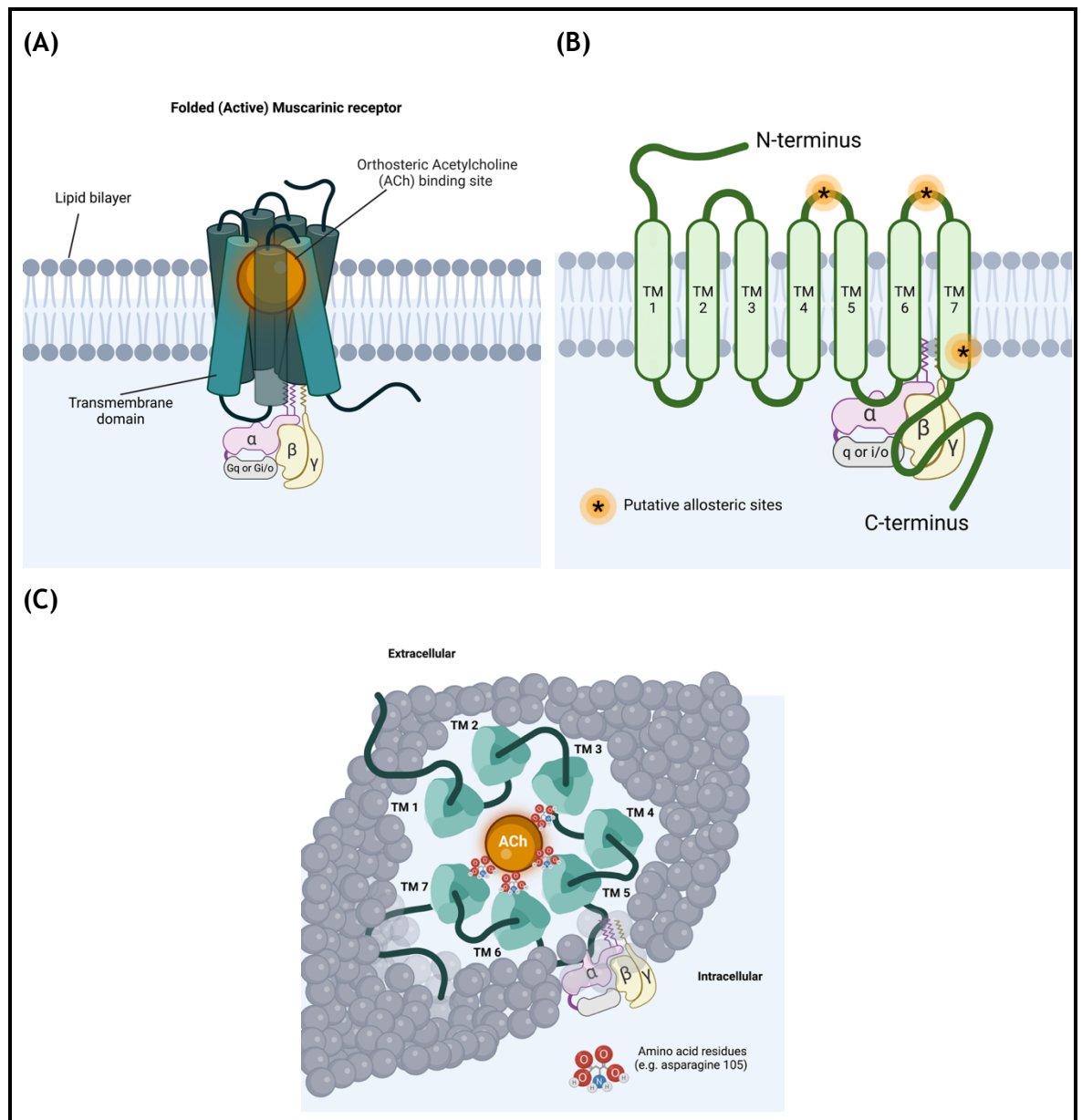


**Figure 1-2** Illustration representing general structure of a muscarinic receptor. (A) Side view of a muscarinic receptor in an active state showing the arrangement of the transmembrane domains around ACh that is binding in the orthosteric site. (B) Simplified arrangements of the seven transmembrane domains connected by extracellular and intercellular loops where: allosteric binding can happen on the second and third extracellular loop, coupling of the  $\alpha$  G protein on the third intracellular loop (C) Extracellular view (top) of a muscarinic receptor showing amino acid residues on transmembrane domains 3, 5, 6, and 7 function in docking ACh in the orthosteric pocket.

Most of the structural knowledge related to muscarinic receptors has been obtained through several indirect approaches and are based on similarity to other members of the GPCRs family (Leach *et al.*, 2012). Hence, the activation

mechanisms of muscarinic receptors are largely based on essential homology with rhodopsin, the only seven transmembrane receptor for which direct three-dimensional structural information has been obtained (Unger *et al.*, 1997; Gether, 2000; Palczewski *et al.*, 2000). Nonetheless, these approaches in defining the structure of muscarinic receptors, despite their limitations, have revealed a wealth of information. Indeed, a significant finding was that there is subtle variability in the amino acids sequence of muscarinic receptors at the extracellular terminal region and at the third intracellular loop which determines their specific activity (Ishii and Kurachi, 2006).

Like most class I GPCRs, muscarinic receptors have a conserved pocket buried deep within the transmembrane region for the purpose of binding designated ligands (Eglen, 2005). From a pharmacological point of view, this is called the orthosteric binding site. Most muscarinic ligands, such as ACh and muscarine, bind to this site specifically on points located on transmembrane domains TM3, TM5, TM6, and TM7 (Hulme *et al.*, 2003) (Figure 1-2). Furthermore, when a ligand binds to these domains it binds to amino acid residues that are critical in the binding of the positively charged headgroup. In the case of ACh, it is predicted to bind to the asparagine 105 (Asp105), a residue conserved in most Class I GPCRs (Eglen, 2005). Apart from Asp105, five more key residues were identified to be unique to the whole muscarinic receptor family. However, these residues and the whole arrangement of the orthosteric binding site is reportedly similar across all five muscarinic subtypes (Hulme, Birdsall and Buckley, 1990). This notion was confirmed when the first studies that described the molecular organization of muscarinic receptor subtypes M2 and M3 were published (Haga *et al.*, 2012; Kruse *et al.*, 2012). Comparison of these subtypes revealed that the residues lining the orthosteric binding site are conserved absolutely in sequence and, moreover, are positioned almost identically in space in both receptors (Kruse *et al.*, 2014). This in principal is what made subtype identification of muscarinic receptors difficult as well as the frequent co-expression of more than one receptor subtype in the same tissues (Jöhren and Höltje, 2002; Wess, Eglen and Gautam, 2007). Indeed, although there are other related minor differences between these subtypes, efforts to exploit these variations in hope of developing subtype selective compounds have far been proven challenging (Kruse *et al.*, 2013).

Given the challenges in developing muscarinic subtype selective compounds that act through the orthosteric site, research shifted the focus to another structural component referred to as allosteric sites. From a pharmacological perspective, sites where a ligand binds to that are remote to the endogenous binding site are termed allosteric. There is good evidence that muscarinic receptors possess numerous allosteric sites (Birdsall and Lazareno, 2005) (Figure 1-2). The nature of these sites is different to the original orthosteric site in their structural location, mode of function, and even vary between the five muscarinic subtypes (Birdsall and Lazareno, 2005). Most of the evidence points to their location on the extracellular domain of the receptor, namely between the second and the third extracellular loops (Prilla *et al.*, 2006). Even though receptor activation is largely mediated through the orthosteric site, allosteric targeting ligands modulate the function of a receptor in a different way (Suno, Asada and Kobayashi, 2016). When a ligand or a compound designed to bind to a receptor through an allosteric site, it does not directly compete with the endogenous orthosteric ligands (neurotransmitter or hormone). It essentially acts to modulate the binding and effects of orthosteric ligands, and therefore, the ability to influence the activity of the receptor (Mohr, Tränkle and Holzgrabe, 2003). Such allosteric ligands can even activate the receptor in the absence of an orthosteric ligand (Jakubik and El-Fakahany, 2016). These features and their variant occurrence across muscarinic subtypes impart them unique subtype functional selectivity. On these bases, allosteric modulators are intensively becoming the focus of studies looking at identification of subtype selectivity of muscarinic receptor (Kruse *et al.*, 2014). However, these studies are limited by the complexity of allosteric interactions and the lower affinity of developed compounds aimed to identify them (Jakubik and El-Fakahany, 2016).

### 1.1.3.2 Expression

Muscarinic receptors now are arguably expressed by almost all mammalian cells (Wessler and Kirkpatrick, 2008). Although their expression and activity are better understood in the neuronal system, they play an integral role in non-neuronal tissue and cells. As these receptors couple differently to associated G proteins, they are capable of initiating multiple downstream signalling events. Based on downstream functionality of the coupled G proteins, they are commonly divided into two groups; stimulatory (M1, M3, and M5) or inhibitory (M2 and M4) (Maeda

*et al.*, 2019). The stimulatory group, M1, M3, and M5 muscarinic receptors couple to subunit  $\alpha$  of the Gq/11 family. The inhibitory group, M2 and M4 muscarinic receptors couple to the  $\alpha$  subunit of Gi and Go (Eglen, 2005). This coupling mechanism is preferential in nature and based partially on the muscarinic agonist or ligand. For an example, stimulation of the M2 muscarinic receptor using common muscarinic agonists was reported to activate both Gi/o and Gs proteins, which makes the M2 signalling pattern more difficult to predict (Kebig *et al.*, 2009). In principle, the ligand activates the GPCRs which initiate downstream second messengers depending on the activated G proteins (Eglen, 2005).

The downstream signalling events of mAChRs depends on the expression pattern of the activated subtypes as well as the state or environmental conditions that governs these receptors (Eglen, 2005). Indeed, mAChRs may undergo frequent modification in their expression pattern and physiological functions in their natural environment or *in vivo*, as opposed to what is reported in cell-free preparations and recombinant system (Muramatsu *et al.*, 2016). This could be due to internal and external environmental conditions, either pathological or developmental such as phenotypic cell functions, sex, disease state, and state of cell differentiation (Resende and Adhikari, 2009). In addition, various patterns of mAChR subtypes have been witnessed across different non-neuronal cell types. The diversity of mAChRs expression pattern is further discussed in “1.2”

The expression pattern and numbers of mAChRs are modified by receptor internalisation. This happens in response to agonist-induced stimulation as a mechanism to regulate receptor numbers on the cell surface and thus sensitivity to long-term stimulation. The process is not fully clear; however, it has been suggested that agonist-induced internalisation is a common feature of mAChRs (Reiner and Nathanson, 2012). Following the internalisation process, the receptor may recycle back to the cell surface or start a degradation course resulting in permanent loss (Van Koppen, 2001). Further evidence suggests that cell type and receptor subtype influence the process of receptor desensitization (Anderson, Goldstein and Brown, 1977; Schlador, Grubbs and Nathanson, 2000).

### 1.1.3.3 Function

Downstream signalling and thus function of mAChRs depends on multiple factors among which are the activated G proteins, cell type, and property of the agonist.

However, a pattern of signalling has been reported based on the receptor coupled G proteins (Figure 1-3). Activation of Gq coupled mAChRs (i.e., stimulatory group; M1, M3, and M5) generate protein kinase C (PKC) and increase calcium ( $\text{Ca}^{2+}$ ) intracellularly. This happens through downstream signalling via Phospholipase C that generates diacylglycerol (DAG) and inositol triphosphate ( $\text{IP}_3$ ) secondary messengers. These messengers provide the stimulatory action by increasing PKC and  $\text{Ca}^{2+}$  influx (van Koppen and Kaiser, 2003). Activation of Gi/o coupled mAChRs (i.e., inhibitory group; M2 and M4) reduce cyclic adenosine monophosphate levels (cAMP), extend the opening of potassium channels, and reduce the intracellular  $\text{Ca}^{2+}$  levels. This happens through downstream signalling that reduces adenylyl cyclase which then results in decreased protein kinase A (Zholos, Zholos and Bolton, 2004; Eglen, 2005) (Figure 1-3). This leads to the inhibitory reaction within the cell in response to reduction in cAMP, reduction in intracellular  $\text{Ca}^{2+}$  ions, and continued efflux of  $\text{K}^+$  ions. Moreover, it has been reported that the  $\beta\gamma$ -subunits of the Gi-proteins coupled to the M2 mAChR may modulate Akt (previously known as protein kinase B) signaling by means of upstream Phosphoinositide 3-kinase (PI3K) activation (Botticelli *et al.*, 2022).

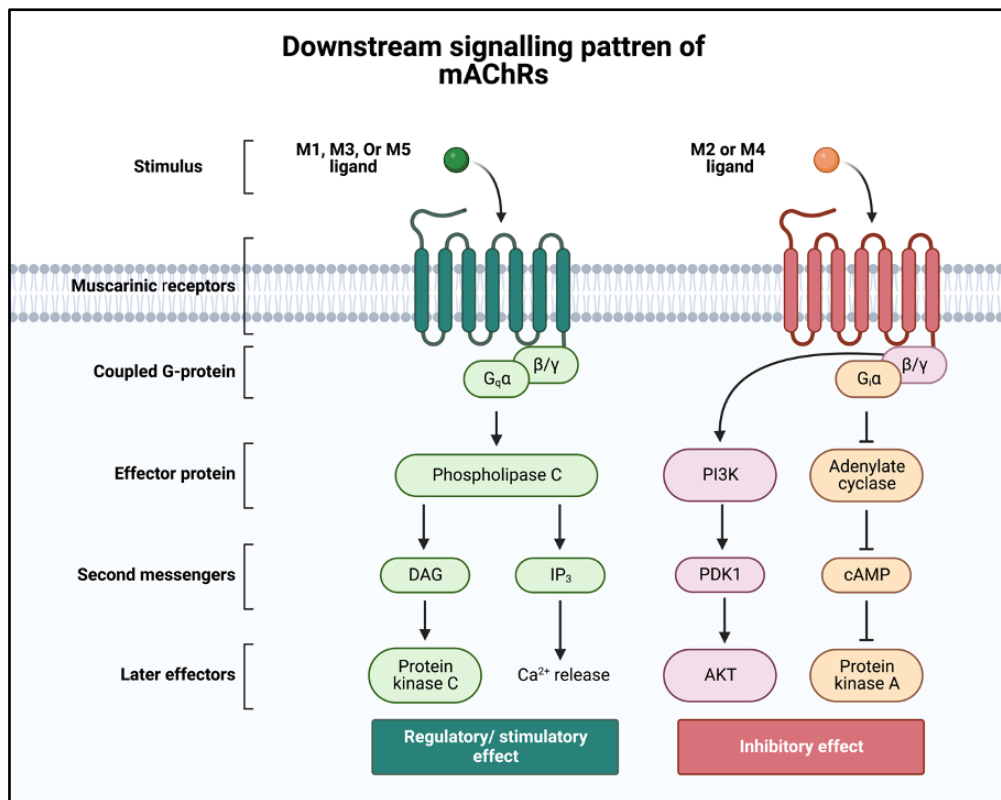


**Figure 1-3 Overview of the metabotropic downstream signalling phases of muscarinic receptors (mAChRs). Signalling of a mAChR is largely based on the coupled g proteins. Stimulation of coupled g proteins lead to activating effector proteins that further activate secondary messengers and so late effectors that will initiate cellular response. In case of M1, M3, and M5, the Gq protein produce a regulatory/ stimulatory effect through a cascade of**

**events. While the M2 and M4 couple to the Gi protein to produce an inhibitory effect through a different cascade of events. Additionally, the  $\beta\gamma$ -subunits of the Gi-proteins, in the M2 subtype produce an inhibitory effect through a different auxiliary pathway.**

The downstream signalling pattern of mAChRs can also be dependent on cell type. Indeed, there is a cell-dependent diversity of downstream effectors in response to mAChRs stimulation. For an example, in the heart, M2 downstream signalling leads to contraction in vascular smooth muscle cells, however, through an increase in intracellular  $\text{Ca}^{2+}$  levels (Rubanyi, 1991). While in the same tissue, vascular smooth muscle cells relaxation happens in response to nitric oxide production as a result of M3 downstream signalling (Van Zwieten and Doods, 1995). Cell-dependent diversity of downstream signalling of mAChRs have also been reported in cancer cells. Colon cancer cell lines and prostate carcinoma cells proliferation is prompted via M3 activation (Williams, 2003). However, in several small cell lung carcinoma cell lines the same receptor (M3) activation leads to an arrest in DNA synthesis (Williams, 2003). Consequently, diverse signalling dependent-pathways can be involved in mAChR function. This facilitates these receptors involvement in a wide range of pathways that leads to regulation of basic cell functions, such as gene expression, mitogenesis, differentiation, cytoskeletal organization, as well as controlling the activity of ion channels (Wessler, Kirkpatrick and Racke, 1999).

Signalling of mAChRs can also be dependent upon the agonist or ligand. The notion that a mAChR is capable of coupling to multiple cellular effectors indicate a biased agonism interplay that depends on the property of the agonist (Kenakin, 2007). Signalling through these cellular effectors is therefore dependent upon the selectivity and strength of the receptor stimulus (Kenakin, 2007). Furthermore, mAChRs are capable of adopting multiple receptor conformations depending on the stimulus (Gether, 2000; Kenakin, 2002). Antagonists modify mAChRs conformations to prevent access to coupled G proteins, while agonist elect conformations that allow interaction with coupled G proteins. Given these key properties, massive efforts were directed to develop compounds that selectively agonise, modulate or antagonise each receptor subtype to meet therapeutic objectives and study their individual function (Gether, 2000; Kenakin, 2002, 2007). Initially, compounds that imitate ACh action were found naturally, including the agonist muscarine (from which mAChRs derives their name), pilocarpine, or antagonists like atropine (Eglen, 2005). Pilocarpine is now indicated in treatment of glaucoma, ocular hypertension, and salivary gland dysfunction (Wiseman and Faulds, 1995; Vivino *et al.*, 1999). Atropine is now indicated in treatment of amblyopia and sinus bradycardia (Scheinman, Thorburn

and Abbott, 1975; Holmes *et al.*, 2003; Marrs, Maynard and Sidell, 2007). Since then, several mAChRs agonists and antagonists have emerged, where some are naturally occurring while others have been developed as subtype-selective compounds (Eglen, Choppin and Watson, 2001; van Koppen and Kaiser, 2003). However, selectivity of these compounds is still questionable as they should not be considered absolute due to the fact that it is still difficult to fully understand the exact role of each subtype *in vivo* (Ishii and Kurachi, 2006).

## 1.2 Acetylcholine receptors in mesenchymal stem cells

### 1.2.1 Mesenchymal stem cells

Stem cells are a group of undifferentiated cells that have the ability to self-renew and differentiate into multiple cell types. While this definition is broad, it is important in the context of what is reported in the literature especially when it comes to mesenchymal stem cells. There has been an ongoing controversy about the terminology used for stem cells, and terms such as “mesenchymal stem cell” and “mesenchymal stromal cell” have been used interchangeably (Sipp, Robey and Turner, 2018). This has led to the assumption that the two terms are the same, whereas “stromal” refers loosely to a bulk population from which a minor population of “stem cells” arise. Indeed, it is recommended to keep the acronym “MSCs” for mesenchymal stem cells, however, it needs to be supported by evidence demonstrating the “stemness” traits of self-renewal and differentiation properties as well as annotation of the source of these cells (Viswanathan *et al.*, 2019).

Stem cells are present in the embryonic, foetal, and adult stages of life. Stem cells are usually classified according to their differentiation potential, or potency (Smith, 2006). Pluripotent stem cells display the ability to differentiate into cells of the three primary germ layers (ectoderm, mesoderm, and endoderm), from which all tissues and organs develop (P De Miguel, Fuentes-Julián and Alcaina, 2010). Embryonic stem cells (ESCs), in early stage of development, are the only naturally occurring pluripotent stem cell (Thomson *et al.*, 1998). However, adult somatic cells can be genetically reprogrammed to an ESC-like state, and these are referred to as induced pluripotent stem cells (iPSCs) (Takahashi and Yamanaka, 2006). Multipotent stem cells are defined by their ability to differentiate into various cell types, but typically within a single germ layer. Multipotent stem cells are found in most tissues postnatally and are usually known as adult stem cells (Bacakova *et al.*, 2018). Mesenchymal stem cells (MSCs) are broadly an example of multipotent cell (Ratajczak *et al.*, 2012). Unipotent stem cells (USCs), are tissue specific adult stem cells tasked with the repair of the tissues in which they reside. They differentiate into only one specific cell type and form a single lineage (Kolios and Moodley, 2013). Both pluripotent and multipotent stem cells have been utilised in regenerative applications. Although multipotent stem cells exhibit

lower potency compared to pluripotent stem cells, their application in regenerative medicine is favourable as they circumvent the ethical and legal issues associated with using ESCs and the genetic instability associated with iPSCs (Kolios and Moodley, 2013).

The MSCs are a group of multipotent adult stem cells initially isolated from bone marrow (Friedenstein *et al.*, 1974). MSCs have now been isolated from various other tissues, including adipose tissue (Zuk *et al.*, 2002), dental pulp (Gronthos *et al.*, 2002), peripheral blood (Chong *et al.*, 2012), salivary glands (Aure, Arany and Ovitt, 2015), skeletal muscle (Nombela-Arrieta, Ritz and Silberstein, 2011), skin (Sellheyer and Krahl, 2010), and placental tissue (Rogers and Casper, 2004; Troyer and Weiss, 2008; Wang, Qu and Zhao, 2012) (Figure 1-4). The International Society of Cellular Therapy set three criteria to define stem cells as MSCs: (i) ability to adhere to plastic; (ii) expression of cell surface markers (e.g. CD73, CD90, and CD105) and lack of hematopoietic markers (e.g. CD14, CD34, and CD45) and class II major histocompatibility complex molecules; (iii) ability to differentiate down mesodermal lineages (Horwitz *et al.*, 2005; Liu, Zhuge and Velazquez, 2009; Orbay, Tobita and Mizuno, 2012). Generally, cultured MSCs present these features, however some differences have been observed between MSCs of different origins (Mafi *et al.*, 2011). MSCs tend to differentiate down mesodermal lineages, however, under appropriate stimuli, it has been suggested that MSCs are capable of differentiation into tissues of endodermal and neuroectodermal lineages (Liu, Zhuge and Velazquez, 2009). As MSCs are self-renewing cells with immunomodulatory properties and the ability to be differentiated into several lineages (Pittenger *et al.*, 1999; Kolf, Cho and Tuan, 2007; Bernardo and Fibbe, 2013; Matuskova *et al.*, 2018) they are a vital resource for tissue engineering, regenerative medicine, and cell-based therapy research (Pittenger *et al.*, 1999; Heubach *et al.*, 2004; Wang, Qu and Zhao, 2012).

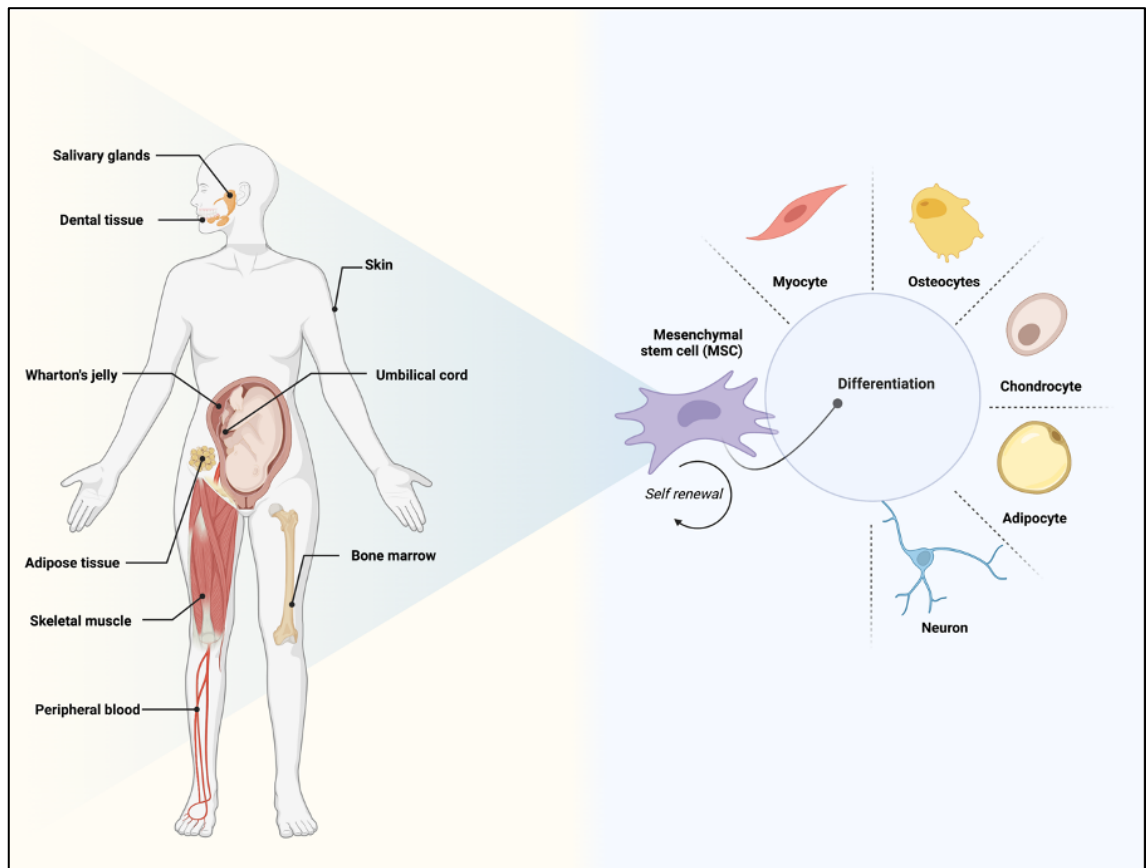


**Figure 1-4** The possible origin and differentiation potential of MSCs. MSCs have been isolated from different parts of the adult body and are usually annotated according to the source of their harvest (e.g., Bone Marrow-MSCs). The differentiation potential of these stem/progenitor cells and self-renewal properties vary according to multiple factors such as origin, isolation, and culture. The figure broadly describes the different types of cells that can be differentiated from MSCs.

Growth factors that have been identified to play a role in controlling MSC fate include basic fibroblast growth factor (bFGF) (Benavente *et al.*, 2003) and bone morphogenic proteins (BMPs) (Diefenderfer *et al.*, 2003). Furthermore, receptors, such as the epidermal growth factor receptor (EGFR) (Krampera *et al.*, 2005) and the interleukin-6 receptor (IL-6R) (Erices *et al.*, 2002), have also been shown to regulate MSC function. The Wnt 3a (Boland *et al.*, 2004), Wnt/ $\beta$ -catenin (Liu *et al.*, 2011), and Notch (Li *et al.*, 2006) intracellular signalling pathways are major regulators of MSC proliferation and differentiation and transcription factors, such as *SOX9* (Furumatsu *et al.*, 2005) and *RUNX2* (Xu *et al.*, 2015), have been shown to influence MSCs commitment to differentiation towards particular lineages. However, our knowledge of the receptors and associated signalling pathways that influence MSC fate is far from complete. Indeed, non-neuronal cholinergic receptors and their associated signalling pathways have also been suggested to modulate MSC function.

Despite being known to regulate cell differentiation, the role of the non-neuronal cholinergic system in stem cells is still relatively unexplored. Several types of stem cell express components of the non-neuronal cholinergic signalling system including functional AChRs. This includes non-neural stem cells, such as embryonic stem cells (Paraoanu *et al.*, 2007), hematopoietic stem cells (Serobyán *et al.*, 2007), skeletal muscle stem cells (Grassi *et al.*, 2004), and MSCs (Hoogduijn, Cheng and Genever, 2009; Piovesana *et al.*, 2018). There is sufficient evidence to conclude that MSCs express a functional cholinergic system and studies suggest a role for ACh in regulating stem cell properties (Hoogduijn, Cheng and Genever, 2009; Piovesana *et al.*, 2018). Therefore, it can be hypothesised that MSCs have cholinergic properties which play important roles in determining their fate. (Piovesana *et al.*, 2018).

## 1.2.2 Expression of Muscarinic Receptors in Mesenchymal Stem Cells

Note: part of this section has been published in *Stem Cells and Development* Peer-reviewed journal (Alqahtani *et al.*, 2023)

### 1.2.2.1 Bone marrow MSCs (BM-MSCs)

All five mAChRs have been identified in human MSCs (Table 1-1). Hoogduijn *et al.* were the first to investigate cholinergic signalling in MSCs (Hoogduijn, Cheng and Genever, 2009). Using polymerase chain reaction (PCR), the authors demonstrated that human bone marrow MSCs (BM-MSCs) express the M2 receptor gene (*CHRM2*). Moreover, the authors suggested that expression was dynamic given that only half of the BM-MSCs were positive for the M2 protein. Confirmation that BM-MSCs express a functional M2 receptor was demonstrated as stimulation with muscarine increased intracellular Calcium ( $Ca^{2+}$ ) concentration and downregulated production of cyclic adenosine 3',5'-monophosphate (cAMP). Intracellular  $Ca^{2+}$  and cAMP were previously proven to regulate MSC proliferation and differentiation (Chu *et al.*, 2006). Furthermore, muscarine induced an increase in the levels of phosphorylation of the extracellular signal-regulated protein kinases 1 and 2 (ERK1 and ERK2) (Hoogduijn, Cheng and Genever, 2009); the ERK1/2 pathway has been linked to control differentiation and phosphorylation of transcription factors such as PPAR $\gamma$  and RUNX2 which are required for adipose and osteogenic differentiation, respectively (Ge *et al.*, 2007, 2016; Dalby, García and Salmeron-Sanchez, 2018). These data imply that the M2 receptor activates downstream signalling pathways that govern MSC proliferation and differentiation.

Expression of M1, M2 and M3 receptor genes (*CHRM1*, *CHRM2* and *CHRM3*) in BM-MSCs has also been reported (Danielyan *et al.*, 2009). Upregulated expression of these receptors after treatment with erythropoietin under both normoxic and hypoxic conditions was reported in BM-MSCs and likely marked the induced neuronal like cell differentiation. Treatment of BM-MSCs with ACh led to an increase in concentration of intracellular  $Ca^{2+}$  which was hypothesised to be mediated by M1 and M3 receptors and further influenced the phospholipase C and inositol-1,4,5-triphosphate (IP3) signalling axis. Although it was hypothesised that the effects of ACh on BM-MSCs are mediated by the M1 and M3 receptor, the influence of other mAChRs subtypes (e.g., M2) was not investigated in detail. The

M2 and M4 receptors, despite being thought to modulate inhibitory signalling pathways, have been shown to stimulate phospholipase C activity (Zhu and Birnbaumer, 1996). In addition, ACh is a universal cholinergic agonist, and, therefore, the influence of the nAChRs could also not be excluded.

Expression of M2 and M3 receptor genes (*CHRM2* and *CHRM3*) was reported in a study exploring mAChRs expression in human BM-MSCs, induced pluripotent stem cells (iPSCs) and MSCs derived from human iPSCs (iPS-MSCs) (Weist *et al.*, 2018). Interestingly, the M2 gene (*CHRM2*) is expressed in native iPSCs and during the differentiation phase into iPS-MSCs, but it was not detected at the end of the differentiation period. This implied that MSCs generated from iPSCs lose M2 expression. Consistent expression of the M2 receptor gene (*CHRM2*) in BM-MSCs was however observed despite donor-dependent variability. Expression of the M3 receptor gene (*CHRM3*) also varied during the differentiation process into iPS-MSCs. M3 receptor gene (*CHRM3*) expression was detected in native iPSCs, decreased during the differentiation process, and increased again at the end stage of differentiation into iPS-MSCs. Unlike the BM-MSCs, where the M3 receptor gene (*CHRM3*) was clearly expressed. The authors suggest that the variation in the expression profile among the different cell types might contribute to different signalling capabilities, which in turn may lead to their different biological characteristics. Variation in mAChRs expression pattern between passages and upon differentiation of MSC has indeed been reported in a study investigating human BM-MSCs (Yegani *et al.*, 2020). Real time PCR showed downregulation in expression of the M1 (*CHRM1*) and M5 (*CHRM5*) receptor genes in consecutive passages as well as during both osteogenic and adipogenic differentiation. Furthermore, the study reported treatment with atropine, a general muscarinic antagonist, significantly upregulated expression of the M4 receptor gene (*CHRM4*) during adipogenic differentiation of BM-MSCs.

Expression of the M3 receptor was detected at both the mRNA and protein level in mouse BM-MSCs (Mona *et al.*, 2019). The M3 receptor was localised primarily to the endoplasmic reticulum in the investigated BM-MSCs and as such were not competent to signal. This was confirmed in agonist studies. It may be the case that during differentiation membrane translocation occurs and enables functional M3 receptor signalling. However, this hypothesis was not investigated further. Rat BM-MSCs have been shown to express M1 and M4 receptors at the protein level and

the M1 receptor was found to be localised in both the cytoplasm and cell membrane (Tang *et al.*, 2012). Interestingly, fluorescence-activated cell sorting (FACS) analysis only showed a third of the rat BM-MSCs expressed the M1 receptor. Treatment with ACh, a universal cholinergic agonist, caused enhanced migration of rat BM-MSCs in a dose-and time-dependent manner with no effect on proliferation. The effect of ACh on rat BM-MSCs migration was hypothesised to be mediated by the M1 receptor using atropine, a general muscarinic receptor antagonist. Indeed, activation of the M1 receptor was shown to trigger the ERK1/2 and Protein Kinase C (PKC) signalling pathways with release of Ca<sup>2+</sup> which in turn regulated migration (Tang *et al.*, 2012).

#### 1.2.2.2 Adipose derived MSCs (AD-MSCs)

Human adipose-derived MSCs (AD-MSCs) express the M1 and M2 receptor genes (*CHRM1* and *CHRM2*) and expression of both were upregulated following cardiogenic differentiation and denoted as markers for cardiomyocytes (Chang *et al.*, 2012). Interestingly, native AD-MSCs only express the M2 receptor gene (*CHRM2*), while expression of the M1 receptor gene (*CHRM1*) was only detected once AD-MSCs were differentiated into cardiomyocytes. Another study demonstrated changes in the pattern of mAChR gene expression upon AD-MSCs differentiation (Nery *et al.*, 2019). Expression of all five mAChR genes (*CHRM1* - *CHRM5*) fluctuated throughout the differentiation of AD-MSCs into cells that expressed neural proteins. Expression levels of the M1 (*CHRM1*), M3 (*CHRM3*) and M4 (*CHRM4*) receptor genes rose during the differentiation process. In contrast, expression levels of the M2 (*CHRM2*) and M5 (*CHRM5*) receptor genes declined during the differentiation process; however, expression of the M2 (*CHRM2*) receptor gene recovered towards the end of differentiation. Furthermore, AD-MSCs isolated from rats express functional M2 receptor (Piovesana *et al.*, 2018). Rat AD-MSCs have been demonstrated to express the M1 (*CHRM1*), M2 (*CHRM2*) and M3 (*CHRM3*) receptor genes and expression of the M2 receptor was confirmed at the protein level. Stimulation of AD-MSCs with arecaidine propargyl ester hydrobromide (APE), a selective M2 agonist, caused autocrine upregulation of expression of the M2 gene (*CHRM2*). In addition, activation of the M2 receptor inhibited AD-MSC proliferation, migration, and cell cycle. However, these effects were reversed when the agonist was withdrawn. Selectivity of APE for the M2 receptor in AD-MSCs was also confirmed using methoctramine, an antagonist with

preference for the M2 receptor. Additionally, activation of the M2 receptor resulted in down regulated expression of key genes involved in cell proliferation and migration (*cyclinD1*, *PCNA*, *c-jun*, *PDGFR-B*, *CXCR4* and *CXCR7*). These findings are in agreement with the hypothesised role of the M2 receptor as an inhibitory mAChRs and suggests that M2 receptor activation places AD-MSCs in a quiescent state.

#### **1.2.2.3 Salivary gland derived stem cells (SGDCs)**

Two studies isolated the M3 receptor protein from porcine salivary gland derived stem cells (SGDCs) (Ferreira *et al.*, 2019; Urkasemsin *et al.*, 2019) Both studies reported an increase in intracellular Ca<sup>2+</sup> activity upon stimulating the porcine SGDCs with carbachol and suggested that this effect is mediated via the M3 receptor. However, carbachol is an ACh analogue that can mimic the effect of ACh on both mAChRs and nAChRs. Both studies viewed the M3 receptor as a salivary gland marker of generated salivary gland organoids and do not report expression of other AChRs, or present data for the selectivity of carbachol to the SGDC M3 receptor.

#### **1.2.2.4 Reaming debris-derived MSCs (RD-MSCs)**

Harvested MSCs from reaming debris (RD-MSCs) during surgery of long bone diaphyseal fractures of male and female patients with osteoporosis, and MSCs from healthy donors, have been differentiated down osteogenic, chondrogenic, and adipogenic lineages and expression of mAChR genes was shown to be differential and dynamic (Zablotni *et al.*, 2015). Indeed, only the M4 (*CHRM4*) and M5 (*CHRM5*) receptor genes were expressed in RD-MSCs isolated from male donors, while female donors expressed the M2 (*CHRM2*), M4 (*CHRM4*), and M5 (*CHRM5*) receptor genes. RD-MSCs from female donors with osteoporosis showed no differences in the mAChR expression profile to RD-MSCs from healthy female donors. However, expression of the specific subtype of mAChRs showed a degree of subject specificity in both undifferentiated RD-MSCs and RD-MSCs differentiated down specific lineages. This was hypothesised to be related to donor-specific conditions. However, the observed differences in mAChRs expression by RD-MSCs pre- and post- differentiation is compelling evidence for a role of mAChRs in regulating MSC differentiation.

### 1.2.2.5 Foetal membrane MSCs (FM-MSCs)

In a study that investigated mAChR gene expression in MSCs isolated from human foetal membrane (FM-MSCs), the authors report variation in the expression pattern of mAChR genes between passages and upon differentiation of FM-MSCs (Yegani *et al.*, 2020). Indeed, by passage three, FM-MSCs demonstrated upregulated expression of the M1 (*CHRM1*) receptor gene in addition to differentiation down both osteogenic and adipogenic lineages. Expression of the M2 (*CHRM2*) receptor gene was downregulated during differentiation of FM-MSCs down an osteogenic lineage and expression of the M3 (*CHRM3*) receptor gene was maintained throughout the differentiation process. Treatment of FM-MSCs with atropine, a general muscarinic antagonist, enhanced their viability and upregulated expression of the M1 (*CHRM1*) receptor gene during osteogenic differentiation. However, atropine treatment had no effect on the ability of FM-MSCs to differentiate down adipogenic or osteogenic lineages. The authors suggest that the M1 receptor may play an important role in differentiation of FM-MSCs. However, without selective stimulation or knockout experiments, it remains unclear which mAChRs are functional in FM-MSCs as atropine is a general muscarinic antagonist that can act on all mAChRs.

### 1.2.2.6 Umbilical cord-derived MSCs (UC-MSCs)

Expression of the M2 (*CHRM2*), M3 (*CHRM3*), and M4 (*CHRM4*) receptor genes was detected in human MSCs derived from the umbilical cord (UC-MSCs) (Kotova *et al.*, 2020). Stimulation of UC-MSCs with ACh induces an intracellular Ca<sup>2+</sup> response. The authors indicated that the ACh-induced response is mediated by the M3 receptor via the phosphoinositide 3-kinase (PIK3) axis. The authors viewed the M3 receptor as the best candidate to investigate Ca<sup>2+</sup> intracellular signalling mediated by the PIK3 axis. This is based on how mAChRs, naturally, couple to G proteins and mediate downstream signalling. The M1, M3, and M5 receptors couple to G proteins known to influence Ca<sup>2+</sup> mobilisation, while M2 and M4 couple to G proteins that inhibit adenylate cyclase. Indeed, the authors showed data demonstrating that a selective M3-antagonist abolished the induced effects of ACh on UC-MSCs (Kotova *et al.*, 2020). Interestingly, the authors also reported the ability of a PIK3 inhibitor to abolish the induced effects of ACh on UC-MSCs, suggesting that the PIK3 inhibitor might function by obstructing the ACh binding site of the M3 receptor.

### 1.2.2.7 Summary

In summary, studies suggest involvement of mAChRs in activating signalling pathways that regulate MSCs function. For example, the M2 receptor has been suggested to activate the ERK1/2 pathway in BM-MSCs (Hoogduijn, Cheng and Genever, 2009), while the M1 and M3 receptors influence the IP3 signalling axis of the same MSCs type (Danielyan *et al.*, 2009). These data imply mAChRs can activate downstream signalling pathways that govern MSC function. However, only one study in AD-MSCs has to date has provided direct evidence for a role of mAChRs (the M2 receptor) in inhibiting proliferation, migration, and the cell cycle (Piovesana *et al.*, 2018).

**Table 1-1 Summary of muscarinic receptors in MSCs. N/A: not assessed.**

Muscarinic subtype	Species	mRNA expression	Protein expression	Functional expression
M1	Human	BM-MSCs (Danielyan <i>et al.</i> , 2009; Yegani <i>et al.</i> , 2020)		BM-MSCs (Danielyan <i>et al.</i> , 2009)
		FM-MSCs (Yegani <i>et al.</i> , 2020)	N/A	
	Rat	AD-MSCs (Nery <i>et al.</i> , 2019)		
		AD-MSCs (Piovesana <i>et al.</i> , 2018)	BM-MSCs (Tang <i>et al.</i> , 2012)	BM-MSCs (Tang <i>et al.</i> , 2012)
		BM-MSCs (Tang <i>et al.</i> , 2012)		
M2	Human	BM-MSCs (Danielyan <i>et al.</i> , 2009; Hoogduijn, Cheng and Genever, 2009; Weist <i>et al.</i> , 2018)	BM-MSCs (Hoogduijn, Cheng and Genever, 2009)	BM-MSCs (Hoogduijn, Cheng and Genever, 2009)
		FM-MSCs (Yegani <i>et al.</i> , 2020)		
		AD-MSCs (Chang <i>et al.</i> , 2012; Nery <i>et al.</i> , 2019)		
	Rat	RD-MSCs (Zablotni <i>et al.</i> , 2015)		
		UC-MSCs (Kotova <i>et al.</i> , 2020)		
		AD-MSCs (Piovesana <i>et al.</i> , 2018)	AD-MSCs (Piovesana <i>et al.</i> , 2018)	AD-MSCs (Piovesana <i>et al.</i> , 2018)

M3	Human	BM-MSCs (Danielyan et al., 2009; Weist et al., 2018; Yegani et al., 2020)	N/A	BM-MSCs (Danielyan et al., 2009)
		iPS-MSCs (Weist et al., 2018)		UC-MSCs (Kotova et al., 2020)
		FM-MSCs (Yegani et al., 2020)		
		AD-MSCs (Nery et al., 2019)		
	Rat	AD-MSCs (Piovesana et al., 2018)	N/A	N/A
	Mouse	BM-MSCs (Mona et al., 2019)	BM-MSCs (Mona et al., 2019)	N/A
	Porcine	N/A	SGDCs (Ferreira et al., 2019; Urkasemsin et al., 2019)	SGDCs (Ferreira et al., 2019; Urkasemsin et al., 2019)
M4	Human	BM-MSCs (Yegani et al., 2020)	N/A	N/A
		RD-MSCs (Zablotni et al., 2015)		
	Rat	BM-MSCs (Tang et al., 2012)	N/A	N/A
M5	Human	BM-MSCs (Yegani et al., 2020)	N/A	N/A
		AD-MSCs (Nery et al., 2019)		
		RD-MSCs (Zablotni et al., 2015)		

### 1.2.3 Expression of Nicotinic Receptors in Mesenchymal Stem Cells

#### 1.2.3.1 Bone marrow MSCs (BM-MSCs)

Expression of the nAChR subunits have been reported in MSCs (Table 1-2). In BM-MSCs, Hoogduijn *et al.*, detected gene and protein expression of the  $\alpha 3$ ,  $\alpha 5$ , and  $\alpha 7$ nAChR subunits (Hoogduijn, Cheng and Genever, 2009). Confirmation of functional nAChR expression was determined by stimulation with nicotine which led to an increase in intracellular calcium and an increase in the levels of phosphorylation of ERK1 and ERK2. However, this was observed in only half of the BM-MSc population upon stimulation with nicotine. It was, however, suggested that the nicotine induced effects are mediated through the  $\alpha 7$ nAChR in BM-MSCs as the study showed an increase in levels of phosphorylated ERK in C3H10T1/2 cells (functionally similar cells to MSCs), transfected with the  $\alpha 7$ nAChR construct, after stimulation with nicotine. Although nicotine is a general nicotinic agonist, it remains unclear if the other nAChRs that the authors identified to be expressed by BM-MSCs could have contributed to these observations.

Variation in the expression profile of nAChR genes has been reported between human BM-MSCs, iPSCs, and MSCs derived from human iPSCs (iPS-MSCs) (Weist *et al.*, 2018). Native iPSCs do not express the  $\alpha 1$  subunit (*CHRNA1*) gene; however, both iPS-MSCs and BM-MSCs express transcripts of this gene. The genes for the  $\alpha 3$ ,  $\alpha 4$ ,  $\alpha 5$ ,  $\alpha 7$ ,  $\alpha 9$ , and B1 subunits (*CHRNA3*, *CHRNA4*, *CHRNA5*, *CHRNA7*, *CHRNA9*, and *CHRNB1*) were strongly expressed in iPSCs and during the generation of iPS-MSCs. However, they were only weakly expressed in generated iPS-MSCs. While BM-MSCs showed donor dependent expression of  $\alpha 4$ ,  $\alpha 5$ ,  $\alpha 7$ , and B1 subunit genes (*CHRNA4*, *CHRNA5*, *CHRNA7*, and *CHRNB1*), the B2 and B4 subunit genes (*CHRNB2*, and *CHRNB4*) were only expressed at low levels in iPSCs and during the generation of iPS-MSCs. Differential expression profiles of nAChR genes have been reported in human MSCs (hMSCs) (Schraufstatter, DiScipio and Khaldoyanidi, 2010). Gene expression of the  $\alpha 1$ ,  $\alpha 2$ ,  $\alpha 3$ ,  $\alpha 4$ ,  $\alpha 5$ ,  $\alpha 7$ ,  $\alpha 9$ , B2, B3 and B4 subunits (*CHRNA2*, *CHRNA3*, *CHRNA4*, *CHRNA5*, *CHRNA7*, *CHRNA9*, *CHRNB2*, *CHRNB3*, and *CHRNB4*) were confirmed in hMSCs (Schraufstatter, DiScipio and Khaldoyanidi, 2010). Further analysis confirmed protein expression of the  $\alpha 7$ , B2, and B4 nAChR subunits. The study also provided evidence of functional nAChRs in hMSCs via stimulation with nicotine. Indeed, treatment with 1  $\mu$ M nicotine or less induced

spontaneous migration of hMSC; however, higher doses ( $>1 \mu\text{M}$ ) caused cell death. Furthermore, the study provided evidence that nicotine inhibits C3a- and bFGF-induced migration in hMSCs. Moreover, the study provided data showing the nicotine-induced effects are mediated through the  $\alpha 7\text{nAChR}$  in hMSCs. Indeed, the  $\alpha 7\text{nAChR}$  selective antagonist  $\alpha$ -bungarotoxin ( $\alpha$ -BTX) was shown to abolish the inhibitory effects of nicotine. The study also provided *in vivo* data demonstrating impaired migration of transplanted hMSCs to the bone marrow and spleen in mice as a result of nicotine exposure. Indeed, in a separate study, it has been suggested that higher doses of nicotine cause apoptosis and impair proliferation, while at non-toxic concentrations it decreases the migratory potential of MSCs (Chan and Huang, 2020).

A functional heteropentameric  $\alpha 4\beta 2\text{nAChR}$  has been reported in rat BM-MSCs (Xiao *et al.*, 2019). Indeed, stimulation with nicotine suppressed the osteogenic potential of rat BM-MSCs in a concentration-dependent manner. Nicotine ( $>0.1 \mu\text{M}$ ) had a negative effect on the expression of osteogenesis markers such as: *Runx2*, *BSP*, *Col1*, and *OCN*. Higher concentrations of nicotine ( $10 \mu\text{M}$ ) significantly inhibited mineralisation of differentiated rat BM-MSCs. The authors indicated that suppressed rat BM-MSCs osteogenesis occurs due to nicotine promoting the activity of the angiotensin-converting enzyme (ACE) and activating the bone renin angiotensin system (RAS). This was confirmed using dihydro- $\beta$ -erythroidine, a selective inhibitor of the  $\alpha 4\beta 2\text{nAChR}$ , which partially counteracted the nicotine-induced expression of ACE and activation of the RAS system. In a separate *in vivo* study, expression of a functional  $\alpha 7\text{nAChR}$  in rat BM-MSCs has been reported (Tie *et al.*, 2018). The study showed that nicotine impaired the ability of BM-MSCs to repair cartilage defects in rats. Indeed, nicotine suppressed chondrogenic differentiation of rat BM-MSCs as evidenced by reduced safranin-O staining of newly formed cartilage tissue. Additionally, nicotine inhibited expression of chondrogenic markers such as *Col2A1* and *Sox9* in rat BM-MSCs regenerated tissue. The authors indicate that the  $\alpha 7\text{nAChR}$  mediates nicotine's ability to downregulate *Col2A1* expression by suppressing its upstream effector *Sox9*. Indeed, the study provides evidence of involvement of the  $\alpha 7\text{nAChR}$  in mediating the effect of nicotine as methyllycaconitine, a specific  $\alpha 7\text{nAChR}$  antagonist, inhibited nicotine-induced  $\text{Ca}^{2+}$  influx in rat BM-MSCs. Furthermore, repressed BM-MSC chondrogenesis is thought to occur via the  $\text{Ca}^{2+}$ /calcineurin/NFATc2 signalling pathway upon nicotine stimulation. The study demonstrated that nicotine

decreased cytoplasmic dephosphorylated NFATc2 with concomitant nuclear translocation of NFATc2 in response to an increase in intracellular  $\text{Ca}^{2+}$ . NFATc2 is capable of binding to the Sox9 promoter, thus decreasing Sox9 expression. These nicotine-induced effects were abolished when BM-MSCs were pre-treated with methyllycaconitine, indicating the involvement of the  $\alpha 7$ nAChR in attenuating the  $\text{Ca}^{2+}$ /calcineurin/NFATc2 signalling pathway.

### 1.2.3.2 Adipose-derived MSCs (AD-MSCs)

Human AD-MSCs express both the  $\alpha$  and  $\beta$  nAChR subunits (Nery *et al.*, 2019). Expression of the  $\alpha 7$  and  $\beta 4$  nAChR subunits (*CHRNA7*, and *CHRNB4*) were upregulated while the  $\alpha 3$ ,  $\alpha 6$ , and  $\beta 2$  nAChR subunits (*CHRNA3*, *CHRNA6*, and *CHRNB2*) were significantly downregulated in neuronal differentiated AD-MSCs. Functional nAChRs were confirmed as nicotine induced an increase in intracellular  $\text{Ca}^{2+}$ , most significantly when AD-MSCs underwent neuronal differentiation. However, no data eluding to which nAChRs mediate the effect of nicotine is reported. In another study, AD-MSCs derived from rats were found to express a functional  $\alpha 7$ nAChR (Pernarella *et al.*, 2020). Indeed, stimulation with ICH3, a selective  $\alpha 7$ nAChR agonist, inhibits rat AD-MSCs proliferation. Further analysis confirms that the  $\alpha 7$ nAChR inhibits AD-MSCs proliferation by promoting cell cycle arrest via downregulation of *Cyclin D1* expression. However, activation of the  $\alpha 7$ nAChR significantly enhanced rat AD-MSCs migration via upregulation of CXCR4, a chemokine receptor that also mediates cellular migration. Both these effects could be counteracted using  $\alpha$ -BTX, an  $\alpha 7$ nAChR selective antagonist. Interestingly, ICH3 treatment of AD-MSCs also increased protein expression of the M2 mAChR suggesting a potential cross-interaction mechanism between m and nAChRs.

### 1.2.3.3 Periodontal ligament derived MSCs (PDL-MSCs)

Human periodontal ligament derived MSCs (PDL-MSCs) have been reported to express the  $\alpha 7$  and  $\beta 4$  nAChR subunit genes (*CHRNA7*, and *CHRNB4*) and nicotine stimulation amplifies their expression (Kim *et al.*, 2012). Nicotine stimulation had a negative impact on PDL-MSCs viability in a dose dependent manner. Higher concentrations of nicotine,  $> 100 \mu\text{M}$ , were associated with increased DNA fragmentation in PDL-MSCs and accumulation of cells in subG1 phase of the cell cycle, the phase associated with apoptosis. Indeed, nicotine in millimolar levels

activated apoptotic pathways in PDL-MSCs and increased expression of p53, a pro-apoptotic marker, was evident after only 30 min treatment with ten mM nicotine. This was associated with a decrease in levels of the Bcl-2 anti-apoptotic protein and an increase in the well-known apoptotic marker caspase-3. However, the nicotine-induced apoptosis was blocked when PDL-MSCs were pre-treated with  $\alpha$ -BTX, the aforementioned  $\alpha$ 7nAChR-specific antagonist. Thus, confirming the role of the  $\alpha$ 7nAChR in mediating the nicotine-induced effects on apoptosis in PDL-MSCs. Data from a study by Zhou *et al* confirmed that PDL-MSCs express a functional  $\alpha$ 7nAChR and nicotine inhibited PDL-MSCs proliferation in a dose dependent manner (Zhou *et al.*, 2013). Moreover, stimulation with nicotine dose-dependently impaired osteogenic differentiation of PDL-MSCs. Indeed, differentiated PDL-MSCs showed significant decreases in bone mineralisation associated with decreased expression of osteogenic genes and protein markers (ALP, OCN, BSP, and RUNX2). However, the nicotine-induced impairment of differentiation was partially reversed by  $\alpha$ -BTX, suggesting that the  $\alpha$ 7nAChR regulates, to an extent, PDL-MSCs osteogenic differentiation. In fact, both gene and protein expression of the  $\alpha$ 7nAChR in osteo-differentiated PDL-MSCs is increased when nicotine is present. This suggests the involvement of the  $\alpha$ 7nAChR and cholinergic signalling in the process of osteogenesis. In fact, several *in vivo* and *in vitro* studies in chick and mouse have reported involvement of ACh dependent pathways regulating skeletogenesis and bone development (Spieker *et al.*, 2016, 2017; Thangaraj *et al.*, 2016). In which it was suggested that  $\alpha$ 7nAChR mediated the nicotine inhibitory effects on cartilage and bone formation (Spieker *et al.*, 2017). All which are supportive of a role for cholinergic regulation in bone development. In addition, nicotine-stimulated nAChRs can initiate relevant downstream signalling pathways. Indeed, it was shown that the  $\alpha$ 7nAChR mediates the downstream effects of nicotine through the wnt/ $\beta$ -catenin pathway in PDL-MSCs (Zhou *et al.*, 2013). Nicotine stimulation of PDL-MSCs lead to a decrease in protein expression of wnt-related factors, DKK-1 and GSK-3 $\beta$ , and an increase in the expression of active- $\beta$ -catenin protein. The latter has been previously shown in a separate study to suppress PDL-MSCs osteogenic differentiation (Liu *et al.*, 2011). However, in the presence of  $\alpha$ -BTX, all these effects were reversed, again providing further evidence of a functional  $\alpha$ 7nAChR modulating the wnt/ $\beta$ -catenin pathway in PDL-MSCs (Zhou *et al.*, 2013).

#### 1.2.3.4 Wharton's Jelly MSCs (WJ-MSCs)

Human Wharton's Jelly MSCs (WJ-MSCs), derived from the mucous connective tissue between the amniotic epithelium and the umbilical vessels found in the umbilical cord, express genes encoding the  $\alpha 3$ ,  $\alpha 5$ ,  $\alpha 7$ ,  $\beta 2$ , and  $\beta 4$  nAChR subunits (*CHRNA3*, *CHRNA5*, *CHRNA7*, *CHRNB2*, and *CHRNB4*) (X. Yang *et al.*, 2017). WJ-MSCs, in response to nicotine treatment, demonstrate significantly decreased proliferation but no change in viability, apoptosis or necrosis. The chondrogenic differentiation capacity of WJ-MSCs was impaired, to an extent, by nicotine. Indeed, while nicotine treatment did not affect the collagen output of differentiated WJ-MSCs, it did impair the quality of the collagenous matrix formed, as determined by the proteoglycan content. This was asserted to be due to the downregulated expression of chondrogenic markers including *Sox9*, *Col2a1* and *aggrecan*. The authors suggested that the  $\alpha 7$ nAChR mediated the nicotine-induced effects in WJ-MSCs as it induced  $Ca^{2+}$  influx into the cells. In a separate study, human WJ-MSCs were confirmed to express a functional  $\alpha 7$ nAChR as well as the  $\alpha 3$  and  $\alpha 9$  nAChR subunit genes (*CHRNA3*, and *CHRNA9*) (Lykhmus *et al.*, 2019). Furthermore, injection of human WJ-MSCs into  $\alpha 7$ nAChR deficient mice demonstrated improved episodic memory and suggest increased regenerative potential of WJ-MSCs to improve cognitive functions via the  $\alpha 7$ nAChR.

#### 1.2.3.5 Reaming debris-derived MSCs (RD-MSCs)

Expression profile data available for nAChRs provides interesting insight into variation dependent upon sex and health of RD-MSC donors (Zablotni *et al.*, 2015). For example, the  $\alpha 5$ ,  $\alpha 7$ , and  $\alpha 9$  nAChR subunit genes (*CHRNA5*, *CHRNA7*, and *CHRNA9*) were expressed in RD-MSCs isolated from all donor groups (male and female, healthy and diseased). In contrast, the  $\alpha 2$ ,  $\alpha 6$ , and  $\alpha 10$  nAChR subunits (*CHRNA2*, *CHRNA6*, and *CHRNA10*) were only expressed in RD-MSCs isolated from diseased female donors and the  $\alpha 3$  nAChR subunit gene (*CHRNA3*) was only expressed in RD-MSCs isolated from diseased male donors. The study also reported variations in expression of certain nAChR subunits between different differentiated lineages. However, the  $\alpha 7$  subunit gene (*CHRNA7*) was expressed in RD-MSCs differentiated down all lineages (osteogenic, chondrogenic, and adipogenic lineages). Furthermore, the  $\alpha 3$  subunit gene (*CHRNA3*) was expressed in adipocytes generated from female RD-MSC donors; but not by adipocytes

generated from male RD-MSCs donors. Therefore, it can be concluded that the expression profile of the nAChR subunits is dynamic in RD-MSCs.

### 1.2.3.6 Summary

In summary, the aforementioned studies provide evidence that MSCs express functional nAChRs that have been shown to mediate the impact of nicotine. These in turn activate signalling pathways such as the ERK1/2 (Hoogduijn, Cheng and Genever, 2009), Ca<sup>2+</sup>/calcineurin/NFATc2 (Tie *et al.*, 2018), and wnt/ $\beta$ -catenin pathway that are involved in MSC function (Zhou *et al.*, 2013). However, there is limited direct evidence for a role of a specific nAChR in translating the effect of nicotine. One example of a demonstrated direct effect is in the case of the  $\alpha$ 7nAChR which appears to mediate nicotine inhibitory effects on hMSCs migration (Schraufstatter, DiScipio and Khaldoyanidi, 2010). Additionally, impaired chondrogenic differentiation of BM-MSCs in response to nicotine has been demonstrated to be mediated through  $\alpha$ 7nAChR (Tie *et al.*, 2018). Interestingly, the  $\alpha$ 7nAChR was shown to inhibit AD-MSCs proliferation but enhances migration (Pernarella *et al.*, 2020). In PDL-MSCs, the  $\alpha$ 7nAChR mediates nicotine-induced apoptosis (Kim *et al.*, 2012), and to an extent impaired these cells' ability to undergo osteogenic differentiation (Zhou *et al.*, 2013). However, in BM-MSCs the  $\alpha$ 4 $\beta$ 2nAChR was shown to suppress cells' osteogenic potential in response to nicotine (Xiao *et al.*, 2019).

**Table 1-2 Summary of nicotinic receptors in MSCs. N/A: not assessed.**

Nicotinic subunit	Species	mRNA expression	Protein expression	Functional expression
$\alpha$ 1	Human	BM-MSCs (Weist <i>et al.</i> , 2018)	N/A	N/A
		iPS-MSCs (Weist <i>et al.</i> , 2018)		
$\alpha$ 2	Human	MSCs (Schraufstatter, DiScipio and Khaldoyanidi, 2010)	N/A	N/A
		RD-MSCs (Zablotni <i>et al.</i> , 2015)		
$\alpha$ 3	Human	BM-MSCs (Hoogduijn, Cheng and Genever, 2009)	BM-MSCs (Hoogduijn, Cheng and Genever, 2009)	N/A

		AD-MSCs (Nery et al., 2019) RD-MSCs (Zablotni et al., 2015) MSCs (Schraufstatter, DiScipio and Khaldoyanidi, 2010) WJ-MSCs (X. Yang et al., 2017)	WJ-MSCs (Lykhmus et al., 2019)	
$\alpha 4$	Human	BM-MSCs (Nery et al., 2019) MSCs (Schraufstatter, DiScipio and Khaldoyanidi, 2010)	N/A	N/A
$\alpha 5$	Human	BM-MSCs (Hoogduijn, Cheng and Genever, 2009; Weist et al., 2018) iPS-MSCs (Weist et al., 2018) RD-MSCs (Zablotni et al., 2015) MSCs (Schraufstatter, DiScipio and Khaldoyanidi, 2010) WJ-MSCs (X. Yang et al., 2017)	BM-MSCs (Hoogduijn, Cheng and Genever, 2009)	N/A
$\alpha 6$	Human	AD-MSCs (Nery et al., 2019) RD-MSCs (Zablotni et al., 2015)	N/A	N/A
$\alpha 7$	Human	BM-MSCs (Hoogduijn, Cheng and Genever, 2009; Weist et al., 2018) iPS-MSCs (Weist et al., 2018) RD-MSCs (Zablotni et al., 2015) AD-MSCs (Nery et al., 2019) MSCs (Schraufstatter, DiScipio and Khaldoyanidi, 2010) PDL-MSC (Kim et al., 2012; Zhou et al., 2013) WJ-MSCs (X. Yang et al., 2017)	BM-MSCs (Hoogduijn, Cheng and Genever, 2009) MSCs (Schraufstatter, DiScipio and Khaldoyanidi, 2010) PDL-MSCs (Zhou et al., 2013) WJ-MSCs (X. Yang et al., 2017; Lykhmus et al., 2019)	BM-MSCs (Hoogduijn, Cheng and Genever, 2009) MSCs (Schraufstatter, DiScipio and Khaldoyanidi, 2010) PDL-MSCs (Kim et al., 2012; Zhou et al., 2013) WJ-MSCs (X. Yang et al., 2017; Lykhmus et al., 2019)
	Rat	BM-MSCs (Tie et al., 2018)	BM-MSCs (Tie et al., 2018)	BM-MSCs (Tie et al., 2018)

		AD-MSCs (Pernarella et al., 2020)	AD-MSCs (Pernarella et al., 2020)	AD-MSCs (Pernarella et al., 2020)
$\alpha 9$	Human	iPS-MSCs (Weist et al., 2018) MSCs (Schraufstatter, DiScipio and Khaldoyanidi, 2010)	WJ-MSCs (Lykhmus et al., 2019)	N/A
$\alpha 10$	Human	RD-MSCs (Zablotni et al., 2015)	N/A	N/A
B1	Human	BM-MSCs (Weist et al., 2018)	N/A	N/A
B2	Human	AD-MSCs (Nery et al., 2019) MSCs (Schraufstatter, DiScipio and Khaldoyanidi, 2010) WJ-MSCs (X. Yang et al., 2017)	MSCs (Schraufstatter, DiScipio and Khaldoyanidi, 2010)	N/A
B3	Human	MSCs (Schraufstatter, DiScipio and Khaldoyanidi, 2010)	N/A	N/A
B4	Human	AD-MSCs (Nery et al., 2019) MSCs (Schraufstatter, DiScipio and Khaldoyanidi, 2010) PDL-MSCs (Kim et al., 2012) WJ-MSCs (X. Yang et al., 2017)	MSCs (Schraufstatter, DiScipio and Khaldoyanidi, 2010)	N/A
$\alpha 4\beta 2$	Human	BM-MSCs (Xiao et al., 2019)	N/A	BM-MSCs (Xiao et al., 2019)

### 1.2.4 Conclusion

The studies presented in this review showed the widespread expression of AChRs in MSCs and demonstrates the involvement of these receptors in MSCs function. It appears that AChRs expression in MSCs is dynamic, dependent on the type of MSCs, and can be individually based on donor or differentiation lineage. However, expression of all mAChR subtypes have been identified in most of MSCs studied as well as both the  $\alpha$  and  $\beta$  nAChR subunits. Furthermore, consistent expression of a particular AChR subtypes across different types of MSCs has been observed. For example, the M3 mAChR and  $\alpha 7$ nAChR are expressed in multiple types of MSCs. This may suggest central roles of these subtypes in regulating MSC function.

#### 1.2.4.1 Downstream signalling of Acetylcholine receptors in MSCs

Some of the presented studies examined the downstream effects of AChR activation on MSCs regenerative potential. In stem cell therapy, the regenerative output is determined by the ability of the cells to migrate, proliferate, and differentiate. The presented findings showed involvement of major pathways involved in regulating these functions. In the MAPK/ERK pathway, phosphorylation of ERKs are known to regulate proliferation and differentiation of stem cells (Michailovici *et al.*, 2014). As described herein, both muscarinic and nicotinic AChRs were shown to be involved in triggering this signalling pathway cascade in MSCs. Indeed, as AChRs activation facilitates downstream signalling pathways that influence cell homeostasis, they have the capability to influence the regenerative potential of MSCs. However, it is the presence of a subtype functional AChRs that determines specific downstream signalling cascade activation and therefore cell fate. In the case of mAChRs, downstream signalling is mostly dependent on the coupled G protein (Figure 1-5). Indeed, the stimulatory group of mAChRs (i.e., M1, M3, and M5) coupled to Gq proteins mainly influence Ca<sup>2+</sup> influx in MSCs. While the inhibitory group of mAChRs (M2 and M4) coupled to Gi proteins mainly influence cAMP production. Furthermore, both groups of mAChRs share a common downstream pathway for ERK1/2 activation. Dependent on the mAChRs subtype, this can result in promoting MSCs function, e.g., M1 regulating BM-MSCs migration (Tang *et al.*, 2012), or inhibiting MSCs growth, e.g., M2 inhibiting AD-MSC proliferation (Piovesana *et al.*, 2018).

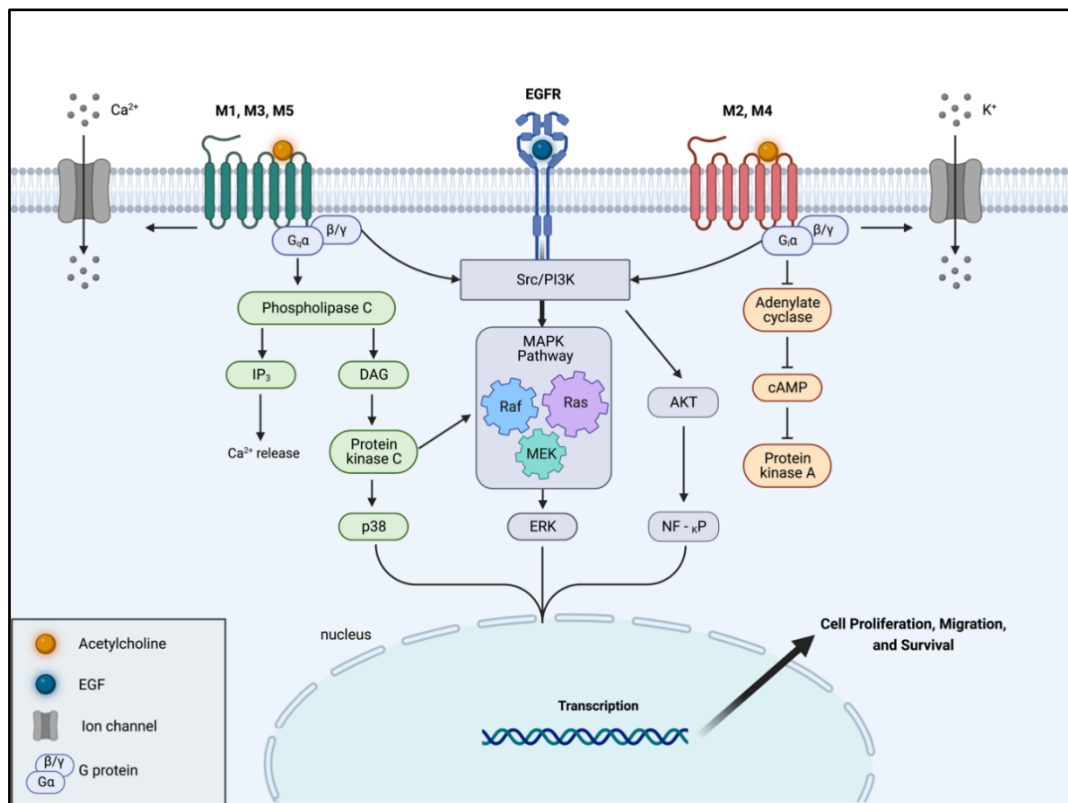


**Figure 1-5 Metabotropic signalling of muscarinic receptors.** Upon stimulation with acetylcholine, or a subunit specific agonist, M1, M3 and M5 receptors activate Phospholipase C (PLC) resulting in downstream protein kinase C (PKC) activation and an increase in IP<sub>3</sub> and Ca<sup>2+</sup> levels. PKC can also activate the MAPK cascade and ERK1/2. M2 and M4 subtypes inhibit the activity of the adenylyl cyclase, leading to a decrease in intracellular cAMP. In addition, mAChRs can activate ion channels. Common pathways for all mAChRs are the activation of ERK1/2 via a Src/PI3K pathway. The M2 subtype may also modulate Akt signaling by means of upstream PI3K activation, influencing transcription factors regulating proliferation.

In the case of nAChRs, these receptors are mainly gated ion channels, for example the most characterised in MSCs is the  $\alpha 7$ nAChRs which modulates intracellular Ca<sup>2+</sup> concentration. Most of the reviewed studies examined downstream effects of nAChRs activation through activation with nicotine. It may have been the focus of these studies to determine the impact of nicotine on the overall potential of treated MSCs. Indeed, nicotine had an overall negative impact on MSCs regenerative potential. The majority of the studies identified the  $\alpha 7$ nAChR in mediating nicotine's effects on MSCs. The consequent changes in the intracellular Ca<sup>2+</sup> concentrations can initiate several signalling cascades (Figure 1-6). This can involve MAPK effectors, via the PI3K pathway or in conjugation with other pathways, such as the calcineurin/NFATc2 or wnt/ $\beta$ -catenin pathways. In most of the studies, this results in inhibition of MSC growth or even in initiation of apoptosis. While other studies showed inhibition or suppression of MSCs potential to differentiate as seen with chondrogenic differentiation of BM-MSCs (Tie *et al.*, 2018) and osteogenic differentiation of PDL-MSCs (Zhou *et al.*, 2013).

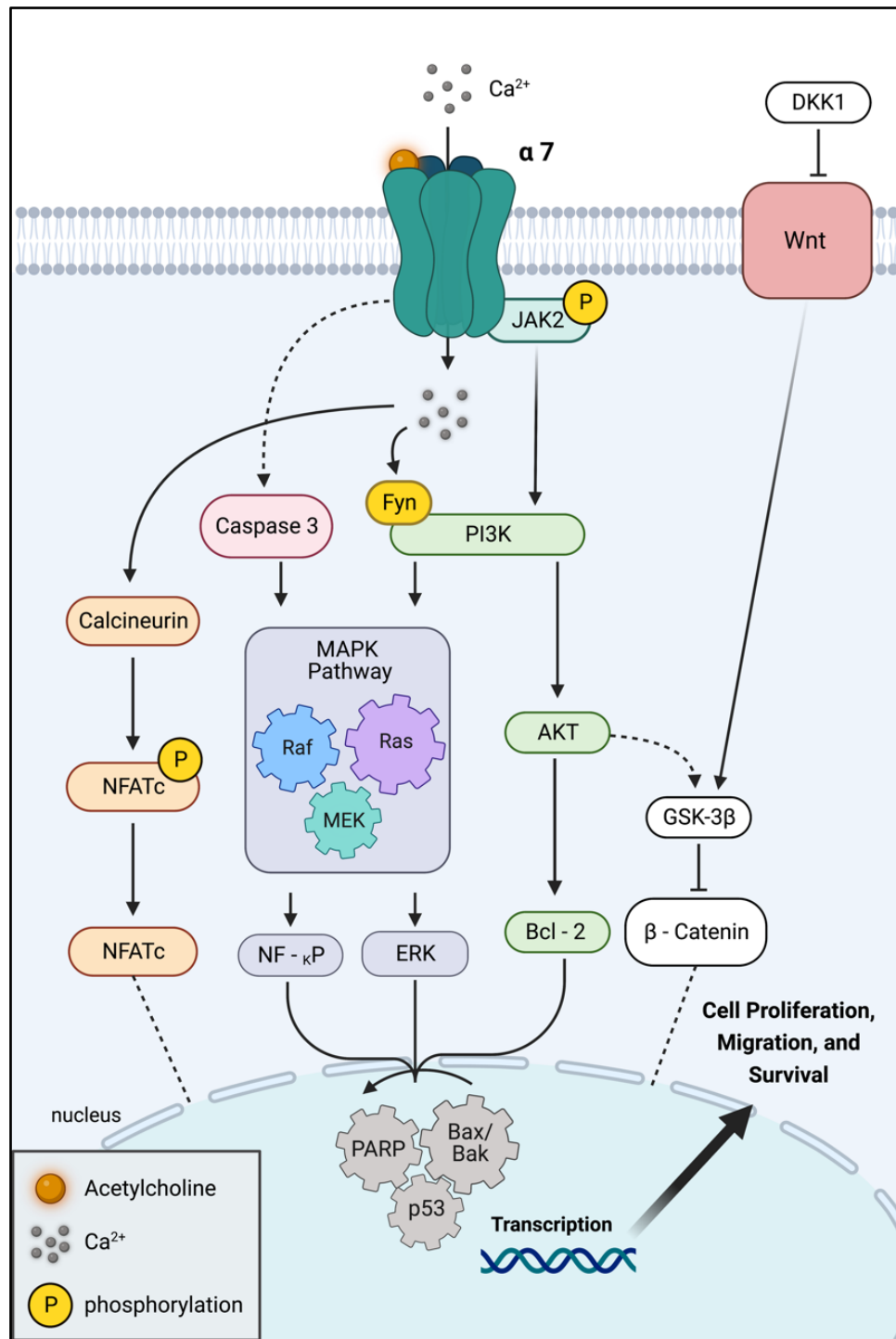


**Figure 1-6** Diagram depicting the  $\alpha 7$ nAChR signalling pathway. Upon stimulation with acetylcholine, or a subunit specific agonist, nAChRs increase cytosolic  $\text{ca}^{2+}$  concentration, initiating several signalling cascades. The  $\text{Ca}^{2+}$  influx with activation of calcineurin can induce NFATc dephosphorylation and translocation back to the nucleus. This recruits transcription factors that govern cell differentiation. Similarly, the  $\alpha 7$ nAChR, via the wnt/AKT pathway, can translocate  $\beta$ -catenin into the nucleus and subsequently activate expression of target genes that modulate differentiation. Common signalling pathways activated by nAChRs include the MAPK via PI3K pathway. This can occur in a Fyn dependent manner or by means of upstream phosphorylation of JAK2. Additionally, Inhibition of JAK2 activates caspase 3, leading also to activation of the MAPK downstream signalling pathway. Later effectors such as NF-KP, ERK, and Bcl-2 signal nuclear transcription factors (e.g., PARP, Bax/Bak, and p53) were found to play a role in the downstream signalling of  $\alpha 7$ nAChR activation. Depending on the downstream signalling pathways activated these pathways can impinge on transcription factors that control synthesis and repair of DNA or promote apoptosis; consequently, influencing cell proliferation, migration, and survival.

#### 1.2.4.2 Acetylcholine receptors as a potential target to regulate MSC function

The evidence suggests that AChRs may present as a promising therapeutic target to control the regenerative potential of MSCs. Indeed, the reviewed studies presented data for subtype-selective AChR agonists and antagonists in manipulating stem cell function. For example, the selective M2 agonist APE placed AD-MSCs in a quiescent state without affecting the viability of the cells (Piovesana *et al.*, 2018). This may be favourable during transplant and for directing *in vivo* regeneration. Migration, an important function of stem cell therapy during *in vivo* regeneration, can be controlled via AChRs. Indeed, the M2 selective agonist APE suppressed AD-MSCs migration via the M2 mAChRs (Piovesana *et al.*, 2018). Another promising option is to block undesirable AChR function through selective and non-selective antagonists. For instance, atropine the general mAChRs antagonist was able to enhance FM-MSCs viability by blocking the M1 receptor (Yegani *et al.*, 2020). It is not unexpected that mAChRs have this central role in MSCs, these receptors were shown to be influential in many body systems e.g., nervous, cardiovascular, and muscular (Kruse *et al.*, 2014). As mAChRs are GPCRs, they belong to the most successful therapeutically targeted family of proteins that continue to be a major focus of biomedical research (Jacoby *et al.*, 2006; Lappano and Maggiolini, 2011; Sriram and Insel, 2018).

Non excitable cells are now known to express a plethora of ion channels, and these are also interesting targets for pharmacological intervention. Here, MSCs were shown to express several subunits of nAChRs forming functional receptors that are susceptible to pharmacological stimulation. Indeed, the selective  $\alpha 7$ nAChR agonist ICH3, was shown to enhance MSCs migration (Pernarella *et al.*, 2020). Likewise,  $\alpha$ -BTX, the  $\alpha 7$ nAChR selective antagonist had the ability to block the detrimental effects of nicotine in several MSCs (Kim *et al.*, 2012; Zhou *et al.*, 2013; Chan and Huang, 2020). These data display an interesting potential for targeting ion channels that influence MSC function. It is also worth mentioning that other classical excitable ion channels are being investigated in control of MSC phenotype. Worthy of mention are the Piezo ion channels, which regulate osteogenesis of MSCs by regulating the expression of *BMP2* (Cheng *et al.*, 2010) and migration via adenosine triphosphate (ATP) release (Mousawi *et al.*, 2020). Likewise, of interest are the Transient Receptor Potential (TRP) ion channels

which can influence MSCs differentiation (Tsimbouri *et al.*, 2017), cell cycle (Hong *et al.*, 2020) and survival (Cheng *et al.*, 2010).

Acetylcholine signalling, mediated by muscarinic and nicotinic AChRs, is indeed involved in regulating MSC function. Targeting both muscarinic and nicotinic AChRs with pharmacological agents may therefore reveal novel mechanisms to tune MSC function and thus their regenerative output. Indeed, there is a plethora of AChRs agonists and antagonists licensed for the treatment of a variety of diseases (Decker, Meyer and Sullivan, 2001; Kruse *et al.*, 2014; Sriram and Insel, 2018; Verma *et al.*, 2018) and these have yet to be explored with regards to their effects on the regenerative potential of MSCs and the possibility of their re-purposing into the regenerative medicine arena. Furthermore, there is more to learn about the metabotropic downstream signalling of mAChRs in MSCs and indeed even if they do play a naturally occurring role in MSC homeostasis or differentiation. It is therefore imperative that more studies are undertaken to investigate the precise functions of AChRs in MSCs.

## 1.3 Dental pulp stem cells (DPSCs)

A number of stem cell populations have been characterised and identified in the oral and maxillofacial region, where collectively they are referred to as dental mesenchymal stem cells (Figure 1-7). In particular, dental pulp stem cells (DPSCs) display impressive properties that make them an ideal candidate for future stem cell-based therapies and not only in the field of dentistry. The following section attempts to give an overview of these cells and their differentiation potential.

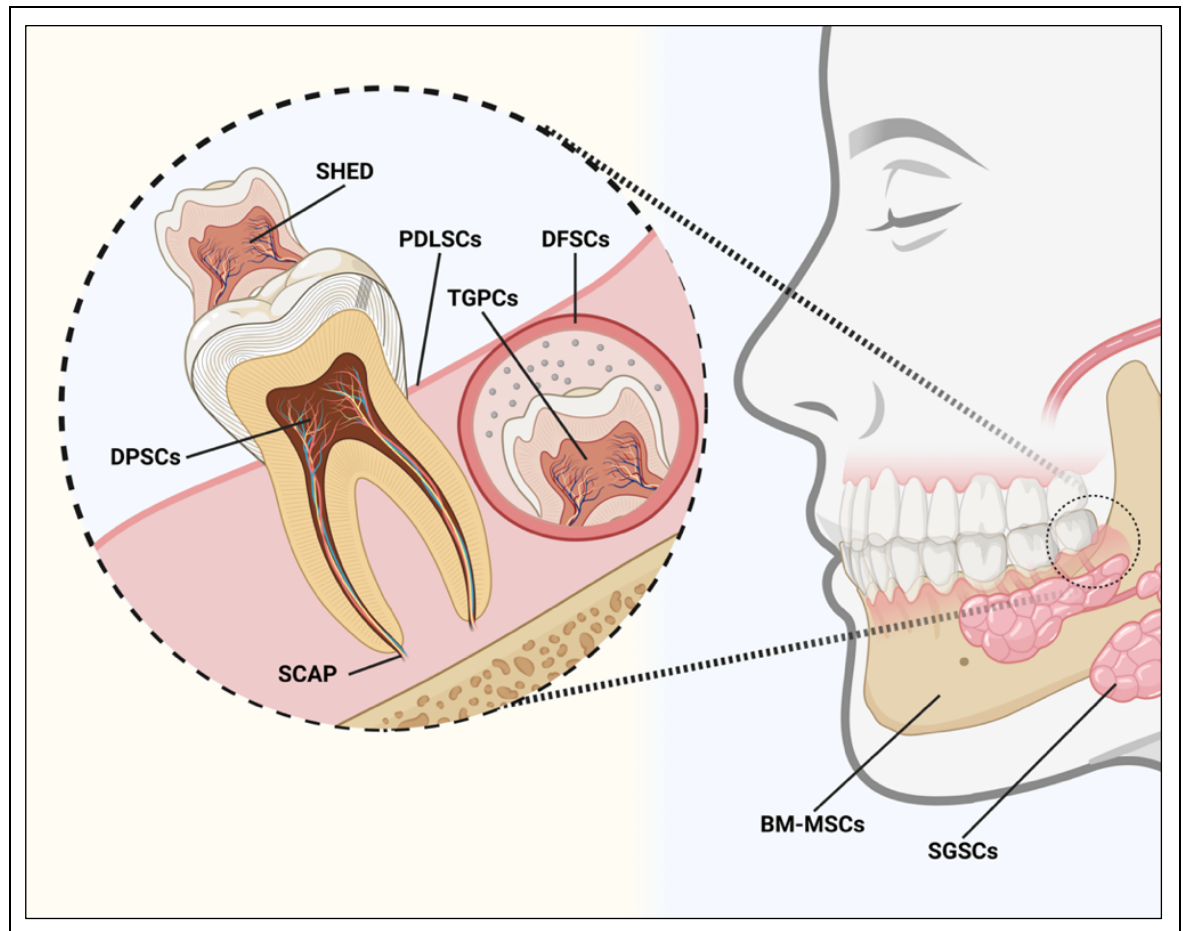


**Figure 1-7 Sources of adult stem cells in the oral and maxillofacial region. BM-MSCs: bone marrow- MSCs from orofacial bone; DPSCs: dental pulp stem cells; SHED: stem cells from human exfoliated deciduous teeth; PDLSCs: periodontal ligament stem cells; DFSCs: dental follicle stem cells; TGPCs: tooth germ progenitor cells; SCAP: stem cells from the apical papilla SGSCs: salivary gland-derived stem cells.**

### 1.3.1 Characteristics and properties of DPSCs

DPSCs were the first population of stem cells isolated and identified from the pulp cavity of adult permanent teeth (Gronthos *et al.*, 2000). These cells are characterised as self-renewing multipotent cells that possess a high level of clonogenicity and proliferation capacity (Gronthos *et al.*, 2002). DPSCs are derived

from the ectodermal layer where they originate from migrating neural crest cells (Chai *et al.*, 2000; Miletich and Sharpe, 2004; Hu, Liu and Wang, 2018). They display mesenchymal like properties in terms of their fibroblast-like morphology, attachment to a plastic surface, *in vitro* ability to form colonies, and multi lineage differentiation potential. (Martens *et al.*, 2013). Indeed, DPSCs have been demonstrated to differentiate into several cell types including odontoblast-like cells (i.e., cells differentiated *in vitro* with phenotypic characteristics of odontoblasts), osteoblasts, adipocytes, neurocytes, chondrocytes, myocytes and chondrocytes *in vitro* and *in vivo* (Zhang *et al.*, 2006; d'Aquino *et al.*, 2007; Carinci *et al.*, 2008; Armiñán *et al.*, 2009). However, there are still hurdles in translating these findings to clinical applications and even in reproducing some of these findings in culture. This is broadly due to difficulties in setting up consistent homogenous primary cell cultures. The following discuss's identity and properties of DPSCs in an attempt to explain discrepancies reported by the literature.

DPSCs possess immunophenotype and immunosuppressive properties that are similar to MSCs. That is expression of several cluster of differentiation markers and negative expression of hematopoietic makers or human leukocyte antigen (HLA). However, there seems to be discrepancies and inconsistencies between studies reporting the immunophenotype of DPSCs (Ledesma-Martínez, Mendoza-Núñez and Santiago-Osorio, 2016) (

Table 1-3). Several arguments have been proposed to the cause of these discrepancies, notably, DPSCs have no exclusive markers to identify them and may even have a different immunophenotype to MSCs (Sonoyama *et al.*, 2006; Espagnolle *et al.*, 2014). Another proposed reason is the presence of other populations of dental stem cells in the pulp which have different biological activities (Ledesma-Martínez, Mendoza-Núñez and Santiago-Osorio, 2016). It has been reported that DPSCs reside within two stem cell niches; the perivascular region and a second niche around the cervical area adjacent to the odontoblastic layer (Martens *et al.*, 2012). Thus, the notion that DPSCs are expected to only express several common markers to identify them as MSCs (Kawashima, 2012). However, what is now accepted is that DPSCs are a heterogeneous population of cells, thus, and this may explain the reported variation of DPSCs characteristics (Kok *et al.*, 2022).

Indeed, Gronthos and co-workers postulated the existence of a hierarchy of progenitor cells in adult dental pulp in which the majority of DPSCs are slow proliferative progenitors, and only a fraction reveal stemness properties of self-renewal and multipotency (Gronthos *et al.*, 2002). This demonstrates that the adult human pulp bears a source of stem and stromal cells, of which only particular subpopulations are capable of superior regenerative properties. Based on this, the current advancements are towards establishing cellular markers to characterise DPSC subpopulations, thus, leading to a better and consistent way of utilising these cells in regenerative applications. The review by (Kok *et al.*, 2022) summarise these markers in identifying DPSCs subpopulations with distinct characteristics and suggests that these subpopulations reside in more stem cell niches than originally reported. What is now known is that a small minority of DPSC subpopulations are high proliferative multipotent cells with self-renewal ability and these arguably maintain the stem cell pool, while the majority of DPSCs are low proliferative cells with limited potency (Alraies *et al.*, 2017; Alaidaroos *et al.*, 2021). When these high proliferative subpopulations of DPSCs are cultured, they display longer telomeres that shorten during expansion, eventually, resulting in the loss of their proliferative and multipotency characteristic (Alraies *et al.*, 2017; Alaidaroos *et al.*, 2021). This arguably is where the majority of low proliferative-limited potency DPSCs originate from and strengthen the notion of a hierarchical arrangement of DPSCs in the pulp. Apart from the hierarchical stages of DPSCs, the mesodermal or neuroectodermal origin of the cells, and their origin

from different stem cell niches, are also factors that determine DPSCs heterogeneity (Huang, Gronthos and Shi, 2009; Pisciotta, Carnevale, *et al.*, 2015). Furthermore, extrinsic factors such as isolation method, culture conditions; and intrinsic factors such as donor age and inner-donor variation, are all suggested to determine DPSCs heterogeneity (for a review see (Nel *et al.*, 2022)). This outlines the importance of distinguishing DPSCs subpopulations to identify which pose the desired traits for prospective regenerative procedures, as even the low proliferative subpopulations, with limited potency, have been suggested to be capable of regeneration of specialised tissues (Kok *et al.*, 2022).

**Table 1-3 Reported variation of human DPSCs phenotype characteristics. The variation in these markers indicate the heterogenous populations isolated and used in DPSCs regenerative studies.**

CD antigen expression		Other representative markers		Reference
Positive	Negative	Positive	Negative	
CD13, CD29, CD44, CD73, CD90, CD146, CD166				(Akpınar et al., 2014)
CD29, CD44, CD63, CD73, CD90, CD166	CD34, CD45			(Suchánek et al., 2010)
CD29, CD73, CD90	CD14, CD45		HLA-DR	(Werle et al., 2016)
CD44, CD73, CD90, CD105	CD14, CD31, CD45		HLA-DR	(Bray et al., 2014)
CD44, CD73, CD90, CD166	CD34, CD45		HLA-DR	(Govindasamy, Abdullah, <i>et al.</i> , 2010)
CD29, CD73, CD90	CD14, CD34, CD45		HLA-DR	(Lindemann et al., 2014)
CD73, CD90, CD105, CD146	CD14, CD34, CD45			(Pivoriūnas et al., 2009)
CD34, CD90	CD45			(Laino et al., 2005)
CD9, CD10, CD44, CD49, CD90, CD105, CD106, CD146		STRO-1		(Lindroos et al., 2008)
CD90, CD105, CD146	CD45			(Shoi et al., 2014)
CD117		Oct3/4, NANOG		(Ishkitiev et al., 2010)
CD34, CD117	CD45			(Yang et al., 2009)
CD29, CD44		STRO-1		(Jo et al., 2007)
CD29, CD34, CD44, CD106, CD146		STRO-1		(Liu et al., 2009)
CD146	CD45, CD73, CD105	STRO-1, NANOG		(Dissanayaka et al., 2011)
		Oct4, NANOG, SSEA-3, TRA-1-60, TRA-1-81		(Kerkis et al., 2006)

One significant property of DPSCs is their immunosuppressive activity. It has been reported that this population of stem cells display an increased immunosuppressive action when compared to BM-MSCs (Pierdomenico *et al.*, 2005). Indeed, DPSCs were reported to express several immunomodulators such as Fas ligand, heme oxygenase-1, hepatic growth factors (HGF), human leukocyte antigen-G5, indoleamine-2, 3-dioxygenase, interleukins-6 and -10, matrix metalloproteinases, nitric oxide, Prostaglandin E2, and transforming growth factor- $\beta$  (Demircan *et al.*, 2011; Tomic *et al.*, 2011; Zhao *et al.*, 2012). Furthermore, activation of the widely present Toll-like receptors (TLRs) across the immune system have been shown to initiate DPSCs immunosuppressive response (Li *et al.*, 2014). In fact, DPSCs express all 10 known human TLRs and are responsive to inflammatory stimuli (El-Sayed, Klingebiel and Dörfer, 2016). DPSCs were also shown to be capable of inducing apoptosis of activated T-cells *in vitro* through Fas ligand (Zhao *et al.*, 2012). Indeed, several lines of evidence showed involvement of DPSCs in the innate and adaptive immune responses (for a review see (Shang, Shao and Ge, 2021). These properties make DPSCs an ideal candidate for procedures that involve host immune reactions.

One noteworthy propriety of DPSCs is their ability to survive cryopreservation. Several studies have shown that these cells maintain their stem cell properties after cryopreservation. Indeed, DPSCs isolation and culture was efficiently achieved from cryopreserved whole teeth (Papaccio *et al.*, 2006; Zhang *et al.*, 2006; Perry *et al.*, 2008). The significance of this is the ability to cryopreserve extracted human teeth, either intact or carious (Louvrier *et al.*, 2018), which are routinely discarded. Thus, offering an unprecedented opportunity of a multipotent stem cell source that can be used in tissue engineering and regeneration applications or research.

### **1.3.2 Isolation and culture of DPSCs**

Studies reporting the multi-differentiation properties of DPSCs (i.e. adipogenic, chondrogenic, neurogenic lineages) identified that the culture conditions and isolation method are important factors in inducing this variation of different populations or lineages (Martens *et al.*, 2013). There are mainly two methods for the isolation of DPSCs, namely, the explant or outgrowth method, and by enzymatic digestion (Gronthos *et al.*, 2000; Spath *et al.*, 2010). The latter was the

method that was used in the initial identification of DPSCs more than a decade ago (Gronthos *et al.*, 2000). In this method, the dental pulp is digested using collagenase or a combination of collagenase and dispase, after which the resulting cell suspension is seeded into culture dishes. The culture contains growth medium, essentially Dulbecco's modified Eagle's medium (DMEM), and may be supplemented with foetal bovine serum (FBS) and nutrient additives. In the DPSC-outgrowth method, the pulp tissue is surgically extracted, sliced into 2-mm<sup>3</sup> pieces, and directly grown in culture dishes containing DMEM, 10% FBS, and occasionally cytokines are added. During the incubation period, multiplication of stem cells occurs with desirable numbers after 2-3 passages. So far, no isolation methods display superiority over the other in terms of clinical applications, proliferative capacity, or karyotypic stability. However, most protocols utilise the enzymatic digestion method, and some groups tuned this method to increase efficiency of the isolation and maintenance process (Kerkis and Caplan, 2011; Jung *et al.*, 2012).

The initial growth of DPSCs on a plastic surface is distinguished by the formation of colonies, which can be sub-cultured usually through various passages as they tend to expand in culture (Bakopoulou *et al.*, 2011). Remarkably, DPSCs were found to retain their plasticity and ability to form mineralised nodules *in vitro* after being grown for long periods. Studies have shown that DPSCs can achieve 60-80 population doublings in different culture medium (Ledesma-Martínez, Mendoza-Núñez and Santiago-Osorio, 2016). However, MSCs in general may lose some biological activities following prolonged expansion, which may induce senescence after 20 to 40 population doublings or passages. Therefore, the number of passages that produce the most favourable *in vivo* effect is of most importance in clinical applications. Whilst the data for DPSCs are limited, MSC clinical trials exploring *ex vivo* expansion reports that the smaller the passage number (e.g. first and second passage) correlates with a better therapeutic response (Choi *et al.*, 2010; von Bahr *et al.*, 2012).

The proliferation rate of MSCs, in general, depends on the composition of the medium and added supplements. Other factors play a major role in culturing MSCs such as: culture substrate area, seeding density, and incubation environment (Carbon dioxide-oxygen concentrations and temperature) (Jung *et al.*, 2012). Although DPSCs would grow under the same culture conditions as MSCs, there are

subtle differences that can affect their expansion rate. For example, oxygen concentration in conventional cell-cultures ranges from 18- 21%, which can be a hyperoxic environment for DPSCs on account that these cells reside in the dental pulp where O<sub>2</sub> concentration ranges from 3-6%. (Mohyeldin, Garzón-Muvdi and Quiñones-Hinojosa, 2010). Indeed, proliferation rate of DPSCs under conventional culture conditions (21% O<sub>2</sub>) were shown to be reduced compared to a lower O<sub>2</sub> concentration (i.e., 3% O<sub>2</sub>) (El Alami et al., 2014). Because of this, DPSCs incubation under conventional cell-culture O<sub>2</sub> concentrations may result in harvesting low yields of viable cells.

Culturing protocols for DPSCs involves the use of growth supplements such as FBS, and albeit this supplement is fairly safe for human therapeutic purposes, the use of non-human supplements is still a matter open to argument in clinical applications (Reinhardt, Stühler and Blümel, 2011). This is also intensified by the unknown FBS composition and its variation between batches. Although, no risks were observed in transplanted DPSCs cultured in serum medium, various methods of serum-free culture were proposed in response to these concerns. For an example, DPSCs grown in a serum-free medium were shown to display no reduction in colony forming ability compared with FBS containing medium and were able to form the desired dentine-like structures (Takeda-Kawaguchi *et al.*, 2014). This highlights the possibility of DPSCs expansion in conditions that are relatively safe for human therapeutic applications without compromising the properties of these cells.

### **1.3.3 Differentiation and applications of DPSCs:**

Most of the current understanding of human DPSCs is derived from animal experiments, where human DPSCs and scaffolds are prepared *in vitro*, and then transplanted *in vivo* in subcutaneous regions or within a tooth body. The literature almost exclusively reports formation of dental tissue-like cells such as: pulp, dentine, or odontoblast like tissue (Ledesma-Martínez, Mendoza-Núñez and Santiago-Osorio, 2016) (Table 1-4). Additionally, other types of tissue generation have been reported when DPSCs are cultured in osteo-inductive conditions such as: mineralised deposits, osteoblasts, and the formation of bone nodules. Furthermore, human orthotopic transplantation studies reported successful bone defect repair and formation of osteocyte-like cells (d'Aquino et al., 2009).



**Table 1-4 Transplantation studies using human DPSCs. Non-human host were immunodeficient animals.**

Host	Results	Reference
Mice	Formation of pulp, dentine, and odontoblast-like tissue.	(Gronthos et al., 2000)
Mice and Swine	Formation of pulp tissue, dentine, and cementum.	(Sonoyama et al., 2006)
Mice	Generation of odontoblast-like cells and a collagen-like matrix. Formation of dentine, pulp-like tissue.	(Wang <i>et al.</i> , 2010)
Mice	Formation of dentine-like tissue.	(Chun et al., 2010)
Mice	Mineralized tissue formation.	(Chen et al., 2012)
Mice	Mineralized tissue formation. Formation of soft pulp-like tissue.	(Yang et al., 2009)
Mice	Formation of dentine-like matrix.	(Sun et al., 2014)
Mice	Differentiation into osteoblasts and odontoblast-like cells.	(Batouli et al., 2003)
Mice	Generation of dentine pulp-like structure.	(Takeda et al., 2008)
Rats	Bone nodule formation.	(Graziano et al., 2008)
Mice	Mineralised tissue formation.	(Ikeda et al., 2009)
Mice	Formation of pulp-like tissue.	(Huang et al., 2008)
Mice	Mineralised tissue formation.	(Demarco et al., 2010)
Mice	Formation of pulp-like structure lined with odontoblast-like cells.	(Lee et al., 2011)
Mice	Generation of pulp-like and periodontal ligament type tissue.	(Lei et al., 2014)
Mice	Mineralised tissue and dentine formation.	(Tran and Doan, 2015)
Human	Formation of bone in the extracted socket and repair of periodontal tissue.	(d'Aquino et al., 2009)
Human	Repair of human mandible bone defects with compact and uniformly vascularized bone.	(Giuliani et al., 2013)

Interestingly, DPSCs were successfully reprogrammed into iPSCs which opens a whole field of applications in regenerative medicine (Yan *et al.*, 2010) Likewise, iPSCs can be reprogrammed from non-dental cells to be applied in dental tissue

regeneration or even generating a whole tooth-like structure (Cai *et al.*, 2013). Outside the scope of pulpal regeneration, DPSCs were successfully able to repair periodontal defects through differentiation and generation of periodontal-like tissue (Khorsand *et al.*, 2013; Hu *et al.*, 2016). Additionally, due to the ability of DPSCs to form mineralised tissue or osteocyte-like cells, they present as ideal candidates for reconstructing alveolar bone defects. The morbidity associated with harvesting BM-MSCs gave greater opportunity for the utilisation of DPSCs in the management of dental bone defects. In fact, DPSCs display a higher proliferation rate, and may have increased mineralisation potential compared to BM-MSC (Alge *et al.*, 2010). Furthermore, DPSCs displayed powerful potential in peripheral nerve repair of facial nerve and inferior alveolar nerve (Sasaki *et al.*, 2011; Ullah *et al.*, 2017).

The DPSCs additionally display powerful regenerative potential outside the scope of dental research. DPSCs can differentiate into neurocytes and possess neural properties as in expression of neuronal markers and exerting neurotrophic factors (Arthur *et al.*, 2008, 2009; Kiraly *et al.*, 2009; Király *et al.*, 2011). In fact, DPSCs are likely to trans-differentiate into functional neurons, since they originate from the neural crest (Arthur *et al.*, 2008, 2009; Kiraly *et al.*, 2009; Király *et al.*, 2011). These properties suggest a powerful potential for DPSCs in guided cell-based therapy for neurological disorders. And while neural stem cells are considered the optimal source in managing these disorders, they present difficulties in harvesting compared to DPSCs (Arthur *et al.*, 2008, 2009; Kiraly *et al.*, 2009; Király *et al.*, 2011). There are now several protocols for neuronal differentiation of DPSCs such as direct transplantation into the animal brain, culture medium treatment using a mixture of neuronal inducing agents, or *in vitro* generation of neurospheres (Arthur *et al.*, 2008, 2009; Kiraly *et al.*, 2009; Király *et al.*, 2011). Other possible applications of DPSCs have emerged from their ability to differentiate into endothelial-like cells. Increased blood vessel markers were noted when DPSCs were cultured with VEGF (Park *et al.*, 2015; Zhu, Dissanayaka and Zhang, 2019). In addition, DPSCs may display endothelial features through formation of capillary-like structures (Janebodin *et al.*, 2013). However, the true nature of this differentiation *in vivo* is still open to dispute, even with DPSC inducing neovascularization in two animal hosts. This may be to do with locating DPSCs near the newly regenerated capillaries instead of incorporation within the blood vessel wall (Gandia *et al.*, 2008; Nakashima, Iohara and Sugiyama, 2009).

Nevertheless, the multidifferentiation capabilities of DPSCs have made them applicable in several medicinal fields, and the literature is evermore growing to the possibilities offered by these cells (Table 1-5).

**Table 1-5 Non-dental therapeutic applications of DPSCs.**

Applications	Reference
Corneal epithelium regeneration	(Syed-Picard et al., 2015; Kushnerev et al., 2016)
Central nervous system (CNS) injuries	(Király <i>et al.</i> , 2011; Sakai <i>et al.</i> , 2012; Nicola <i>et al.</i> , 2016; C. Yang <i>et al.</i> , 2017)
Craniofacial bone defects	(de Mendonça Costa et al., 2008; Chamieh et al., 2016)
Brain ischaemia (stroke)	(Yang et al., 2009; Sugiyama et al., 2011; Leong et al., 2012)
Liver fibrosis	(Ishkitiev et al., 2012)
Myocardial infarction (MI)	(Gandia et al., 2008)
Duchene muscular dystrophy (DMD)	(Pisciotta, Riccio, <i>et al.</i> , 2015)
Acute renal failure (ARF)	(Barros et al., 2015)
Diabetes	(V Govindasamy <i>et al.</i> , 2011; Carnevale <i>et al.</i> , 2013)
Parkinson's disease (PD)	(Gnanasegaran et al., 2017)

### 1.3.4 Limitation and barriers in DPSCs utilisations

Heterogenicity of DPSCs constitute as the main influence in the lack of consensus between studies that investigate the regenerative potential of these cells. This is also further amplified once *in vitro* results are attempted *in vivo* or in clinical application. Inconsistency in the differentiation potential and dentine formation has been observed between in *in vitro* and *in vivo* studies (Gronthos *et al.*, 2002; Nakashima *et al.*, 2017; Min *et al.*, 2021). Indeed, the contrast in reported differentiation potential and regenerative output of DPSCs stand as the main limitation in translating research to clinical applications. There is even a debate on the current markers used to identify DPSCs. Furthermore, the expression of the widely used surface markers is affected by several factors relating to culture conditions (Alraies *et al.*, 2017; Noda *et al.*, 2019; Qu *et al.*, 2020). This only highlights the numerous factors that influence the regenerative potential of harvested DPSCs. Indeed, factors involved in the isolation of DPSCs also need to be considered. To name a few, the donor age and health, the integrity or status

of the pulp, and variability between the donors. (Sun *et al.*, 2014; Wu *et al.*, 2015; Pagella *et al.*, 2021)

Among the barriers in DPSC utilisation is the number of cells needed for a regenerative clinical procedure. As discussed above, the high proliferative multipotent subpopulations with self-renewal ability constitute the minority of DPSCs isolated from the pulp. This, combined with the fact that DPSC diverse subpopulations represent only a fraction of the total cells within the pulp, make it more challenging in harvesting multipotent stem cells. Furthermore, *ex vivo* expansion of multipotent DPSC subpopulations is met with difficulties confounded in limited population doublings before senescence and the loss of differentiation potential as doublings increase (Kobayashi *et al.*, 2020). All of the above demonstrate the required efforts needed to expand the necessary amounts and right type of population for cell-based therapies.

Nevertheless, research is evermore growing to better understand the identity of the cells, their origin, and the subpopulations required for different regenerative characteristics. Indeed, the future holds promise with respect to identifying markers specific to DPSCs or subpopulations capable of superior regenerative characteristics. For example, Single-cell Raman spectroscopy (SCRM) is a technology that has been used to identify DPSC subpopulations (Alraies *et al.*, 2019). This non-invasive technique offers the ability to *in situ* identify DPSCs subpopulations with contrasting regenerative characteristics.

## 1.4 Summary

In this chapter, the non-neuronal cholinergic system has been presented in which the signalling of this system occurs in cells that are independent from the classic neuronal system. This system is largely based on ACh and its receptors; muscarinic and nicotinic (m and n-AChRs). Both m and n-AChRs are further divided into several subtypes or units. Each family of the AChRs has a specialised function independent from the other, and thus can initiate different and diverse signalling cascades that ultimately control cellular homeostasis. The mAChRs are the metabotropic receptors of ACh, which once stimulated start a chain of events triggering multiple cellular pathways. These receptors are coupled to G proteins that will eventually determine cellular response through sets of downstream signalling events. The mAChR- G protein interplay functions in a way that the

receptor acts as a vessel for the ligand and determines the binding selectivity. The coupled G proteins, depending on the ligand and coupling efficiency, trigger a selected downstream effector and second messenger that ultimately results in a cellular response. Based on this pattern of signalling, mAChRs are divided into a stimulatory group (M1, M3, and M5 mAChRs) and an inhibitory group (M2 and M4 mAChRs). There is sufficient evidence showing AChRs, including the mAChRs, modulate cellular function in non-neuronal cells. In this chapter detailed information about MSCs has been provided showing expression of functional AChRs. Indeed, AChR expression in MSCs is dynamic, dependent on the type of MSCs, and can be individually based on donor or differentiation lineage. The presented findings show involvement of major pathways in modulating MSCs regenerative potential. This suggests that AChRs may present as a promising therapeutic target to control the regenerative potential of MSCs. The DPSCs are a group of stem cells that share similar characteristics with MSCs. However, DPSCs are multipotent stem cells that are easily isolated with less morbidity compared with some MSCs. Moreover, DPSCs display powerful regenerative potential and properties that are even greater compared to well-known MSCs. For this, DPSCs are gaining more traction in medicinal regenerative applications. There is limited evidence of expression of functional AChRs in DPSCs, thus, it is worthy to explore novel pathways that could potentially be tuned from a regenerative perspective.

## 1.5 Project hypothesis and aims

The idea to characterise AChRs expression and their role in DPSCs behaviour and function is based on current reported literature. Non-neuronal ACh is a powerful multifunctional cyto-transmitter involved in numerous cellular processes including modulating gene expression, cellular proliferation, cytoskeletal organization, cell-cell contact. In addition, receptors of this cyto-transmitter are expressed in a number of stem cell populations, including MSCs. The findings of aforementioned MSC studies present evidence of AChRs regulating cell proliferation, survival and migration. Taking all of this into consideration, and the shared characteristics of DPSCs with MSCs, it is hypothesised that DPSCs might express AChR(s), among which are receptor(s) that play a key role in DPSCs regenerative potential.

The aims of this project were: (1) investigate the expression of AChRs in DPSCs, (2) confirm functional expression of AChRs, and (3) dissect the effect of the most predominately expressed AChR on DPSCs function.

## **2 Expression Of Acetylcholine Receptors In Dental Pulp Stem Cells And Methodology Development**

## 2.1 Introduction

The presence and function of AChRs have been characterized in several non-neuronal human cells, and there are multiple published reviews describing their role (Wessler, Kirkpatrick and Racké, 1998; Wessler, Kilbinger, *et al.*, 2001; Kawashima and Fujii, 2008; Wessler and Kirkpatrick, 2008). Moreover, the presence of functional AChRs have been described in stem cell populations, including MSCs. However, studies that investigate the role of AChRs in modulating MSCs regenerative potential are scarce. It is known that MSCs express functional AChRs that can be attuned to control these cells' regenerative characteristics (Danielyan *et al.*, 2009; Hoogduijn, Cheng and Genever, 2009; Piovesana *et al.*, 2018; Pernarella *et al.*, 2020). DPSCs are stem cells capable of multipotent differentiation which share similar properties to MSCs and can be easily isolated and cultured. DPSCs, especially ones isolated from intact teeth, have been popular in the development of cell-based regenerative therapies from a dental origin (Kok *et al.*, 2022). This might be due to the number of studies involving DPSCs compared to the other dental driven stem cells, or the controlled environment from which these cells have been harvested (e.g., uninfamed intact pulp of teeth extracted for elective procedures). Thus, DPSCs can be considered an excellent alternative to study AChRs function and be used to develop methods to determine how activation of AChRs can modulate the regenerative output of stem cells.

At present, only one study suggested expression of AChRs in DPSCs. The study suggests that DPSCs express the  $\alpha 7$ nAChR (Wang *et al.*, 2017). The data were obtained using stem cells that were extracted from deciduous (i.e., stem cells from human exfoliated deciduous teeth (SHED)) and adult teeth (i.e., DPSCs), thus, it is unclear which group of stem cells expressed the  $\alpha 7$ nAChR. The authors suggest involvement of the  $\alpha 7$ nAChR in modulating osteoclastogenesis resulting in deciduous teeth root resorption. In human dental pulp residing cells (i.e. cell such as DPSCs, odontoblasts, endothelial cells, immune cells, and neurons), expression of nAChRs was detected (Yanagita *et al.*, 2008). The authors report that nicotine, presumably via nAChRs, suppresses the cytodifferentiation and mineralisation of isolated pulpal cells. However, the study did not report characterisation of the cell type that is positive for the expressed nAChRs. In a another study it was reported that  $\alpha 7$ nAChR expression changes during development, suggesting

functional pleiotropy in the tooth developmental process (Rogers and Gahring, 2012).

In dental pulp tissue, the presence mAChRs has also been detected. Interestingly, mAChRs expression in pulpitis differ to healthy pulp (Sterin-Borda *et al.*, 2011). It is suggested that progressive inflammation of the pulp caused drastic changes in the expression pattern of mAChR subtypes. In particular, the M1 and M3 mAChR subtypes expression levels fluctuated between inflamed and healthy pulps. Other studies report the presence of functional mAChRs in dental pulp (Yu *et al.*, 2001; Borda *et al.*, 2007; De Couto *et al.*, 2009; De Couto Pita *et al.*, 2009), however, scarce evidence exist about the role of these receptors in modulating tissue repair or proliferation and differentiation of the pulp tissue or cells. Furthermore, there is currently no available evidence of the presence of mAChRs in DPSCs. Thus, a non-neuronal cholinergic signalling pathway is still to be investigated and determined whether it affects DPSCs potential in regeneration.

In this chapter, the aim is to investigate expression of AChRs and development of methodologies that will assist in subsequent investigations of the role of AChRs on DPSCs function.

## 2.2 Materials and Methods

### 2.2.1 Cells and cell culture

Human DPSCs, isolated from extracted adult third molars of a 17 year old male donor, were supplied by Lonza (h-DPSCs, PT-5025, Lonza Inc, UK) and cultured according to the supplier's instructions. Briefly, DPSCs were seeded in 75-cm<sup>2</sup> flasks at 5,000-6,000 cells/cm<sup>2</sup>. The supplier claim expression of stemness markers such as: CD105, CD166, CD29, CD90, and CD73, and negative expression of hematopoietic stem cells markers such as: CD34, CD45, and CD133. Thus, fulfilling the international society of cellular therapy criteria to define stem cells as MSCs. Furthermore, supplied DPSCs are guaranteed these properties up to ten population doublings. Originally the supplier's medium (BulletKit™ Medium, PT-3005, Lonza Inc, UK) was used to generate several stock cryovials. Subsequently, medium was changed to Knock-out Dulbecco's modified Eagle's medium (DMEM-KO™ Media, Gibco, 10829-018) supplemented with 10% foetal bovine serum, 200 mM L-Glutamine (Sigma, G7513), and 5% Penicillin-Streptomycin solution (Gibco, 15140). This is based on findings that showed optimal conditions for this population of stem cells when grown with DMEM-KO (Rodas-Junco and Villicaña, 2017). Medium was refreshed every three days, and when flasks were approximately 90% confluent, cells were passaged by detaching with trypsin-EDTA (Gibco™, 11560626, 0.025%). Cultures were maintained at sub-confluent levels at 37 °C in a humidified atmosphere with 5% CO<sub>2</sub>. The DPSCs that were used for the following experiments are between passages four and six. Cell growth and expression of stemness gene markers such as: *THY1*, *ENG*, and *PTPRC* (CD90, CD105, and CD45) (Table 2-1) were evaluated after switching culture media to ensure no deleterious effects on DPSC stemness properties

#### 2.2.1.1 Development of osteogenic differentiation protocol

To establish osteogenic differentiation capabilities, DPSCs were seeded in 24-well plates and cultured in complete culture medium (DMEM-KO) at a seeding density of 1X10<sup>4</sup> per well. When cells reached 85-90% confluence (48-72 hrs), medium was changed to induction medium which was composed of regular culture medium (DMEM-KO) supplemented with: 100 nM dexamethasone (D4902, Sigma-Aldrich), 50 µM ascorbic acid-2-phosphate (A4403, Sigma-Aldrich), and 10 mM β-

glycerophosphate (G9422, Sigma-Aldrich). Plates were then incubated at 37°C 5% CO<sub>2</sub> for 7, 14, 21, and 28 days and media changed twice per week. At each time point, total RNA was isolated from the adherent cells to investigate osteogenesis gene markers (Table 2-1). Moreover, cells were subjected to Alizarin Red and Von Kossa (Sigma-Aldrich) staining to detect the formation of mineralised nodules.

For the Alizarin red staining, cells were stained at each time point of the osteogenic experiment as previously described (Gregory et al., 2004). Briefly, cells were washed three times with PBS and fixed with 4% paraformaldehyde in PBS and incubated at 37°C 5% CO<sub>2</sub> for 30 min. Subsequently, cells were washed three times with distilled water (dH<sub>2</sub>O), then stained with Alizarin red S (40 mmol/L, pH 4.2, Sigma-Aldrich) and incubated on a shaker for 1 h at room temperature (RT). The staining agent was then discarded, and the cells were washed three times with dH<sub>2</sub>O with an extended 1 mL PBS wash for ten min. Plates were tilted to facilitate removal of excess liquid and placed on a light box to acquire images. Images were taken using a 16-megapixel (77-degree) lens camera (Samsung ST200F) with no resolution less than 4,032 x 1,908 pixels. Plates were stored at -20°C prior to dye extraction. To quantify the formation of the stained calcium nodules, 200 µL of 10% acetic acid was added to each well and the plate was shaken for 30 min. The cells were then scraped off the plate and transferred to an Eppendorf tube. After vortexing, the stained cells were heated to 85°C in a water bath incubator for ten min and then transferred to ice for five min. The stained cells were centrifuged at 15,000 g for 15 min, and the supernatant was transferred to a new tube. To neutralize the acetic acid solution, 100 µL of 10% ammonium hydroxide was added into the tube and mixed by pipetting. Finally, 50 µL of the mixture was transferred to a 96-well plate for reading on a spectrophotometer (FLUOstar Omega microplate reader) at 405 nm.

For the Von Kossa stain, cells were washed and fixed in the same manner described for the Alizarin red stain above. Subsequently, cells were washed three times with PBS and 200 µL of silver nitrate (Silver plating kit, 100362, Sigma-Aldrich) was added to each well. Plates were exposed to ultraviolet light (Ultraviolet Crosslinker, uvc-508) for 30 min, then rinsed three times with dH<sub>2</sub>O. The reaction was terminated by the addition of 200 µL sodium thiosulfate (Silver plating kit, Sigma-Aldrich) and incubated for ten min at RT. Finally, cells were washed three times with dH<sub>2</sub>O. Images were taken using the same method above.

## **2.2.2 Transcript expression**

### **2.2.2.1 Ribonucleic acid (RNA) Extraction**

Total RNA was extracted using an RNA isolation kit (RNeasy Mini Kit, 74104 Qiagen, UK) following the manufacturer's protocol. Briefly, 350 µL of sample in the RLT buffer was disrupted by vortexing for 30 sec. Then 350 µL of 70% ethanol was mixed with the lysate, transferred into a RNeasy Mini spin column, and centrifuged for 15 sec at 10,000 rpm and the resultant flow-through was discarded. Then 350 µL of RW1 buffer was added to the column, centrifuged for 15 sec at 10,000 rpm, and flow-through was discarded. To ensure the extracted RNA was free from DNA contamination, a DNase digestion kit was used, as per manufacturer's instructions (RNase-Free DNase Set, 79254, Qiagen, UK). This was performed by adding 350 µL of RW1 buffer, centrifugation for 15 sec at 10,000 rpm, and discarding the flow-through. Next, 80 µL of the DNase mix (10 µL DNase I stock solution and 70 µL RDD Buffer) was added on to the column and then incubated at RT for 15 min. After incubation, the columns were washed again with 350 µL of RW1 buffer by centrifugation for 15 sec at 10,000 rpm and the flow-through was discarded. Subsequently, 500 µL of RPE buffer was added and the column centrifuged for 15 sec at 10,000 rpm, and the flow-through was discarded. Next, 500 µL of RPE buffer was added and the column centrifuged for two min at 10,000 rpm, and the flow-through was discarded. The RNeasy Mini column was then transferred into a new collection tube and centrifuged for one minute at full speed (14,000 rpm) to dry the membrane. Finally, 30 µL RNase-free H<sub>2</sub>O was added to the column which was centrifuged for one minute at 10,000 rpm. To ensure the maximum RNA concentration was achieved, the eluted RNA was then passed through the membrane once more as described above.

### **2.2.2.2 Ribonucleic acid (RNA) quantification**

Quantification of sample concentration and integrity was performed according to the Spectrophotometer program instructions RNA-40 Nucleic Acids (NanoDrop-1000, Thermofisher). Briefly, one µL of above RNA elute for each sample was read and the concentrations were recorded in ng/µL. Samples with a 260/280 nm ratio of 1.8 to 2.2 were deemed to be of high quality and were used for subsequent reverse transcription.

### 2.2.2.3 Reverse Transcription into complementary deoxyribonucleic acid (cDNA)

To ensure equal amount of cDNA synthesis across all, samples were standardised to the lowest sample's RNA yield. The reverse transcription into cDNA was performed according to the manufacturer's protocol (High-Capacity cDNA Reverse Transcription Kit, 4368814, Applied Biosystems™ UK). Briefly, ten µL of the standardised RNA sample was added to ten µL of the High-Capacity RNA-to-cDNA™ reverse transcription master-mix. A reverse transcriptase negative control was also prepared using a master-mix which did not contain the reverse transcriptase enzyme. Samples were briefly centrifuged to remove any air bubbles and loaded on to the thermal cycler (Primus 96 Thermal Cycler, MWG Biotech Inc). Finally, reverse transcription was performed by incubating at 25 °C for ten min, followed by 37 °C for 120 min, then 85 °C for five min, and finally 4 °C until samples were stored for analysis.

### 2.2.2.4 Polymerase chain reaction (PCR) and quantitative (q-PCR) analysis

Primer sequences for gene expression investigated in this chapter are provided in Table 2-1 (cholinergic primers were adapted from (Weist *et al.*, 2018)). Target gene primers and the prepared cDNA samples were mixed with the fast SYBR Green Master Mix (Fast SYBR™ Green Master Mix 4385610, Applied Biosystems™, UK) following manufacturer's instructions. Briefly, five µL of the cDNA sample was added to two µL of the investigated gene primers (forward and reverse) and all were mixed with ten µL of the fast SYBR Green Master Mix. The mixture final volume of 20 µL was made up using RNase-free H<sub>2</sub>O. Negative reverse transcriptase controls and no template controls (i.e., cDNA replaced by RNase-free H<sub>2</sub>O) were also included. All were then loaded into a 96-well plate (MicroAmp™ Fast Optical 96-Well Reaction Plate, 4346907, Applied Biosystems), sealed, and centrifuged for two min at 4500 rpm. Then, plates were loaded on to a q-PCR machine (StepOnePlus™ Real-Time PCR System, Applied Biosystems). Finally, the PCR reaction was performed under the following conditions: two-minutes polymerase activation step at 95 °C, followed by 40 cycles at 95 °C for five sec and 60 °C for 30 s, with and without a melt curve cycle at 65-95 °C (0.5 °C increments) for five sec/step.

For cholinergic genes (i.e., ACh receptors, synthesis, transportation, and degradation genes), twenty-five microliters of each PCR products were analysed by electrophoresis in 2% (w/v) agarose gels with 0.5 mg/mL ethidium bromide. 100 bp markers (New England Biolabs, N3231) were used for size estimation. Electrophoresis run for one hour at 100 volts, and images were acquired using a BIO-RAD GEL DOC XR (Bio-Rad Molecular Imager Gel Doc XR+, 1708195).

For q-PCR, each sample was analysed in duplicate, and expression of the genes of interest were normalised to the housekeeping gene GAPDH. For control versus treated experiments, relative expression was quantified using the  $2^{-\Delta\Delta Ct}$  method (Livak and Schmittgen, 2001). For estimating relative abundance of a gene transcript, delta CT value were calculated as previously described (Czechowski *et al.*, 2004; Linardou *et al.*, 2012). The distribution of normalized mRNA expression of investigated genes is described as  $40 - \Delta CT$  values (40 is the total number of PCR cycles in a run, CT is cycle threshold value, and  $\Delta CT$  is the CT value of housekeeping gene (*GAPDH*) subtracted by target gene).

**Table 2-1 Primer sequences for genes investigated in chapter 2.**

Primer	Sequence
<i>ACHE-R, E</i>	Fwd: CGGGTCTACGCCTACGTCTTTGAACACCGTGCTTC Rev: ATGGGTGAAGCCTGGGCAGGTG
<i>ACHE-S</i>	Fwd: CGGGTCTACGCCTACGTCTTTGAACACCGTGCTTC Rev: CACAGGTCTGAGCAGCGATCCTGCTTGCTG
<i>ALP</i>	Fwd: ATGAAGGAAAAGCCAAGCAG Rev: CCACCAAATGTGAAGACGTG
<i>BCHE</i>	Fwd: AGACTGGGTAGATGATCAGAGACCTGAAAACCTACCG Rev: GACAGGCCAGCTTGTGCTATTGTTCTGAGTCTCAT
<i>BGLAP</i>	Fwd: CGCTACCTGTATCAATGGCTGG Rev: CTCCTGAAAGCCGATGTGGTCA
<i>BMP2</i>	Fwd: GCTAGTAACTTTTGGCCATGATG Rev: GCGTTTCCGCTGTTTGTGTT
<i>CHAT</i>	Fwd: GGAGATGTTCTGCTGCTATG Rev: GGAGGTGAAACCTAGTGGCA
<i>CHRM1</i>	Fwd: AGACGCCAGGCAAAGGGGGTGG Rev: CACGGGGCTTCTGGCCCTTGCC
<i>CHRM2</i>	Fwd: ACAAGAAGGAGCCTGTTGCCAACC

	Rev: CAATCTTGCGGGCTACAATATTCTG
<i>CHRM3</i>	Fwd: GACAGAAAACCTTTGTCCACCCAC Rev: AGAAGTCTTAGCTGTGTCCACGGC
<i>CHRM4</i>	Fwd: TCCTCAAGAGCCCACTAATGAAGC Rev: TTCTTGCGCACCTGGTTGCGAGC
<i>CHRM5</i>	Fwd: CTCACCACCTGTAGCAGCTACCC Rev: CTCTCTTTCGTTTGGTCATTTGATG
<i>CHRNA1</i>	Fwd: GCGGCAGAGTGGAAGTA Rev: CCCTAGTGGTCTCGTGGTT
<i>CHRNA2</i>	Fwd: TCACCCTGTCCATCGTCAT Rev: ACTTCCAGTCCTCCTTCACC
<i>CHRNA3</i>	Fwd: CCATGTCTCAGCTGGTG Rev: GTCCTTGAGGTTTATGGA
<i>CHRNA4</i>	Fwd: TGGGTACGCAGGGTCTTCC Rev: GCTCAGCCGGCACATCCA
<i>CHRNA5</i>	Fwd: CCATCATCTTCAAAAGTCATA Rev: CCCATTTATAAATAACAGGAAC
<i>CHRNA6</i>	Fwd: TGGGAAAACAGTGAATGGGAAATC Rev: GGTTGGGGTGCGGTAGTGTATG
<i>CHRNA7</i>	Fwd: CGCCACATTCCACACTAAC Rev: ACCTTTCACCTCCTTGGCC
<i>CHRNA9</i>	Fwd: CTACAATGGCAATCAGGTGG Rev: ATGATGGTCAACGCAGTGG
<i>CHRNA10</i>	Fwd: TCTCAAGCTGTTCCGTGACC Rev: AAGGCTGCTACATCCACGC
<i>CHRNB1</i>	Fwd: CCGCCGCAAGCCTCTCTTCT Rev: GCCCGGTTTGGACCATCGAT
<i>CHRNB2</i>	Fwd: CAGCTCATCAGTGTGCA Rev: GTGCGGTCGTAGGTCCA
<i>CHRNB3</i>	Fwd: TCATCCCCAGAGAAAGAGG Rev: TGTACTACCTGGCTGATAAAATGT
<i>CHRNB4</i>	Fwd: CTGAAACAGGAATGGACT Rev: CCATGTCTATCTCCGTGT
<i>CHRNA10</i>	Fwd: GGCCTCACACTCTCCAACC Rev: GGGTGATCTCTTTGGCCGTAT
<i>CHRNE</i>	Fwd: GAACTGCGTCTTTATCACCA Rev: TACGTCTGAGAGCGGAAAATA
<i>CHRNA10</i>	Fwd: GGTGGCCCTCTACTGCAA

	Rev: TTCTGTAGCCGGGACTGG
<i>COL1A1</i>	Fwd: CCATGTGAAATTGTCTCCCA Rev: GGGGCAAGACAGTGATTGAA
<i>ENG</i>	Fwd: CCACTAGCCAGGTCTCGAAG Rev: GATGCAGGAAGACACTGCTG
<i>GAPDH</i>	Fwd: GCAGGGGGGAGCCAAAAGGG Rev: TGCCAGCCCCAGCGTCAAAG
<i>IBSP</i>	Fwd: GGCAGTAGTGACTCATCCGAAG Rev: GAAAGTGTGGTATTCTCAGCCTC
<i>PTPRC</i>	Fwd: CTTCAGTGGTCCCATTGTGGTG Rev: CCACTTTGTTCTCGGCTTCCAG
<i>RUNX2</i>	Fwd: GGTCAGATGCAGGCGGCCC Rev: TACGTGTGGTAGCGCGTGGC
<i>SLC18A3</i>	Fwd: TACCCTACGGAGAGCGAAGA Rev: CTGTAGAGGCGAACATGACG
<i>SPP1</i>	Fwd: GAAGTTTCGCAGACCTGACAT Rev: GTATGCACCATTCAACTCCTCG
<i>Thy1</i>	Fwd: GAAGGTCCTCTACTTATCCGCC Rev: TGATGCCCTCACACTTGACCAG

## 2.2.3 Screening of functional acetylcholine receptors

### 2.2.3.1 Proliferation assessment via methylthiazol tetrazolium (MTT) assay

To assess functionality of detected AChRs, DPSCs proliferation was assessed in response to stimulation by commercially available AChRs agonists and antagonists (Table 2-2). Briefly, cells were seeded into 96-well plates at a density of  $1 \times 10^4$  cells/well and were grown in regular media (DMEM-KO). After allowing the cells to adhere overnight, they were treated with a serial dilution of AChRs agonists and antagonists. Consensus in literature when using cholinergic stimulus is in the range of  $\mu\text{M}$  for agonists and  $\text{nM}$  for antagonists, thus, a ten-fold serial dilution of was prepared accordingly. After 72 h, viable cell numbers were assessed using a colorimetric assay based on 3-(4,5-dimethyl thiazol 2-y1) -2,5-diphenyl tetrazolium bromide (0.5 mg/mL MTT, M2128, Sigma-Aldrich). For each well, medium was replaced with 100  $\mu\text{L}$  MTT solution (0.5 mg/mL diluted in PBS) and incubated for 4 h at  $37^\circ\text{C}$  and 5%  $\text{CO}_2$ . Subsequently, the dye was replaced

with 100  $\mu$ L of dimethyl sulfoxide (DMSO, D8418, Sigma-Aldrich) per well and further incubated for one hour at 37°C and 5% CO<sub>2</sub>. Finally, plates were shaken at 250 rpm for five min and optical density readings were performed on a microplate reader (FLUOstar Omega microplate reader) at 545 nm (measurement wavelength) and 650 nm (reference wavelength).

**Table 2-2 Commercially available Acetylcholine receptors agonists and antagonists. In this study, a ten-fold serial dilution in the range of  $\mu$ M for agonists and nM for antagonists was prepared.**

Name (supplier, catalogue number)	Advertised effect	Concentration used in this study
Acetylcholine chloride (ACh) (Sigma-Aldrich, A6625)	Non-selective agonists that act on both the n- and mAChRs	0.1, 1, 10, 50, 100 $\mu$ M
Carbamoylcholine chloride (CCH) (Tocris, 2810)	Cholinergic receptor agonist that acts on both the n- and mAChRs	0.1, 1, 10, 50, 100 $\mu$ M
Muscarine chloride hydrate (MCH) (Sigma-Aldrich, M104)	General mAChRs agonist	0.1, 1, 10, 50, 100 $\mu$ M
Pilocarpine hydrochloride (PHCl) (Tocris, 0694)	General mAChRs agonist	0.1, 1, 10, 50, 100 $\mu$ M
Nicotine detartrate (Nic) (Sigma-Aldrich, N0590200)	General nAChRs agonist	0.1, 1, 10, 50, 100 $\mu$ M
Atropine (ATR) (Sigma-Aldrich, A0132)	Potent, competitive, non-selective mAChRs antagonist	1, 10, 100, 1000 nM
McN-A 343 (McN) (Sigma-Aldrich, C7041)	M1 > M2 mAChRs agonist	0.1, 1, 10, 50, 100 $\mu$ M
Arecaidine propargyl ester hydrobromide (APE) (Sigma-Aldrich, A140)	Potent mAChRs agonist exhibiting selectivity for M2	0.1, 1, 10, 50, 100 $\mu$ M
Pirenzepine (PZ) (Sigma-Aldrich, P7412)	Selective M1 antagonist	1, 10, 100, 1000 nM
Methoctramine (Meth) (Sigma-Aldrich, M105)	Selective M2 antagonist at nM concentrations	1, 10, 100, 1000 nM
4-DAMP (Sigma-Aldrich, SML0255)	M3 antagonist	1, 10, 100, 1000 nM
A-85380 dihydrochloride (Tocris, 5017)	High affinity and selective agonist for $\alpha$ 4 $\beta$ 2nAChR	0.1, 1, 10, 50, 100 $\mu$ M
SIB 1508Y maleate (SIB) (Tocris, 4766)	High affinity agonist for $\alpha$ 4 $\beta$ 2nAChRs	
Dihydro- $\beta$ -erythroidine hydrobromide (DhBE) (Tocris, 2349)	$\alpha$ 4 $\beta$ 2nAChR antagonist	1, 10, 100, 1000 nM
AR-R 17779 (ARR) (Abcam, ab142817)	Selective agonist for $\alpha$ 7nAChRs	0.1, 1, 10, 50, 100 $\mu$ M

$\alpha$ -Bungarotoxin ( $\alpha$ -Bun) (Tocris, 2133)	nAChRs selective antagonist for $\alpha 7$ receptors	1, 10, 100, 1000 nM
--	--	---------------------

---

### 2.2.3.2 Pharmacological competition assays

Pharmacological competitions to determine agonists selectivity were carried out. This was done by pre-treating cells with a specific subtype AChR antagonists 2 hours prior to adding the agonist in accordance with literature (Piovesana,2018, Jakubik et al,2014, Alessandrini et al,2015). For agonists, a final concentration of 100  $\mu$ M was used and 0.01  $\mu$ M was used for antagonists. Untreated cells that received normal media were utilised as controls. Treatments were carried out for 72 h and cell growth was assessed using the MTT assay as described above.

## 2.2.4 Protein expression

### 2.2.4.1 Immunofluorescence

The DPSCs were plated on glass coverslips in a 24-well plate at a seeding density of  $1 \times 10^5$  cells/well in complete medium (DMEM-KO) and allowed to adhere overnight. The following day, cells were washed with phosphate-buffered saline (PBS) twice and fixed with 4% paraformaldehyde in PBS for 15 min at RT. The cells were subjected to three washes in PBS with 0.1% Tween 20 (TPBS), permeabilized with 0.1% Triton™ X-100 for 15 minutes, and incubated in TPBS solution containing 1% Bovine Serum Albumin (BSA) for one hour at RT. The cells were then washed with TPBS and incubated with a Rabbit monoclonal M2 antibody (1:1000, ab109226, Abcam UK), a Rabbit polyclonal M3 antibody (1:1000, ab126168, Abcam UK), and a Rabbit polyclonal M5 antibody (1:1000, ab186830, Abcam UK), all diluted in 1% BSA-PBS solution at 4 °C overnight. The next day, the cells were washed with TPBS three times for a total of 15 min. After washes, cells were incubated with a Goat Anti-Rabbit secondary antibody (1:1000, Goat anti-Rabbit IgG (H+L) Alexa Fluor™ 647, A-21245, Invitrogen) diluted in 1% BSA in PBS for one hour in the dark at RT. After three washes in TPBS, cells were then stained with Alexa Fluor 488 phalloidin (1:1000, Alexa Fluor™ 488, A12379, Invitrogen) for 30 minutes at RT for labelling of actin filaments. After three washes in TPBS, coverslips were moved on to glass slides and mounted with VECTASHIELD Antifade mounting medium with DAPI (4',6-diamidino-2-phenylindole) mounting medium.

Images were captured using an EVOS FL digital inverted microscope (EVOS FL Cell Imaging System, Thermo Scientific) equipped with a monochrome camera and a 40x phase objective. Images for two-channel merges were created by the built-in microscope software.

#### **2.2.4.2 Western blot**

Proteins were extracted from DPSCs that were seeded in a 75-cm<sup>2</sup> flasks after five days in their normal culture. A cell lysate was prepared according to supplier's instruction. Briefly, after centrifugation, cells were resuspended in ice-cold PBS and centrifuged for five min at 1200 rpm. Supernatant was then discarded, and cells were resuspended in 1ml ice cold RIPA buffer (50 mM Tris-HCl (pH 8.0), 150 mM sodium chloride, 0.1% Triton X-100, 0.5% sodium deoxycholate, 0.1% sodium dodecyl sulphate) supplemented with protease inhibitor cocktail (cOmplete™ ULTRA Tablets, Roche, 5892970001, Sigma-Aldrich UK). Cells were then incubated on ice for 20 min, followed by 20 min centrifugation at 12,000 rpm, at 4 °C. Protein content in cleared supernatant lysate was then quantified via a bicinchoninic acid assay (BCA) kit according to supplier's instructions (Pierce™ BCA Protein Assay Kit, 23225, Thermo Scientific™).

For the electrophoresis step, a Mini Gel Tank and Blot Module set was used to run and blot the gels (NW2000, Invitrogen™ UK) according to the manufacturer's instructions. First, protein samples (standardised to 30 µg/mL) were prepared for denaturation using an LDS Sample Buffer (NuPAGE™ LDS Sample Buffer, NP0007, Invitrogen™ UK) under reducing conditions using 500 mM dithiothreitol (DTT) as a reducing agent (Bolt™ Sample Reducing Agent, B0009, Invitrogen™ UK). Then, samples were boiled at 70 °C for ten minutes. The denatured protein samples were then loaded and separated on a 4-12% Bis-Tris gel (Bolt™ Bis-Tris Plus Mini Protein Gels, 4-12%, 1.0 mm, NW04120, Invitrogen™ UK). A chemiluminescent pre-stained protein ladder (Precision Plus Protein™ WesternC™ Blotting Standards, 1610376, Bio-Rad UK) was also loaded according to manufacturer instructions. The electrophoresis running conditions were set at 20 min at 200 V (Voltage) and current starting at 160 mA, according to running buffer supplier's instructions (Bolt™ MES SDS Running Buffer, B0002, Invitrogen™ UK).

Once separation was complete, the proteins were transferred from the gel onto a nitrocellulose membrane (88018, Thermo Scientific™ UK). Membrane preparation

and assembly were performed according to the protocol supplied by the blot module manufacturer (NW2000, Invitrogen™ UK). A compatible Bis-Tris transfer buffer (25 mM Bicine, 25 mM Bis-Tris, 1 mM EDTA, pH 7.2) (Bolt™ Transfer Buffer, BT0006, Invitrogen™ UK) was used. Transfer conditions were set to 60 min at 12 V and current starting at 160 mA.

Successful protein transfer was checked using Ponceau S stain (Biotium Ponceau S stain, BT22001, Bioscience UK) as per suppliers' instruction. Then, membranes were washed twice with d.H<sub>2</sub>O for a total of 15 min. Subsequently, the membranes were incubated in a blocking buffer (5% BSA in TPBS) on a rocking plate for one hour at RT. Afterwards, membranes were washed with TPBS and incubated with a Rabbit monoclonal M2 antibody (1:10,000, ab109226, Abcam UK), a Rabbit polyclonal M3 antibody (1:10,000, ab126168, Abcam UK), Rabbit polyclonal M5 antibody (1:10,000, ab186830, Abcam UK), Mouse monoclonal GAPDH Antibody (1:20,000, AM4300, Invitrogen™ UK), all diluted in the blocking buffer at 4 °C overnight. The next day, membranes were washed with TPBS three times for a total of 15 min. After washes, membranes were incubated with Goat Anti-Rabbit secondary antibody (1:20,000, Goat Anti-Rabbit IgG H&L (HRP), ab6721, Abcam UK), Goat Anti-Mouse secondary antibody (1:20,000, Goat Anti-Mouse IgG H&L (HRP), A28177, Invitrogen™ UK), and a combatable secondary antibody for the ladder chemiluminescent detection (1:20,000 Precision Protein™ StrepTactin-HRP Conjugate, 1610381, Bio-Rad UK), all diluted in the blocking buffer for one hour in the dark at RT. Membranes were then washed with TPBS three times for a total of 15 min, and a final wash with PBS for five min performed. The protein bands were visualised using an enhanced chemiluminescence (ECL) detection kit (Pierce™ ECL, 32109, Thermo Scientific™ UK) as per suppliers' instructions. Visualization and analysis were digitally performed using Bio-Rad imaging software (Chemidoc) with exposure setting as chemiluminescence 30 sec intervals for a total of three min. Protein samples of Human embryonic kidney cells (HEK 293) and Human squamous cell carcinoma (TR146) were used as controls and prepared as above.

### **2.2.5 Statistical analysis**

Statistical analysis was performed with GraphPad Prism for macOS (GraphPad Software, Inc., La Jolla, CA, USA) statistical packages. Normal distribution of the

investigated samples was assessed using Shapiro-wilk normality test. To analyse statistical differences of more than two conditions one-way ANOVA with Dunnett's multiple comparison or Kruskal-Wallis and Dunn's tests were used. For analysis of more than two conditions with multiple independent variables (i.e., time points), two-way ANOVA- with Šídák's post-test multiple comparisons was used. Analysis of two conditions was done with an unpaired t test followed by a Mann-Whitney test. The data are presented as mean  $\pm$  Standard Error of the Mean (SEM) with a difference of  $P < 0.05$  considered statistically significant.

## **2.3 Results**

### **2.3.1 Media type did not affect dental pulp stem cells stemness**

There was no significant difference in DPSCs proliferation in DMEM-KO compared to supplier's medium (BulletKit™) as measured by MTT assay (Figure 2-1 A). DPSCs are reported to be positive for different markers including CD90 and CD105, they also do not express CD45 among several other hematopoietic stem cell markers (Aydin and Şahin, 2019). To validate that using DMEM-KO did not compromise DPSCs stemness properties, expression of these stemness markers were determined by gene expression analysis. The results demonstrate positive expression of CD90 and CD105 and negative expression of CD45 in both media types with no differences (Figure 2-1 B). These results indicate that DPSCs maintain their stemness properties in DMEM-KO as reported for BulletKit™ media. Based on these results, all subsequent analysis were performed using DMEM-KO.

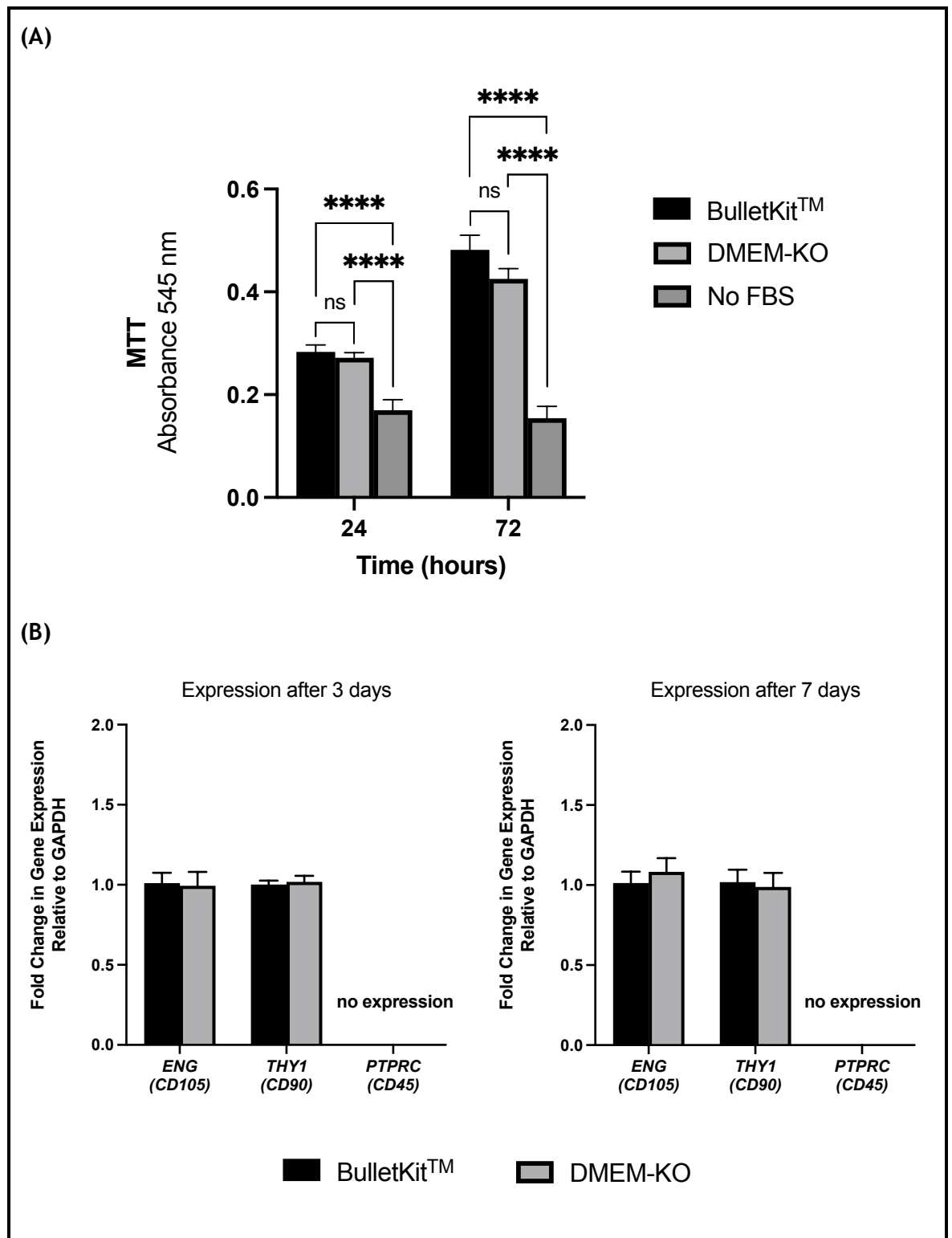
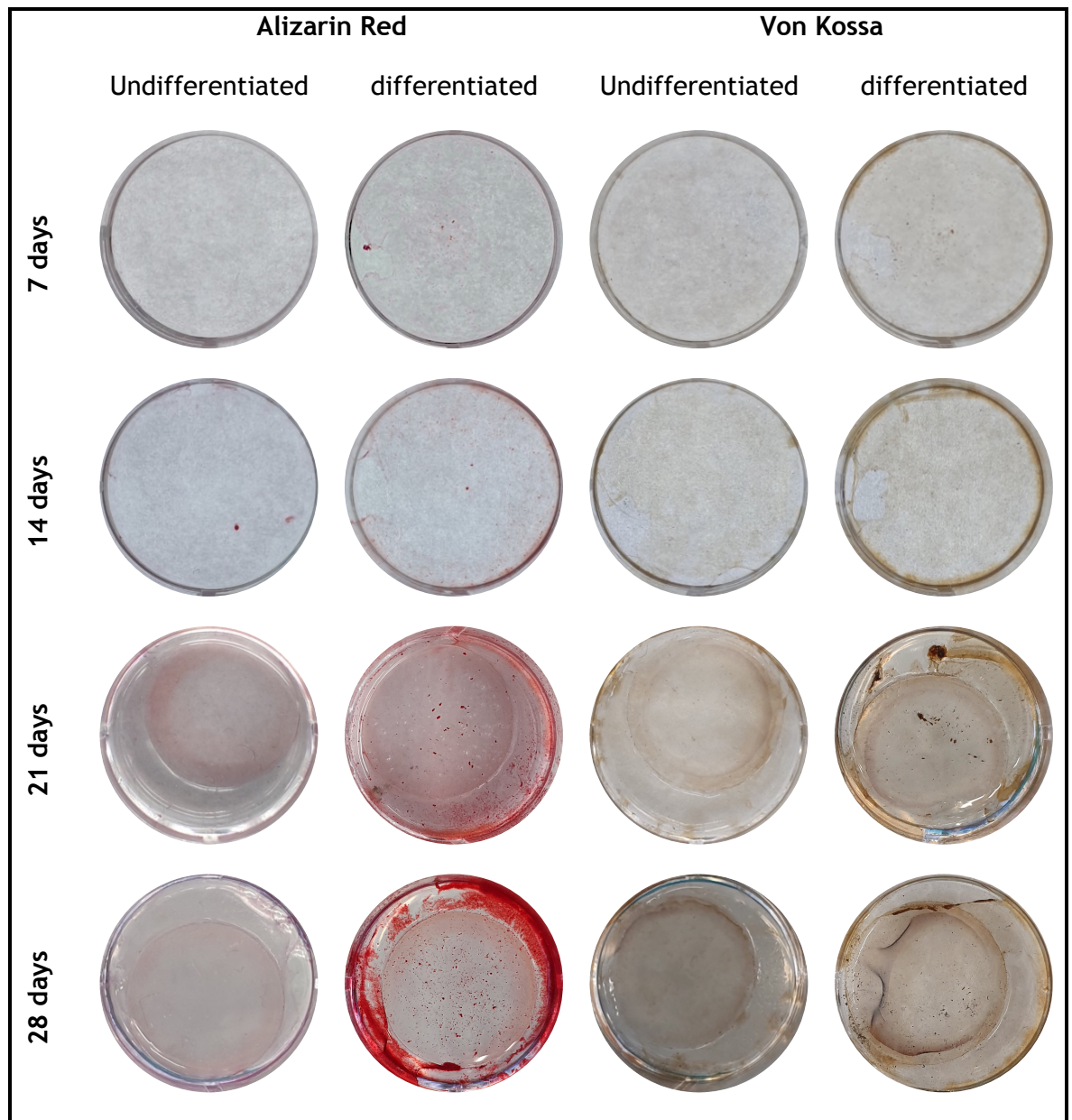


Figure 2-1 Stemness properties of DPSCs in different media types. (A) MTT assay showing DPSCs proliferation in the two different media types after 24 and 72 h, where cells proliferation displays no significant difference. Cells' proliferation in DMEM-KO medium with no growth serum (i.e., NO FBS) were used as a negative control and exhibited significantly reduced growth (\*\*\*\* $p < 0.0001$ ). (B) Stemness markers expression after three and seven days of DPSCs culture in the two different media types exhibiting no differences. Gene expression is presented as mean fold change relative to the housekeeping gene (*GAPDH*). Data for all are from three independent experiments ( $n = 3$ ).

Furthermore, to validate differentiation of DPSCs towards a particular lineage, *in vitro* osteogenic differentiation was evaluated. DPSCs differentiation into osteoblast-like cells confirmed their ability for osteogenic differentiation. The capability of DPSCs to form mineralised nodules *in vitro* was evaluated by matrix mineralisation visualised by Alizarin Red and Von Kossa staining (Figure 2-2). Quantification of the Alizarin red stain showed significant mineralisation after 21 and 28 days of differentiation compared to undifferentiated controls ( $P < 0.0001$ ) (Figure 2-3). Additionally, significant mineralisation stain is witnessed after 28 days of differentiation compared to 21 days ( $P < 0.0001$ ), which is comparable to the mineralised nodules images (Figure 2-2). Furthermore, changes in expression of key genes reported to be involved in the osteogenic differentiation (Orapiriyakul *et al.*, 2020) were analysed. Significant upregulation was witnessed for five out of seven investigated genes (Figure 2-4). The *ALP* gene exhibited significant upregulated expression at week two and three ( $P < 0.01$ ) of differentiation. While *BGLAP* exhibited significant elevated expression at week two ( $P < 0.001$ ). The *BMP2* gene displayed significant upregulated expression at weeks one ( $P < 0.05$ ) and two ( $P < 0.01$ ). The *IBSP* gene expression significantly increased three-folds at week four ( $P < 0.0001$ ). While the *SPP1* gene exhibited more than six folds significant increase at week four ( $P < 0.001$ ). Both *COL1A1* and *RUNX2* genes were found to exhibit constitutive expression across the experimental time course.



**Figure 2-2 Mineralisation of differentiated DPSCs. Alizarin reds stain of differentiated DPSCs showing vast extracellular calcium deposits as red mineralisation spots, whereas the controls (Undifferentiated) is only slightly reddish. Von Kossa stain shows calcium deposits as black nodules compared to control (Undifferentiated). Notably, Mineralisation deposits are more distinguishable in the 21 and 28-day samples. Images are representative of duplicate wells from three independent experiments ( $n = 3$ ).**

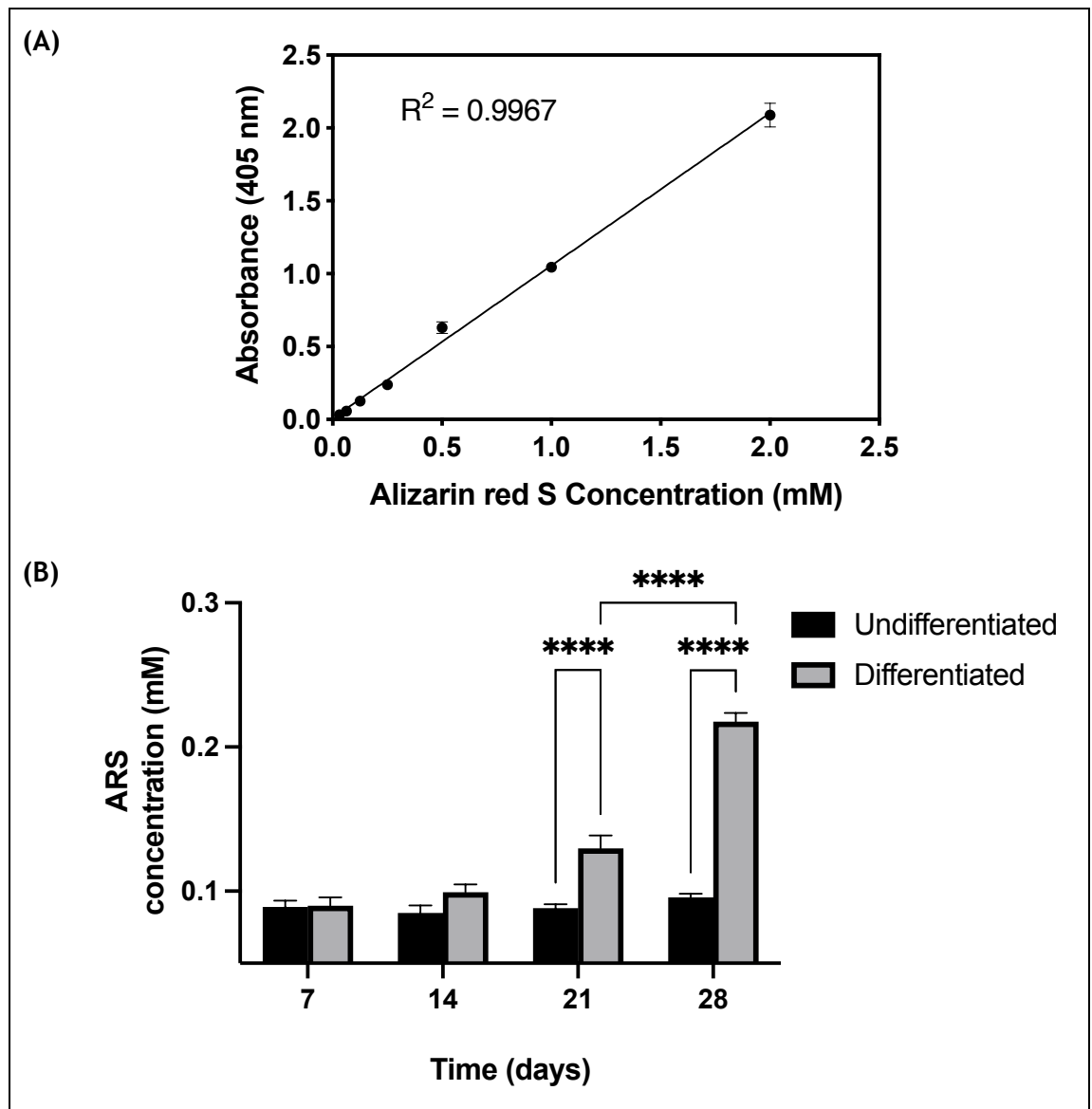


Figure 2-3 Alizarin Red stain quantification. (A) Alizarin Red stain standard curve using a serial dilution of known concentrations of the Alizarin Red stain. The data shows a representative standard curve from three independent experiments (B) Alizarin Red stain concentrations (in relation to known concentrations obtained by the standard curve) of differentiated DPSC samples compared to undifferentiated DPSC controls across the four weeks of osteogenic differentiation. Differentiated samples after 21 and 28 days produce the most significant mineralisation compared to undifferentiated controls (\*\*\*\* $p < 0.0001$ ). Differentiated samples after 28 days produce more significant mineralisation compared to 21 days (\*\*\*\* $p < 0.0001$ ). Values are reported as mean  $\pm$  SEM of mM concentration. Data presented is from duplicate wells of three independent experiments ( $n = 3$ ).

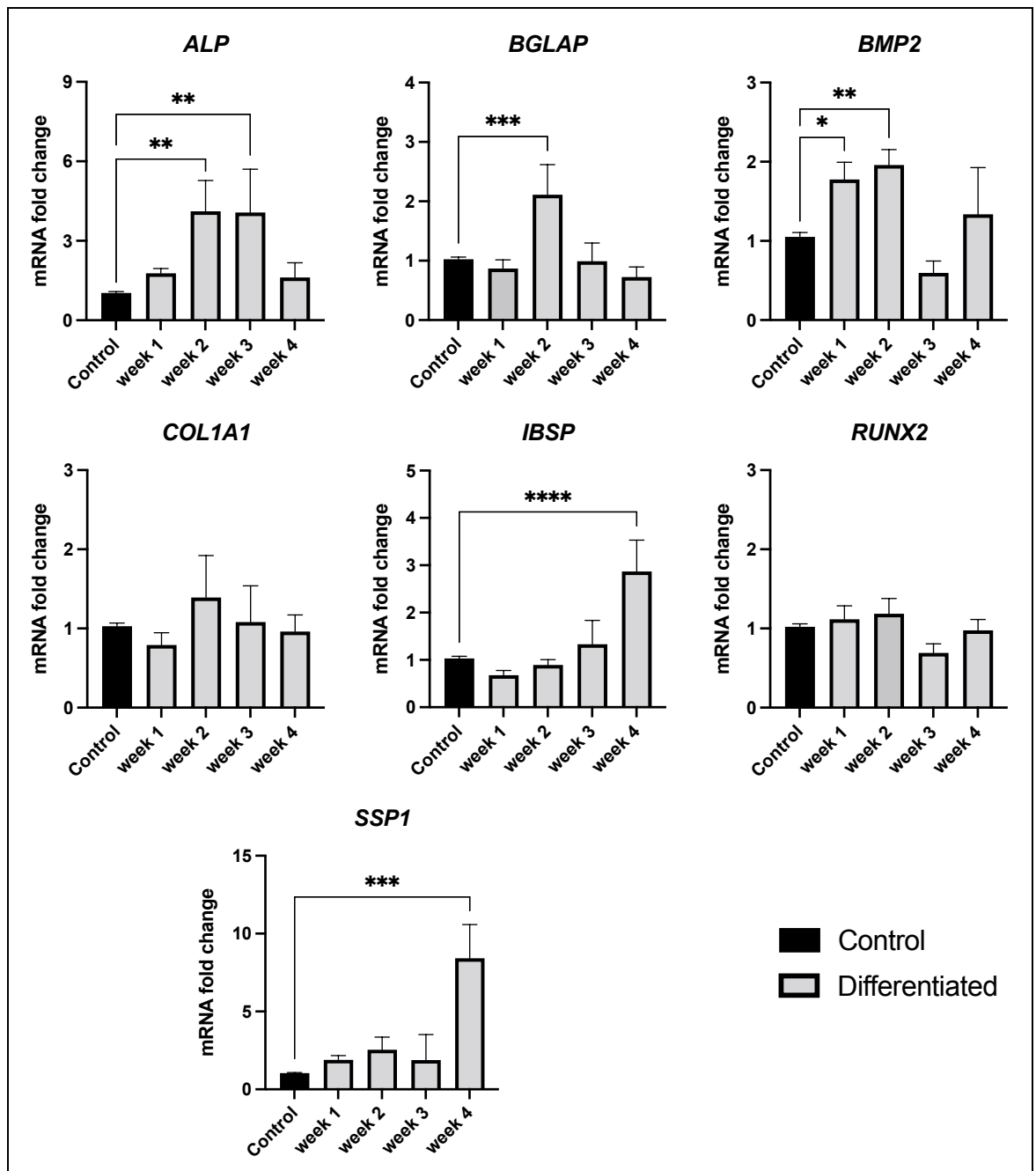


Figure 2-4 Gene expression of seven osteogenic markers. Data for all are derived from duplicate wells of three independent experiments and is presented as mean fold change compared to the control (cells that did not undergo osteogenic differentiation) using the  $2^{-\Delta\Delta C_t}$  method (Livak and Schmittgen, 2001). Gene expression is relative to the housekeeping gene (*GAPDH*). A difference of  $P < 0.05$  was considered statistically significant. (\*  $p < 0.05$ , \*\*  $p < 0.01$ , \*\*\*  $p < 0.001$ , \*\*\*\*  $p < 0.0001$ ).

### 2.3.2 Detection of muscarinic and nicotinic transcripts:

Gene expression for AChRs in DPSCs were determined using end-point PCR and qPCR. To compare the relative abundance of the transcript of each AChRs in DPSCs, the delta CT ( $\Delta$ CT: housekeeping gene (*GAPDH*) subtracted by target gene) values were subtracted from the total number of PCR cycles (40) and presented as  $40 - \Delta$ CT. Regarding mAChRs transcript expression, the data showed expression of the *CHRM2*, *CHRM3*, and *CHRM5* gene (M2, M3 and M5 muscarinic subtypes) in DPSCs (Figure 2-5 A). However, the band representing the *CHRM3* transcript appears below the expected approximate size. The q-PCR results also showed expression of the *CHRM2*, *CHRM3*, and *CHRM5* transcripts (Figure 2-5 B). The  $40 - \Delta$ CT indicates that the M2 muscarinic receptor encoded by the *CHRM2* gene is the most abundant among the detected muscarinic subtype transcripts. Moreover, melt curve analysis confirms on-target amplification for detected transcripts including the *CHRM3* gene (Sup 2-1)

With regards to nicotinic receptor subunit transcript expression, the data that showed a single band expression at the expected approximate size for *CHRNA1*, *CHRNA4*, *CHRNA5*, *CHRNA7*, *CHRNB3*, *CHRNB4*, and *CHRNE* transcripts ( $\alpha$ 1,  $\alpha$ 4,  $\alpha$ 5,  $\alpha$ 7,  $\beta$ 3,  $\beta$ 4, and  $\epsilon$  subunits) (Figure 2-6 A). However, the q-PCR results showed expression of the *CHRNA4*, *CHRNA7*, *CHRNA9*, *CHRNB1*, *CHRNB2*, and *CHRNE* genes ( $\alpha$ 4,  $\alpha$ 7,  $\alpha$ 9,  $\beta$ 1,  $\beta$ 2, and  $\epsilon$ ) (Figure 2-6 B). Among the expressed nicotinic subunits, it appears that the  $\alpha$ 4 subunit encoded by *CHRNA4* gene is the most abundantly expressed in DPSCs. However, melt curve analysis confirms on-target amplification only for *CHRNA7*, *CHRNB1*, *CHRNB2* and *CHRNE* transcripts (Sup 2-2).

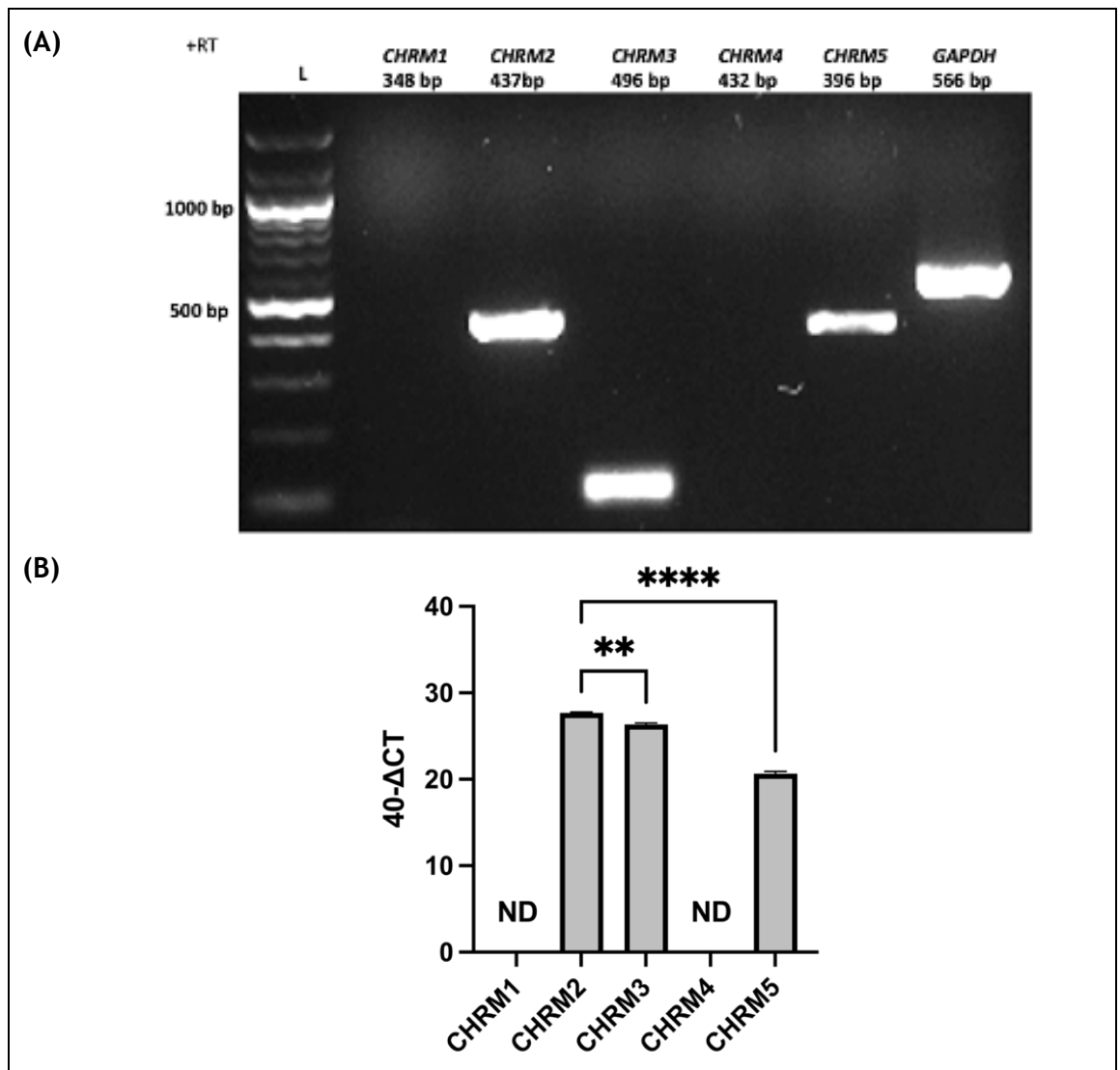


Figure 2-5 Gene expression of muscarinic receptors in DPSCs. (A) Representative data from the end point PCR showing PCR product bands for each transcript, in which bands of *CHRM2*, *CHRM3*, and *CHRM5* were detected. Only the bands of *CHRM2* and *CHRM5* appear at the expected approximate size. The intense bands represent 500 and 1000 bp on the ladder (L). (B) Distribution of normalised mRNA expression (40 - ΔCT values) of mAChRs in DPSCs. Expression of muscarinic subtype 2, 3 and 5 (*CHRM2*, *CHRM3*, and *CHRM5*) with predominate expression of muscarinic subtype 2 is shown (*CHRM2*). CT, cycle threshold; ND, Undetected. Data for all are from duplicate wells of three independent experiments and is presented as mean fold change compared to the highest 40 - ΔCT values. (\*\* p< 0.01, \*\*\*\* p<0.0001).



In summary, it is expected that DPSCs express several AChRs (Table 2-3). For the mAChRs a pattern of M2 > M3 > M5 was confirmed. For nAChRs, based on detected nicotinic subunits, it is predicted on known arrangements that DPSCs express a homopentameric  $\alpha 7$ nAChR and a heteropentameric  $\alpha 4\beta 2$ nAChR.

**Table 2-3 Summary of Acetylcholine receptors expression in DPSCs. Detected (+); undetected (-). A melt curve of one single amplicon indicates that the amplified double-stranded DNA products are a single discrete species and thus considered detected (+). The presence of multiple peaks in the melt curve indicates off-target amplification products and thus considered undetected (-).**

Receptor Family	Gene	RT-PCR	q-PCR	Melt curve
Muscarinic	<i>CHRM1</i>	-	-	-
	<i>CHRM2</i>	+	+	+
	<i>CHRM3</i>	-	+	+
	<i>CHRM4</i>	-	-	-
	<i>CHRM5</i>	+	+	+
Nicotinic	<i>CHRNA1</i>	+	-	-
	<i>CHRNA2</i>	-	-	-
	<i>CHRNA3</i>	-	-	-
	<i>CHRNA4</i>	+	+	-
	<i>CHRNA5</i>	+	-	-
	<i>CHRNA6</i>	-	-	-
	<i>CHRNA7</i>	+	+	+
	<i>CHRNA9</i>	-	+	-
	<i>CHRNA10</i>	-	-	-
	<i>CHRNB1</i>	-	+	+
	<i>CHRNB2</i>	-	+	+
	<i>CHRNB3</i>	+	-	-
	<i>CHRNB4</i>	+	-	-
	<i>CHRND</i>	-	-	-
	<i>CHRNE</i>	+	+	+
<i>CHRNG</i>	-	-	-	

### 2.3.3 Detection of acetylcholine synthesis, transportation, and degradation transcripts:

Expression of genes involved in ACh synthesis, transportation, and degradation in DPSCs were also investigated. Among the two genes known to hydrolyse ACh, *ACHE* and *BCHE*, DPSCs express *ACHE* which is a gene encoding Acetylcholinesterase (Figure 2-7). In particular, DPSCs express the erythrocyte variant E of the *ACHE* gene. Genes known for ACh synthesis and transportation such as *CHAT* (choline acetyltransferase), and *CRAT* (Carnitine O-Acetyltransferase), were not detected in DPSCs. Expression analysis of the vesicular acetylcholine transporter (VACHT), that is encoded by the *SLC18A3* gene, showed multiple bands on the end point PCR (Figure 2-7 A) and therefore was deemed non-specific binding of the primers used in the investigation. In addition, no expression of *SLC18A3* was detected via q-PCR (Figure 2-7 B). Therefore, it was concluded that *SLC18A3* is not expressed in DPSCs.

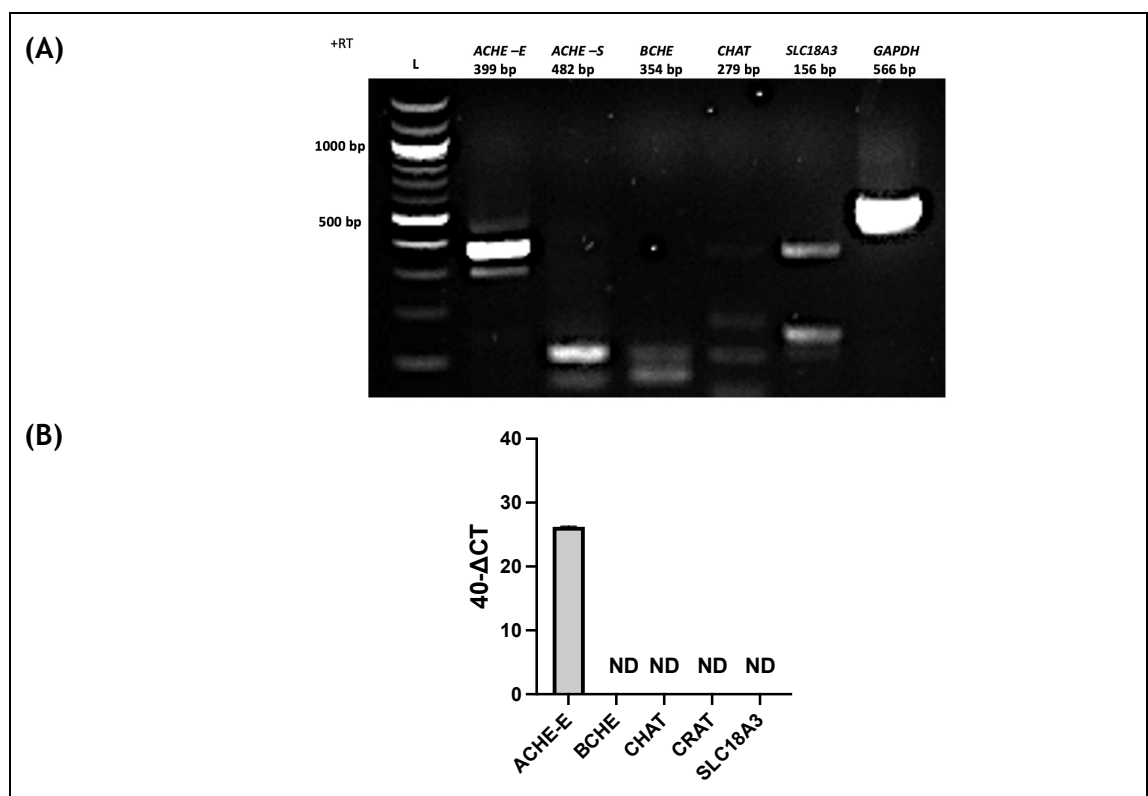


Figure 2-7 Gene expression of acetylcholine synthesis, transportation, and degradation components in DPSCs. (A) Representative data from the end point PCR showing PCR product bands for each transcript, in which the only band appearing at the expected approximate size is for *ACHE-E*. The intense bands represent 500 and 1000 bp on the ladder (L). (B) Distribution of normalised mRNA expression (40 - ΔCT values) showing only *ACHE*. CT, cycle threshold; ND, Undetected. Data for all are from duplicate wells of three independent experiments and is presented as mean fold change compared to the highest 40 - ΔCT values.

### 2.3.4 Expression of functional muscarinic and nicotinic receptors:

To evaluate functionality of detected AChRs, DPSCs proliferation was evaluated using the MTT assay. The metabolic activity assessed via MTT is proportional to the total number of cells in a well. To this end, DPSCs were treated with different types of agonists in the range of 0.1- 100  $\mu\text{M}$  for 72 h. Overall, a consistent response is witnessed when using concentrations of  $\geq 50 \mu\text{M}$  (Figure 2-8). The general non-specific agonists acting on both m and nAChRs such as Acetylcholine (ACh) and Carbamoylcholine chloride (CCh) were shown to enhance DPSCs proliferation most significantly at 100  $\mu\text{M}$  compared to untreated cells (i.e., CTRL) (Figure 2-8 A). Among the non-selective muscarinic agonists that do not display selectivity to a certain mAChR subtype, only Pilocarpine hydrochloride (PHCl) seems to enhance DPSCs proliferation most significantly at 100  $\mu\text{M}$  (Figure 2-8 B). The non-selective nicotinic agonist, Nicotine (Nic), that do not display selectivity to a certain nAChR subtype, inhibit DPSCs proliferation most significantly at 10-50  $\mu\text{M}$  (Figure 2-8 C).

Furthermore, to assess subtype functionality of detected AChRs, DPSCs proliferation was evaluated in response to several subtype selective agonists. DPSCs proliferation was inhibited in the presence of M1 > M2 preferred agonist McN-A 343 (McN) most significantly at 50 and 100  $\mu\text{M}$ , and in presence of the M2 selective agonist Arecaidine propargyl ester (APE) most significantly at 100  $\mu\text{M}$ . (Figure 2-9 A). DPSCs proliferation was slightly enhanced in the presence of the  $\alpha 7$  agonist AR-R 17779 (ARR) at 0.1  $\mu\text{M}$ , while it was inhibited slightly in the presence of the  $\alpha 4\beta 2$  agonist SIB 1508Y maleate (SIB) at 100  $\mu\text{M}$ .

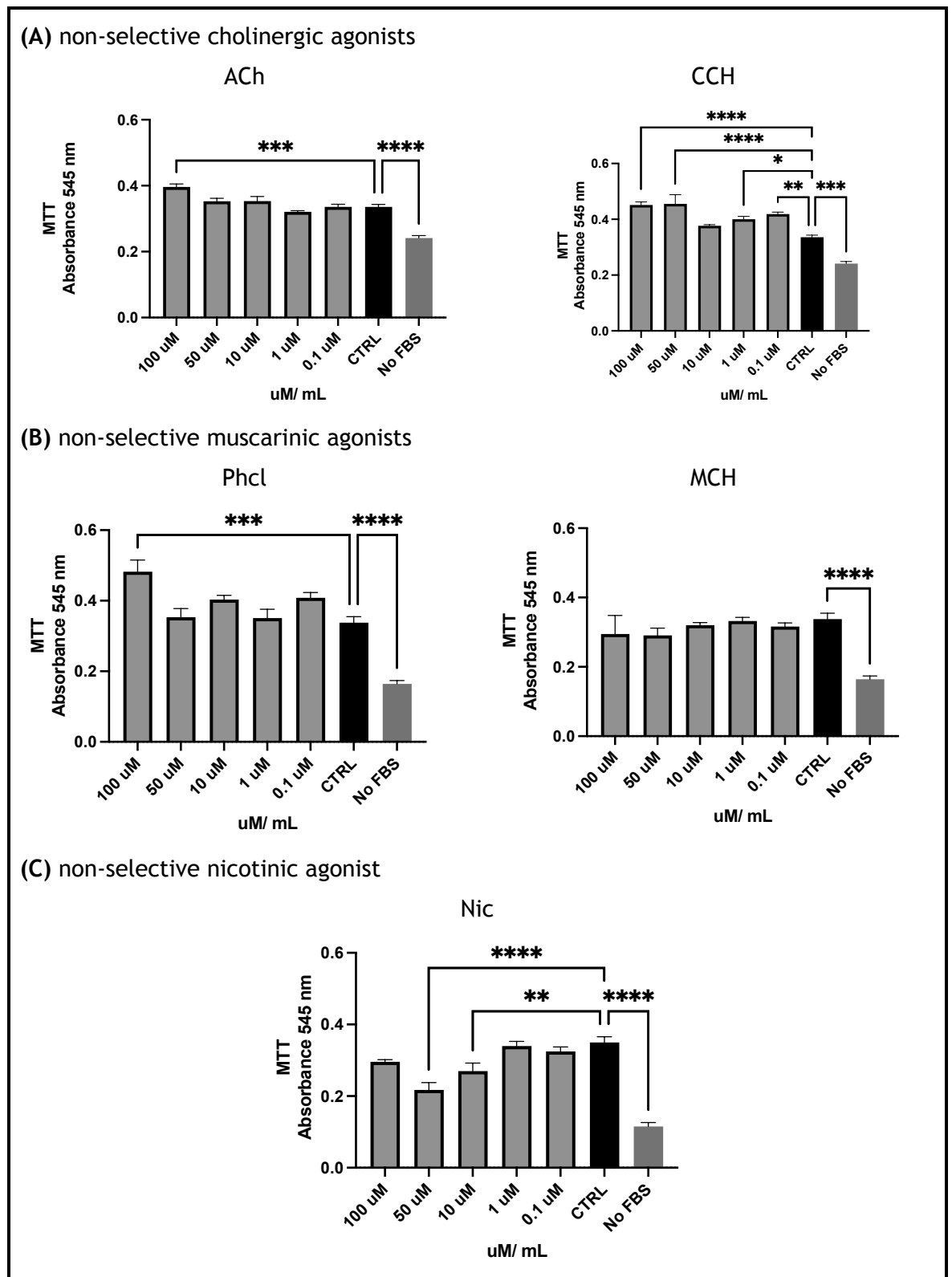
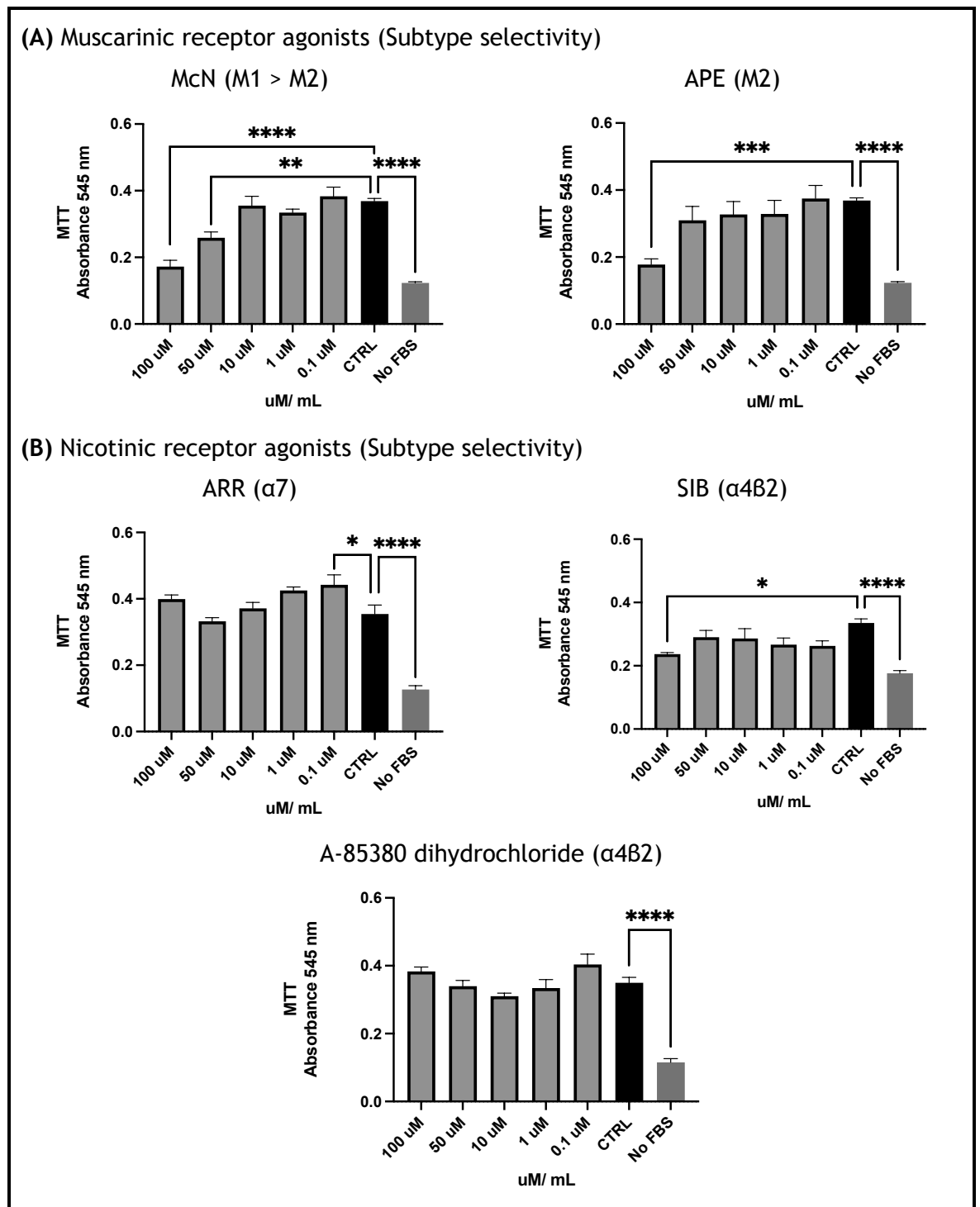


Figure 2-8 Viable cell number of DPSCs after 72 h treatment with several non-selective agonists. (A) non-selective cholinergic agonists, Acetylcholine (ACh) and Carbamoylcholine chloride (CCH) enhance DPSCs proliferation most significantly at 100  $\mu$ M. (B) non-selective muscarinic agonists, only Pilocarpine hydrochloride (PHCI) shown to enhance DPSCs proliferation most significantly at 100  $\mu$ M, while Muscarine chloride (MCH) did not influence DPSCs proliferation. (C) non-selective nicotinic agonist, Nicotine (Nic) inhibit DPSCs proliferation most significantly at 10 and 50  $\mu$ M. Comparison made to untreated group (CTRL), negative control are cells without serum (No FBS). Data for all are from duplicate wells of three independent experiments (\*  $p < 0.05$ , \*\*  $p < 0.01$ , \*\*\*  $p < 0.001$ , \*\*\*\*  $p < 0.0001$ ).



**Figure 2-9 Proliferation of DPSCs after 72 h treatment with several subtype selective agonists. (A) Selective muscarinic receptor agonists, McN-A 343 (McN) and Arecaidine propargyl ester (APE) inhibit DPSCs proliferation most significantly at 100  $\mu$ M. (B) Selective nicotinic receptor agonists, AR-R 17779 (ARR) enhance proliferation at 0.1  $\mu$ M, SIB 1508Y maleate (SIB) inhibit proliferation at 100  $\mu$ M, and A 85380 dihydrochloride do not elicit a response. Comparison made to untreated group (CTRL); negative control are cells without serum (No FBS). Data for all are of three independent experiments (\*  $p < 0.05$ , \*\*  $p < 0.01$ , \*\*\* $p < 0.001$ , \*\*\*\*  $p < 0.0001$ ).**

### 2.3.5 Subtype specific muscarinic and nicotinic agonists

Antagonists in the range of nM, either nonselective or subtype specific, do not produce an effect on their own (Figure 2-10). Therefore, to confirm that the effect witnessed upon DPSCs proliferation with a subtype specific agonist is specific to the investigated m or n-AChRs, the DPSCs were pre-treated with subtype specific antagonists for two hours. The notion is that the subtype specific antagonists will negate the effect of the subtype specific agonist and thus confirm selectivity of the agonist for the proposed receptor subtype. The data showed that the inhibition of proliferation observed with both the M1 preferring agonist McN-A 343 (McN) and M2 selective agonist Arecaidine propargyl ester (APE) was inhibited by the M2 selective antagonist Methoctramine (Meth) (Figure 2-11 A). This implied that DPSCs express a functional M2 mAChR giving that McN can stimulate M2 in the absence of M1 and the ability of the M2 selective antagonist (Meth) to cancel its inhibitory effect on DPSCs proliferation. The data for the nAChRs showed that the  $\alpha 7$  selective antagonist  $\alpha$ -Bungarotoxin ( $\alpha$ -Bun) was able to inhibit the effect of the  $\alpha 7$  agonist AR-R 17779 (ARR). In addition, the  $\alpha 4\beta 2$  selective antagonist Dihydro-  $\beta$ -erythroidine (DhBE) was able to inhibit the effect of the  $\alpha 4\beta 2$  selective agonist SIB 1508Y maleate (SIB) (Figure 2-11 B). To this end, it is concluded that DPSCs express functional M2 mAChRs,  $\alpha 7$  and  $\alpha 4\beta 2$ nAChRs based on the commercially available pharmacological subtype specific agonist and antagonist interactions.

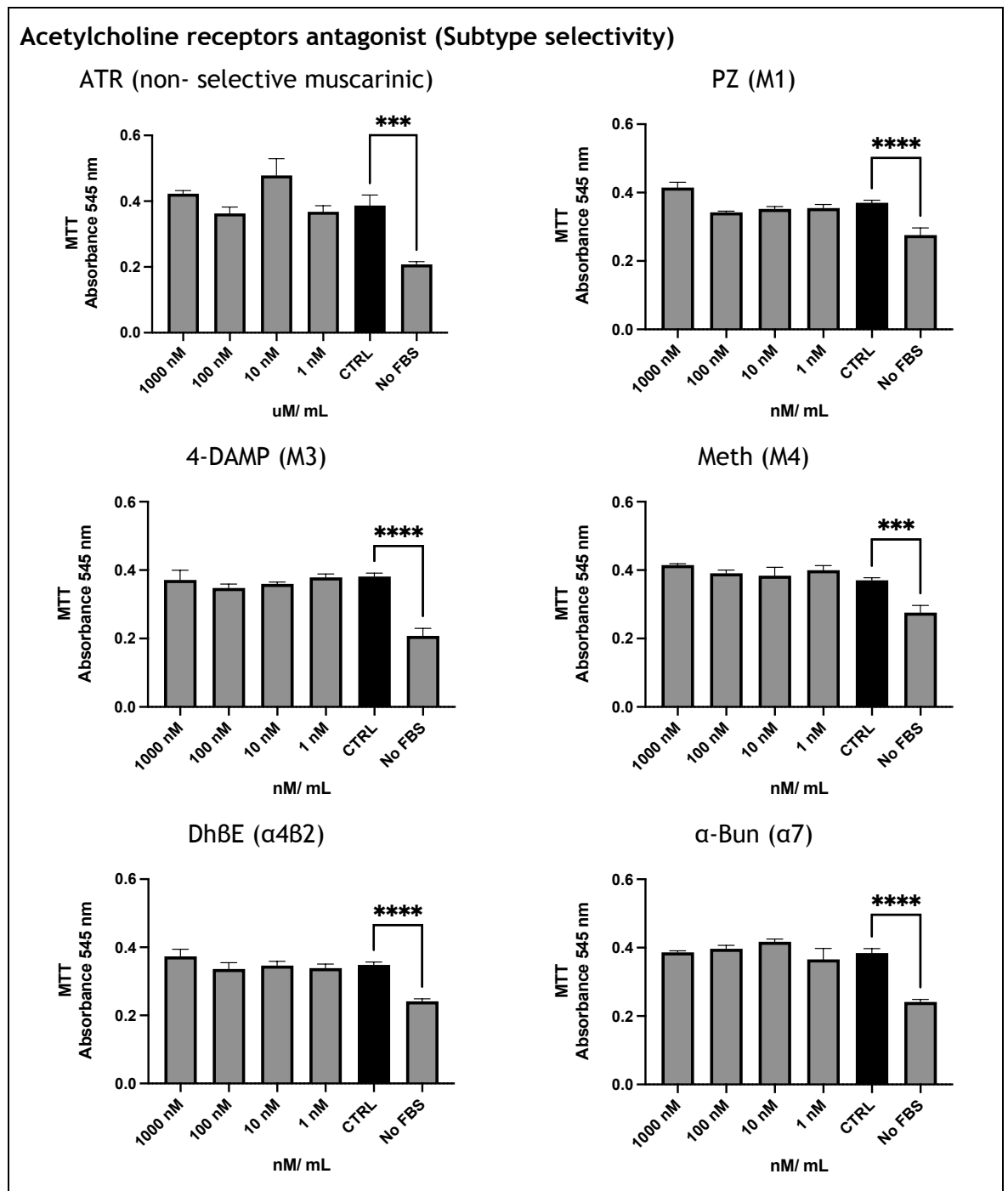


**Figure 2-10** Viable cell number of DPSCs after 72 h treatment with several acetylcholine receptors antagonist. Antagonist in the range of 1-1000 nM do not produce an effect on DPSCs proliferation. Comparison made to untreated group (CTRL); negative control are cells without serum (No FBS). Data for all are of duplicate wells of three independent experiments (\*\* $p < 0.001$ , \*\*\*\*  $p < 0.0001$ ).

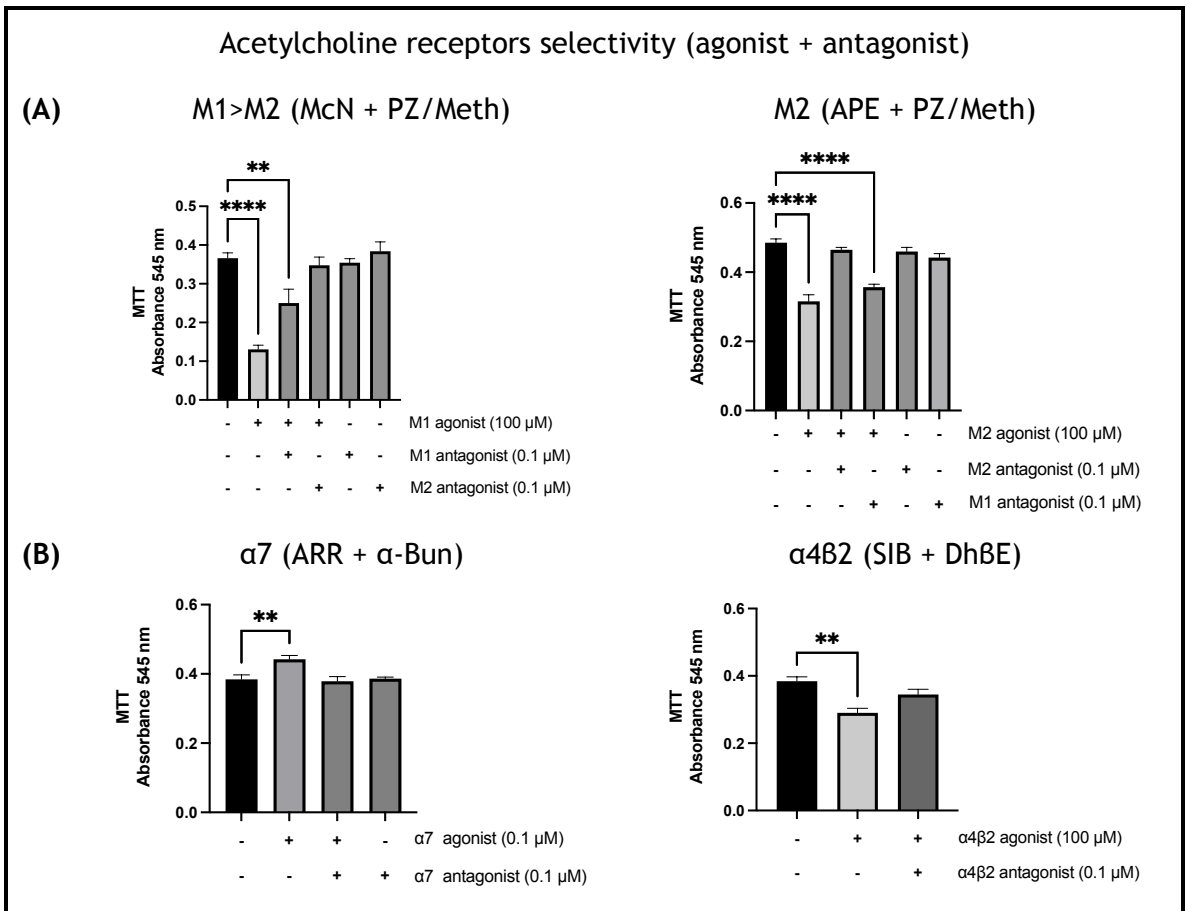


**Figure 2-11 Subtype specific acetylcholine receptors agonist selectivity. (A) Data shows that the M2 selective agonist methoctramine (Meth) cancelled the effect of both the M1 preferring agonist McN-A 343 (McN) and M2 selective agonist Arecaidine propargyl ester (APE). (B) Data shows the ability of the  $\alpha 7$  selective antagonist  $\alpha$ -Bungarotoxin ( $\alpha$ -Bun) to cancel the effect of the  $\alpha 7$  agonist AR-R 17779 (ARR), and the  $\alpha 4\beta 2$  selective antagonist Dihydro-  $\beta$ -erythroidine (Dh $\beta$ E) to cancel the effect of the  $\alpha 4\beta 2$  selective agonist SIB 1508Y maleate (SIB). The concentrations of each agonist used in this study were chose based on the findings reported in Figure 2-9. The concentrations of each antagonist were chosen in all cases was 0.01  $\mu$ M. Statistical analysis was performed comparing each experimental group with the control group (no compounds). Data for all are derived from duplicate wells of three independent experiments (\*\*  $p < 0.01$ , \*\*\*\*  $p < 0.0001$ ).**

### 2.3.6 Expression of muscarinic subtypes 2, 3, and 5 protein

Based on the gene expression of the M2, M3 and M5 genes (*CHRM2*, *CHRM3*, and *CHRM5*), and the profound effect of the M2 selective agonist (APE) on DPSCs growth, this project from here on investigated the muscarinic receptors M2, M3 and M5 protein expression. Thus, cellular expression of these receptors' protein was investigated through immunostaining and western blot. Positive immunostaining for the M2, M3 and M5 receptor was determined in *in vitro* cultured DPSCs. The M2 receptor protein was localised to the cell membrane as well as the cytoplasm (Figure 2-12). The M3 and M5 receptors protein was localised to the cell membrane as well as the cytoplasm and nuclei (Figure 2-13 & Figure 2-14). Immunostaining of these receptors was also carried out using a different secondary antibody conjugated to Alexa Fluor™ 488 (Sup 2-3).

Western blot results complement the immunostaining results, showing detection of M2 receptor protein bands approximately at 52 kDa in DPSCs and control samples (i.e., HEK 293 and TR146 cells) (Figure 2-15 A). Detection of the M3 receptor protein was observed in bands approximately at 75 kDa in DPSCs and control samples, however at a lesser intensity compared to the M2 bands (Figure 2-15 B). Detection of the M5 receptor protein was observed in bands approximately at 100 kDa in DPSCs and control samples, however at a lesser intensity compared to the M2 and the M3 bands (Figure 2-15 C). The loading control GAPDH showed bands of similar intensity approximately at 37 kDa indicating equal protein loading of all investigated cells (Figure 2-15 D). The additional bands in TR146 samples observed at 150 kDa are unknown. These same non-specific bands were detected when the primary antibodies were omitted (Sup 2-1).

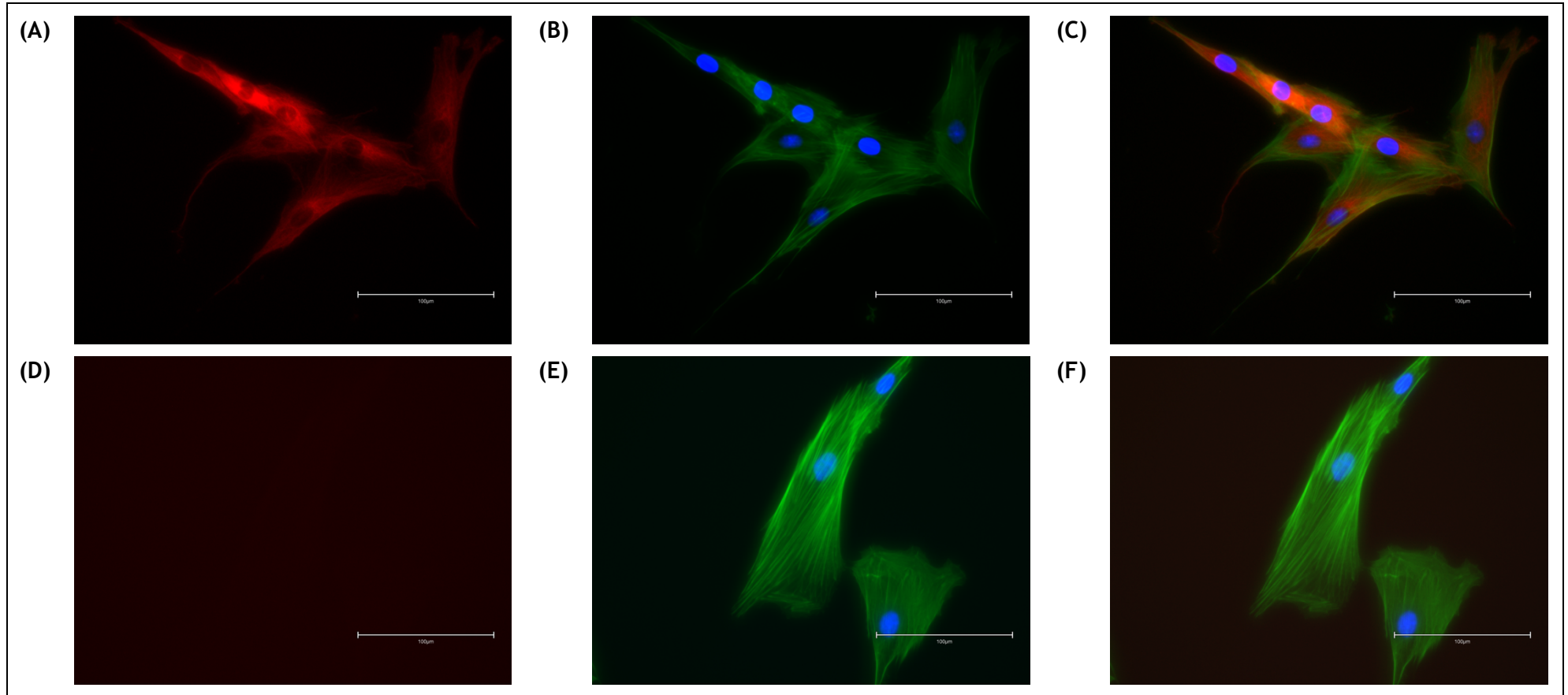


**Figure 2-12 Immunofluorescent staining of the M2 receptor in DPSCs. (A-C) Staining of the M2 receptor: (A) primary antibody revealed expression of the M2 receptor localised to the cell membrane as well as the cytoplasm of DPSCs, (B) merged images showing DPSCs nuclei stained with DAPI (blue) and actin filaments with phalloidin (green), and (C) merged images of (A) and (B). (D-F) Negative control (no primary antibody) showing: (D) no non-specific binding of secondary antibody, (E) merged images showing DPSCs nuclei stained with DAPI (blue) and actin filaments with phalloidin (green), and (F) merged images of (A) and (B). All images shows 2D projections of confocal stacks and are a representative of three independent experiments (n=3). Scale bars = 100 μm.**

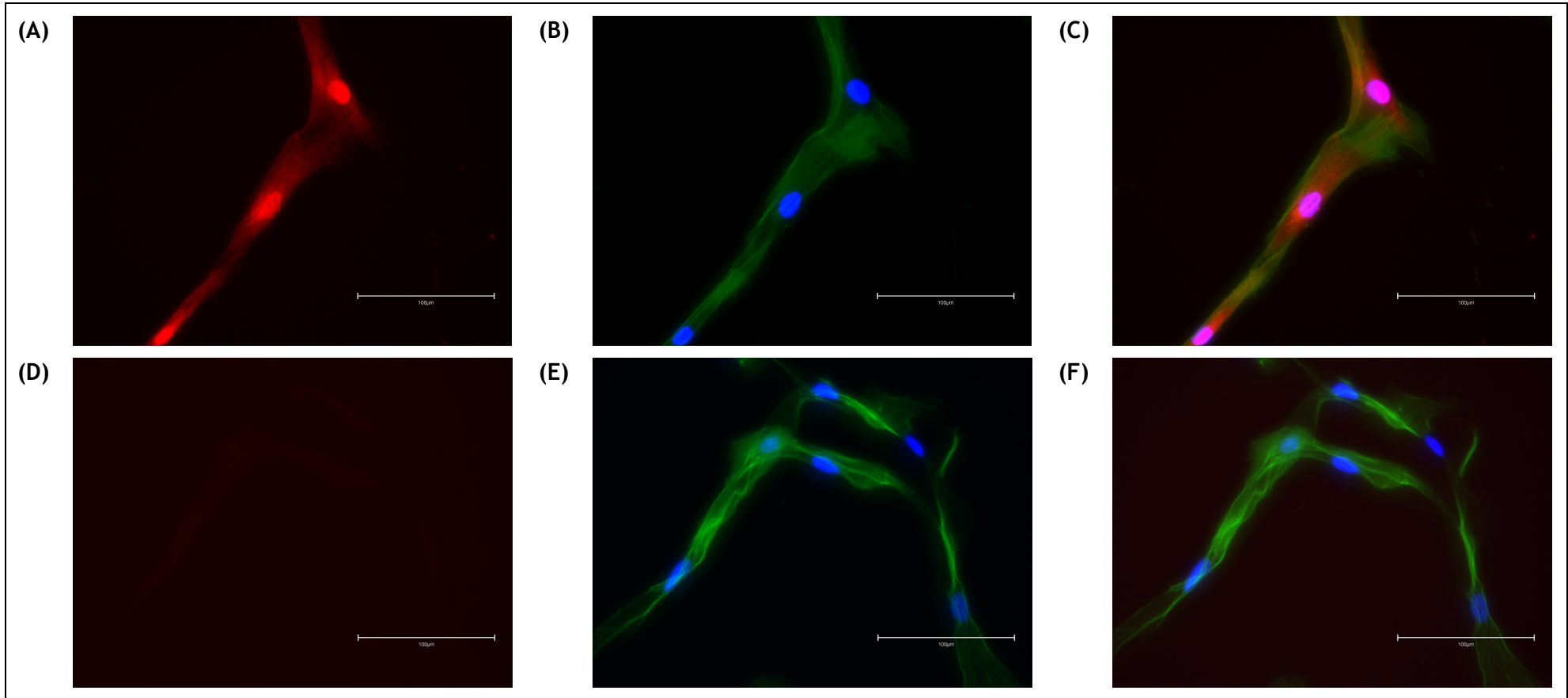


**Figure 2-13 Immunofluorescent staining of the M3 receptor in DPSCs. (A-C) Staining of the M3 receptor: (A) primary antibody revealed expression of the M3 receptor localised to the cell membrane as well as the cytoplasm and nuclei of DPSCs, (B) merged images showing DPSCs nuclei stained with DAPI (blue) and actin filaments with phalloidin (green), and (C) merged images of (A) and (B). (D-F) Negative control (no primary antibody) showing: (D) no non-specific binding of secondary antibody, (E) merged images showing DPSCs nuclei stained with DAPI (blue) and actin filaments with phalloidin (green), and (F) merged images of (A) and (B). All images shows 2D projections of confocal stacks and are a representative of three independent experiments (n=3). Scale bars = 100  $\mu$ m.**

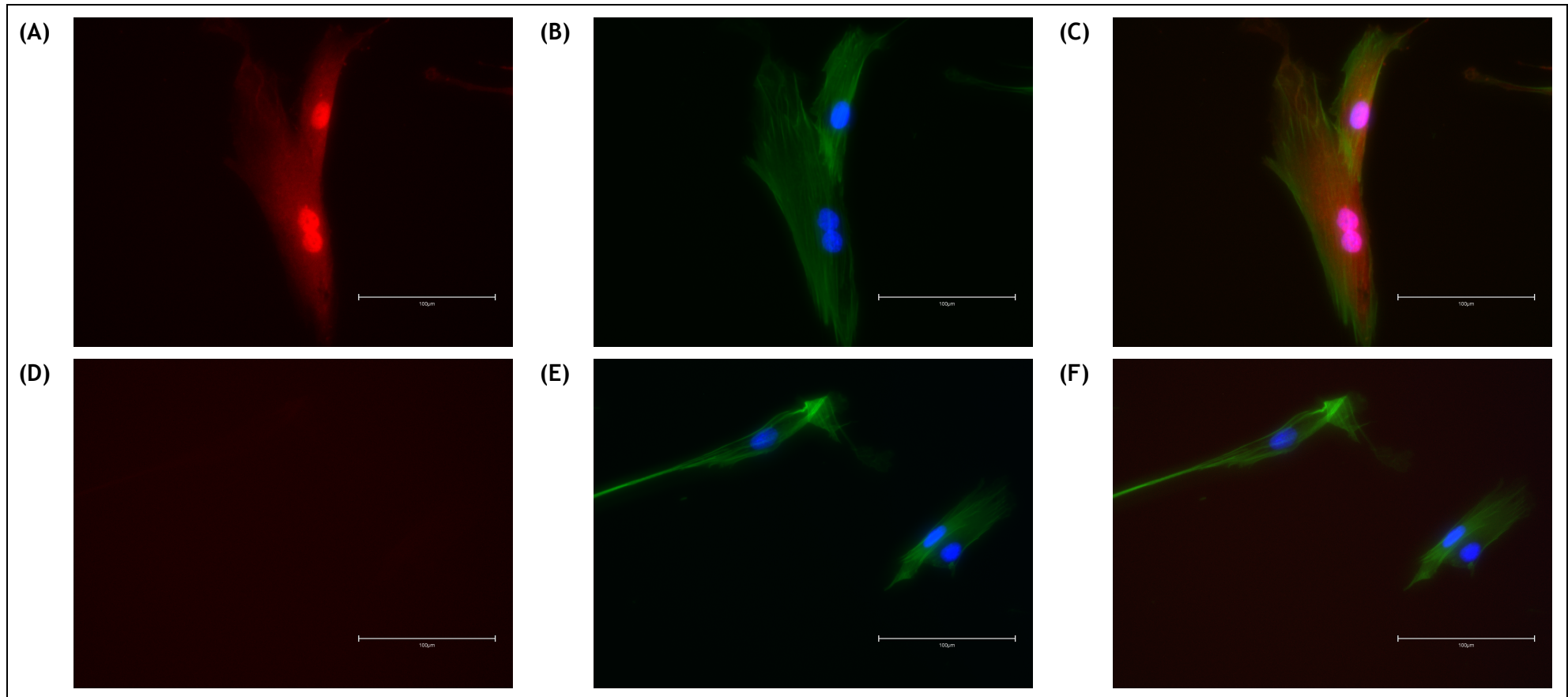


**Figure 2-14 Immunofluorescent staining of the M5 receptor in DPSCs. (A-C) Staining of the M5 receptor: (A) primary antibody revealed expression of the M5 receptor localised to the cell membrane as well as the cytoplasm and nuclei of DPSCs, (B) merged images showing DPSCs nuclei stained with DAPI (blue) and actin filaments with phalloidin (green), and (C) merged images of (A) and (B). (D-F) Negative control (no primary antibody) showing: (D) no non-specific binding of secondary antibody, (E) merged images showing DPSCs nuclei stained with DAPI (blue) and actin filaments with phalloidin (green), and (F) merged images of (A) and (B). All images shows 2D projections of confocal stacks and are a representative of three independent experiments (n=3). Scale bars = 100  $\mu$ m.**

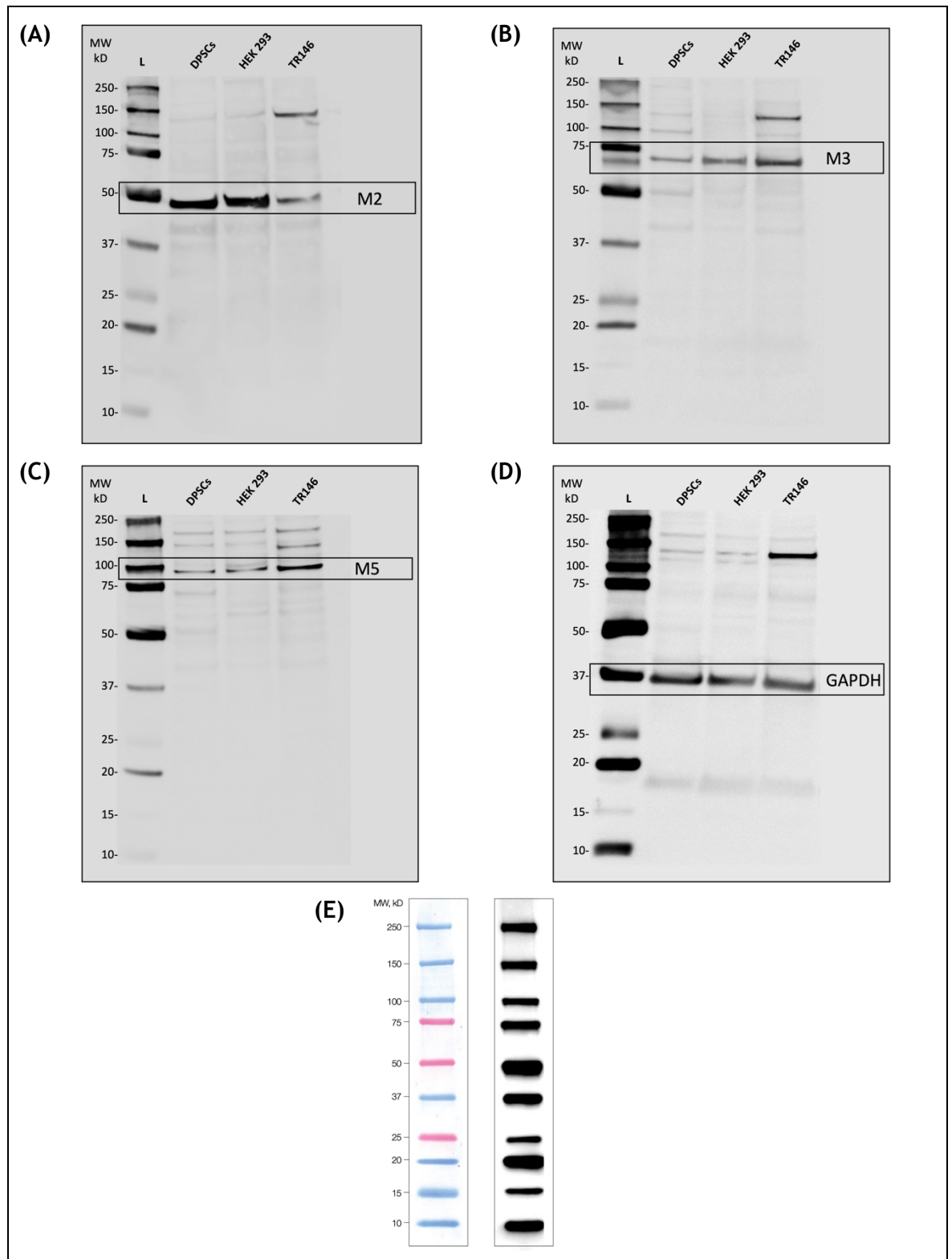


**Figure 2-15** Western blot analysis for the M2, M3, and M5 receptors. (A) M2 protein expression showing bands approximately at 50 kDa for DPSCs, HEK 293, and TR146. (B) M3 protein expression showing bands approximately at 75 kDa for DPSCs, HEK 293, and TR146. (C) M5 protein expression showing bands approximately at 100 kDa for DPSCs, HEK 293, and TR146. (D) GAPDH protein expression as a loading control showing bands approximately at 37 kDa for DPSCs, HEK 293, and TR146. (E) Precision Protein™ StrepTactin-HRP Conjugate (Bio-Rad, 1610380) ladder. (KD or kDa: kilodalton; L: denotes the ladder; MW: molecular weight). Exposure time: 30 sec. Images are representative of three independent experiments (n=3). Additional bands at 150 kDa in TR146 samples are yet unknown.

## 2.4 Discussion

Dental pulp stem cells represent an extraordinary source of stem cells for regeneration, given their multipotentiality and ability for self-renewal. DPSCs can be obtained from extracted adult teeth, rendering these cells to be a very promising resource considering their availability, good accessibility, and insignificant invasiveness in collection. These cells have great potential since they can be amplified and differentiated *in vitro* and transplanted to promote regeneration of several damaged tissues. Culture medium is a very important factor in growing DPSCs and guiding their differentiation output. In this work, the culture medium was changed to DMEM-KO. The rationale was that the supplier's medium (BulletKit™ Medium, Lonza Inc, UK) had anonymous growth supplements, presumably mammalian serum, growth factors, and unknown concentration of ascorbic acid. The osteogenic differentiation culture calls for a specific concentration of ascorbic acid (50 µM), thus it is best practice to have a medium with the ability to control addition of supplements accurately. The DMEM-KO is a well-established medium for DPSCs based on the breadth of literature (Govindasamy, Ronald, *et al.*, 2010; Vijayendran Govindasamy *et al.*, 2011; Alvarez *et al.*, 2015). It showed optimal conditions in terms of maintaining a higher proliferation rate, differentiation potential and lower levels of senescence (Rodas-Junco and Villicaña, 2017). The data herein, showed that DPSCs were able to grow normally in DMEM-KO, compared to the supplier's medium. Moreover, DPSCs continue to express markers of stemness in DMEM-KO. Stem cells are identified through a set of markers known as cluster of differentiation (CD), surface antigens, or stemness markers. Mesenchymal stem cells (MSCs), including DPSCs, express several markers among which are CD90 and CD105 (Aydin and Şahin, 2019). They also should not express hematopoietic stem cell markers like CD45. The results herein suggests that DPSCs maintain their stemness regardless of the media change. Suggesting no alternations had occurred with regards to the status of the investigated DPSCs or their ability to differentiate. In fact, phenotypical data of osteogenic differentiation showed the ability of DPSCs to undergo osteogenesis when using DMEM-KO as a base medium. To this end, this medium was set as default for subsequent investigations.

To establish differentiation capabilities, DPSCs were driven towards an osteogenic lineage. The intention here is to optimise an osteogenic differentiation protocol to serve as control for investigations that involve differentiation. The results herein demonstrate satisfactory osteoblast-like cell differentiation. This is visualised through the formation of mineralised nodules in samples stained with Alizarin red, and also the formation of calcium deposits in samples stained with Von Kossa. Osteogenic differentiation of multipotent stem cells involves a mixture of dexamethasone, ascorbic acid and  $\beta$ -glycerophosphate. There is a plethora of protocols to initiate osteogenic differentiation, which often result in conflicting findings. Therefore, the review by Langenbach and Handschel, 2013 describes a more detailed approach, which was followed in this study (Langenbach and Handschel, 2013). The Alizarin red staining has been used for decades to evaluate cells with rich calcium deposits. The dye binds selectively to calcium salts and is widely used for calcium mineral histochemistry (McGee-Russell, 1958). The protocol described by Gregory et al., 2004 was followed, as it yields more sensitive and reliable results (Gregory et al., 2004). Alizarin red is particularly versatile compared to Von Kossa, in that the dye can be extracted from the stained monolayer and quantified. Indeed, the quantification results of the Alizarin red stain supplement the mineralised nodules images showing significant mineralisation at the end of the osteogenic differentiation. This highlights the transition of the cells into osteoblasts-like cells which are responsible for forming the mineralised nodules. The Von Kossa staining is a marker for osteogenic differentiation and reveals calcium salt deposits in mineralised tissue. This assay is based on the binding of silver ions to the anions of calcium salts and the reduction of silver salts to form dark brown or black metallic silver staining (Wang et al., 2006).

The results here for the osteogenic differentiation report the expression pattern of key genes involved in osteogenic differentiation. It is worthy to consider this differentiation process from a temporal view to establish an understanding of these genes' expression dynamics. Osteogenesis occurs in several stages that can be divided into: proliferation and differentiation, synthesis of extracellular matrix (ECM), and maturation of the ECM through mineralisation deposition (Aubin, 2001). During these stages, the osteoinductive factors in the media: dexamethasone, ascorbic acid, and  $\beta$ -glycerophosphate, play a specialised role.

Dexamethasone initiates the osteogenic differentiation, ascorbic acid promote ECM synthesis, and  $\beta$ -glycerophosphate provides a phosphate source to promote mineralisation (Kärner *et al.*, 2007). In the early stage of osteogenic differentiation, cells proliferate to increase the mass of mineralised tissue (Hanna, Mir and Andre, 2018). Dexamethasone induces *Runx2* expression which starts the osteogenic differentiation process. During this stage cells are changing into pre-osteoblasts (Langenbach and Handschel, 2013; Zhou *et al.*, 2021). The *RUNX2* gene encodes the RUNX2 transcription factor which is a master regulator of osteogenic differentiation (Lian and Stein, 2003; Chen *et al.*, 2009). It elects response elements in the DNA of major osteogenic genes, and thereby orchestrating their expression (Niu *et al.*, 2016). After it initiates and guides osteogenic differentiation, *RUNX2* expression needs to be downregulated in order for the cell to become a mature osteoblast (Komori, 2010a; Bruderer *et al.*, 2014). The results herein, albeit not statistically significant, indicate this downregulation in week 3. However, upregulation of *RUNX2* expression was undetected. Possibly it might have been upregulated earlier than the investigated time course (<7 days) as it is considered an early-stage marker of osteogenic differentiation (Komori, 2010b; Ni *et al.*, 2011). During this early stage, ascorbic acid stimulates collagen type 1 secretion and initiates the formation of ECM (Langenbach and Handschel, 2013). The *COL1A1* gene encodes the pro-alpha1 chains of type I collagen which is secreted from the cell and provides the framework for inorganic deposition and comprises most of the ECM. It plays an essential role in maintaining the biological and structural integrity of the matrix architecture (Cen *et al.*, 2008; Sun *et al.*, 2017). Similar to *RUNX2*, the results indicate that it might have been missed during the early days of differentiation. During the ECM formation, the progressive secretion of collagen type I leads to downstream signalling events that activate *RUNX2* by phosphorylation (Langenbach and Handschel, 2013). This leads *RUNX2* to stimulate expression latterly of phenotype-associated genes more involved with mature osteoblasts-like cells. The bone morphogenetic protein-2 plays an important role during this onset of differentiation. The *BMP-2* gene encodes a secreted ligand of the TGF-beta (transforming growth factor-beta) superfamily of proteins which is necessary for the activity of *RUNX2*, as it induces or promotes *RUNX2* expression as well as other related markers such as *ALP*, *COL1A1* and *BGLAP* (Yamaguchi *et al.*, 2008; Sun *et al.*, 2015). Thus, it has been described as an important regulator in the onset of osteogenic differentiation (Onishi *et al.*, 1998;

Dumic-Cule *et al.*, 2018; Gromolak *et al.*, 2020). The results here showed similar findings of upregulated expression of *BMP-2* at weeks one and two. The mid stage of osteogenic differentiation is marked by inhibition in proliferation associated with conversion of type I procollagen to collagen I and expression of *ALP* (Datta *et al.*, 2006). The *ALP* gene encodes several members of the alkaline phosphatase family of proteins and is considered a mid-stage marker during osteogenesis (Hessle *et al.*, 2002; Gauthier *et al.*, 2017). Results here support this and showed upregulated expression at week two and three. Among proteins encoded by this gene, the tissue-nonspecific alkaline phosphatase glycoprotein is the one reported to play a role in bone matrix mineralisation and production of a calcifiable extracellular matrix during osteogenic differentiation (Hessle *et al.*, 2002; Gauthier *et al.*, 2017). The mRNA expression and onset of ALP enzymatic activity occur at a point where proliferation ceases and before development of the mineralised ECM and the activity of Osteocalcin (Owen *et al.*, 1990; Datta *et al.*, 2006). In this phase, alkaline phosphatase lowers the concentration of the calcification inhibitor, pyrophosphate, and increase concretions of local inorganic phosphate provided by  $\beta$ -glycerophosphate (Golub and Boesze-Battaglia, 2007; Langenbach and Handschel, 2013) This endorses calcification through the formation of hydroxyapatite and mineral deposition for maturation of the mineralised extracellular matrix (Gulseren *et al.*, 2015). At this stage the ECM is formed and progresses into the mineralisation stage, where non-collagenous proteins assume their role marking the late stage of osteogenesis. These non-collagenous proteins are known as bone markers for the fact that they are more associated with the osteoblast phenotype (Fedarko *et al.*, 2004; Hanna, Mir and Andre, 2018). These proteins, including osteocalcin, bone sialoprotein, and osteopontin, play a major part in ECM mineralisation (Staines, MacRae and Farquharson, 2012; Hanna, Mir and Andre, 2018). Osteocalcin is encoded by the *BGLAP* gene, an osteoblast-specific gene that is upregulated via *RUNX2* (Lian and Stein, 2003). Osteocalcin is a non-collagenous protein that binds to hydroxyapatite and ultimately regulates bone mineralisation through modulating osteoblast and osteoclast activity (Shimizu *et al.*, 2014). This marker has been reported to be associated with latter stages of differentiation (Ni *et al.*, 2011; Wang *et al.*, 2012), in which it initiates the mineral deposition by binding to the calcium phosphate crystals that are stained by Alizarin red and Von Kossa stains. Osteocalcin is expressed, during the late phases of osteogenesis, in conjunction with the

mineralisation of the bone extracellular matrix, thus, suggesting commitment towards a mature osteoblast differentiation (Stein and Lian, 1993; Neve, Corrado and Cantatore, 2013). In the results presented here, an increased expression of *BGLAP* mRNA was observed at week two. Although the literature describes the protein expression as a late-stage marker, gene expression has been detected in mid stages of osteogenic differentiation (Boufker *et al.*, 2011; TAIRA *et al.*, 2012; Hatakeyama *et al.*, 2013; Calabrese *et al.*, 2016). Bone sialoprotein or integrin-binding sialoprotein is encoded by the *IBSP* gene, which is one of the significant components of the bone ECM (Ma *et al.*, 2018). This is due to the fact that bone sialoprotein has been suggested to be the main nucleator of hydroxyapatite crystal formation (Frank *et al.*, 2002; Ogata, 2008). Additionally, this protein has a very high affinity to bind calcium, distinguishing its role in ECM mineralisation (Ganss, Kim and Sodek, 1999). Bone sialoprotein expression is indicative of ECM maturation and the late stage of osteogenic differentiation (Carvalho *et al.*, 2021). The results presented here are in agreement, showing upregulated expression in the last week of differentiation. Osteopontin, encoded by the *SSP1* gene, is another non-collagenous protein essential for the process of mineralisation (Sodek, Ganss and McKee, 2000). This protein displays high affinity for calcium and has been suggested to influence calcium phosphate nucleation during ECM mineralisation (Boskey, 1995). Osteopontin expression during osteogenic differentiation inhibits the mineralisation process (McKee and Nanci, 1996), arguably in order to maintain promote maturation of the ECM as it can influence bone mass, mineral size, and orientation alongside osteocalcin (Turner *et al.*, 2010). Osteopontin expression was previously reported in the late and intermediate stages of differentiation (Liu *et al.*, 2008; Carvalho *et al.*, 2019). The results herein for this gene showed more than six folds upregulation of expression in the last two weeks, which suggest activity in the later stage of differentiation. In light of this, these genes gave an insight into the process of DPSCs osteogeneses under normal conditions. Moving forward, these results will serve as a control for future experiments investigating DPSCs differentiation.

Although there is a good body of evidence about DPSCs capabilities, there is more to learn about mechanisms and pathways that regulate DPSCs activity. Most notably, an ancient and powerful one; the non-neuronal cholinergic pathway. ACh plays an important role in this pathway, through binding to its receptors it

modulates cellular proliferation, differentiation, and migration in several non-neuronal cell types, including MSCs (Ma et al., 2000; Oddo and LaFerla, 2006; Hoogduijn, Cheng and Genever, 2009; Asrican et al., 2016). However, no clear evidence on the role of ACh and its receptors has been reported in DPSCs. DPSCs share several properties with MSCs, then again, studies investigating the role of non-neuronal cholinergic mechanisms are scarce in MSCs. Findings of MSCs studies suggest a role of ACh in regulating stem cell function (Tang et al., 2012). In this light, the goal was to assess whether DPSCs express AChRs, and determine if expressed AChRs are functional. Initially, RT-PCR analysis of m- and nAChRs expression was investigated. This method is a cost-effective approach to confirm expression of AChRs. Furthermore, q-PCR data confirmed expression of detected AChRs and allowed quantification of the most abundantly expressed AChR subtypes or subunits. The relative abundance of a gene transcript was presented as  $40^{-\Delta CT}$  values. Although, this might not be an ideal way to calculate transcripts abundance, it allows a relative estimation as previously described (Czechowski *et al.*, 2004; Linardou *et al.*, 2012). The melt curves analysis adds validity by demonstrating specificity of the primers employed in the analysis, and thus adds additional validity to the data demonstrating expression of specific AChR subtypes or subunits. Based on all the three methods, DPSCs were suggested to express transcripts for the M2, M3, and M5 mAChRs. For nAChRs, based on the type of detected nicotinic subunits and known subunit conformations described in the literature (Dani and Bertrand, 2007; Albuquerque *et al.*, 2009; Carballosa, Greenberg and Cheung, 2016) DPSCs are suggested to express transcripts encoding a homopentameric  $\alpha 7$ nAChR and a heteropentameric  $\alpha 4\beta 2$ nAChR. Furthermore, DPSCs were suggested to only express transcripts encoding *ACHE* gene which is known to hydrolyse ACh. This and the above data suggest that DPSCs are equipped with machinery to only bind and terminate ACh that is produced locally from a source independent of DPSCs and do not themselves synthesise and secrete ACh. However, this hypothesis requires further investigation.

To begin to determine the function of detected AChRs, DPSCs were treated with several commercially available pharmacological cholinergic agonists. DPSCs proliferation was assessed in response to agonists using an MTT assay. MTT measures active cell metabolism, and thereby quantifies changes in DPSCs proliferation of treated cells. This assay is a sensitive and reliable indicator of

cellular metabolic activity and is preferred over other methods of assessing proliferation such as the ATP and  $^3\text{H}$ -thymidine incorporation assay (Patravale et al., 2012). The assay relies on the viable cells to reduce the yellow water-soluble tetrazolium dye, primarily by the mitochondrial dehydrogenases, to purple colored formazan crystals (Korzeniewski and Callewaert, 1983). The absorbance of the color change is proportional to the total number of cells in a well. Herein, the stimulants used were agonists in  $\mu\text{M}$  range and antagonist in the nM range based on reported literature and concentrations comparable to those of their inhibition constant ( $K_i$ ) (Ragheb *et al.*, 2001; Loreti *et al.*, 2007; De Angelis *et al.*, 2012; Ferretti *et al.*, 2012, 2013; Uggenti *et al.*, 2014; Pacini *et al.*, 2014; Alessandrini *et al.*, 2015; Di Bari *et al.*, 2015; Cristofaro *et al.*, 2018; Piovesana *et al.*, 2018; Cristofaro, Alessandrini, *et al.*, 2020; Cristofaro, Limongi, *et al.*, 2020). The data showed most of the non-selective agonists enhanced DPSCs proliferation at 100  $\mu\text{M}$ . This gave a strong indication that the detected AChRs in DPSCs were functional. The positive response is comparable to the literature for MSCs in which ACh was found to induce migration (Tang *et al.*, 2012), while CCh was shown to increase intracellular  $\text{Ca}^{2+}$  (Sharma *et al.*, 2009) which is involved in the regulation of cell proliferation. Among the non-selective mAChR agonists, MCH did not show an effect on DPSCs proliferation, despite previous findings showing it to promote intracellular  $\text{Ca}^{2+}$  in MSCs (Hoogduijn, Cheng and Genever, 2009). This could be due to MCH acting on all mAChRs, in which some subtypes might cancel each other's downstream effect. It is known that mAChR subtypes are commonly divided into two groups; stimulatory (M1, M3, and M5) or inhibitory (M2 and M4) (Maeda *et al.*, 2019) based on downstream functionality of the coupled G proteins. The stimulatory group, M1, M3, and M5 mAChRs couple to subunit  $\alpha$  of the Gq/11 family and commonly result in an activation effect, while the inhibitory group, M2 and M4 mAChRs couple to the  $\alpha$  subunit of  $G_i$  and  $G_o$  and commonly result in a suppressive effect (Eglen, 2005). Additionally, in ligand and G protein coupled receptor interactions, the ligand's concentration can determine the resultant response, thus the concentrations used in this study might be outside the scope of detection. However, the other non-selective mAChRs agonist, PHCl is shown to promote DPSCs proliferation. This further highlights the complexity of the mAChR response to different ligands based on the ligand- G protein receptor interaction and the mosaic of receptor subtypes expressed by each cell. To the contrary, the non-selective nicotinic agonist (Nic) was shown to have an inhibitory

effect on DPSCs proliferation. This is comparable to findings in MSCs showing the suppressive effect of nicotine (Schraufstatter, DiScipio and Khaldoyanidi, 2010; Kim *et al.*, 2012; Zhou *et al.*, 2013; X. Yang *et al.*, 2017; Xiao *et al.*, 2019).

Further explorations to investigate subtype specific effect on DPSCs proliferation was carried out using receptor subtype specific agonists and antagonists. This enabled the study of functionality of a particular receptor without the risk of activating multiple subtypes as was plausible with the non-selective agonist experiments described previously. The data from the M1 preferring agonist (McN) and M2 selective agonist (APE) demonstrated that they generally inhibited DPSCs proliferation. The data for the M1 preferring agonist (McN) was potentially to be expected as it is also known to activate M2 mAChR in the absence of M1 which DPSCs were found not to express. The inhibitory effect of M2 was comparable to other observation in MSCs literature (Piovesana *et al.*, 2018). The  $\alpha 7$ nAChR selective agonist (ARR) was shown to promote DPSCs proliferation. It was suggested, in the MSCs literature, that  $\alpha 7$ nAChR can increase intracellular calcium and the levels of phosphorylation of ERK1 and ERK2 (Hoogduijn, Cheng and Genever, 2009). However, the consensus amongst all the MSCs literature indicates that the  $\alpha 7$ nAChR promotes the inhibitory effects of nicotine (Kim *et al.*, 2012; Zhou *et al.*, 2013; Tie *et al.*, 2018; Lykhmus *et al.*, 2019; Chan and Huang, 2020). Most of the MSC literature studied the effect of  $\alpha 7$ nAChR through stimulation with nicotine, a general nAChR agonist. In our initial results we report similar inhibitory effect of nicotine on DPSCs proliferation. Therefore, the  $\alpha 7$  or  $\alpha 4\beta 2$ nAChRs can be assumed to have a role in mediating this effect. To the best of knowledge, there is no MSC study that investigated the effect of the  $\alpha 7$ nAChR through stimulation using a specific selective agonist. The use of the selective agonist (ARR) here showed a contradictory effect to the expected inhibitory response of  $\alpha 7$ nAChR activation reported by MSCs upon stimulation with nicotine, a non-selective nicotinic agonist. Therefore, it can be hypothesized that ARR induced proliferation, via the  $\alpha 7$ nAChR, might be related to a ligand specific response that may initiate different downstream signalling pathways. Indeed, it has been shown that ARR, via the  $\alpha 7$ nAChR, can stimulate rat intrahepatic Cholangiocyte proliferation through  $\text{Ca}^{2+}$  ERK1/2-dependent signalling mechanism (Jensen *et al.*, 2013). The  $\alpha 4\beta 2$ nAChR selective agonist (SIB) was shown to have an inhibitory effect on DPSCs proliferation. To the best of our knowledge, SIB has not been

investigated in non-neuronal cells, however it is described as a potent  $\alpha 4\beta 2$  agonist (Parkinson Study Group, 2006). Data for the other  $\alpha 4\beta 2$ nAChR selective agonist, A 85380 dihydrochloride, revealed no effect on DPSCs proliferation. However, the MSCs literature finds the  $\alpha 4\beta 2$  generally to have a suppressive effect (Xiao *et al.*, 2019).

Based on expression of the M2, M3 and M5 genes (*CHRM2*, *CHRM3*, and *CHRM5*), and the profound effect of the M2 agonist (APE) on DPSCs proliferation, the project focused on muscarinic receptors roles in DPSCs function. Muscarinic receptors downstream signalling involves G proteins, and thus they are the metabotropic receptors of ACh. This involves activation of several downstream effectors and secondary messengers in translating muscarinic receptor induced ACh signalling. Most of these secondary messengers are involved in signal transduction of several pathways that control the cells' basic function. For example, the M2 receptor is expressed in several cell types and found to mainly control proliferation (Ma *et al.*, 2000; Loreti *et al.*, 2006; De Angelis *et al.*, 2012; Piovesana *et al.*, 2018) Therefore, the protein presence and distribution of the three detected muscarinic receptors (i.e., M2, M3 and M5) in DPSCs was examined. Expression of the M2 protein was investigated using a monoclonal antibody. The immunofluorescence data showed antigen-antibody binding reaction suggestive of this receptor localised to the cell membrane and cytoplasm of DPSCs. This is in agreement with a reported study on human scleral fibroblasts (Barathi, Weon and Beuerman, 2009) and expected as muscarinic receptors including M2 are transmembrane receptors in nature. However, immunofluorescence data of M3 and M5 showed antigen-antibody binding reaction that involves DPSC nuclei besides the cell membrane and cytoplasm. This might be due to suggestion that the secretory pathway of mAChRs involve perinuclear production of the receptor protein (Yamasaki, Matsui and Watanabe, 2010; Rosemond *et al.*, 2011). Additionally, there are concerns about the selectivity and specificity of available commercial muscarinic antibodies (Jositsch *et al.*, 2009; Pradidarcheep and Michel, 2016). The M2 data herein was generated using a recombinant monoclonal antibody, while the M3 and M5 data were generated using polyclonal antibodies. This can explain the improved sensitivity and specificity observed in the M2 immunofluorescence when compared to the M3 and M5. Indeed, the use of a recombinant monoclonal antibody has been

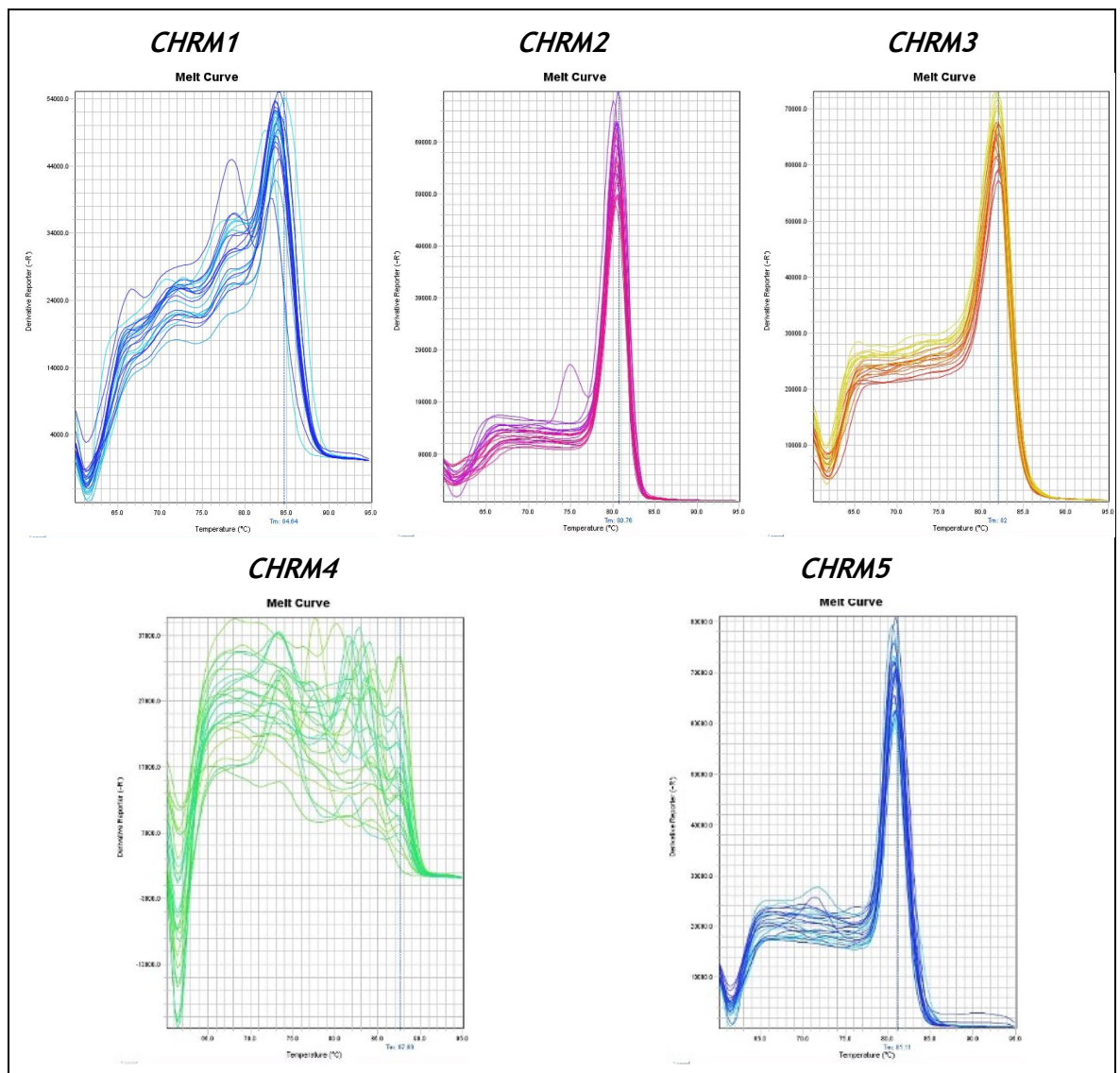
recommend in addressing selectivity and specificity of available commercial antibodies (Neri, Petrul and Roncucci, 1995; Basu *et al.*, 2019).

The expression of the M2, M3 and M5 proteins in DPSCs were further confirmed by Western blot analysis of whole cell lysates. The western blot analysis showed expression of the M2 protein approximately at its predicted molecular weight, in agreement with another publication using the same antibody (Ferrier *et al.*, 2015). The results also showed expression of the M3 and M5 proteins, however, at a lesser intensity compared to M2 expression. This could be attributed to the issues concerning the type of antibodies used as discussed above. The western blot analysis included two other cell types (HEK 293, and TR146) intended as controls. The optimal control, such as Foetal brain lysate, can be challenging to acquire due to ethical constraints. An appropriate alternative was the use of cells that have been shown to express the protein of interest. For example, HEK 293 were shown to express the M2 protein (Roseberry and Hosey, 2001). In fact, HEK 293 are widely used as a pharmacological tool for studying G-protein coupled receptors (Graham *et al.*, 2013). Additionally, muscarinic receptors are widely studied in cancer research and development for antitumor targets (Castillo-González *et al.*, 2015; Sun *et al.*, 2019; Calaf *et al.*, 2022), thus the use of TR146 cell line. Furthermore, the western blot analysis included GAPDH as a loading control, which the data showed relatively equal amounts of proteins between the investigated cell types. The data, especially in TR146 cells, showed an additional band at 150 kDa in all the investigated antibodies. The identity of this band remains unknown, and the band remained despite several attempts to optimise by different methods of protein extraction, preparation, and different antibody concentrations. Additional investigation found these non-specific bands in blots that were performed in the absence of primary antibodies (Sup 2-1). The nature of this interaction is unclear, as this could be non-specific binding of the antibody to molecules present in the samples, such as Fc receptors on the surface of cells (Burry, 2011), or unknown cross-reactivity that is unique to proteins isolated from TR146 cells. A proposed solution that can be investigated in the future is the “Double-blotting” technique (Lasne, 2001). Nevertheless, this additional band does not interfere with the data reported, as the detected mAChRs appear at the same location across three different cell types. The western analysis for the M3 and M5, albeit showing bands at the predicated molecular weight for these

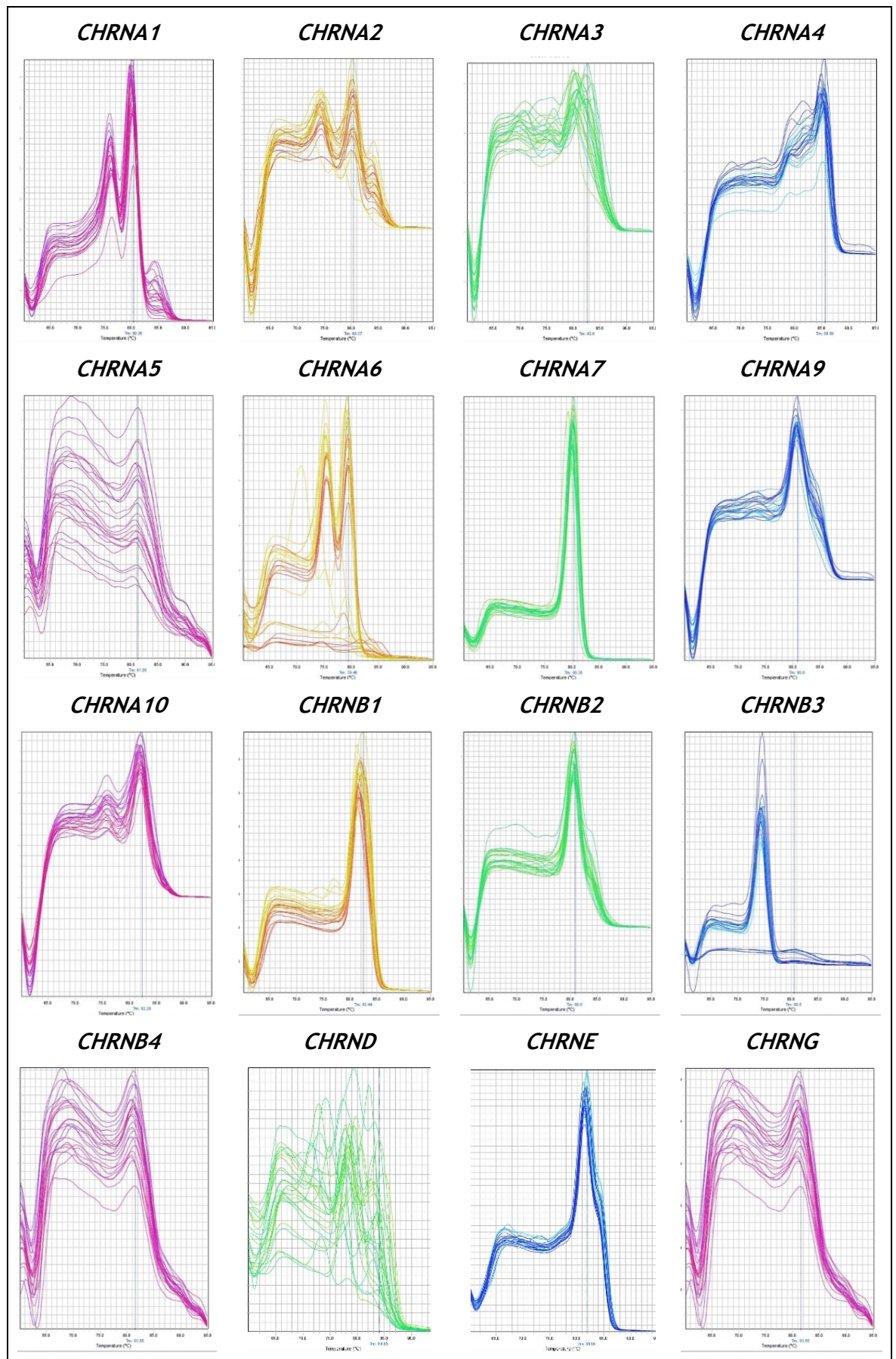
proteins, still require further optimisation to conclude specificity. For example, gene knockout via small interfering RNAs (siRNAs) or short hairpin RNAs (shRNAs) are methods proposed to overcome these issues. For now, however, the results obtained clearly showed functional expression of the M2 muscarinic receptor in DPSCs.

Further exploration to dissect the role of M2 in DPSCs was conducted using this receptor's specific agonist (APE). The notion here is to mimic the action of ACh in activating the M2 mAChR in nature. APE is a synthetic modified alkaloid derived by a metabolite produced by the areca nut (Voigt *et al.*, 2013), and considerable evidence has shown it to be selective for the M2 subtype (Loreti *et al.*, 2007; De Angelis *et al.*, 2012; Ferretti *et al.*, 2013; Alessandrini *et al.*, 2015). Thus, through this agonist, the effect of activating M2 on DPSCs survival, proliferation, cell cycle, migration, and differentiation will be investigated. The following work will refer to APE as the M2 agonist, since it is the only agonist used in this project to activate the M2 receptor.

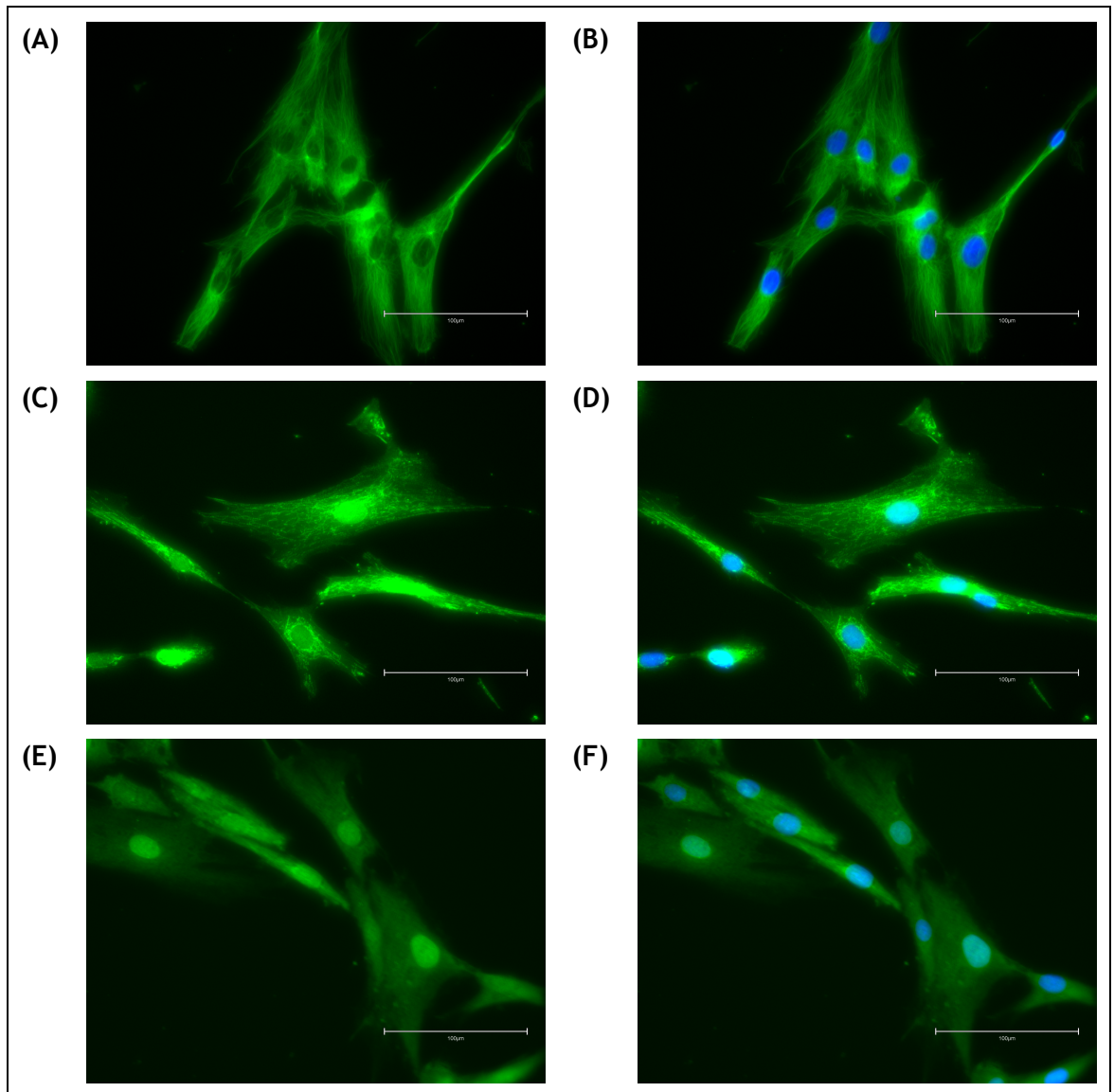
## 2.5 Supplementary



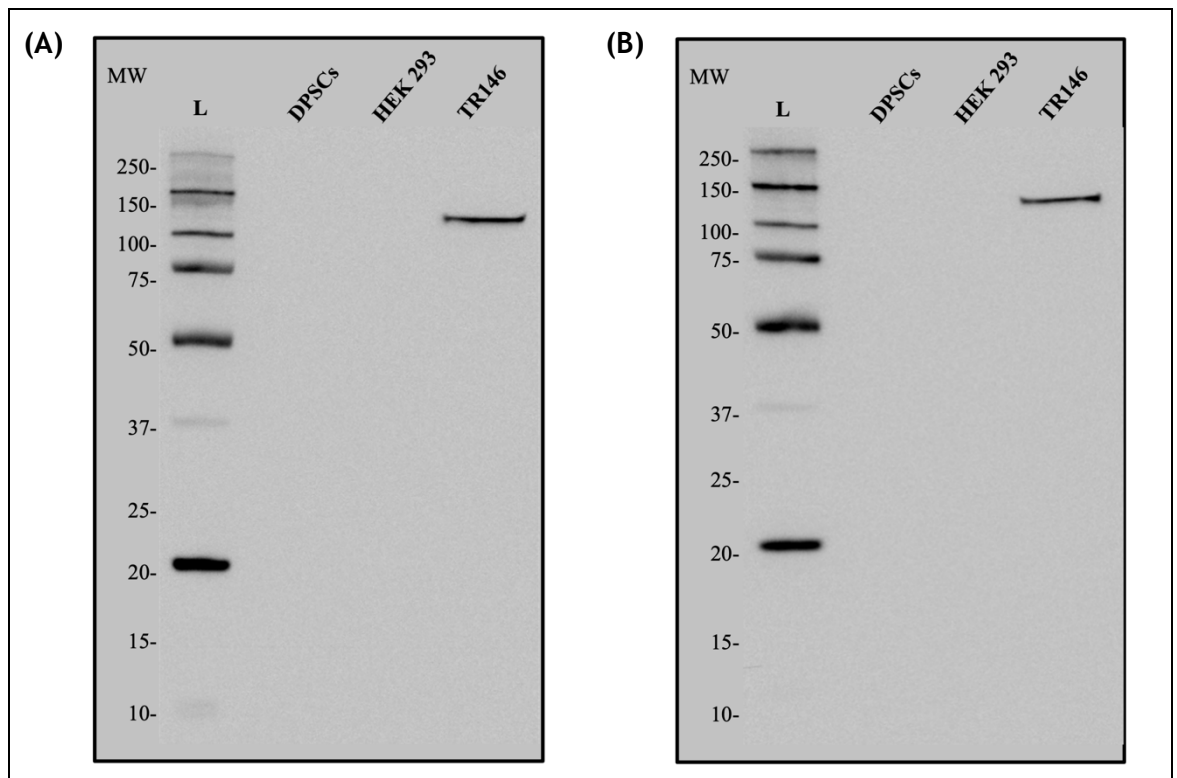
Sup 2-1 Melt curve analysis of muscarinic receptors gene expression. Melt curves for *CHRM2*, *CHRM3* and *CHRM5* subtypes shows a single peak representing a pure, single amplicon. In contrast, the melt curves of *CHRM1* and *CHRM4* showing multiple peaks, a result which is usually interpreted as an off target amplification.



Sup 2-2 Melt curve analysis of nicotinic receptors gene expression. Melt curves for *CHRNA7*, *CHRNB1*, *CHRNB2* and *CHRNE* subunits were the only ones showing a single peak representing a pure, single amplicon. In contrast, the melt curves of the other subunits showing multiple peaks, a result which is usually interpreted as an off-target amplification.



**Sup 2-3 Immunofluorescent staining of the M2, M3 and M5 receptors using Alexa Fluor™ 488 conjugated secondary antibody. (A-B) Staining of the M2 receptor: (A) primary antibody revealed expression of the M2 receptor localised to the cell membrane as well as the cytoplasm of DPSCs, (B) merged images showing DPSCs nuclei stained with DAPI (blue). (C-D) Staining of the M3 receptor: (C) primary antibody revealed expression of the M3 receptor localised to the cell membrane as well as the cytoplasm and nuclei of DPSCs, (D) merged images showing DPSCs nuclei stained with DAPI (blue). (E-F) Staining of the M5 receptor: (E) primary antibody revealed expression of the M5 receptor localised to the cell membrane as well as the cytoplasm and nuclei of DPSCs, (F) merged images showing DPSCs nuclei stained with DAPI (blue). All images shows 2D projections of confocal stacks and are a representative of three independent experiments (n=3). Scale bars = 100 µm.**



**Sup 2-1 Western blot analysis for the non-specific bands present in TR146 sample. Blot were generated following the same protocol, however in the absence of primary antibodies. The band in TR146 sample observed at 150 kDa are detected in (A) Goat Anti-Mouse secondary antibody, and (B) Goat Anti-Rabbit secondary antibody. (L: denotes the ladder; MW: molecular weight). Exposure time: 30 sec. Images are representative of three independent experiments (n=3).**

### **3 Effect of M2 muscarinic receptor stimulation on DPSCs survival, proliferation, and cell cycle**

### 3.1 Introduction

The M2 muscarinic receptor is a subtype of muscarinic receptor that mediates the function of acetylcholine (ACh). This receptor is a G protein-coupled receptor and when stimulated the receptor couples to distinct G protein subunits that in turn activate second messenger signalling pathways as well as gated ion channels (Eglen, 2006). Based on downstream functionality of the coupled G proteins, the M2 muscarinic receptor is grouped in the inhibitory subtype of muscarinic receptors. The receptor couples to the  $\alpha$  subunit of Gi and Go families of G proteins, and the downstream signalling typically results in a suppressive effect (most notably through a reduction in adenylyl cyclase activity) (Eglen, 2005). In addition to other subtypes of muscarinic receptors, the M2 receptor downstream signalling has been found to be involved in regulation of basic cell functions, such as gene expression, mitogenesis, differentiation, cytoskeletal organization, as well as controlling the activity of ion channels (Wessler, Kirkpatrick and Racke, 1999). Despite this, the role of the M2 muscarinic receptor in stem cell populations is still relatively unexplored.

There is sufficient evidence to conclude that Mesenchymal stem cells (MSCs) express ACh receptors, and studies suggest a role for ACh in regulating stem cell properties (See 1.2 for details). However, only a few studies report expression of the M2 gene in MSCs and only two report expression of the M2 muscarinic receptor at the protein level (Hoogduijn, Cheng and Genever, 2009; Piovesana et al., 2018). Furthermore, only one study has to date provided direct evidence for a role of the M2 receptor in inhibiting proliferation, migration and the cell cycle in Adipose derived MSCs (AD-MSCs) (Piovesana *et al.*, 2018). This study used arecaidine propargyl ester (APE), which functions as an analogue of acetylcholine, to confirm the presence of an active M2 receptor in MSCs.

In the previous chapter, expression of *CHRM2* and the M2 receptor protein were reported for the first time in dental pulp stem cells (DPSCs) (2.3.2 & 2.3.6). The expressed M2 was proven to inhibit DPSCs proliferation via its selective agonist APE (2.3.4). Selectivity of APE for the M2 receptor was confirmed via pharmacological competition experiments (2.3.5). Thus, this chapter aimed to further explore the nature of the observed effect of M2 activation on DPSCs proliferation, survival, and cell cycle.

## **3.2 Materials and Methods**

### **3.2.1 Cells and cell culture**

The DPSCs investigated in this chapter were from the same batch used in this project and were between passages four and six. Cells were cultured in normal medium (i.e., DMEM-KO) as described 2.2.1.

### **3.2.2 M2 muscarinic receptor stimulation**

Human DPSCs were plated according to experimental design in regular medium (DMEM-KOTM, Gibco, 10829-018), and allowed to adhere overnight. The following day, cells were treated with the M2 selective agonist APE (Sigma-Aldrich, A140). The M2 agonist (APE) selectivity for the M2 receptor has been confirmed by pharmacological experiments taking the form of agonist-antagonist competition to bound the receptor (For details see 2.3.5). Treatments were carried out over several time points with different concentrations in the range of  $\mu\text{M}$ , and subsequently narrowed to 100  $\mu\text{M}$  for 72 hours based on the proliferation data. Treatments were carried out in triplicate on three independent occasions.

### **3.2.3 Proliferation and recovery**

To evaluate the effect of M2 stimulation on DPSC proliferation, cell metabolism was assessed using a colorimetric assay based on 3-(4,5-dimethyl thiazol 2-y1) - 2,5-diphenyl tetrazolium bromide (MTT, M2128, Sigma-Aldrich). Briefly, DPSCs were plated into a 96-well plates at a density of  $1 \times 10^4$  cells/well. The M2 receptor stimulation described above was carried out over several timepoints (24 - 144 h) using a range of concentrations between 25 - 500  $\mu\text{M}$ . At the end of the treatment, medium was replaced with 100  $\mu\text{L}$  MTT solution (0.5 mg/mL diluted in PBS) and incubated for 4 h at 37°C and 5% CO<sub>2</sub>. Subsequently, the solution was replaced with 200  $\mu\text{L}$  of dimethyl sulfoxide (DMSO, D8418, Sigma-Aldrich) per well and further incubated for one hour at 37°C and 5% CO<sub>2</sub>. Finally, plates were shaken at 250 rpm for 20 min and absorbance readings were performed on a FLUOstar Omega microplate reader at 545 nm wavelength with 650 nm as a reference wavelength.

To assess whether the induced effect of the M2 agonist on DPSCs proliferation was reversible, a recovery analysis was set up. Briefly, after 72 h of the above

treatment, the medium in wells treated with the M2 agonist was discarded and the cells were washed with PBS. Then, fresh growth medium (DMEM-KO™, FBS, L-glut, and P-S) without the M2 agonist was added for another 72 h. Proliferation was determined by measuring metabolic activity using the MTT assay described above (M2128, Sigma-Aldrich).

### **3.2.4 Cytotoxicity and cell survival**

#### **3.2.4.1 Trypan blue analysis**

Cell vitality, after treatment with APE, was evaluated by trypan blue staining. Briefly, DPSCs were plated into 24-well plates at a density of  $1 \times 10^4$  cells/well. At the end of treatment, cells were detached with trypsin-EDTA (Gibco™, 11560626, 0.025%). The cell suspension was centrifuged for five min at 12000 rpm and the pellet was resuspended in fresh medium. Then, 40  $\mu$ L of trypan blue solution (1:10 v/v) (Sigma-Aldrich, T8154) was added to ten  $\mu$ L of cell suspension. After five min, the number of blue-stained cells (not viable) and unstained cells (viable) was evaluated using a Bürcker chamber.

#### **3.2.4.2 Lactate dehydrogenase measurement**

To measure cytotoxicity after treatment with APE, levels of Lactate dehydrogenase (LDH, a stable enzyme in all cell types released from dead cells when membrane is damaged) in supernatants were measured. An LDH cytotoxicity assay kit (Pierce LDH Cytotoxicity Assay Kit, 88953, Thermo Scientific) was used according to manufacturer's instructions. Briefly, DPSCs were plated into 96-well plates at a density of  $1 \times 10^4$  cells/well. The M2 receptor stimulation described in 3.2.2 was carried out for 72 h. At the end of the treatment, 20  $\mu$ L of cell supernatants were plated in a 96-well plate with a blank media control and a positive control (lysed cells). This was then mixed with 20  $\mu$ L of the LDH reaction mix and incubated in the dark for 30 min at room temperature (RT). After incubation, the reaction was stopped by adding 20  $\mu$ L of a stop solution provided by the manufacturer. Absorbance was read at 490 nm with a reference wavelength of 680 nm on a FLUOstar Omega microplate reader. Percentage cytotoxicity was determined as per the manufacturer's instructions: Cytotoxicity (%) = (Test sample - untreated control) / (Positive control - untreated sample). The assay assess the level of plasma membrane damage in a cell population as LDH is a stable enzyme,

present in all cell types, which is rapidly released into the cell culture medium upon damage of the plasma membrane. If present in the culture supernatant, the LDH oxidises lactate to generate NADH, which then reacts with a water-soluble tetrazolium salt (WST) to generate a yellow colour. The intensity of the generated colour correlates directly with the amount of LDH in the supernatant and therefore the number of lysed cells.

#### **3.2.4.3 Cell counting Kit-8 analysis**

To evaluate cell viability, the adherent cells from the experiments described in 3.2.2 were evaluated with a cell counting Kit (CCK-8, CK04, Dojindo Japan). Briefly, ten  $\mu\text{L}$  of the kit solution was added to each well of the plate and incubated for 4 h at  $37^\circ\text{C}$  and 5%  $\text{CO}_2$ . Subsequently, absorbance was read at 450 nm wavelength on a FLUOstar Omega microplate reader. The CCK-8 working principle is based on the reduction of a water-soluble tetrazolium salt, WST-8, to a formazan product by dehydrogenase enzymes in metabolically active cells. Unlike the LDH assay that measures released LDH levels of damaged cells, CCK-8 is used to measure dehydrogenase levels in viable cells, thus, the generated colour correlates directly with the number of viable cells. The added value of this assay is that both the tetrazolium salts and formazan are highly soluble in the tissue culture media, allowing for growth/proliferation analysis on the same cultured cells.

#### **3.2.4.4 Annexin V and Propidium iodide staining**

To determine whether the induced effect of APE causes the cells to lose their vitality by means of apoptosis, an Annexin V-fluorescein isothiocyanate (FITC)/PI detection kit (Abcam, ab14085) was used. The experiment was performed according to the manufacturer's protocol. Briefly, DPSCs were plated into 24-well plates at a density of  $5 \times 10^4$  cells/well. The M2 receptor stimulation described above was carried out for 72 h. Cells were sequentially incubated with five  $\mu\text{L}$  Propidium iodide (PI) binding buffer (50  $\mu\text{g}/\text{mL}$ ) and five  $\mu\text{L}$  Annexin V-FITC (10  $\mu\text{g}/\text{mL}$ ) in the dark. Subsequently, cells were fixed with 2% paraformaldehyde in PBS for 15 min at RT, washed and stained with DAPI (4',6-diamidino-2-phenylindole) mounting medium. Positive controls to detect PI and Annexin v staining were generated using 30% methanol as an inducer of apoptosis, and 70% as an inducer of necrosis. Cells were observed under a fluorescence microscope.

Images were captured using an EVOS FL digital inverted microscope (EVOS FL Cell Imaging System, Thermo Scientific) equipped with monochrome camera and a 40x phase objective. Images for two-channel merges were created by the built-in microscope software. The images were compared to the positive controls.

### 3.2.5 Cell cycle analysis

DPSCs were plated into a 75-cm<sup>2</sup> flasks at a seeding density of  $1.5 \times 10^6$  in regular medium (DMEM-KO<sup>TM</sup>, Gibco, 10829-018), and allowed to adhere overnight. The following day, cells were treated with the selective M2 agonist as described in 3.2.2. To enable analysis of cells in the S phase, cells were incubated with 50  $\mu$ M bromodeoxyuridine (BrdU, Sigma-Aldrich, 19-160) 24 h prior to the end of stimulation with the M2 agonist. At the end of treatment, cells were collected by trypsinisation, centrifuged for five min at 1200 rpm and then fixed in 70% Ethanol overnight. Partial DNA denaturation was performed by incubating the cells in 2N HCl for 30 min at 37 °C, followed by neutralization with 0.1 M sodium tetraborate. Cells were spun out of neutralised acid and washed with 2% FBS in DPBS. Cells were then incubated overnight at 4 °C with anti-BrdU clone MoBU-1 conjugated to AlexaFluor488 (Invitrogen, B35130) in 2% FBS in DPBS. The following day, cells were stained with a Propidium Iodide/ RNase buffer (PI/RNase Staining Buffer, BD biosciences, 550825) for 30 min at RT. Flow cytometry analysis was performed with a flow cytometer (MACSQuant® Analyzer 10 Flow Cytometer, Miltenyi Biotec) with 488 nm wavelength excitation, and  $10^4$  events were collected for each sample. Analyses were performed using FLOWJO V.10 software (Treestar, Inc., Ashland, OR, USA) in which curve fitting was used to estimate the percentages of cells in each phase of the cell cycle and produce BrdU plots. Gating strategy to exclude debris, exclude doublet cells, and to detect BrdU positive cells is presented in the supplementary section of this chapter (Sup 3-2).

### 3.2.6 Quantitative polymerase chain reaction (q-PCR) analysis

DPSCs were stimulated with the M2 agonist as described in 3.2.2. The RNA extraction and generation of cDNA was carried out as described in 2.2.2.1 & 2.2.2.3. Primer sequences for genes involved in proliferation and cell cycle are provided in Table 3-1. Target gene primers and the prepared cDNA samples were

mixed with the fast SYBR Green Master Mix (Fast SYBR™ Green Master Mix 4385610, Applied Biosystems™, UK) described in 2.2.2.4.

**Table 3-1 Primer sequences for genes investigated in chapter 3.**

<b>Primer</b>	<b>Sequence</b>
<i>CCNA1</i>	Fwd: CTCGTAGGAACAGCAGCTATGC Rev: GCTAGAACT TTCAGAAGCAAGTGTTTC
<i>CCNA2</i>	Fwd: GGATGGTAGTTTTGAGTCACCAC Rev: CACGAGGATAGCTCTCATACTGT
<i>CCND1</i>	Fwd: GCTGCGAAGTGGAACCATC Rev: CCTCCTTCTGCACACATTTGAA
<i>CCND2</i>	Fwd: ACCAACACAGACGTGGATTGT Rev: CTCCGACTTGGATCCGTCAC
<i>CCNE2</i>	Fwd: GCCAGCCTTGGGACAATAATG Rev: CTTGCACGTTGAGTTTGGGT
<i>CDC14A</i>	Fwd: CGAGCACTATGACCTCTTCTTCA Rev: AGGCTATCAATGTCCCTGTTCT
<i>CDC25A</i>	Fwd: TTCCTCTTTTTACACCCCAGTCA Rev: TCGGTTGTCAAGGTTTGTAGTTC
<i>CDK2</i>	Fwd: CCAGGAGTTACTTCTATGCCTGA Rev: TTCATCCAGGGGAGGTACAAC
<i>CDK3</i>	Fwd: TGGTGACACTGTGGTATCGC Rev: GGGCTTTTCGAGTCACCATC
<i>CDK4</i>	Fwd: CCCATCAGCACAGTTCGTGA Rev: AACACCAGGGTTACCTTGATCTC
<i>CDKN1A</i>	Fwd: TCTTGTACCCTTGTGCCTCG Rev: CGGCGTTTGGAGTGGTAGAA
<i>CDKN2A</i>	Fwd: CCCTGGATGAAGATGGACGG Rev: GATGGGGTACTGGCTTGGTC
<i>GAPDH</i>	Fwd: GCAGGGGGGAGCCAAAAGGG Rev: TGCCAGCCCCAGCGTCAAAG
<i>GSK3B</i>	Fwd: CGACTAACACCACTGGAAGCT Rev: GGATGGTAGCCAGAGGTGGAT

*PCNA* Fwd: CAAGTAATGTCGATAAAGAGGAGG  
Rev: GTGTCACCGTTGAAGAGAGTGG

---

### 3.2.7 Statistical analysis

Statistical analysis was performed as in 2.2.5.

### 3.3 Results

#### 3.3.1 Activation of the M2 receptor reversibly inhibits DPSCs proliferation

The ability of M2 receptor to modulate DPSCs proliferation was evaluated using the MTT assay. This assay measures viable cell's metabolic activity in proportion to the total number of cells in a well. To this end, DPSCs were treated with the M2 agonist (APE) which was shown in in the previous chapter to be selective for the M2 muscarinic receptor. Here, a more detailed investigation of the M2 agonist concentration and treatment duration is presented. Overall, DPSCs treated with the M2 agonist resulted in an inhibition in proliferation (Figure 3-1). The higher concentrations of M2 agonist, 250  $\mu\text{M}$  and 500  $\mu\text{M}$ , significantly inhibited proliferation as early as 24 h of treatment ( $P < 0.001$ ,  $P < 0.0001$ , respectively) and suppressed proliferation for the remainder of the treatment duration ( $P < 0.0001$ ). DPSCs treated with 100  $\mu\text{M}$  had significantly inhibited proliferation after 48 h and 72 h of treatment ( $P < 0.01$ ,  $P < 0.001$ , respectively). For DPSCs treated with the lower concentrations of M2 agonist, 25  $\mu\text{M}$  and 50  $\mu\text{M}$ , only the 50  $\mu\text{M}$  concentration after 72 h of treatment exhibited significant inhibited proliferation ( $P < 0.05$ ).

To further investigate the nature of the M2 agonist effect on proliferation inhibition, recovery experiments were carried out. DPSCs were treated with different concentrations of the M2 agonist for 72 h and then treatment was withdrawn for the remaining 72 h. The results showed that DPSCs treated with 250  $\mu\text{M}$  and 500  $\mu\text{M}$  of the M2 agonist were not able to recover their proliferation rate after treatment withdrawal and still showed significant inhibition in proliferation ( $P < 0.001$ ,  $P < 0.0001$ , respectively). However, DPSCs treated with 50  $\mu\text{M}$  and 100  $\mu\text{M}$  concentrations display enhanced recovery rate after treatment withdrawal. Altogether, both results (Figure 3-1 & Figure 3-2) suggest that concentrations of 100  $\mu\text{M}$  and below elicit a reversible inhibition in proliferation in a dose dependent manner. Concentrations above 100  $\mu\text{M}$  cause irreversible changes to the DPSCs proliferation and morphological structure (Sup 3-1), thus it may have unknown off-target effect and therefore these concentrations were not used in further investigations. Furthermore, the result suggests that the 100  $\mu\text{M}$  concentrations produced a sustained significant inhibition after 72 h of treatment when compared to the 50  $\mu\text{M}$  (Figure 3-1 & Figure 3-2).

To further confirm that the M2 agonist (APE) at a concentration of 100  $\mu\text{M}$  was able to inhibit DPSCs proliferation in a reversible manner, a more detailed recovery experiment was carried out. This was done by monitoring DPSCs proliferation after 72 h of stimulation the M2 agonist, where one group was allowed to recover for a further 72 h. The results showed the ability of DPSCs to recover their proliferation rate after 144 h displaying less difference to the untreated control (Ctrl) ( $P < 0.05$ ). However, the group that was under constant stimulation with the M2 agonist displayed more significant difference to the untreated control (Ctrl) at the 144 h mark ( $P < 0.0001$ ) (Figure 3-3). The result further showed that the proliferation rate of DPSCs recovery is significantly enhanced after 120 h and 144 h compared to ones that were under constant stimulation with the M2 agonist ( $\#$ :  $P < 0.05$ ,  $P < 0.0001$ , respectively). Based on all the above data, subsequent investigations were performed using 100  $\mu\text{M}$  of the M2 agonist (APE), which is in line with previous literature (Loreti et al., 2007; De Angelis et al., 2012; Ferretti et al., 2012, 2013; Pacini et al., 2014; Alessandrini et al., 2015; Cristofaro et al., 2018; Piovesana et al., 2018).

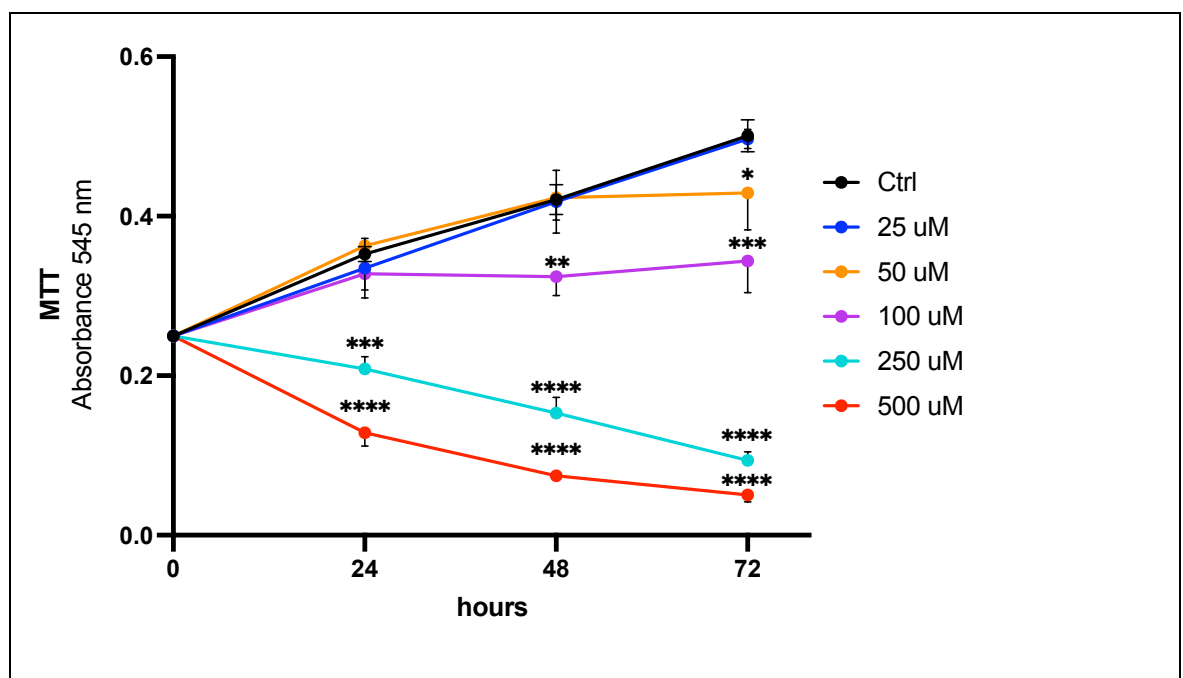
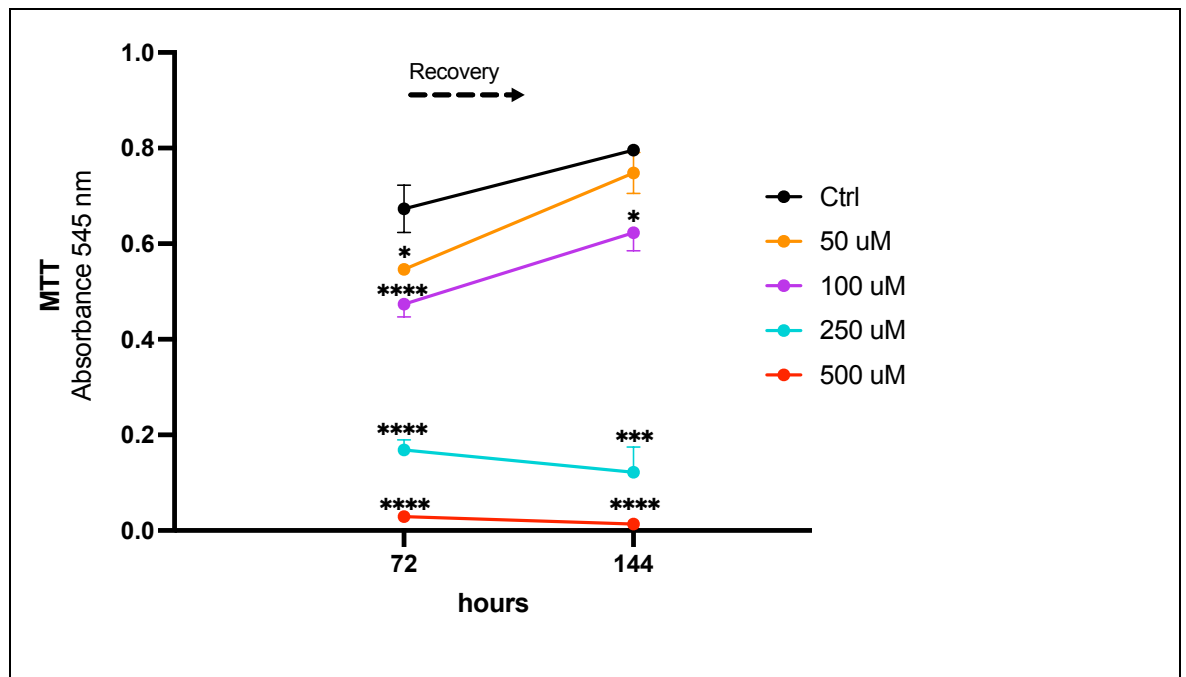
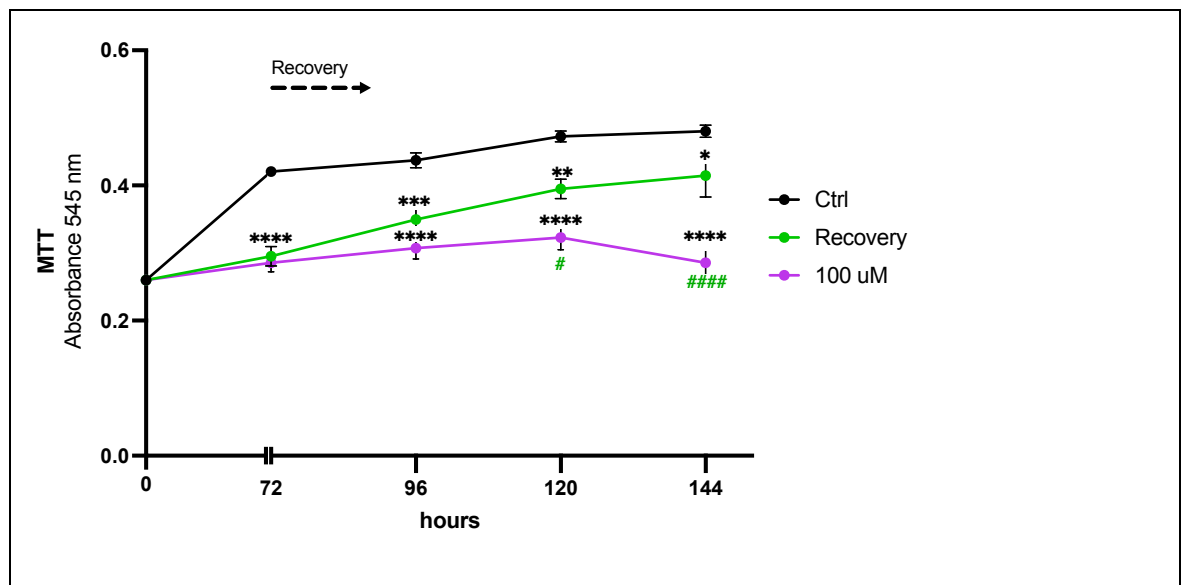


Figure 3-1 Proliferation of DPSCs over a 72 h time course after stimulation with the M2 agonist (APE). Compared to the untreated group (Ctrl), concentrations in the range of 250- 500  $\mu\text{M}$  resulted in the most significant proliferation inhibition, followed by 100  $\mu\text{M}$ , and then 50  $\mu\text{M}$ . The proliferation inhibition occurs timely and, in a dose, dependent manner. Data is derived from duplicate wells of three independent experiments (\*  $p < 0.05$ , \*\*  $p < 0.01$ , \*\*\*  $p < 0.001$ , \*\*\*\*  $p < 0.0001$ ).



**Figure 3-2 Proliferative recovery of DPSCs after stimulation with M2 agonist (APE).** Stimulation caused the expected proliferation inhibition at 72 h most significantly in  $\geq 100 \mu\text{M}$  concentrations. After stimulus was withdrawn, recovery is apparent at 144h in groups that were stimulated with lower concentrations of the M2 agonist (50- 100  $\mu\text{M}$  compared to ones with higher concentrations (250- 500  $\mu\text{M}$ ). Comparison made to the untreated control (Ctrl). Data is derived from duplicate wells of three independent experiments (\*  $p < 0.05$ , \*\*\*  $p < 0.001$ , \*\*\*\*  $p < 0.0001$ ).



**Figure 3-3 Proliferative recovery of DPSCs after stimulation with 100  $\mu\text{M}$  the M2 agonist (APE).** Stimulation caused the expected proliferation inhibition at 72 h. Stimulus was withdrawn from the recovery group and DPSCs proliferation was monitored up to 144 h. Compared to the untreated control (Ctrl), DPSCs in recovery displayed enhanced proliferation rate in relation to the ones that were exposed to APE treatment over the entire time course. Compared to DPSCs in recovery (#) DPSCs that had treatment during the entire time course shows significant inhibition in proliferation as early as 120 h. Data is derived from duplicate wells of three independent experiments (\*  $p < 0.05$ , \*\*\*  $p < 0.001$ , \*\*\*\*  $p < 0.0001$ ).

### 3.3.2 Activation of the M2 receptor does not affect DPSCs viability

While the recovery data above suggest M2 agonist (APE) stimulation at a 100  $\mu\text{M}$  does not have a detrimental effect on cell viability, a more detailed investigation

of cytotoxicity was carried out to discount a role for cell death by necrosis or apoptosis in the induced inhibition of proliferation. The trypan blue staining analysis showed a significant decrease in the total number of unstained (viable) cells after stimulation with the M2 agonist ( $<0.0001$ ) (Figure 3-4 A), supporting the MTT analysis (Figure 3-2 & Figure 3-3) in a role for the agonist in the inhibition of proliferation. Furthermore, the effect is not associated with cell death as there is no difference between untreated and treated conditions in terms of cells that absorbed the trypan stain (Figure 3-4 A). Analysis of released Lactate dehydrogenase (LDH) levels (a specific measure for cytotoxicity) showed the expected cytotoxicity in the positive control (cells treated with lysis buffer), however, the M2 agonist stimulation did not produced any cytotoxic effect on DPSCs compared to the untreated control (cells in normal media) (Figure 3-4 B). Furthermore, the CCK-8 analysis, which measures dehydrogenase levels inside viable cells, showed that M2 agonist stimulated DPSCs are still viable compared to cells deprived of serum (negative control “No FBS”) ( $P <0.001$ ), however, significantly less in numbers compared to unstimulated cells (Ctrl) ( $P <0.0001$ ) (Figure 3-4 C). This supports the above evidence of inhibited proliferation in relation to M2 activation, and further showed no apparent cytotoxicity at least due to cell necrosis.

Cytotoxicity or cell death might still occur through apoptosis, therefore, annexin V staining was employed as a marker of apoptosis. Annexin V binds to a phospholipid called phosphatidylserine that is expressed on the surface of cells in the early stage of apoptosis (Shlomovitz, Speir and Gerlic, 2019). This in combination with Propidium iodide (PI) staining aid to distinguish the difference between apoptosis and necrosis. The results showed absence of both Annexin and PI fluorescence in unstimulated cells (Ctrl) and cells stimulated with  $100 \mu\text{M}$  of the M2 agonist (APE), indicating no apparent apoptosis or necrosis (Figure 3-5 B-C & E-F). Whereas methanol treated DPSCs (positive control) showed an intense bright green colour (Figure 3-5 A), characteristic of the phosphatidylserine translocated across plasma membrane in apoptotic cells. Moreover, the red fluorescence indicates PI stain of the nucleus in the necrotic cells treated with higher concentrations of methanol (Figure 3-5 D). Collectively, these several lines of evidence showed that M2 activation via the M2 agonist does not affect the vitality of the cells.

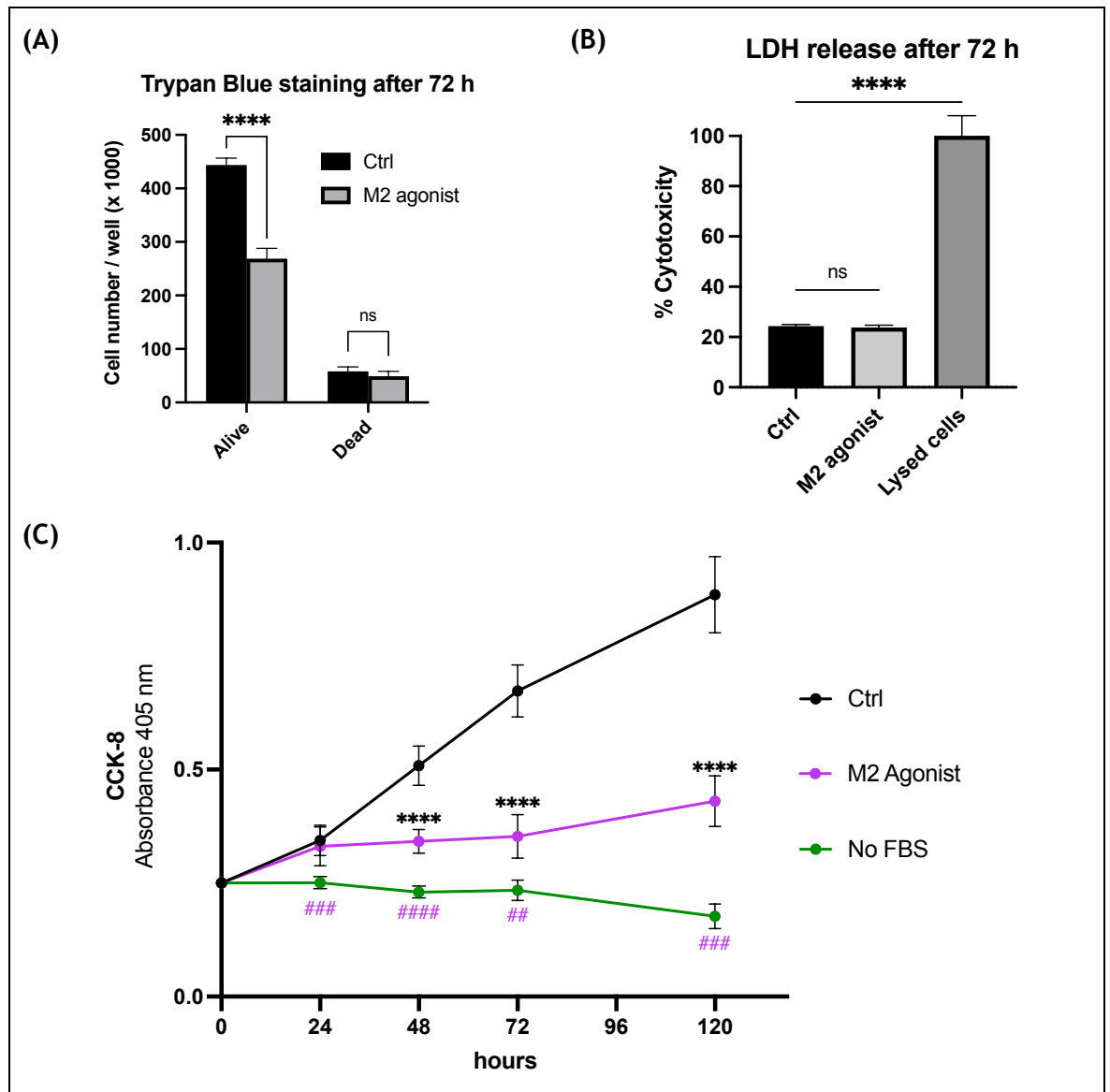


**Figure 3-4 Viability of DPSCs after stimulation with 100  $\mu$ M of the M2 agonist (APE).** (A) Cell growth and survival measured by trypan blue staining showed the number of viable (alive) cells stimulated with the M2 agonist is significantly lower compared to untreated (Ctrl). There is no difference between the number of dead cells present in stimulated or untreated controls (Ctrl). (B) LDH release showed no difference between physiological cell death in untreated control (Ctrl) and cells stimulated with the M2 agonist. The positive control (lysed cells) showed significant cytotoxicity compared to both untreated control (Ctrl) and cells stimulated with the M2 agonist. (C) CCK-8 indicates viability of cells stimulated with the M2 agonist compared to negative control (No FBS) (comparison in #), and significantly less numbers of viable cells compared to unstimulated cells (Ctrl) (comparison in \*). No FBS: cells grown without FBS in the media. Data for all is derived from duplicate wells of three independent experiments (ns: not significant, \*\*\*\*  $p < 0.0001$ ). (##  $p < 0.01$ , ###  $p < 0.001$ , ####  $p < 0.0001$ ).

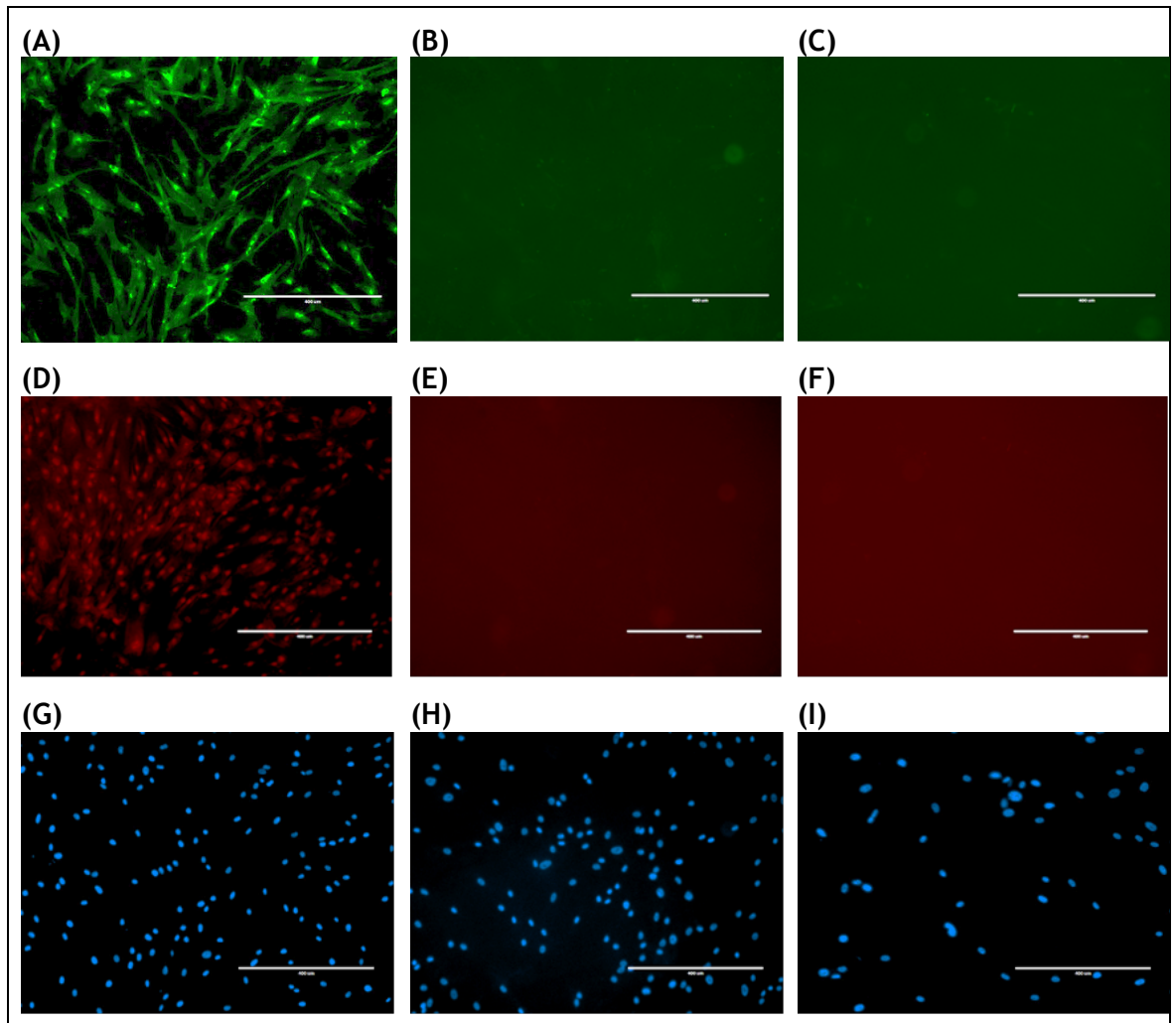


**Figure 3-5** Fluorescent microscopic images of Annexin V/PI stained cells. (A-C) Annexin V staining are only apparent under methanol-induced apoptosis conditions of the positive control (A), while (B & C) shows absence of staining in the untreated control and cells stimulated with the M2 agonist (APE). (D-F) PI staining are only apparent in the damaged nucleus of methanol-induced necrosis of the positive control, while (E & F) shows absence of staining in the untreated control and cells stimulated with the M2 agonist. (G-I) DAPI staining of the nucleus reflecting a smaller number of cells after stimulation with the M2 agonist (I) on account of the inhibited proliferation. Annexin V positive control are cells treated with 30% methanol. PI positive control are cells treated with 70% methanol. Stimulation with the M2 agonist (APE) was carried out for 72h before staining. All images shows 2D projections of confocal stacks and are a representative of three independent experiments. Scale bars = 400  $\mu$ m.

### **3.3.3 Activation of the M2 receptor inhibits cell cycle progression**

The evidence suggests that M2 activation causes a reversible inhibition in proliferation without affecting DPSCs viability. This suggests that M2 signalling may modulate cell cycle progression. Analysis of cell cycle staining was performed via a bi-parametric analysis of BrdU labelling versus propidium iodide-labelled DNA content, allowing analysis of the G1, S, and G2 phases of cell cycle after 72 h of stimulation with the M2 selective agonist (100  $\mu$ M APE). The analysis revealed a significant reduction of stimulated cells in both the G1 and S phases and accumulation of stimulated cells in the G2 phase ( $P < 0.0001$ ) (Figure 3-6). The reduction in the S phase suggested reduction in proliferation as BrdU is used to detect active proliferating cells, where it binds to the newly synthesised DNA of replicating cells during the S phase of the cell cycle (Cecchini, Amiri and Dick, 2012). Furthermore, the accumulation of stimulated cells in the G2 phase suggests a cell cycle arrest at this phase. Thus, the data collectively indicate that M2 activation inhibits DPSCs proliferation by implementing a cell cycle arrest in the G2/M phase just before cell division.

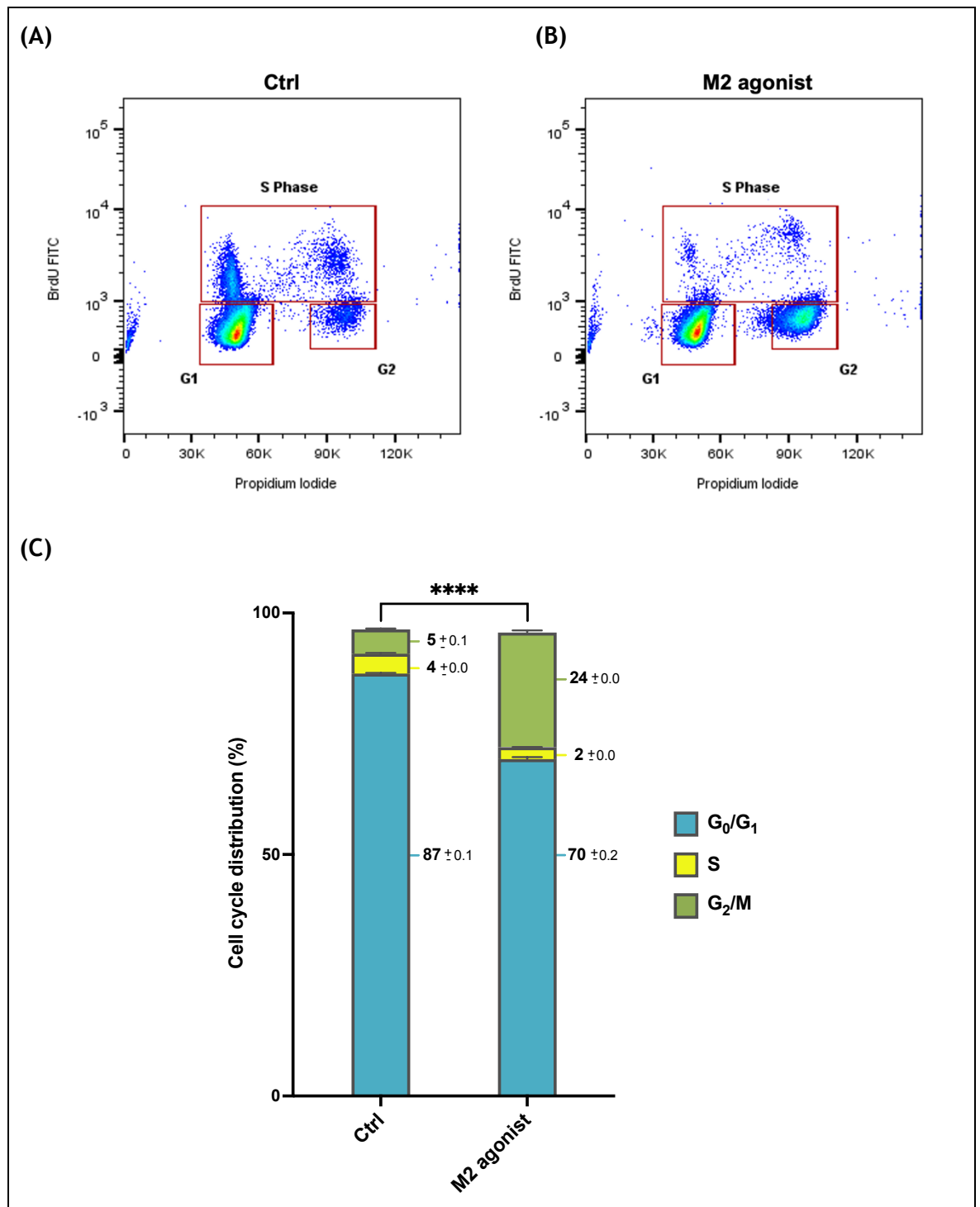


Figure 3-6 Flow cytometry analysis of DPSCs after 72 h of stimulation with the M2 agonist. (A-B) Representative plots of bivariate analysis of BrdU incorporation (ordinate) and propidium iodide- labelled DNA content (abscissa) in (A) untreated control (Ctrl) and (B) cells stimulated with the M2 agonist (100  $\mu$ M APE). The BrdU labelled cell fraction (S Phase) appears reduced after stimulation, while the propidium iodide- labelled cell fraction in G2 phase appears more after stimulation. (C) Quantitative measurement of cell cycle phases showed significant reduction in the percentage of cells in both the G<sub>0</sub>/G<sub>1</sub> and S phase of cells stimulated with the M2 agonist. The analysis also showed significant accumulation of cells in the G<sub>2</sub>/M phase after stimulation with the M2 agonist. Comparison made to the untreated control (Ctrl). Data is derived from duplicate wells of three independent experiments (\*\*\*\*  $p < 0.0001$ ).

Changes in expression of key genes reported to be involved in proliferation and cell cycle were analysed. Significant differential expression was witnessed for ten out of fourteen investigated genes encoding cyclins, cyclin-dependent kinases, and other proteins involved in cellular replication (Figure 3-7). The *CCNA2* gene, known as cyclin- A2, exhibited significant downregulated expression ( $P < 0.0001$ ) following stimulation with the M2 agonist. The *CCNB1* and *CCNB2* genes, known as cyclin- B1 and cyclin- B2, exhibited significant downregulated expression ( $P < 0.01$ ) following stimulation with the M2 agonist. While the *CCND1* and *CCND2* genes, known as cyclin-D 1 and 2, exhibited significant upregulated expressions ( $P < 0.001$ ,  $P < 0.0001$ , respectively). The *CCNE2* gene, known as cyclin-E2, displayed significant upregulated expression following stimulation with the M2 agonist. The *CDC14A* gene, known as cell division cycle 14A, displayed significant upregulated expression ( $P < 0.0001$ ), while *CDC25A* displayed significant downregulated expression ( $P < 0.001$ ). The *CDK4* gene, known as cyclin dependent kinase 4, displayed significant upregulated expression ( $P < 0.0001$ ) following stimulation with the M2 agonist. The *CDKN1A* gene, known as cyclin dependent kinase inhibitor 1A, significantly increased more than six-folds ( $P < 0.0001$ ) following stimulation with the M2 agonist. The *GSK3B* gene, known as glycogen synthase kinase 3 beta, displayed significant upregulated expression ( $P < 0.0001$ ). Similarly, the *PCNA* gene, known as proliferating cell nuclear antigen, displayed significant upregulated expression ( $P < 0.0001$ ) following stimulation with the M2 agonist. All which support evidence of for the involvement of M2 activation in modulating DPSCs proliferation and cell cycle.

Collectively, all the data above indicates that M2 activation via the selective M2 agonist places DPSCs in a quiescent state without affecting their viability. Where upon withdrawing the M2 agonist, DPSCs resume their normal proliferation state.

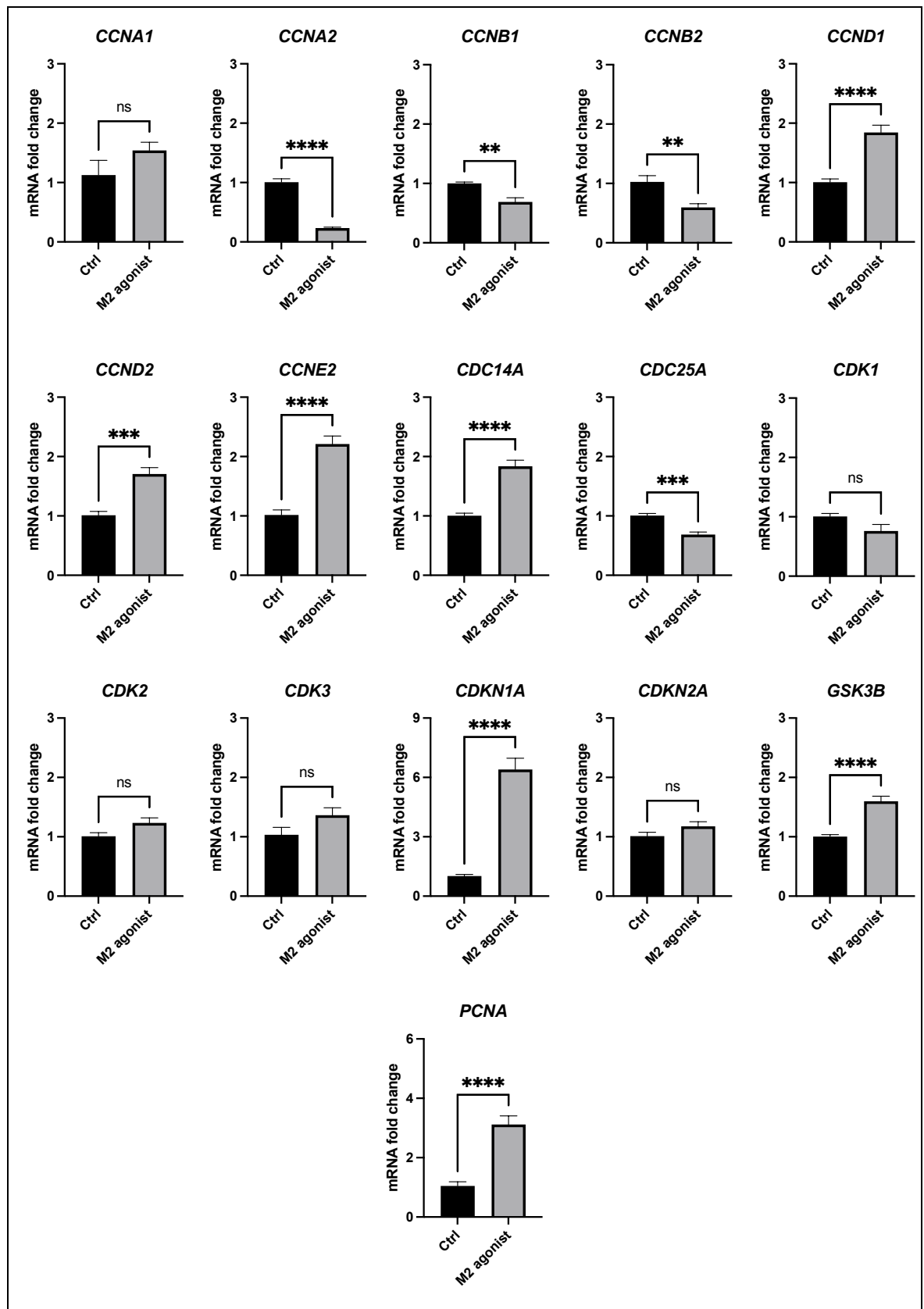


Figure 3-7 Analysis of genes involved in proliferation and cell cycle following stimulation with the M2 agonist for 72 h. Data for all are derived from duplicate wells of three independent experiments and is presented as mean fold change compared to the untreated control (Ctrl) using the  $2^{-\Delta\Delta C_t}$  method (Livak and Schmittgen, 2001). Gene expression is relative to the housekeeping gene (GAPDH). A difference of  $P < 0.05$  was considered statistically significant. (ns: not significant, \*\*\* $p < 0.001$ , \*\*\*\*  $p < 0.0001$ ).

### 3.4 Discussion

In the previous chapter, it was confirmed that DPSCs express three out of five muscarinic receptor transcripts with the M2 muscarinic receptor as the most dominant subtype. Furthermore, the presence and distribution of the M2 protein was confirmed through western blotting and Immunofluorescent analysis. In addition, the initial data suggested functional expression of the M2 receptor upon stimulation with its selective agonist (APE). The selectivity of the M2 agonist (APE) was also confirmed, and the resultant stimulation caused inhibition of DPSCs proliferation. Therefore, this chapter set to explore this further by investigating the nature of this proliferation inhibition and if it had an impact on DPSCs survival, viability and cell cycle progression.

Indeed, to begin to determine the function of M2 receptor, DPSCs were treated with its specific agonist (APE) and the impact of treatment was assessed in terms of cytotoxicity, viability and most notably proliferation. In several cell types (e.g. Schwann cells, oligodendrocytes, glioblastoma cells, bladder cancer cells, and adipose MSCs) the M2 receptor has been found to mainly control cell proliferation (Loreti *et al.*, 2007; De Angelis *et al.*, 2012; Ferretti *et al.*, 2013; Pacini *et al.*, 2014; Piovesana *et al.*, 2018). In human adipose-derived MSCs, activation of this receptor results in inhibition of proliferation and an arrest in cell cycle (Piovesana *et al.*, 2018). This was after stimulation with the same M2 selective agonist (APE). The M2 selective agonist (APE) is a synthetic modified alkaloid derived by a metabolite produced by the areca nut (Voigt *et al.*, 2013), and designed to mimic the effect of acetylcholine when it binds to the M2 receptor in nature. Considerable evidence have shown it to be selective for the M2 subtype and thus has been used to study the function of the M2 receptor (Loreti *et al.*, 2007; De Angelis *et al.*, 2012; Ferretti *et al.*, 2013; Alessandrini *et al.*, 2015). Previous literature investigating the effect of M2 stimulation with the M2 selective agonist (APE) has used concentrations of 100  $\mu\text{M}$  and below (Loreti *et al.*, 2007; De Angelis *et al.*, 2012; Ferretti *et al.*, 2012, 2013; Ugenti *et al.*, 2014; Pacini *et al.*, 2014; Alessandrini *et al.*, 2015; Di Bari *et al.*, 2015; Cristofaro *et al.*, 2018; Piovesana *et al.*, 2018; Cristofaro, Alessandrini, *et al.*, 2020; Cristofaro, Limongi, *et al.*, 2020). Here, concentrations in the  $\mu\text{M}$  range were used over several timepoints

for the fact that DPSCs is a different cell type that have not been explored with the reported agonist.

An assessment of the effect of the M2 agonist was made using an MTT based assay that was intended to measure DPSCs proliferation. This assay measures ability of viable cells to reduce the yellow water-soluble tetrazolium dye, primarily by mitochondria as a marker of metabolic activity, and reflect a colour change that is proportional to the number of assayed cells (Korzeniewski and Callewaert, 1983). The result suggests that the M2 agonist caused a dose and time dependent inhibition of DPSCs proliferation. However, the 100  $\mu\text{M}$  concentration stands as the most appropriate concentration that caused a sustained inhibition after 72 h of stimulation. This is comparable to reported literature which demonstrates that 100  $\mu\text{M}$  of the M2 agonist impaired cell growth or effectively reduced proliferation (Loreti et al., 2007; De Angelis et al., 2012; Ferretti et al., 2012, 2013; Pacini et al., 2014; Alessandrini et al., 2015; Cristofaro et al., 2018; Piovesana et al., 2018). Furthermore, APE stimulated DPSCs were able to recover their proliferation rate once the M2 agonist was withdrawn. Based on this, subsequent investigations were performed using 100  $\mu\text{M}$  of the M2 agonist (APE) for 72 h. The inhibitory effect of the M2 agonist was expected considering the notion that the M2 subtype is an inhibitory muscarinic receptor in nature (Wessler and Kirkpatrick, 2012). The recovery data here suggest M2 agonist stimulation at a 100  $\mu\text{M}$  does not have a detrimental effect on cell viability, however a more detailed investigation of cytotoxicity was warranted. Thus, the following assessment was whether the induced inhibition in proliferation was a sequel to cell death by means of necrosis or apoptosis.

Trypan blue staining is a simple analysis to count the number of live and dead cells (Strober, 1997). The principle of this staining denotes that cells with compromised cell membranes will retain the blue dye and thus suggesting cell necrosis. Similarly, the LDH assay measures the released lactate dehydrogenase enzyme from cells with damaged membrane (i.e., necrotic cells) (Kumar, Nagarajan and Uchil, 2018). Both assays showed that stimulation with the M2 agonist did not exhibit cytotoxic effects on DPSCs. Furthermore, trypan blue staining of live DPSCs support the MTT data by showing reduced total number of cells following stimulation with the M2 agonist. Here arises the need to investigate the viability of stimulated cells. Unlike the LDH assay, the CCK-8 assay measures

dehydrogenase activities within living viable cells that can reduce the WST-8 tetrazolium salt of the CCK-8 kit (2-(2-methoxy-4-nitrophenyl)-3-(4-nitrophenyl)-5-(2,4-disulfophenyl)-2H-tetrazolium, monosodium salt) (Ishiyama *et al.*, 1997). The analysis supports the evidence of induced reduction in the number of cells following stimulation with the M2 agonist, however, it also showed that the cells are still viable compared to cells deprived of serum. Collectively, these lines of evidence suggest that the inhibited proliferation in relation to M2 activation, is not a sequel to cell death at least by necrosis. Here then arises the need to investigate apoptosis, as cytotoxicity or cell death might still occur by this means. Therefore, annexin V staining was employed as a marker of apoptosis. Annexin V combined with PI staining is an excellent method in detecting both necrosis and apoptosis. Apoptosis is detected by binding of the fluorescent-tagged annexin V to an externalised phospholipid expressed by cells in early stage of apoptosis (Cummings and Schnellmann, 2004). This phospholipid, called phosphatidylserine, is expressed on the plasma membrane of the apoptotic cell and generates a green fluorescent signal once bound to an Annexin V-FITC conjugated antibody. The PI staining aims at detecting membrane integrity and necrosis. Necrosis is detected by measuring the permeability of the plasma membrane to the DNA-binding dye of PI to the cell's nucleus (Cummings and Schnellmann, 2004). Normal healthy cells would have an intact plasma membrane that prevents penetration of PI to the nucleus. Whereas methanol treated cells (positive control) exhibit clear fluorescence for both Annexin and PI. Methanol has been used to induce cytotoxicity, induction of apoptotic markers, and investigating cell death (Spyridopoulos *et al.*, 2001; Nguyen, Nguyen and Truong, 2020). Methanol treatment is an excellent method to detect the journey from apoptosis to necrosis. Hence, 30% methanol was used to induce apoptosis which was followed directly by adding the Annexin V-FITC buffer to only capture apoptosis (Figure 3-5 A). While 70% methanol was used to induce necrosis directly and capture necrosis without apoptosis (Figure 3-5 D). The results showed absence of both Annexin and PI fluorescence in unstimulated and stimulated cells, indicative of no apparent apoptosis or necrosis following stimulation with the M2 agonist. Collectively, this is strong evidence that the M2 receptor effect (i.e., inhibition of proliferation via the M2 agonist) is not due to controlled or uncontrolled cell death. Thus, supporting the argument that M2 may contribute to maintain DPSCs in quiescent status.

The analysis of the cell cycle by FACS has confirmed that there is a cell cycle arrest induced by activation of the M2 receptor. Indeed, the M2 agonist caused less cells progressing through the S phase (active synthesis of DNA) compared to untreated cells. The normal cell cycle is comprised of four sequential phases with three major checkpoints (Figure 3-8) (Alberts *et al.*, 2008). The G1 and G2 phases are gap phases where cells grow their size to accommodate proteins and organelles for the required replication. The S phase involves DNA synthesis and chromosome replication, together with the G1 and G2 phases they are referred to as the interphase which is the longest part of the cell cycle. The M phase is the mitotic phase which involves several stages that results in mitosis and the actual division to form two new cells. Progression through the cell cycle phases is controlled by three restriction points or checkpoints that can act as termination points along the cell cycle, where this control system monitors the proper progression of size growth and replication integrity. Cell cycle analysis via flow cytometry enables estimation of the percentages of a cell population in the different phases of the cell cycle. The most common way to achieve this quantitation is by measuring its DNA content, which for an example, doubles during S phase (Alberts *et al.*, 2008). Propidium iodide (PI) was used to label DNA as this method is considered the most widely used for cell cycle analysis (Alberts *et al.*, 2008). The analysis showed that the M2 agonist decreased the percentage of cells in the G1 phase and significant accumulation in the G2 phase. To enable a bi-parametric analysis, BrdU was used to label DNA of active proliferating cells in the S phase. The artificial thymidine analogue bromo-deoxyuridine (BrdU) enables identification of cells progressing through the S phase and incorporating the BrdU molecules into newly synthesised DNA as a substitute for thymidine (Mead and Lefebvre, 2014). The analysis showed reduction of BrdU labelled cells following stimulation with the M2 agonist. Collectively, the data suggest that M2 activation via the M2 agonist causes inhibition in proliferation by arresting the progress of cells prior to division or in the G2/M phase (Figure 3-9).

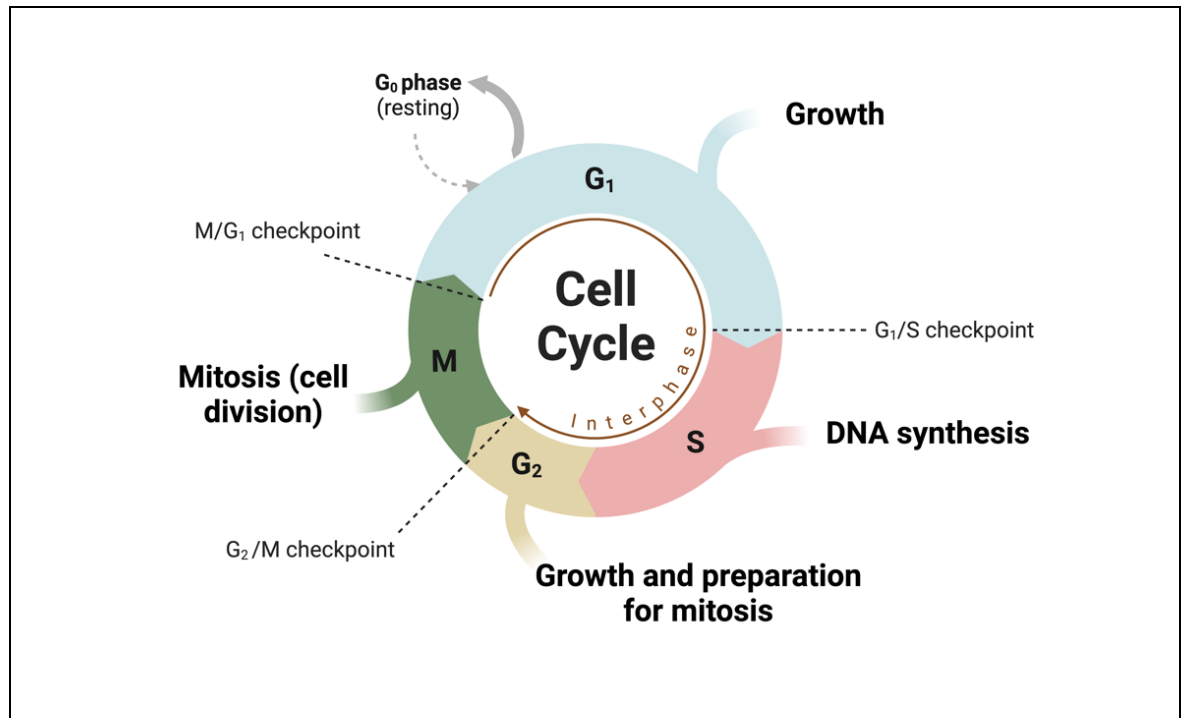


**Figure 3-8 Overview of cell cycle phases.** During entry to the G<sub>1</sub> phase, the cell starts to grow in size and synthesise RNAs and proteins for the daughter cell. As the cell progress into the S phase, DNA synthesis and chromosome replication take place and so that each of the two cells receive one set of DNA. The cell then progresses into another growth phase known as G<sub>2</sub>, where it continues to grow and restructure its content in preparation for mitosis. The G<sub>1</sub>, S, G<sub>2</sub> phases are collectively refer to as the interphase of cell cycle. After the interphase, the M phase begins, where the process of mitosis starts by splitting its DNA continent and organelles into two identical cells, and then complete division of cytoplasm to produce two separate cells. Non replicating cells leave the cell cycle in G<sub>1</sub>, entering the G<sub>0</sub> state, where they remain in a resting phase or a 'quiescent' state. The cell cycle is usually regulated by three main checkpoints. The G<sub>1</sub>/S checkpoint is the point where the cell size and DNA integrity is checked, depending on internal and external conditions it can either commits to enter S phase or revert to the quiescent state at G<sub>0</sub>. The G<sub>2</sub>/M checkpoint is another point where the cell size and DNA replication is checked prior to commitment into M phase. The G<sub>2</sub>/M checkpoint occurs during the M phase, where chromosome spindle attachment is checked before complete division is initiated.

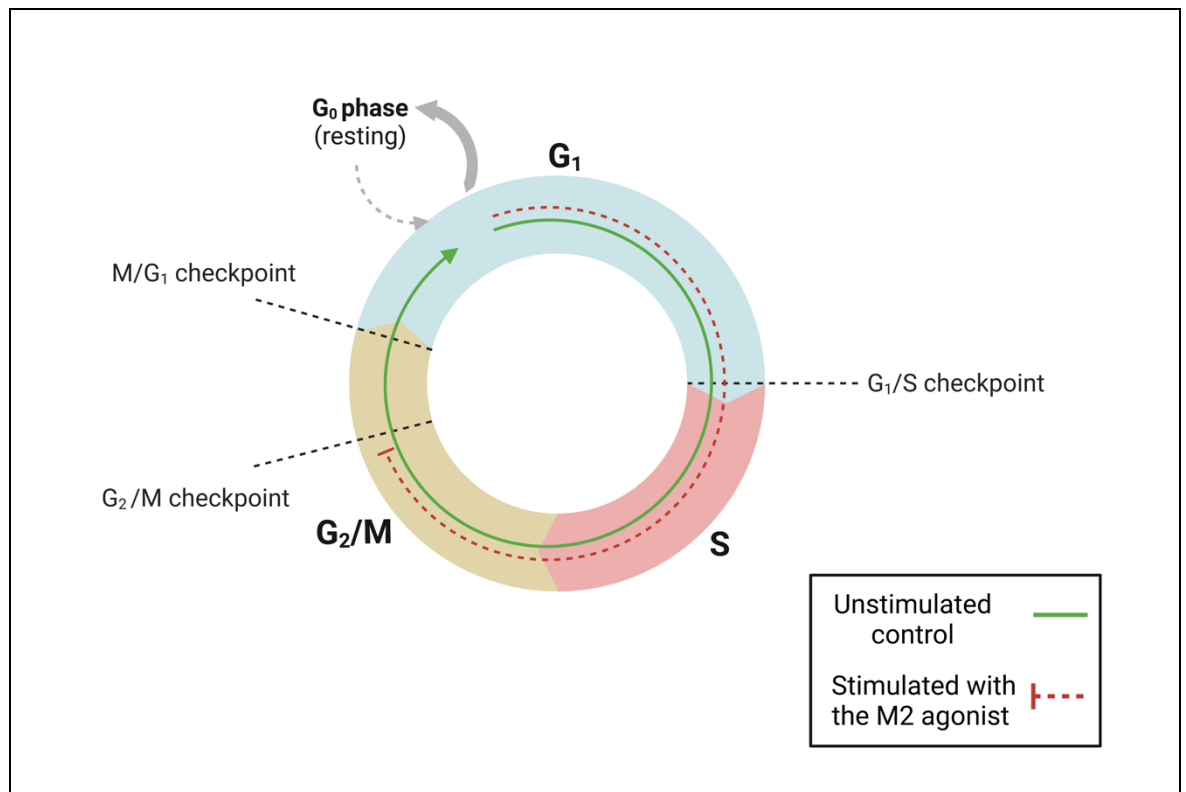


**Figure 3-9 Effect of M2 activation on cell cycle progression. DPSCs are less present in G<sub>1</sub> and S phases and more accumulated in the G<sub>2</sub>/M Phase after stimulation with M2 agonist as determined by the BrdU/PI analysis. DPSCs stimulated with M2 agonist are not progressing through beyond G<sub>2</sub>/M Phase compared with the unstimulated control. It seems that M2 activation arrest DPSCs at the G<sub>2</sub>/M phase.**

The cell cycle analysis further explored the expression pattern of key genes that encode proteins functional in regulating the cell cycle. Indeed, the genes investigated in this chapter are reported to exert an important role in cell cycle control and include cyclins, cyclin-dependent kinases (CDKs), cell division cycle phosphatases (CDCs), and CDK inhibitors (CDKIs) (Vermeulen, Berneman and Van Bockstaele, 2003; Yu, Kovacevic and Richardson, 2007; Satyanarayana and Kaldis, 2009). Cyclins are key proteins that drive the cell cycle and replication process. Cyclins bind and activate their partner kinases, hence, the name cyclin-dependent kinases (CDKs) (Satyanarayana and Kaldis, 2009). Cyclins of the A type (i.e., Cyclin A1 and A2 encoded by *CCNA1* and *CCNA2*, respectively) binds and activates CDK2 and the complex functions in regulating transition through G<sub>1</sub> and S phases of the cell cycle (Martínez-Alonso and Malumbres, 2020). In the S phase, cyclin A replace cyclin E partnership with CDK2, and the new complex cyclin A/CDK2 functions in progressing the cell-cycle through the S phase (Ding *et al.*, 2020). The results here showed downregulated expression of the gene that encode cyclin A2 (i.e., *CCNA2*), supporting the reported results of the M2 agonist in promoting cell cycle arrest. Cyclins of the B type (i.e., Cyclin B1 and B2 encoded by *CCNB1* and *CCNB2*, respectively) activate their catalytic partner CDK1 and the complex promotes

mitosis progression (Gong and Ferrell Jr, 2010). The results here showed downregulated expression of the genes that encode Cyclin B1 and B2 (i.e., *CCNB1* and *CCNB2*), supporting the reported results of the M2 agonist in arresting cell cycle at the G2/M phase as seen in (Figure 3-6). Cyclins of the D type (i.e., Cyclin D1 and D2 encoded by *CCND1* and *CCND2*, respectively) activate their catalytic partners CDK4 and CDK6 and the complex promotes G1 progression of the cell cycle (Sherr, 1994; Satyanarayana and Kaldis, 2009). While Cyclins of the E type (i.e., Cyclin E1 and E2 encoded by *CCNE1* and *CCNE2*, respectively) partner with CDK2 in mammalian cells to regulate entry into S phase (Heller *et al.*, 2011; Yeeles *et al.*, 2015) The results here showed upregulated expression of *CCND1*, *CCND2*, *CCNE2* and *CDK4* genes that encode cyclin D1-2, Cyclin E2, and CDK4. This upregulation is suggestive of an increase in proliferation as cells progress through the G1 phase of the cell cycle as reported in the literature (Aktas, Cai and Cooper, 1997). However, this is in contrast to the observed effect of the M2 agonist in promoting cell cycle arrest. This upregulation can be attributed to a stress-induced gene expression or a mechanism unrelated to cell cycle. For example, it has been reported that ectopic overexpression of cyclin E encourages Embryonic stem cells self-renewal (Coronado *et al.*, 2013; Gonzales *et al.*, 2015). Thus, suggesting that the upregulated expression of cyclin E following M2 agonist stimulation might be attributed to the M2 receptor functioning in retaining DPSCs ability to self-renew.

The cell division cycle phosphatases (CDCs) function in modulating phosphorylation of CDKs. For an example, CDC14A have been reported to dephosphorylate CDK2 that is in partnership with cyclin E, hence, its involvement in the progression of cells from the G1 to S phase of cell cycle (Yu, Kovacevic and Richardson, 2007). However, most of CDC14A protein function takes place in the M phase of the cell cycle (Mocciaro *et al.*, 2010). The results here showed upregulated expression of *CDC14A* following stimulation with the M2 agonist, supporting the accumulation of stimulated cells in the G2/M phase observed in the cell cycle analysis. Another CDC phosphatase required for progression through G1 and S phases of the cell cycle is CDC25A, which dephosphorylates CDK2 that is in partnership with cyclin E (Ekholm and Reed, 2000). Inability of CDC25A to dephosphorylate CDK2 can compromise the transition through the S phase (Bartek and Lukas, 2001). The results here showed downregulated expression of *CDC25A*

gene, in support of a cell cycle arrest after stimulation with the M2 agonist. In fact, overexpression of CDC25A accelerates the G1/S transition by overriding DNA replication restrictions or checkpoints, hence, this expression is usually reported in cancer literature (Molinari *et al.*, 2000).

Key regulators of cell cycle progression are CDK inhibitors (CDKIs). Most notably the P21 protein (encoded by the *CDKN1A* gene) which is a member of CDKIs family that can inactivate all CDKs rendering an arrest in cell cycle (Harper *et al.*, 1993). Indeed, overexpression of P21 can override the function of cyclin D/CDK4,6 complex resulting in an inhibition in the start of the cell cycle (LaBaer *et al.*, 1997; Welcker *et al.*, 1998; Cheng *et al.*, 1999). In this instance, p21 binds the complex by simultaneously binding both the cyclin and CDKs in order to achieve its inhibitory function (Harper *et al.*, 1995; Ball, 1997). Furthermore, P21 is known for its ability to interact and disable the function of various cyclin/CDK complexes, thus it is able to enforce an arrest at any phase of the cell cycle (Harper *et al.*, 1993; Pavletich, 1999). It has been reported that overexpression of p21 can result in a decrease in cells progressing through the S phase (Mansilla *et al.*, 2020). In fact, genetic deletion of p21 gene (*CDKN1A*) was shown to limit human epithelial cell lines to go through their normal cell cycle phases (Spencer *et al.*, 2013; Arora *et al.*, 2017; Barr *et al.*, 2017). The results here showed overexpression of *CDKN1A* by nearly six-folds following stimulation with the M2 agonist. This highlights that p21 might be a strong candidate in endorsing the effect of M2 activation on proliferation and cell cycle progression of DPSCs. Another member of CDKIs family investigated here is *CDKN2A* which encodes the p16 protein. This CDK inhibitor interacts strongly with CDK4 and influences the progression of the cell cycle (Serrano, Hannon and Beach, 1993). The results here showed no changes in *CDKN2A* expression following stimulation with the M2 agonist. This might be due to the nature of the reversible inhibition seen here with the M2 agonist, as the encoded protein p16 is more involved in events that result in an irreversible arrest in proliferation (e.g., cell senescence) (Kumari and Jat, 2021).

The Proliferating Cell Nuclear Antigen (PCNA) protein is an essential regulator of several cellular functions, as it interacts with hundreds of proteins that function in cell-cycle progression, DNA replication, and DNA integrity monitoring processes (Krishna *et al.*, 1994; De Biasio and Blanco, 2013; Boehm, Goldenberg and Washington, 2016; Choe and Moldovan, 2017). In fact, PCNA has been reported to

act as a master conductor of replication-linked processes (Moldovan, Pfander and Jentsch, 2007). For an example, within the context of the cell cycle, PCNA enhances the processivity of DNA synthesis enzymes and tethers polymerases firmly to DNA (Moldovan, Pfander and Jentsch, 2007). It exerts a control over the DNA replication step and prevents re-replication (Ducoux *et al.*, 2001; Xu *et al.*, 2001; Frouin *et al.*, 2003). It is involved in regulating chromatin assembly, CDK inhibition and activation, and mismatch repair during a faulty DNA replication process (Warbrick *et al.*, 1995; Fukami-Kobayashi and Mitsui, 1999; Dzantiev *et al.*, 2004; Moldovan, Pfander and Jentsch, 2006). In particular, overexpression of cyclin D1 in conjunction with PCNA can directly inhibit the DNA synthesis step (i.e., inhibition in S phase progression) (Fukami-Kobayashi and Mitsui, 1999). The p21 protein also have an interaction with PCNA in tuning cell cycle progression and proliferation (Mansilla *et al.*, 2020). In fact, both proteins can interact and modulate proliferation arrest independent from CDKs regulatory function in the cell cycle (Cayrol, Knibiehler and Ducommun, 1998; Cazzalini *et al.*, 2003). In the context of the cell cycle, p21 can regulate PCNA-dependent functions (Mansilla *et al.*, 2020). The results here showed increased expression of *PCNA* following stimulation with the M2 agonist. The overexpression of *PCNA* mRNA is not unexpected. It has been reported that stimulation with the M2 agonist resulted in increased expression pattern of PCNA proteins in human glioblastoma cancer stem cells (Cristofaro, Alessandrini, *et al.*, 2020). The authors suggested that this increase could be because of the accumulation of cells in G1-G2/M phases and not due to increase in proliferation as their data showed similar M2 agonist induced inhibition in proliferation. In another report, the same M2 agonist was used to induced inhibition in proliferation and arrest in the cell cycle of adipose-MSCs (Piovesana *et al.*, 2018). However, the authors showed downregulated expression of PCNA transcript and protein following stimulation with the same M2 agonist (i.e., APE). This difference in *PCNA* gene expression here, in association with the cell cycle arrest by the same M2 agonist, could be attributed to the difference in cell types. It is expected that cells of different types arrested using the same condition can display cell-type specific differences in gene expression (Marescal and Cheeseman, 2020). The increased expression of *PCNA* here might be encouraged by expression of *CDKNA1* or the other hundreds of proteins that PCNA interact with, thus, stands as an interesting area to explore.

The protein kinase Glycogen synthase kinase-3B (GSK-3B), encoded by *GSK3B* gene, can phosphorylate cyclin D1 and CDC25A, and thus have an influence on cell cycle progression (Lin *et al.*, 2020). In the G1 phase of the cell cycle, GSK-3B phosphorylation of cyclin D1 promotes progression of cells through that phase. The results here showed increased expression of both *GSK3B* and *CCND1* mRNA levels following stimulation with the M2 agonist. However, the flow cytometry data indicate an arrest in cell cycle or in particular reduced cell progression in the G1 phase. This disparity in the results suggest that *GSK3B* expression might be unrelated to the expected normal function in cell cycle. GSK-3B have been reported to have a significant influence on a number of biological processes and it is involved in several pathways such as Wnt/ $\beta$ -catenin, Hedgehog, Notch and Mammalian target of rapamycin (mTOR) pathways (Cohen and Frame, 2001; Nishimura *et al.*, 2016). Moreover, this protein kinase acts as a substrate for a variety of proteins that function in cellular metabolism, transcription, translation, cytoskeletal regulation, differentiation and proliferation (Grimes and Jope, 2001; Manoukian and Woodgett, 2002). In addition, *GSK3B* expression is influenced by multiple regulatory mechanisms such as extracellular signal-regulated kinases (ERKs), protein kinase B (known as Akt), protein kinase C (PKC), and protein kinase dependent on Cyclic adenosine monophosphate (cAMP) signalling (Luo, 2009). All of which are involved in metabotropic signalling of muscarinic receptors including the M2 muscarinic receptor (see chapter 1 for a review). This suggest that activation of the M2 receptor triggers several pathways where GSK-3B is involved and are worthy to be explored.

The results here portray that M2 activation is involved in other cellular process in DPSCs as yet to be explored. However, with regards to the observed cell cycle arrest, cell senescence and quiescence needs to be discussed to put the investigated gene expression into context. While cell senescence (cessation of cell division) could be interpreted here, senescence is highly dynamic, multi-step process, that has a distinct phenotypic that does not involve reversible proliferation arrest (Kumari and Jat, 2021). Indeed, cellular senescence is different from quiescence which is another form of cell cycle arrest. Quiescence maintains cells in a non-proliferative status (a poised state), ready to re-enter cell cycle when appropriate conditions are regained. Indeed, the key difference between senescence and quiescence is that cells in the latter state are able to

resume proliferation once the conditions are favourable (e.g., stimulation with growth factors or mitogenic signalling, or as in here after stimulus withdraw) whereas senescent cells can not (Campisi and d'Adda di Fagagna, 2007; Gorgoulis *et al.*, 2019; Kamal *et al.*, 2020). CDKIs promote quiescence and quiescent cells typically display high levels of these proteins (Aktas, Cai and Cooper, 1997; Cheung and Rando, 2013; Arora *et al.*, 2017; Barr *et al.*, 2017). Furthermore, CDKIs genes are upregulated once quiescence is induced, thus, they stand as initial markers of cell cycle arrest (Coller, Sang and Roberts, 2006; Fukada *et al.*, 2007). Measuring the expression levels of CDKIs such as p21 and p16 (encoded by *CDKN1A* and *CDKN2A*, respectively) have been advised as key in detecting the nature of cell cycle arrest, where p21 in particular is not constantly expressed by senescent cells (Da Silva-Álvarez *et al.*, 2019). The results here showed overexpression of *CDKN1A* and no changes in the expression of *CDKN2A*. This is suggestive that the induced cell cycle arrest is via *CDKN1A* that encodes the P21 protein, and thus, quiescence of DPSCs by activation of the M2 receptor is likely.

Quiescence can happen due to transient stress, during which, p53 is induced to activate mechanisms involved in monitoring DNA integrity (Vousden and Prives, 2009; Kasteri *et al.*, 2018). This protein functions as a transcription factor with a central role in maintaining genomic stability. Activation of the p53 protein regulates expression of several anti-proliferative genes, including *CDKN1A* that encodes p21 (Kastenhuber and Lowe, 2017). It has been reported that p21 gene expression increases dramatically upon p53 upregulation (Laptenko *et al.*, 2011). Reverting to the transient stress, cells are able to recover and resume proliferation as the induced stress resolves (Childs *et al.*, 2015). This was observable in recovery data presented here, suggesting that the M2 agonist produces a transient stress to which DPSCs were able to resume their proliferation following M2 agonist withdraw. However, should the induced stress persist or increased, it can lead to sustained expression of p53 and activation of the p16 protein (encoded by the *CDKN2A* gene) that may lead to long-lasting cell cycle arrest and may push cells towards a senescent state (Kumari and Jat, 2021). Here, *CDKN2A* expression is not affected by M2 agonist stimulation, as opposed to *CDKN1A* overexpression. This suggests that M2 activation induces a transient stress on DPSCs proliferation and cell cycle which push the stimulated cells into a quiescence state. Indeed, the quiescent state is associated with a decrease in

basal metabolic activity, and the transition back to proliferation is accompanied by metabolic upregulation (Marescal and Cheeseman, 2020); which both the MTT and CCK8 results here reflect, as they essentially measure cells metabolic activity. Finally, it should be noted that quiescence can happen at late stages of cell cycle (Chassot *et al.*, 2008; Spencer *et al.*, 2013; Gire and Dulić, 2015), which strengthen future research direction to focus on the G2/M checkpoint.

The involvement of the proteins encoded by the investigated genes in this chapter are well established in cell cycle control. The ones involved in progression of the cell cycle and their interactions are illustrated in (Figure 3-10). The data here present interesting insights worthy to investigate protein expression of these genes and see if they align with investigated gene expression. Furthermore, it appears that M2 activation is involved in triggering other diverse pathways. For example, p21 expression is regulated by various factors apart from p53 such as myoblast determination protein 1 (MyoD), signal transducer and activator of transcription (STAT) protein, and CCAAT-enhancer binding protein  $\alpha$  (C/EBP $\alpha$ ) (Coller, Sang and Roberts, 2006). Additionally, the mTOR pathway is a regulator of proliferation and in association with p53, it can determine the fate of cell cycle arrest (Korotchkina *et al.*, 2010). Therefore, further research exploring these pathways and proteins interactions is worthy. Another limitation encountered in this chapter is the heterogeneity of the investigated DPSCs, as it remains unclear which subpopulations contributed to the observed effect on proliferation and cell cycle. Overall, the presented data here give an insight into the effect of M2 activation on cell cycle progression.

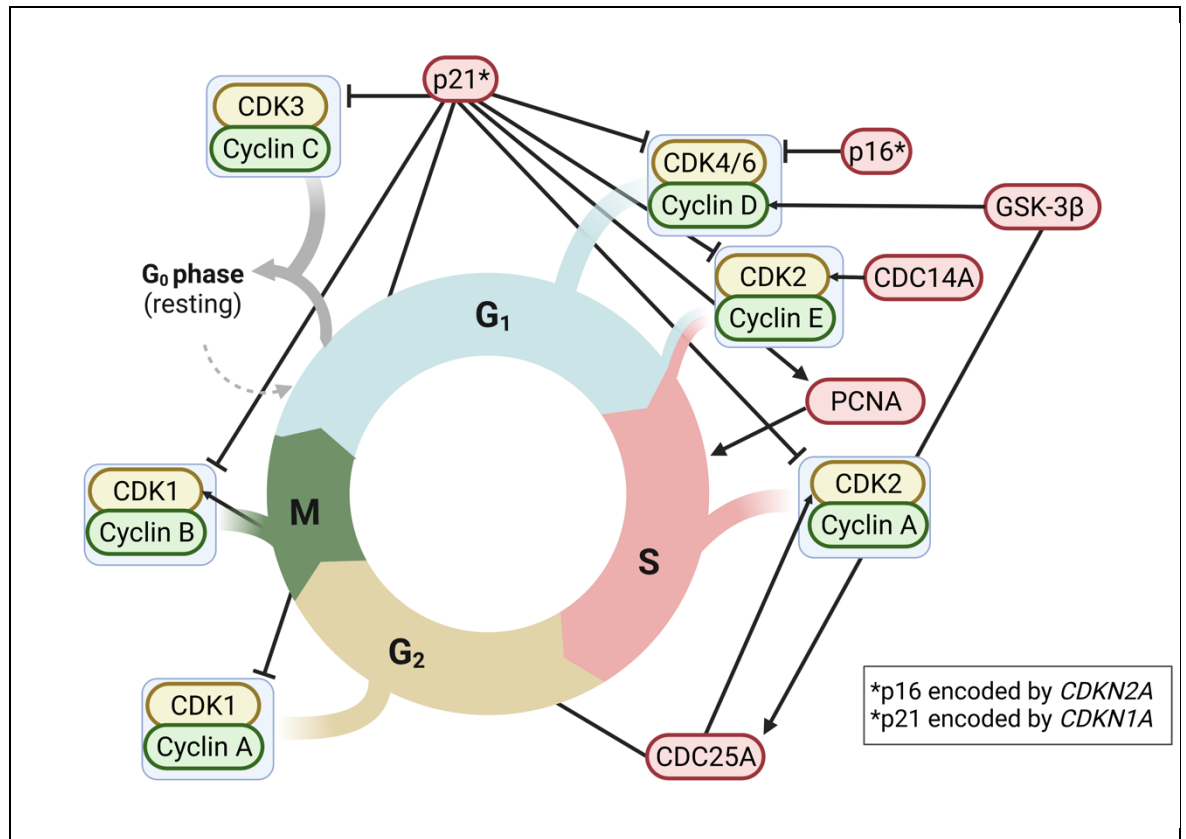
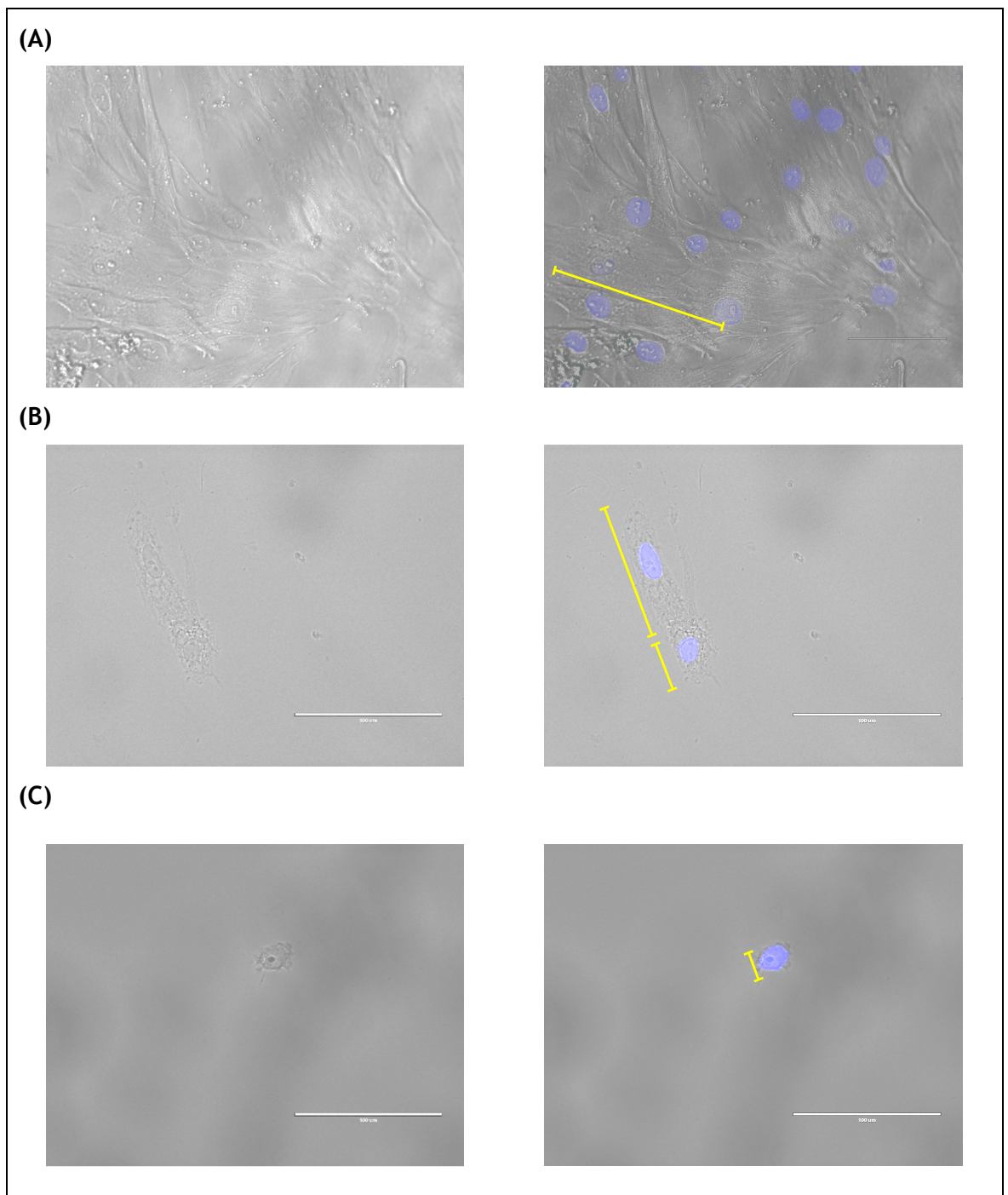
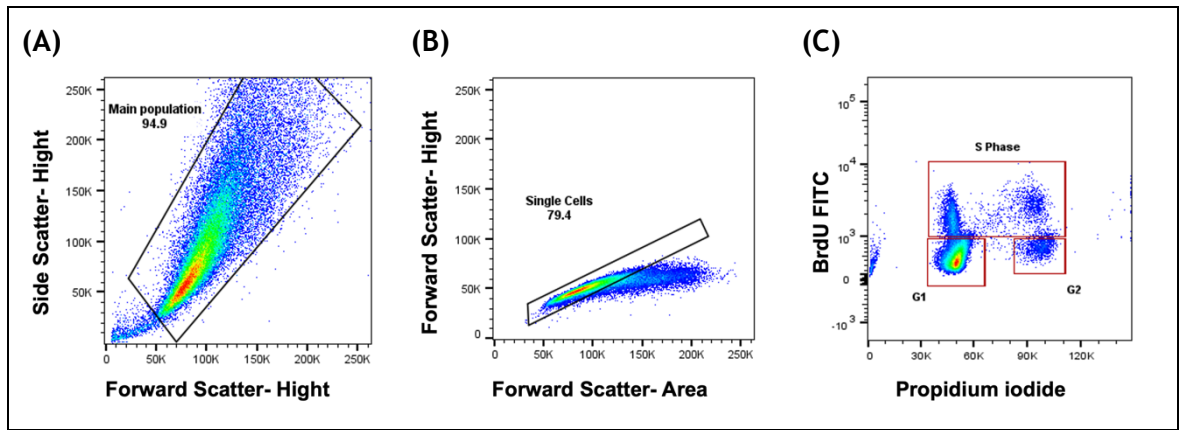


**Figure 3-10 Overview of cell cycle progression.** The cell cycle is regulated by many CDKs which form complexes with their associated cyclin partners. Cells exit the cell cycle and enter the resting state (G<sub>0</sub> phase) are regulated by cyclin C-CDK3. Synthesis of cyclin D in partner with CDK4/6 results in driving the start of the cell cycle. Activation of cyclin D-CDK4/6 complex activates cyclin E and cyclin A that function in promoting the S phase progression. In the S phase, cyclin A removes cyclin E and forms the new complex cyclin A-CDK2, which signals the end of S phase driving the transition to the G<sub>2</sub> phase. In the G<sub>2</sub> phase, cyclin A-CDK1 becomes activated which leads to progression to the M phase. Upon mitosis, cyclin B removes cyclin A and forms the new complex cyclin B-CDK2. Finally, deregulation of CDK1 enables chromosome separation and the completion of mitosis. Regulators of cyclins, CDKs, and cell cycle progression are shown in red. The functions of CDK4 can be inhibited by p16 which is a member of CDK inhibitors family. The protein kinase GSK-3 $\beta$  influence functions of cyclin D1 and CDC25A, thus have a regulatory role on cell cycle progression. The p21 protein is another member of CDK inhibitors family that can inhibit all the CDKs, and thus arrest cell cycle in any phase. Furthermore, it interacts with PCNA, and subsequently modulate the progression of cell cycle and proliferation. The phosphatase CDC14A target CDK2 that is in partner with cyclin E and influence the progression from the G<sub>1</sub> to S phase of cell cycle. The other phosphatase CDC25A target CDK2 that is in partner with cyclin A and CDK1 that is in partner with cyclin B, thus influence the transition through the S and M phases.

### 3.5 Supplementary



**Sup 3-1 Structure of DPSCs following 72 h treatment with higher concentrations of the M2 agonist. (A) Semi-confluent layer of DPSCs under light microscopic displaying normal spindle shape appearance of DPSCs with immunofluorescent staining of the nuclei with DAPI on right. (B) Morphology undergoes changes, as cells shrink and round up following treatment with 250  $\mu\text{M}$  of the M2 agonist, yellow arrow shows some cells with morphological changes, while others maintain their normal shape. (C) Complete loss of normal morphology after treatment with 500  $\mu\text{M}$  of the M2 agonist, indicating a dose response effect. All images shows a 2D projections of confocal stacks. Scale bars for images in (A) = 75  $\mu\text{m}$ , and for (B-C) = 100  $\mu\text{m}$ .**



Sup 3-2 Flow cytometry gating strategy. (A) Forward and side scatter plot to gate on main cells population and to exclude debris present in bottom left corner. (B) Forward scatter-height against forward scatter-area to enable gating that excludes doublet cells. (C) BrdU labelled area against PI-labelled DNA to enable detection of BrdU positive cells in S Phase and visualisation of G1 and G2 phases (gating showing is of untreated control).

## **4 Effect of M2 muscarinic receptor stimulation on DPSCs stemness, migration and differentiation**

## 4.1 Introduction

Dental pulp stem cells (DPSCs) were the first population of stem cells isolated and identified from the pulp cavity of adult permanent teeth (Gronthos *et al.*, 2000). These cells are characterised as self-renewing multipotent cells that possess a high level of clonogenicity and proliferation capacity (Gronthos *et al.*, 2002). Due to the fact that these cells are derived from the ectodermal layer originating from migrating neural crest cells, they possess unique characteristics (Chai *et al.*, 2000; Miletich and Sharpe, 2004; Hu, Liu and Wang, 2018). DPSCs display mesenchymal like properties in terms of their morphology, attachment to a plastic surface, ability to form colonies, expression of mesenchymal stemness markers, and multi lineage differentiation potential (Martens *et al.*, 2013). However, DPSCs also express markers associated with neural stem cells (NSCs) (e.g., Nestin, neuronal N-tubulin, Sox-2 and NSE), and some pluripotency markers similar to embryonic stem cells (ESCs) (e.g., Nanog, Oct4, Sox-2 and Rex-1) (Cheng *et al.*, 2008; Kiraly *et al.*, 2009; Patel *et al.*, 2009; Karbanová *et al.*, 2011; Atari *et al.*, 2012; Sakai *et al.*, 2012). Hence, the rise of the argument that DPSCs are a more naïve population of stem cells that share, but not entirely, similar characteristics with mesenchymal stem cells (MSCs). Indeed, these properties of DPSCs give them the potential to differentiate into osteoblasts, adipocytes, neurocytes, myocytes and chondrocytes *in vitro* and *in vivo* (Zhang *et al.*, 2006; d'Aquino *et al.*, 2007; Carinci *et al.*, 2008; Armiñán *et al.*, 2009; Lan *et al.*, 2019). Therefore, DPSCs are considered an ideal candidate for cell-based therapies owing the fact that these cells are easily obtained without invasive procedures. Therefore, it is worthy to explore novel pathways that could potentially be targeted to manipulate DPSCs regenerative potential. One worthy of exploration is the non-neuronal cholinergic pathway mediated by acetylcholine (ACh) and acetylcholine receptors.

Expression of functional ACh receptors has been reported in different types of MSCs and there is sufficient evidence to suggest their involvement in regulating MSCs function (see chapter 1 for a review). In particular, the M2 muscarinic ACh receptor which is expressed by several different types of MSCs. In bone marrow MSCs (BM-MSCs) it is suggested that the M2 receptor activates downstream signalling pathways that govern these cells' proliferation and differentiation (Hoogduijn, Cheng and Genever, 2009). In adipose-derived MSCs (AD-MSCs) it was

reported that activation of the M2 receptor inhibited these cells' proliferation, migration, and cell cycle (Piovesana *et al.*, 2018). In foetal membrane MSCs (FM-MSCs) expression of the M2 gene (*CHRM2*) was downregulated during differentiation towards an osteogenic lineage (Yegani *et al.*, 2020). These data suggest an active role of the M2 receptor in regulating MSCs proliferation, migration, and differentiation. However, there is still no direct evidence of the involvement of the M2 receptor in regulating MSCs stemness or differentiation potential. Furthermore, the role of the M2 receptor in DPSCs function have not been explored.

In the previous chapter, the data showed that M2 activation, via its selective agonist APE, inhibited DPSCs proliferation through a cell cycle arrest (See 3.3.3 for details). This inhibition occurs in a reversible manner and was shown to not influence DPSCs viability and survival (See 3.3.1 & 3.3.2 for details). It appears that the M2 receptor functions in placing DPSCs in a quiescent state. Therefore, this chapter set to explore this further by investigating the effect of M2 activation on DPSCs stemness, migration and differentiation potential.

## 4.2 Materials and Methods

### 4.2.1 Cells and cell culture

The DPSCs investigated in this chapter were from the same batch used in this project and were between passages four and six. Cells were cultured in normal medium (i.e., DMEM-KO) as described 2.2.1.

### 4.2.2 M2 muscarinic receptor stimulation

DPSCs were treated with the M2 selective agonist as described in 3.2.2. Treatments were carried out in duplicates on three independent occasions over several time points according to experimental design of the investigated assay.

### 4.2.3 Migration

To determine if M2 stimulation, via the M2 selective agonist, affects DPSCs migration, a wound healing assays was performed as described by (Liang, Park and Guan, 2007). The cells were plated on a 6-well plate at a seeding density of  $2 \times 10^5$  in regular medium (DMEM-KO™, Gibco, 10829-018). The following day, cells were treated with the M2 selective agonist (100  $\mu$ M APE), with and without the M2 selective antagonist (0.01  $\mu$ M Meth), and a scratch was made up with a sterile 200  $\mu$ L pipette tip (TipOne® Filter Tips, Starlab). Mitomycin C (50 ng/mL, Fisher BioReagents, 10182953) was added to the medium of treated and untreated cells to exclude the possible influence of cell proliferation. The cells were photographed using an EVOS FL digital inverted microscope (EVOS FL Cell Imaging System, Thermo Scientific) at the start 0 h (t0) and after eight hours (t8). The cells were then stained with phalloidin (1:1000, Alexa Fluor™ 488, A12379, Invitrogen) for 30 minutes at RT to label actin filaments and acquire a better visualisation of the area covered during DPSCs migration. The space between the two fronts at the start and after eight hours was then measured using ImageJ 64 imaging software (NIH, USA: Schneider, Rasband and Eliceiri, 2012). The two values were subtracted (t0-t8), obtaining the covered space by the cells in the experimental time chosen.

#### 4.2.4 Stemness

To validate if M2 activation affects stemness of DPSCs, gene expression of stemness markers was evaluated by qPCR. The DPSCs supplier (Lonza Inc, PT-5025, UK) validation report suggests they express CD105, CD166, CD29, CD90, and CD73, and do not express CD34, CD45, and CD133. Therefore, expression of CD90, CD105, CD73 and CD45 genes were evaluated after DPSCs stimulation with the M2 selective agonist (100  $\mu$ M APE) for 72 hours. Furthermore, genes of transcription factors that regulate and maintain self-renewal and pluripotency such as Oct4, Nanog and Sox-2, were also evaluated.

#### 4.2.5 Osteogenic differentiation

To evaluate the effect of M2 stimulation on the differentiation capabilities of DPSCs, an osteogenic differentiation experiment was set up. The M2 selective agonist (100  $\mu$ M APE) was used during the osteogenic differentiation experiment to activate the M2 receptor. Briefly, Cells were seeded in 24-well plates and cultured in complete culture medium (DMEM-KO<sup>TM</sup>, Gibco, 10829-018) at a seeding density of  $1 \times 10^4$  per well. When cells reached 85-90% confluence (48-72 hrs), medium was changed to osteogenic inductive medium as described in 2.2.1.1. The M2 selective agonist (100  $\mu$ M APE) was added to the osteogenic inductive medium at the onset and during different timepoints to observe its effect on and during the differentiation process. Plates were incubated at 37°C, 5% CO<sub>2</sub> for 7, 14, 21, and 28 days, and medium was refreshed twice per week. At each time point, the plates designated for analysis of gene markers involved in osteogenesis were prepared for RNA extraction by adding a lysis buffer (RLT, RNeasy Mini Kit, 74104 Qiagen, UK) and harvested into eppendorfs for subsequent RNA isolation as described in 2.2.2.1. The remaining plates were designated for mineralisation stains at the end of differentiation (i.e., 28 days) and processed according to each staining protocol.

To detect the formation of mineralised nodules after the osteogenic differentiation, cells were subjected to Alizarin Red (40 mmol/L, pH 4.2, A5533, Sigma-Aldrich) and Von Kossa (Silver plating kit, 100362, Sigma-Aldrich) staining as described in 2.2.1.1. Quantification of the Alizarin Red stain (ARS) was also carried out according to the protocol described in 2.2.1.1.

## 4.2.6 Quantitative polymerase chain reaction (q-PCR) analysis

The RNA extraction and generation of cDNA was carried out as described in (2.2.2.1 & 2.2.2.3). Primer sequences for genes involved in stemness, migration and osteogenic differentiation are provided in Table 4-1 . Target gene primers and the prepared cDNA samples were mixed with the fast SYBR Green Master Mix (Fast SYBR™ Green Master Mix 4385610, Applied Biosystems™, UK) as described in 2.2.2.4.

**Table 4-1 Primer sequences for genes investigated in chapter 4.**

Primer	Sequence
<i>ALP</i>	Fwd: ATGAAGGAAAAGCCAAGCAG Rev: CCACCAAATGTGAAGACGTG
<i>BMP2</i>	Fwd: GCTAGTAACTTTTGGCCATGATG Rev: GCGTTTCCGCTGTTTGTGTT
<i>COL1A1</i>	Fwd: CCATGTGAAATTGTCTCCCA Rev: GGGGCAAGACAGTGATTGAA
<i>ENG</i>	Fwd: CCACTAGCCAGGTCTCGAAG Rev: GATGCAGGAAGACACTGCTG
<i>GAPDH</i>	Fwd: GCAGGGGGGAGCCAAAAGGG Rev: TGCCAGCCCCAGCGTCAAAG
<i>NANOG</i>	Fwd: CAGAAGGCCTCAGCACCTAC Rev: ATTGTTCCAGGTCTGGTTGC
<i>NT5E</i>	Fwd: CAGTACCAGGGCACTATCTGG Rev: AGTGGCCCCTTTGCTTTAAT
<i>OCT4</i>	Fwd: GACAGGGGGAGGGGAGGAGCTA Rev: CTTCCCTCCAACAGTTGCCCAA
<i>PTPRC</i>	Fwd: CTTCAAGTGGTCCCATTGTGGTG Rev: CCACTTTGTTCTCGGCTTCCAG
<i>RUNX2</i>	Fwd: GGTCAGATGCAGGCGGCCC Rev: TACGTGTGGTAGCGCGTGGC
<i>SOX-2</i>	Fwd: AATGCCTTCATGGTGTGGTC Rev: CGGGGCCGGTATTTATAATC
<i>SPP1</i>	Fwd: GAAGTTTCGCAGACCTGACAT

Rev: GTATGCACCATTCAACTCCTCG

---

*THY1*

Fwd: GAAGGTCCTCTACTTATCCGCC

Rev: TGATGCCCTCACACTTGACCAG

---

#### 4.2.7 Statistical analysis

Statistical analysis was performed as in 2.2.5.

## 4.3 Results

### 4.3.1 M2 receptor activation inhibit DPSCs migration

To evaluate the effect of M2 receptor activation on DPSCs migration, a wound healing technique was performed in the presence of the M2 selective agonist (100  $\mu$ M APE), with and without the M2 selective antagonist (0.01  $\mu$ M Meth). To exclude the influence of cell proliferation, co-treatment with mitomycin C (an anti-tumour drug able to arrest cell proliferation) was also performed. The distance of the wound gap between the two fronts was measured after eight hours (t8) in the treated and untreated cells and compared, respectively, with the distance measured at the time the scratch was created 0 h (t0). The results indicated that the presence of M2 agonist alone impaired cell migration, while co-treatment with the M2 antagonist was able to cancel that effect (Figure 4-1). Fluorescence staining showed clear images of cells migrating into the created wound in the untreated control and cells stimulated with both the M2 agonist and antagonist compared to cells stimulated with the M2 agonist alone (Figure 4-1 G-I). Higher magnification images of the fluorescence staining showed better visualisation of how cells treated with the M2 agonist alone was unable to cover the scratch space (Sup 4-1). The data further suggest that selective activation of the M2 receptor significantly inhibits DPSCs migration ( $P < 0.0001$ ) (Figure 4-1 J).

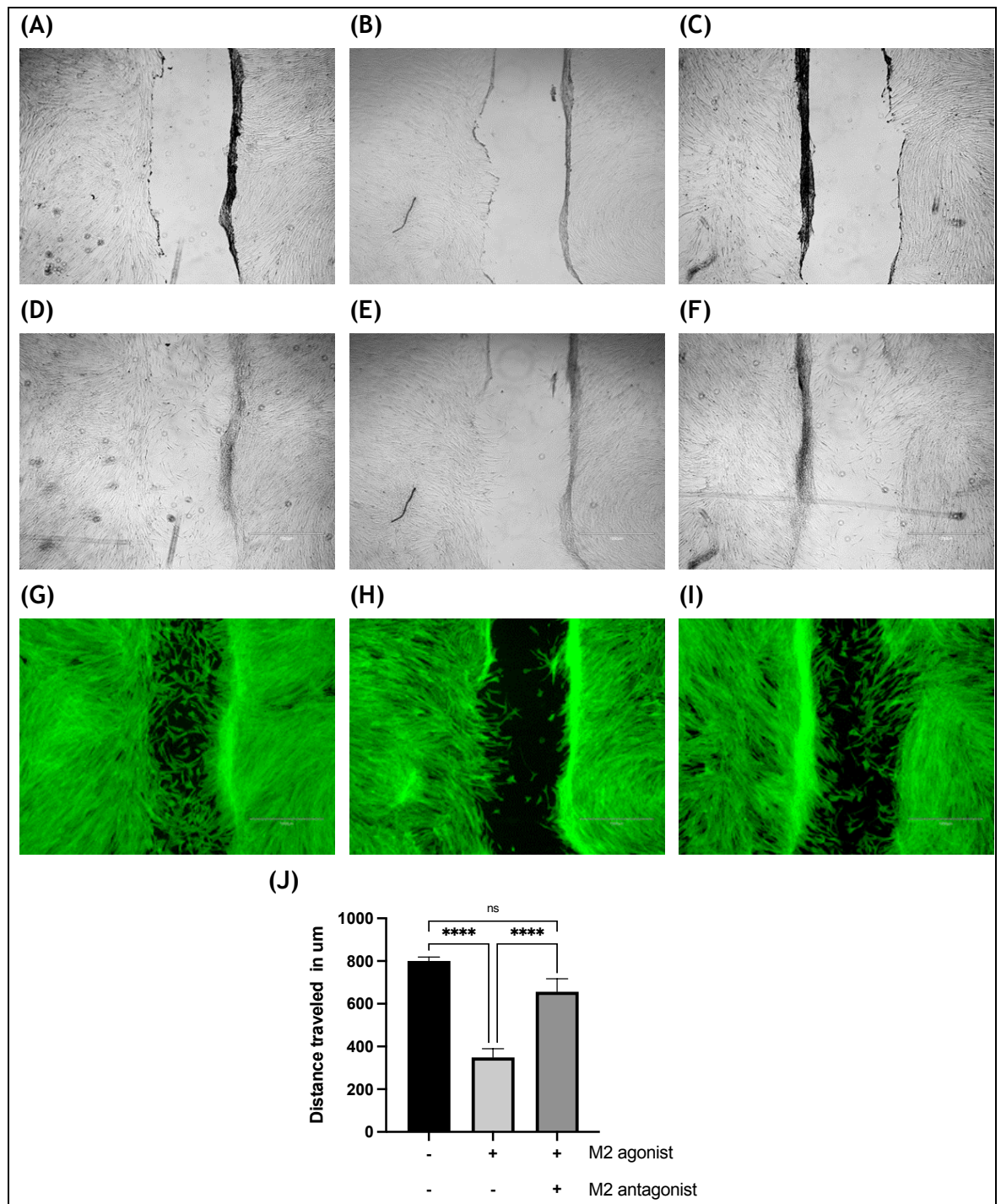


**Figure 4-1 Migration of DPSCs after stimulation with the M2 selective agonist for eight hours. (A-C) Microscopic images at 0 h (t<sub>0</sub>) of the created scratch (A) cells monolayer of the untreated control, (B) cells stimulated with the M2 selective agonist (100 μM APE), and (C) cells stimulated with both the M2 agonist and antagonist (100 μM APE, 0.01 μM Meth, respectively). (D-F) Microscopic images after eight hours (t<sub>8</sub>) showing cells migration into the scratch space of the untreated control (D) and cells stimulated with both the M2 agonist and antagonist (F), while cells stimulated with the M2 agonist alone (E) showed inhibition in migratory ability. (G-I) Fluorescent microscopic images shows enhanced visualisation of inhibited migration of cells stimulated with the M2 agonist alone (H), and inability to cover the scratch space. (J) The distance of the gap between the two fronts was measured by subtracting t<sub>8</sub> from t<sub>0</sub> showing a significant inhibition of DPSCs migration after M2 stimulation with its selective agonist. All investigated conditions (treated and untreated) were co-treated with mitomycin C; this investigation does not have a control without mitomycin C. All images shows 2D projections of confocal stacks and are a representative of a duplicates of three independent experiments. Scale bars = 1200 μm. Statistical data is derived from duplicate wells of three independent experiments (ns: not significant, \*\*\*\* p<0.0001).**

### 4.3.2 M2 receptor activation does not affect DPSCs stemness

DPSCs are positive for MSCs-stemness markers including CD90, CD105, and CD73, they also do not express CD45 among several other hematopoietic stem cell markers (Aydin and Şahin, 2019). Furthermore, DPSCs also express markers of pluripotency such as: Oct4, Nanog, and Sox2 (Ahmed *et al.*, 2016). To validate that the inhibitory effect of M2 activation is not due to spontaneous differentiation, expression of these markers was determined by gene expression analysis following 72 h of stimulation with the M2 selective agonist (100 µM APE). The results demonstrate that DPSCs still express the MSCs-stemness markers CD90 (*THY1*), CD105 (*ENG*), and CD73 (*NT5E*), the pluripotency markers Oct4, Nanog, and Sox2 mRNA transcripts, and do not express the hematopoietic stem cell marker CD45 (*PTPRC*) (Figure 4-2). Indicating that these stemness and pluripotency markers did not significantly alter after stimulation with M2 selective agonist (100 µM APE) for 72 h, demonstrating that DPSCs maintain their stemness properties following M2 activation.

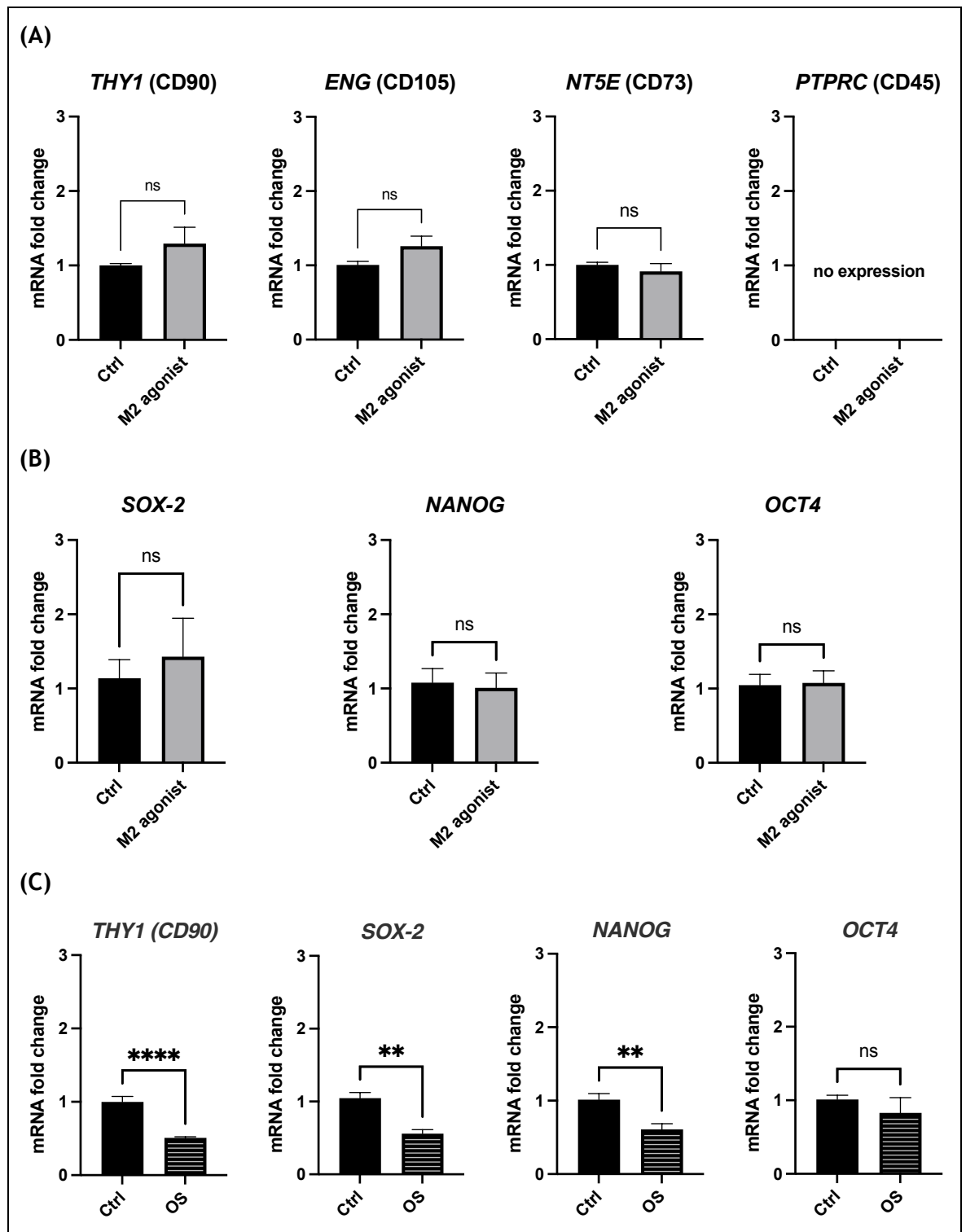


**Figure 4-2** Stemness properties of DPSCs after stimulation with the M2 selective agonist for 72 h. (A) expression of stemness markers showing no difference in genes expression between untreated (ctrl) and cells stimulated with the M2 agonist. (B) Expression of pluripotency markers also shows no difference in genes expression between untreated control (Ctrl) and cells stimulated with the M2 agonist. (C) Expression of investigated markers showing downregulated levels in cells undergoing osteogenic differentiation (OS). Data for all are derived from duplicate wells of three independent experiments and is presented as mean fold change compared to the control (untreated cells) using the  $2^{-\Delta\Delta CT}$  method (Livak and Schmittgen, 2001). Gene expression is relative to the housekeeping gene (*GAPDH*). A difference of  $P < 0.05$  was considered statistically significant. (ns: not significant).

### 4.3.3 M2 receptor activation modulate DPSCs osteogenic differentiation.

To evaluate the effect of M2 receptor activation on DPSCs differentiation potential, the M2 selective agonist (100  $\mu$ M APE) was added to the osteo-inductive medium at the start of differentiation and at different timepoints during the differentiation process. Differentiation into osteoblast-like cells was confirmed phenotypically through the evaluation of the formation of mineralised nodules by Alizarin Red (ARS) and Von Kossa staining. The ARS showed clear reduction of mineralised deposits in the differentiated cells that were stimulated with the M2 agonist compared to the untreated differentiated cells (Figure 4-3 A-C). To investigate this further, the M2 agonist was added at different time points during the differentiation process (i.e., 7, 14, and 21 days), and results showed very little to no mineralisation when the agonist is added at earlier timepoints of differentiation (Figure 4-3 D-F). Quantification of the ARS showed the difference in the mineralisation concentrations upon stimulation with the M2 agonist (Figure 4-3 G). The results support the images of the stains, showing significant reduction of mineralised deposits in the differentiated cells that were stimulated with the M2 agonist compared to the untreated differentiated cells. The Von Kossa staining showed similar results, i.e., clear absence of mineralised deposits in the differentiated cells that were stimulated with the M2 agonist compared to the untreated differentiated cells (Figure 4-4). The staining images also showed very little to no mineralisation when the M2 agonist is added at earlier timepoints of differentiation (Figure 4-4 D-F).

Changes in expression of key genes reported to be involved in osteogenic differentiation were evaluated *via* q-PCR analysis after 3 and 14 days of differentiation. In general, differentiated cells in the presence of the M2 agonist showed significantly downregulated expression compared to untreated osteogenic differentiated cells (OS) (Figure 4-5). The *ALP* gene exhibited significant downregulated expression in differentiated cells with the M2 agonist compared to untreated differentiated cells ( $P < 0.0001$ ). Similarly, the *BMP2*, *COL1A1*, and *SPP1* genes displaying significant downregulated expression in differentiated cells with the M2 agonist compared to untreated differentiated cells ( $P < 0.001$ ,  $P < 0.0001$ ,  $P < 0.05$ , respectively). There was no difference in the expression of *RUNX2* between differentiated cells with the M2 agonist and untreated differentiated

cells, both groups display significant upregulation of this gene expression compared to the undifferentiated control ( $P < 0.0001$ ). Collectively, these results indicate that M2 activation via the M2 selective agonist hinders DPSCs ability to undergo osteogenic differentiation.

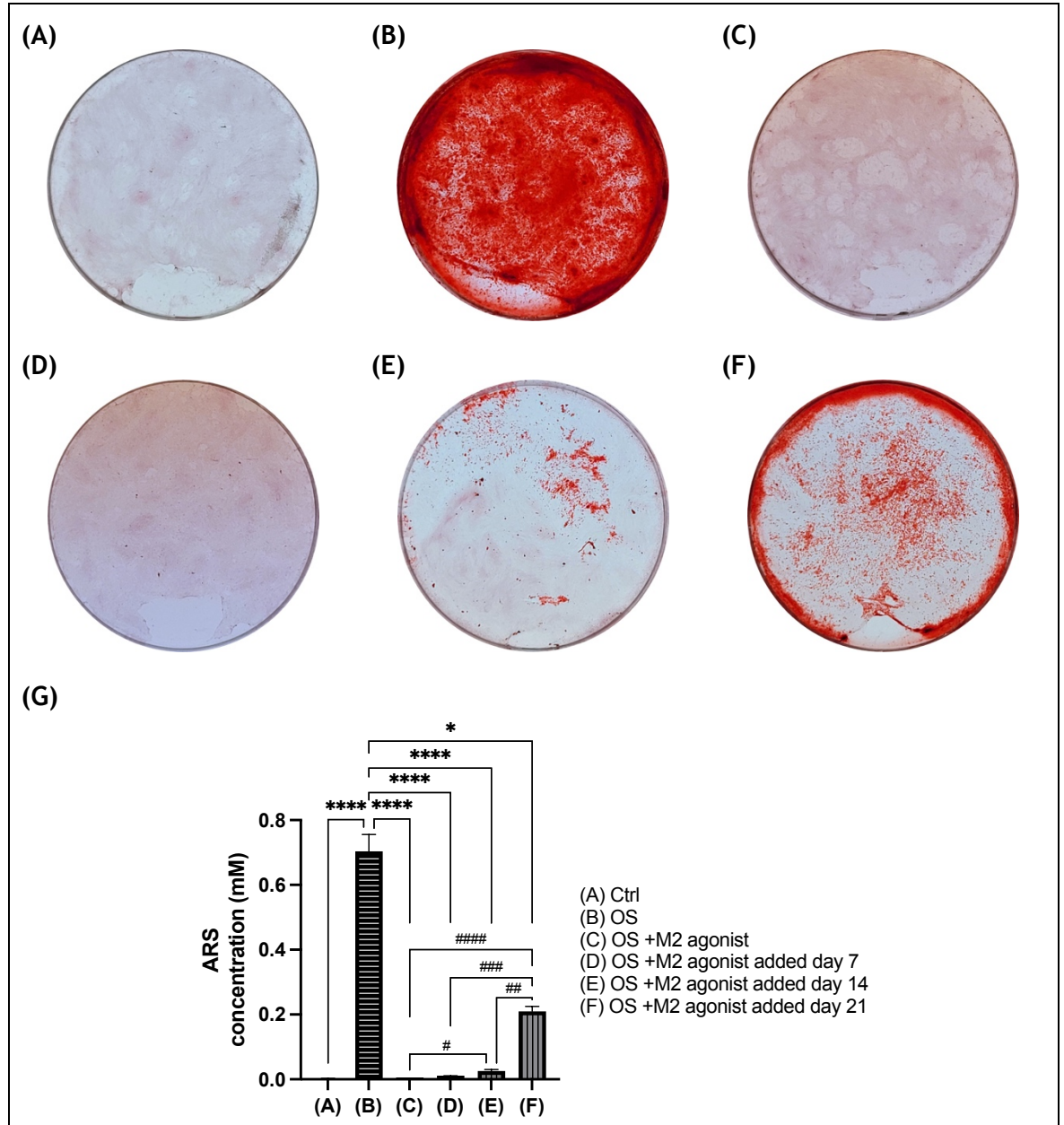


**Figure 4-3 Alizarin reds staining of DPSCs osteogenic differentiation with M2 agonist stimulation. (A-C) Mineralisation stain showing vast extracellular calcium deposits as red mineralisation spots in differentiated DPSCs (B), whereas the undifferentiated control (A) and differentiated cells with the M2 agonist (C) is only slightly reddish. (D-F) shows the effect of adding the M2 agonist during the differentiation process at seven days (D), 14 days (E), and 21 days (F). (G) Alizarin Red stain quantification of the stain concentrations showing significantly less mineralisation compared to cells that had undergone osteogenic differentiation (\*\*\*\* $p < 0.0001$  for A-E, \* $p < 0.05$  for F). Comparison of osteogenic differentiated cells with the M2 agonist shows significant mineralisation in differentiated cells with the M2 agonist added at day 21 compared with day 14, day seven, and since the start of the differentiation process ## $p < 0.01$  for E, ### $p < 0.001$  for D, and #### $p < 0.0001$  for C). Images are representative of duplicate wells from three independent experiments ( $n = 3$ ). Values are reported as mean  $\pm$  SEM of mM concentration. Data presented is from duplicate wells of three independent experiments ( $n = 3$ ).**

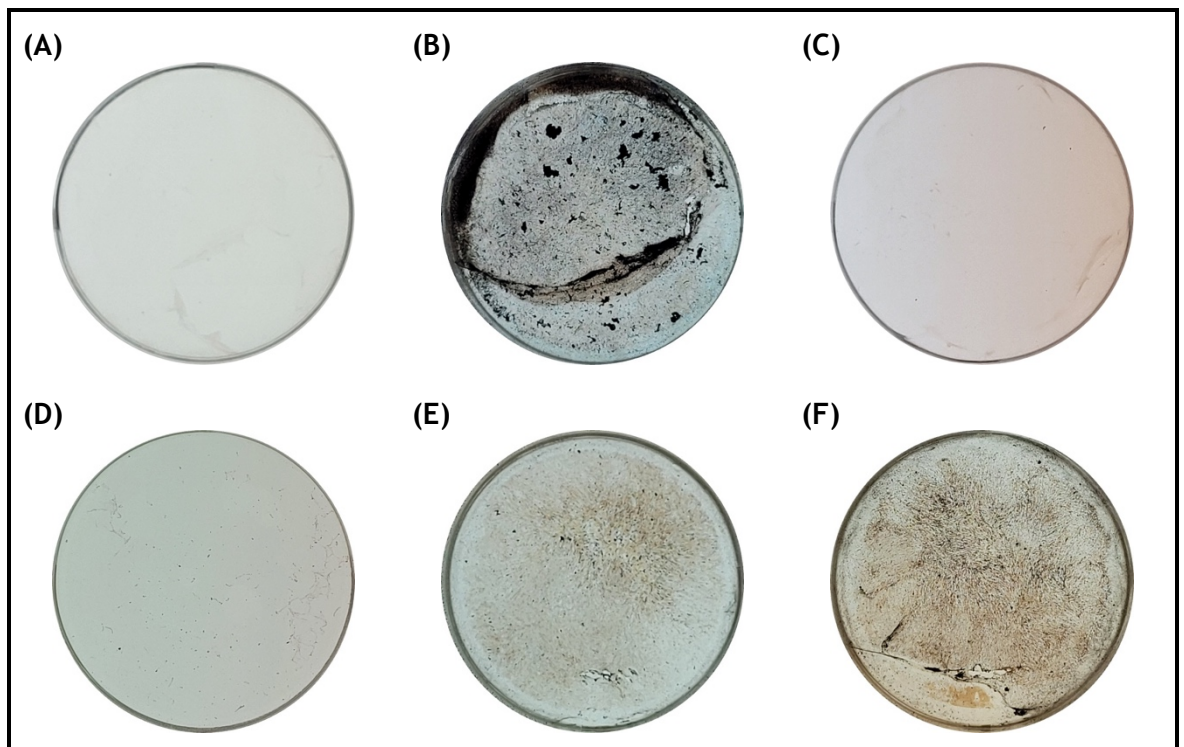


**Figure 4-4** Von Kossa staining of DPSCs osteogenic differentiation with M2 agonist stimulation. (A-C) shows calcium deposits as black nodules in differentiated DPSCs (B), whereas the undifferentiated control (A) and differentiated cells with the M2 agonist (C) is only slightly brownish. (D-F) shows the effect of adding the M2 agonist during the differentiation process at seven days (D), 14 days (E), and 21 days (F). Images are representative of duplicate wells from three independent experiments ( $n = 3$ ).

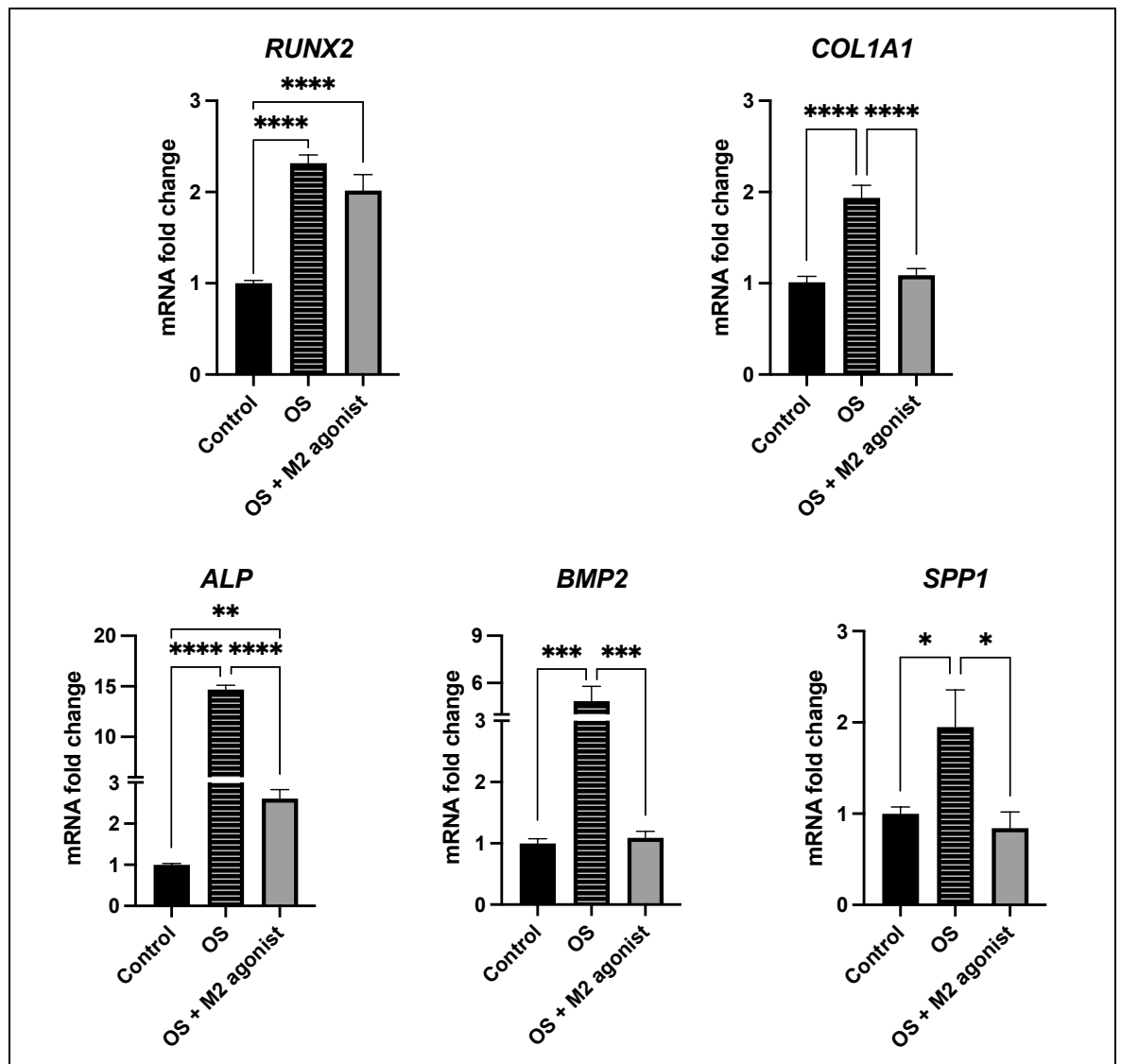


Figure 4-5 Gene expression of osteogenic markers following stimulation with the M2 agonist. Expression of *RUNX2* and *COL1A1* was investigated after 3 days of differentiation; expression of *ALP*, *BMP2*, and *SPP1* was investigated after 14 days of differentiation. Data for all are derived from duplicate wells of three independent experiments and is presented as mean fold change compared to the control (untreated cells that hadn't gone osteogenic differentiation) using the  $2^{-\Delta\Delta CT}$  method (Livak and Schmittgen, 2001). Gene expression is relative to the housekeeping gene (*GAPDH*). A difference of  $P < 0.05$  was considered statistically significant. (\*  $p < 0.05$ , \*\*  $p < 0.01$ , \*\*\*  $p < 0.001$ , \*\*\*\*  $p < 0.0001$ ). OS: osteogenically differentiated.

## 4.4 Discussion

In the previous chapter, data was presented showing that M2 activation, via its selective agonist (100  $\mu$ M APE) inhibited DPSCs proliferation. Indeed, the results of M2 activation was associated with inhibited proliferation without impacting DPSC survival or viability. Furthermore, the induced inhibition in proliferation was traced to a cell cycle arrest. It was concluded that M2 activation places DPSCs in a quiescent state. However, it could be argued that this M2-induced effect is causing the cells to stop proliferating in order to differentiate. Therefore, this chapter set to explore this by investigating the effect of M2 activation on DPSCs stemness, in addition to two other main functions of stem cells, migration and differentiation.

Stem cells are identified through a set of markers known as cluster of differentiation (CD), surface antigens, or stemness markers. Mesenchymal stem cells, including DPSCs, express several of these markers among which are CD90, CD73 and CD105 (Aydin and Şahin, 2019). They also should not express hematopoietic stem cell markers like CD45 (Gronthos *et al.*, 2002). Therefore, if M2 activation is causing spontaneous differentiation, differential expression of these stemness markers would have been detected. However, the results herein suggests that DPSCs maintain their stemness after treatment with the M2 agonist. Highlighting the fact that M2 activation does not interfere with DPSCs stem cell functionality. DPSCs are in fact a unique population of stem cells owing to their ectodermal origin from migrating neural crest cells (Lan *et al.*, 2019). This enables this type of cells to also express several pluripotency markers similar to embryonic stem cells (ESCs) and a number of neural stem cell (NSC) markers (Figure 4-6) (Cheng *et al.*, 2008; Kiraly *et al.*, 2009; Patel *et al.*, 2009; Karbanová *et al.*, 2011; Atari *et al.*, 2012; Sakai *et al.*, 2012). The results herein showed that DPSCs maintain expression of the three investigated pluripotency markers (i.e., Oct4, Nanog, and Sox2) after treatment with the selective M2 agonist. It was only during osteogenic differentiation that DPSCs were shown to exhibit downregulated expression of the investigated stemness/pluripotency markers (Figure 4-2 C), comparable to what has been reported in the literature (Okajcekova *et al.*, 2020). Collectively, these results support the argument that M2 activation places DPSCs

in a 'quiescent state' preserving their stemness properties and self-renewal potential.

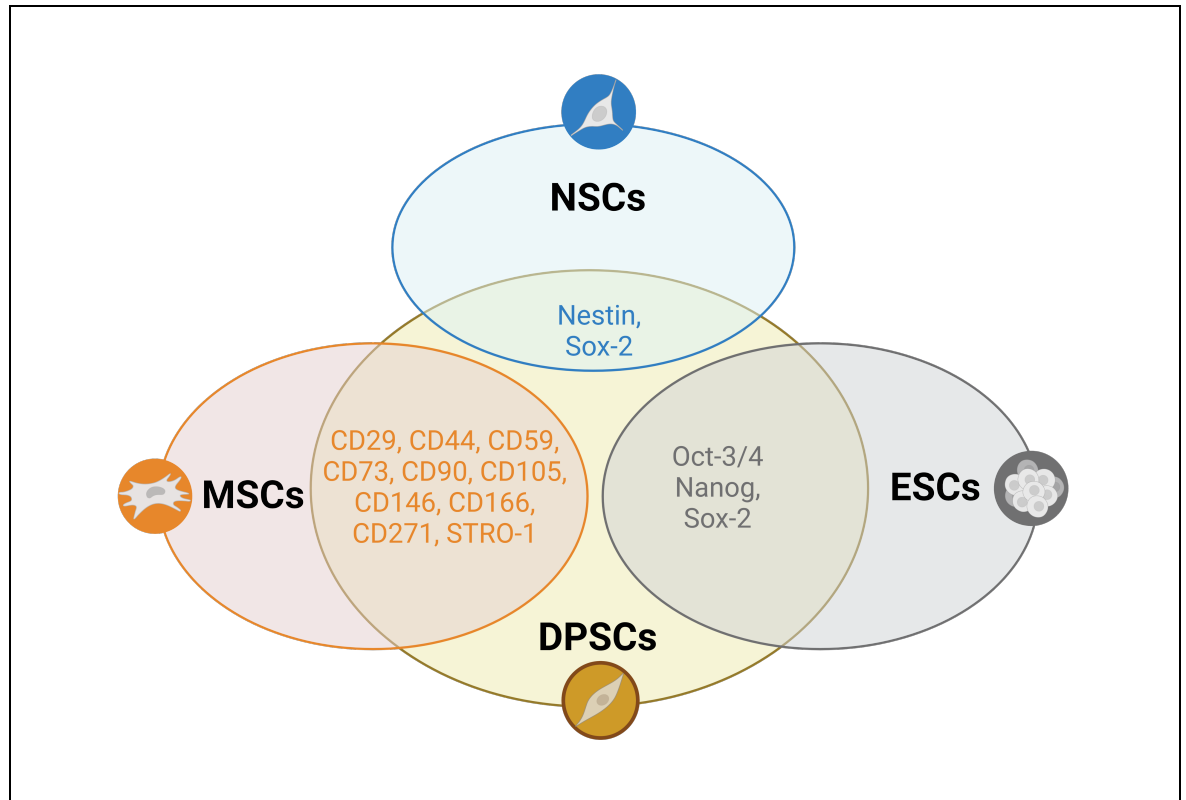


**Figure 4-6 Overview of DPSCs stemness markers. DPSCs identifiable stemness markers overlapped with markers related to mesenchymal stem cells (MSCs), neuronal stem cells (NSCs), and embryonic stem cells (ESCs).**

Stem cell migration is an essential function that enables these cells to respond and move towards the site of stimuli in order to execute their intended regenerative or remodelling functions. Indeed, the response to stimuli and movement of stem cells towards a site of injury or stimulus depends on the cells' migration characteristics (Sonnemann and Bement, 2011; Szabó and Mayor, 2016). In this process, stem cells leave their niche in response to signalling and move towards the site of stimulus to carry out their regenerative function (Te Boekhorst, Preziosi and Friedl, 2016). The DPSCs, for an example, display an inherent migratory response to tooth injury, leading to repair of the affected dentin and assuming the role of the lost odontoblasts (Howard, Murray and Namerow, 2010). It is suggested that transit amplifying cells, committed progenitors for odontoblast differentiation, are the first to respond to tooth injury, whereas the multipotent subpopulation of DPSCs assume the role progenitors production and progenitors orchestrating pulp response (Ishikawa *et al.*, 2010). Depending on the severity of the injury and time (i.e., loss of odontoblast committed progenitors), it is suggested that the multipotent subpopulation of DPSCs can migrate to be involved

directly in the repair process. Moreover, DPSCs seem to exhibit superior migration potential compared to other MSCs such as adipose-derived and bone marrow MSCs, thus making them an attractive source in the field of regenerative medicine (Ishizaka *et al.*, 2013; Lan *et al.*, 2019). Herein, the involvement of the M2 muscarinic receptor in modulating DPSCs migration potential is reported. This not only provides an insight into the involvement of cholinergic pathways in DPSCs function but may provide the opportunity for pharmacologically controlling stem cell migration *in vivo*.

There is sufficient evidence linking both muscarinic and nicotinic acetylcholine receptors in modulating MSCs migration (see chapter 1 for review), most notably, the inhibitory action of the M2 muscarinic receptor on AD-MSCs (Piovesana *et al.*, 2018). The present work reports similar findings with the data showing selective activation of the M2 receptor suppressed DPSCs migration. However, this was determined using a wound healing test, which fundamentally examines the ability of cells to occupy a created wound. This is based on the fact that cells intrinsically tend to move directionally *in vitro* (Petrie, Doyle and Yamada, 2009). Whilst a three-dimensional migration assay would be considered a more appropriate representative of an *in vivo* environment, replication of this assay in culture is reportedly a complex and challenging task compared to the two-dimensional wound healing assay (Decaestecker *et al.*, 2007). Indeed, for initial assessment of migration, the wound healing assay is regarded as an easy and accurate method with high reproducibility to study cells' migration in response to a stimulus (Tremel *et al.*, 2009). Although this assay is widely recognised and reproducible (Liang, Park and Guan, 2007), in the present work mitomycin C was added to the culture medium (treated and untreated cells). This was to exclude the influence of cell proliferation as this drug is known to arrest cell proliferation (Hidalgo San Jose *et al.*, 2018). To this end, the collective evidence so far demonstrates that activation of the M2 receptor inhibits DPSCs proliferation and migration, while maintaining their stemness and viability. This further support the argument that M2 induced DPSCs to go in a quiescent state.

Osteogenic differentiation of MSCs and DPSCs is one of the most studied differentiation protocols in these cells (Seong *et al.*, 2010; Brar and Toor, 2012; Langenbach and Handschel, 2013; Liu *et al.*, 2015; Aydin and Şahin, 2019) Hence, it was used in this study to determine the effects of M2 receptor activation on the

differentiation potential of DPSCs. The work here aimed at investigating the effect of M2 activation, via its selective agonist, on the osteogenic differentiation of DPSCs and during the differentiation process itself. Phenotypic features of osteogenesis are typically detected after 28 days through mineralisation stains. Alizarin red and Von kossa staining are the most frequently used means to detect this mineralisation deposit. Alizarin red staining binds selectively to calcium salts and is widely used for calcium mineral histochemistry (McGee-Russell, 1958). Von Kossa staining reveals calcium deposits in mineralised tissue by binding of silver ions to calcium phosphate and the reduction form dark brown or black metallic silver staining (Wang *et al.*, 2006). The data herein showed well-defined mineralised deposits of both stains in the differentiated control signifying successful osteogenic differentiation. However, significant absences of mineralised deposits are witnessed in differentiated cells stimulated with the M2 agonist compared to the differentiated cells without treatment. Indicating involvement of M2 in hindering the differentiation process. To investigate this further, different time points were examined in the presences of the M2 agonist during the differentiation process. The results showed that adding the M2 agonist early on the process of differentiation, limits the ability of cells to produce mineralisation. Moreover, when the agonist was added to what is believed to be cells committed to an osteoblast lineage (i.e., day 14-21) it reduces the amount of mineralisation deposits. This was quantifiable in the Alizarin-stained cells, as this stain is particularly versatile compared to Von Kossa. In the ARS, the dye can be extracted from the stained monolayer and quantified according to a standard curve using a serial dilution of known concentrations of the stain. The ARS quantifiable data support the images of the stain and provides a time-dependent relationship between mineralisation deposits and the time that M2 agonist is introduced to the differentiation process. The results showed almost undetectable stain in differentiated cells stimulated with the M2 agonist (i.e., OS + M2) compared to the 0.7 mM ARS of differentiated cells without treatment (i.e., OS). The results showed more detectable stain in differentiated cells where the M2 agonist was added at day 21 of the differentiation process (i.e., OS + M2 at day 21) compared with when the M2 agonist was added at day seven and 14 (i.e., OS + M2 at day seven and 21). These data showed that not only does M2 activation inhibit DPSCs ability to undergo osteogenic differentiation, but it also actively

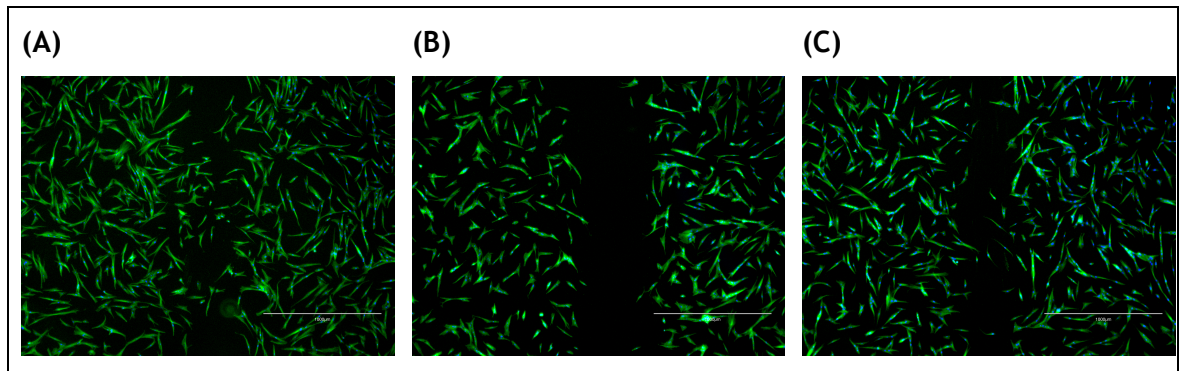
interferes with their commitment to an osteoblast lineage. This signifies a potential role of the M2 receptor in differentiation of DPSCs.

Gene expression analysis of key genes involved in osteogenic differentiation additionally reflects similar results to the phenotypic data. Among the investigated genes is *RUNX2*, which is a master regulator of osteogenic differentiation (Lian and Stein, 2003; Chen *et al.*, 2009). It activates response elements in the DNA of major osteogenic genes, and thereby orchestrates their expression (Niu *et al.*, 2016). The results herein showed significant expression of this gene in both unstimulated differentiated control (OS) and differentiated cells stimulated with the M2 agonist (OS + M2 agonist). This was expected as *RUNX2* is considered an early-stage marker of osteogenic differentiation (Komori, 2010b; Ni *et al.*, 2011). However, the OS + M2 agonist group showed a trend of lesser expression for the remaining investigated genes. For example, *COL1A1* expression exhibits no changes in the OS + M2 agonist group compared to the undifferentiated control, whereas it was significantly upregulated in differentiated cells (i.e., OS group). Besides *RUNX2*, the *COL1A1* gene is arguably an essential osteogenesis marker. This gene provides the framework for inorganic deposition and comprises most of the extracellular matrix, thus plays an essential role in maintaining the biological and structural integrity of the bone matrix architecture (Cen *et al.*, 2008; Sun *et al.*, 2017). Another key osteogenesis marker is *ALP*, which plays a role in bone matrix mineralization and production of a calcifiable extracellular matrix (Hessle *et al.*, 2002; Gauthier *et al.*, 2017). The results herein showed that despite its upregulation in the OS +M2 agonist group, compared to the undifferentiated control, its expression is significantly downregulated compared to the differentiated control (i.e., OS group). The results also showed significant downregulated expression of *BMP2* and *SPP1* in the OS +M2 agonist group compared to the OS group. Collectively, the data indicated that activation of the M2 receptor prevents upregulation of key markers in osteogenic differentiation (The importance of these markers are discussed in detail in chapter 2). Once more, this gives an insight to the potential involvement of the M2 receptor in regulating DPSCs differentiation, at least their osteogenic potential. Indeed, one of the interesting findings was the upregulation of the M2 transcript and protein (*CHRM2*) upon initiation of the DPSCs osteogenic differentiation process (Sup 4-2). This, besides the unexpected upregulation expression of *Runx2* in differentiated cells

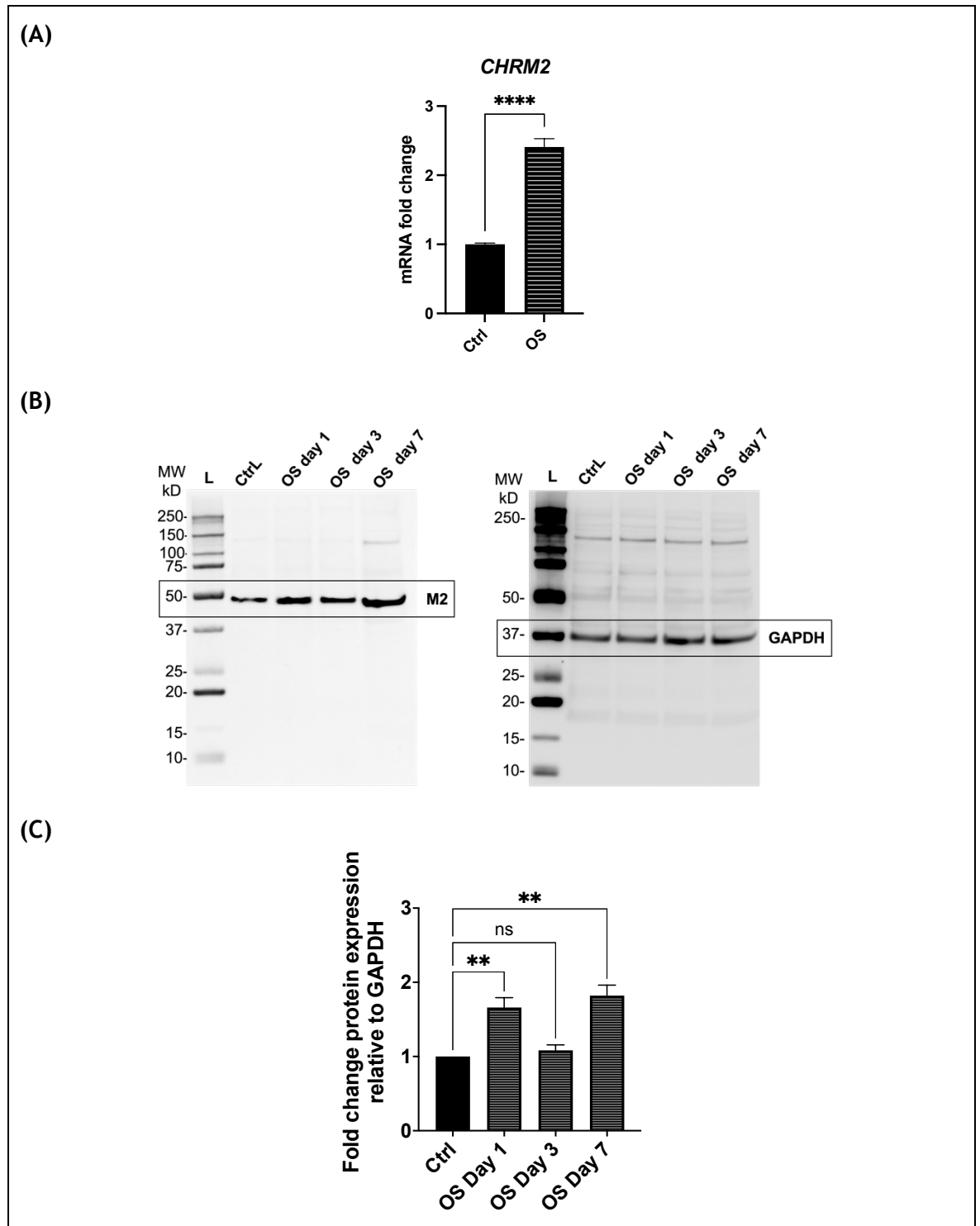
stimulated with the M2 agonist (OS +M2 agonist) (Figure 4-5), suggest that the M2 receptor maybe involved in pathways besides those regulating DPSCs osteogenic differentiation.

In this chapter, the data suggested that activation of the M2 receptor inhibited DPSCs migration while maintaining their stemness. To this end, it could be hypothesised that M2 functions to preserve DPSCs in their niche or a microenvironment of quiescence and a self-renewable state. Furthermore, this appeared to be generally the case upon attempting to drive DPSCs to undergo osteogenesis. Indeed, stimulation of the M2 receptor, via its selective agonist, interfered with DPSCs ability to commit to an osteoblast lineage. This highlights the involvement of this receptor and related pathways to the basic functions of DPSCs. After all, muscarinic receptors expression and function are dynamic in nature and the fact that they are coupled to G proteins means they are capable of initiating several signalling pathways on the account that the downstream signalling of G proteins involve a wide range of secondary messengers (Eglen, 2005; Wessler and Kirkpatrick, 2008; Resende and Adhikari, 2009). Moving forward, it seems appropriate to investigate the wider effects of M2 activation in DPSCs and the potential pathways and processes that it governs.

## 4.5 Supplementary



**Sup 4-1 Higher magnification of fluorescent microscopic images of DPSCs migration. (A) untreated cells, (B) cells treated with the M2 agonist alone, and (C) cells treated with both the M2 agonist and antagonist. Cells stimulated with the M2 agonist alone (B) shows inability to cover the scratch space. All images shows 2D projections of confocal stacks and are a representative of three independent experiments. Scale bars = 1000  $\mu\text{m}$ .**



Sup 4-2 Expression of the M2 receptor following DPSCs osteogenic differentiation. (A) Gene expression data of the M2 mRNA transcript (CHRM2) showing significant upregulated expression after one day of osteogenic differentiation (OS) compared to the undifferentiated control (Ctrl). The data is presented as mean fold change compared to the control (undifferentiated cells) using the  $2^{-\Delta\Delta CT}$  method (Livak and Schmittgen, 2001). Gene expression is relative to the housekeeping gene (GAPDH). (B) Representative western blots of the M2 and GAPDH protein expressions in the undifferentiated control (Ctrl) and cells undergone osteogenic differentiation for one, three, and seven days (OS Day 1, 3, and 7). (C) Densitometric analysis of the M2 protein bands compared to the corresponding loading control (GAPDH) bands showing significant M2 protein levels after one and seven days of osteogenic differentiation (OS Day 1 and 7) compared to the undifferentiated control (Ctrl). All data is derived from duplicates of three independent experiments. A difference of  $P < 0.05$  was considered statistically significant. (ns: not significant, \*\*  $p < 0.01$ , \*\*\*\*  $p < 0.0001$ , OS: osteogenic differentiated cells).

## **5 Activated pathways in response to M2 muscarinic receptor activation.**

## 5.1 Introduction

Muscarinic receptors (mAChRs) are the metabotropic receptors of ACh and their stimulation initiates a cascade of intracellular signalling events owing to their structure and mode of downstream signalling as they couple to several types of G-proteins (Eglen, 2006; Wess, Eglen and Gautam, 2007; Resende and Adhikari, 2009). As these receptors become activated, the coupled G proteins can trigger downstream signalling of hundreds or even thousands of second messenger molecules (Hur and Kim, 2002). As a result, their activation can modulate a plethora of pathways involved in regulating gene expression and cellular functions such as replication, differentiation, cytoskeletal organisation and activity of ion channels (Wessler, Kirkpatrick and Racke, 1999).

Based on downstream functionality of the coupled G proteins, mAChRs are commonly divided into two groups; stimulatory (M1, M3, and M5) or inhibitory (M2 and M4) (Maeda *et al.*, 2019). The stimulatory group, M1, M3, and M5 mAChRs couple to the subunit  $\alpha$  of the Gq/11 family of G proteins. While the inhibitory group, M2 and M4 mAChRs couple to the  $\alpha$  subunit of Gi and Go families of G proteins (Eglen, 2005). The M2 mAChR in particular, has been reported to couple to other families of G proteins such as the Gs family of G proteins, rendering its downstream signalling pattern more difficult to predict (Kebig *et al.*, 2009). Nevertheless, several common effector proteins and secondary messengers have been identified in the downstream signalling of mAChRs including the M2 subtype. These include protein kinase B (PKB, or Akt), phosphoinositide-3-kinase (PI3K), protein kinase C (PKC), inositol triphosphate (IP3), and diacylglycerol (DAG). These effectors and messengers are involved in downstream signalling of multiple pathways (See 1.2.4.1 for details).

In the context of studying the role of muscarinic receptors in stem cells functions, the literature describes identification of functional receptors in different type of MSCs (see chapter 1 for a review). Indeed, there is evidence to suggest mAChRs involvement in regulating MSCs function. In particular, the M2 mAChR has been suggested to be involved in governing BM-MSCs proliferation and differentiation (Hoogduijn, Cheng and Genever, 2009). Furthermore the M2 mAChR has been reported to inhibit AD-MSCs proliferation, migration, and cell cycle progression (Piovesana *et al.*, 2018). Additionally, this mAChR has been suggested to be

involved in FM-MSCs osteogenic differentiation (Yegani *et al.*, 2020). These data suggest an active role of the M2 mAChR in regulating MSCs. Research has also identified a few pathways that the M2 mAChR utilises to transduce its effects. Namely in MSCs, the mitogen-activated protein kinases/ extracellular signal-regulated kinases 1 & 2 (MAPK/ERK 1 & 2) pathways (Hoogduijn, Cheng and Genever, 2009) and the C-X-C motif chemokine ligand 12 - 7/4 receptors (CXCL12-CXCR7/4) axis (Piovesana *et al.*, 2019) have been reported to be involved in the downstream signalling of the M2 receptor. While the Neuregulin-1/ (NRG1)/erbB pathway (Piovesana *et al.*, 2022), PI3K/Akt/mammalian target of rapamycin (mTOR) pathway (Botticelli *et al.*, 2022), NF-E2 p45-related factor 2/antioxidant response element (Nrf2/ARE) signalling pathway (Luo *et al.*, 2020), and the protein kinase A/mTOR (PKA/mTOR) pathway (Dong *et al.*, 2018) have been reported to be involved in the downstream signalling of this receptor in several other cell types. All of these showed there are multiple distinct pathways involved in the downstream signalling of the M2 mAChR.

In the previous chapters, the data showed expression of a functional M2 mAChR in DPSCs. Activation of the M2 receptor via its selective agonist (APE) inhibited the proliferation of DPSCs in a reversible manner without affecting viability or stemness (See 3.3.1, 3.3.2, and 4.3.2 for details). Further analysis showed that this inhibition is through a cell cycle arrest (See 3.3.3 for details). Analysis of DPSCs migration and differentiation showed M2 activation suppressed these functions (See 4.3.1 & 4.3.3 for details). In this chapter, the aim was to unravel the signalling pathways and transcriptomic changes that influence these observed effects, as well as taking a more holistic view of the cellular process involved in M2 activation. This was largely carried out via transcriptomic sequencing of DPSCs after stimulation with the M2 receptor selective agonist (APE) and followed by investigating the involvement of the MAPK/ERK pathway.

## **5.2 Materials and Methods**

### **5.2.1 Cells and cell culture**

The DPSCs investigated in this chapter were from the same batch used in this project and were between passages four and six. Cells were cultured in normal medium (i.e., DMEM-KO) as described 2.2.1.

### **5.2.2 M2 muscarinic receptor stimulation**

DPSCs were treated with the M2 selective agonist as described in 3.2.2. Treatments were carried out in duplicates on three independent occasions over several time points according to experimental design of the investigated assay.

### **5.2.3 RNA sequencing**

#### **5.2.3.1 Sample preparation and RNA isolation**

DPSCs were stimulated with the M2 agonist as described in 3.2.2., for 4 and 24 hours (h). The RNA extraction was carried out as described in 2.2.2.1. The quality and quantity of RNA was checked using a Bioanalyzer (Agilent RNA 6000 Nano Kit, Bioanalyzer 2100 system, Agilent Technologies, CA, USA). Samples with a minimum RNA integrity number (RIN) of 7.0 and a minimum quantity of 0.4 µg (≥ 20 ng/µL) were deemed acceptable and sent for sequencing (Novogene Co., LTD, Cambridge, UK).

#### **5.2.3.1 RNA sequencing workflow:**

RNA sequencing was performed by Novogene, UK. This involved three stages with three quality assurance checkpoints (Figure 5-1). Briefly, samples were subjected to their 'in house' assessment of RNA quality and quantity to confirm that they met the minimum requirement for sequencing. This was followed by RNA library preparation by polyA capture using the NEB Next® Ultra™ RNA Library Prep Kit. The constructed library was subjected to a quality control checkpoint to check quantification and size distribution of cDNA. Then samples were analysed on a Novaseq 6000 (an Illumina based platform) sequencing platform.

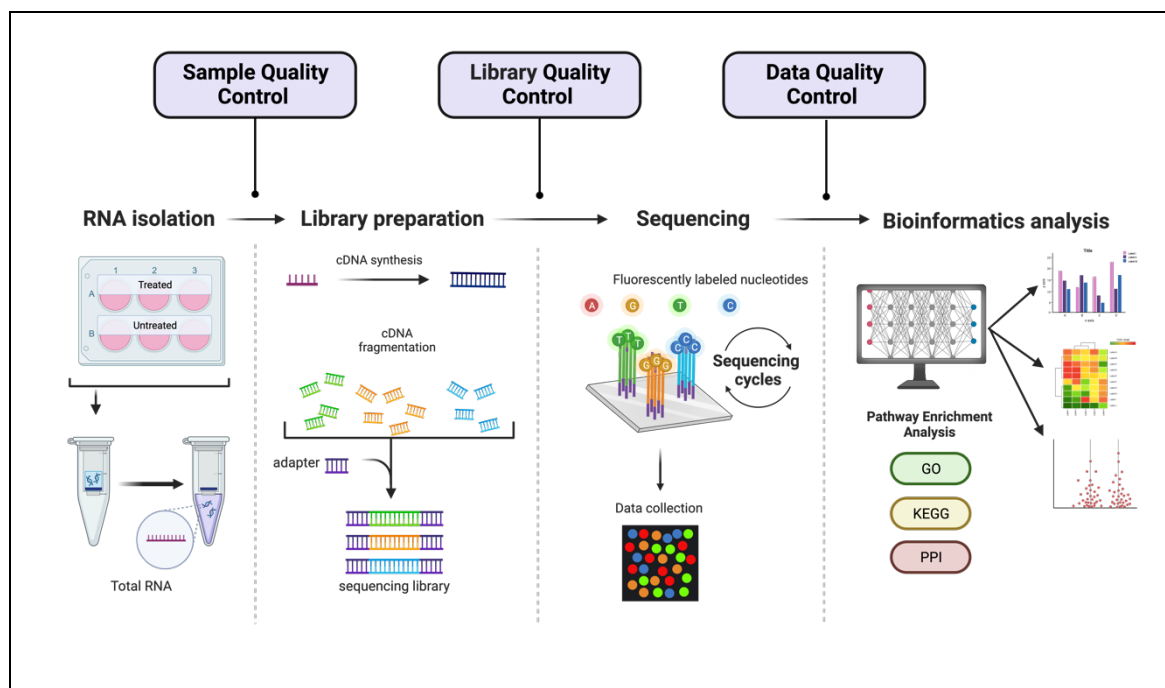


**Figure 5-1** Experimental procedures and sequencing workflow. Total RNA was isolated from treated and untreated cells. Samples were then sent to Novogene for library preparation, sequencing and bioinformatics analysis through an in-house perl scripts.

### 5.2.3.2 Analysis pipeline:

Bioinformatic analysis was performed by Novogene (Novogene Co., LTD, Cambridge, UK). Raw data (raw reads) of fastq format were processed through in-house perl scripts. A summary of the analysis pipeline is illustrated in (Figure 5-2).

#### 5.2.3.2.1 Quality control

Raw data (raw reads) of fastq format were firstly processed through in-house perl scripts. In this step, clean data (clean reads) were obtained by removing reads containing adapter, reads containing poly-N and low-quality reads from the raw data. All the downstream analyses were based on the high-quality clean data.

#### 5.2.3.2.2 Reads mapping to the reference genome

Reference genome and gene model annotation files were downloaded from the National Center for Biotechnology Information genome website directly (NCBI Bethesda (MD), 1988). Index of the reference genome was built using Hisat2 (v2.0.5) (Kim, Langmead and Salzberg, 2015) and paired-end clean reads were aligned to the reference genome (Human Genome Assembly GRCh38.p14) using Hisat2 (v2.0.5). Selecting Hisat2 as the mapping tool enabled generation of a database of splice junctions based on the gene model annotation file and thus allowed better mapping than using alternative non-splice mapping tools.

#### 5.2.3.2.3 Novel transcripts prediction

The mapped reads for each sample were assembled by StringTie (v1.3.3b) (Pertea *et al.*, 2015) in a reference-based approach. StringTie uses a novel network flow algorithm as well as an optional *de novo* assembly step to assemble and quantitate full length transcripts representing multiple splice variants for each gene locus.

#### 5.2.3.2.4 Quantification of gene expression

The featureCounts (v1.5.0-p3) (Liao, Smyth and Shi, 2014) was used to count the reads mapped to each gene. Next, the Fragments Per Kilobase of transcript sequence per Millions base pairs sequenced (FPKM) of each gene was calculated based on the length of the gene and number of reads mapped to this gene. FPKM considers the effect of sequencing depth and gene length for the read counts at the same time and is currently the most commonly used method for estimating gene expression levels (Guo *et al.*, 2013).

#### 5.2.3.2.5 Differential expression analysis

Differential expression analysis of two conditions/groups (two biological replicates per condition) was performed using the DESeq2 R package (1.20.0) (Love, Huber and Anders, 2014). DESeq2 provide statistical routines for determining differential expression in digital gene expression data using a model based on the negative binomial distribution. The resulting P-values were corrected and presented as p adjusted values (padj) using the Benjamini and Hochberg's approach for controlling the false discovery rate. Genes with a padj  $\leq 0.05$  found by DESeq2 were assigned as significantly differentially expressed.

#### 5.2.3.2.6 Gene set enrichment analysis

Gene Set Enrichment Analysis (GSEA) is a computational approach to determine if a pre- defined gene set showed a significant consistent difference between two biological states. The genes were ranked according to the degree of differential expression in the two samples, and then the predefined gene set were tested to see if they were enriched at the top or bottom of the list. Gene set enrichment analysis can determine subtle expression changes. The local version of the GSEA analysis tool <http://www.broadinstitute.org/gsea/index.jsp>, GO, KEGG data set were used for GSEA independently.

### 5.2.3.2.7 Pathways enrichment analysis of differentially expressed genes

Gene Ontology (GO) enrichment analysis of differentially expressed genes was implemented by the clusterProfiler R package, in which gene length bias was corrected (Wu *et al.*, 2021). GO terms with a  $p_{adj} \leq 0.05$  were considered significantly enriched by differential expressed genes. The Kyoto Encyclopaedia of Genes and Genomes (KEGG) is a database resource for understanding high-level functions and utilities of the biological system, such as the cell, the organism and the ecosystem, from molecular-level information, especially large-scale molecular datasets generated by genome sequencing and other high-through put experimental technologies (<http://www.genome.jp/kegg/>). The R package clusterProfiler was used to test the statistical enrichment of differential expression genes in KEGG pathways.

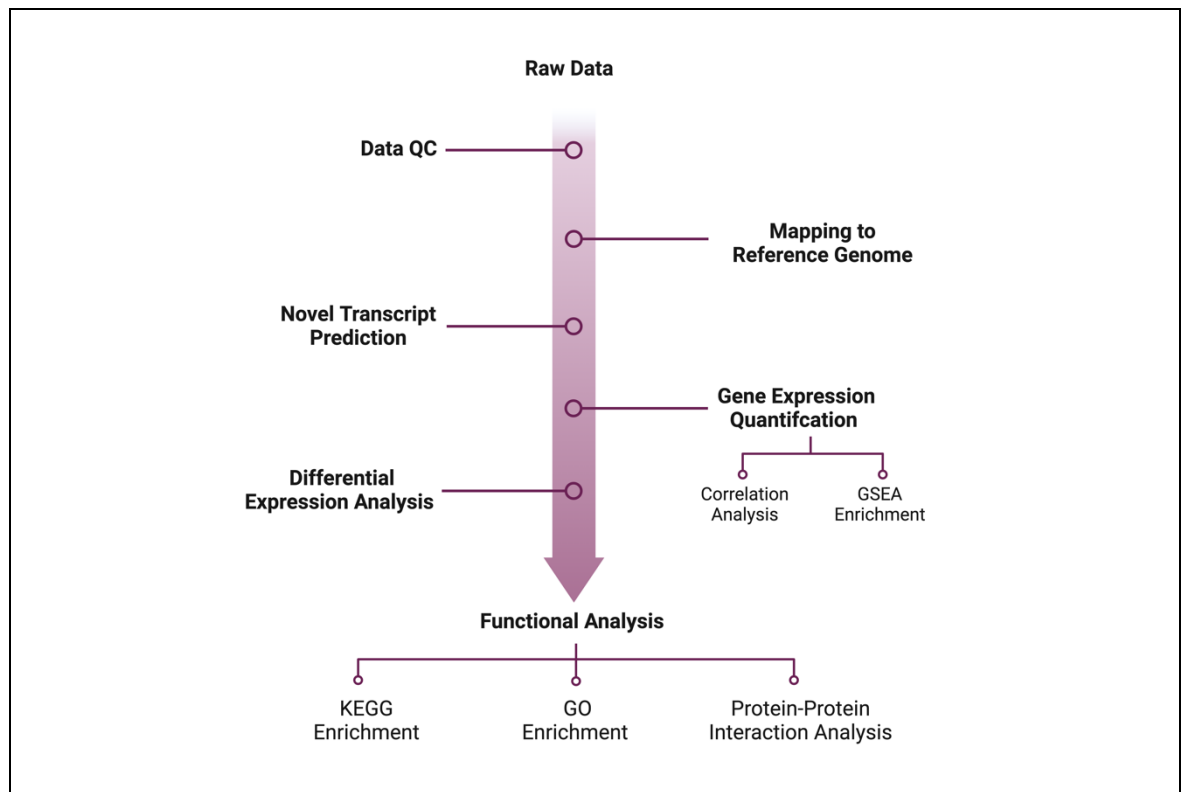


**Figure 5-2 Bioinformatic analysis pipeline.** The schematic diagram shows the bioinformatics pipeline used by Novogene for data analysis. Raw sequences were subjected to a quality control checkpoint to achieve high quality reads. Reads were mapped to the human reference genome, and the aligned transcripts were assembled and quantified. Differentially expressed genes were analysed for significant pathways enrichment using different databases.

#### **5.2.4 ERK1/2 Enzyme-linked immunosorbent assay**

To evaluate the involvement of the mitogen-activated protein kinases/extracellular signal-regulated kinases 1 & 2 (MAPK/ERK 1 & 2) pathway in the downstream signalling of the M2 muscarinic receptor, a sandwich enzyme-linked immunosorbent assay (ELISA) was used to measure phosphorylation of ERK1 and ERK2 (Phospho-ERK1 (T202/Y204)/ERK2 (T185/Y187) DuoSet IC ELISA, DYC1018, R&D Systems) following manufacturer's instructions. Briefly, DPSCs were incubated with the selective M2 agonist (APE) between 0 - 40 minutes (min) at 37°C. The cells were rinsed twice with PBS, lysed with lysis buffer, and incubated on ice for 15 min. Samples were then centrifuged at 2000 x g for five min and only supernatant was kept for the assay. Bicinchoninic acid assay (Pierce™ BCA Protein Assay Kit, 23225, Thermo Scientific™) was carried out to standardise protein concentrations between samples. The capture antibody was incubated in a 96-well plate overnight at room temperature (RT). The following day, the antibody was aspirated, and wells were washed three times with the wash buffer. The wells were incubated with the blocking buffer for one hour at RT. Then, wells were washed three times and the Phospho-ERK1/ERK2 standard and samples were loaded into the plate and incubated for two hours at RT. This was followed by another wash step and the detection antibody was loaded into the plate and incubated for two hours at RT. This was followed by another wash step and Streptavidin-HRP A was loaded into the plate and incubated for 20 min at RT. This was followed by another wash step and substrate solution (1:1, H<sub>2</sub>O<sub>2</sub>: Tetramethylbenzidine) was loaded into the plate and incubated for 20 min at RT in the dark. Finally, the stop solution (2 N Sulfuric Acid) was added to each well, and the plate was read on a microplate reader (FLUOstar Omega microplate reader) at 450 nm (measurement wavelength) and 540 nm (reference wavelength). The concentrations of phospho-ERK1/2 in the cell lysates were determined using a calibration curve with recombinant human phospho-ERK2 (Thr85/Tyr187) and the differences were compared with the untreated control.

#### **5.2.5 Quantitative polymerase chain reaction (q-PCR) analysis**

Primer sequences for genes involved the ERK 1/2 pathway are provided in Table 5-1. Target gene primers and the prepared cDNA samples were mixed with the

Chapter 5: Activated pathways in response to M2 muscarinic receptor activation.

fast SYBR Green Master Mix (Fast SYBR™ Green Master Mix 4385610, Applied Biosystems™, UK) described in 2.2.2.4.

**Table 5-1 Primer sequences for genes investigated in chapter 5.**

Primer	Sequence
<i>GAPDH</i>	Fwd: GCAGGGGGGAGCCAAAAGGG Rev: TGCCAGCCCCAGCGTCAAAG
<i>MAPK1</i>	Fwd: ACACCAACCTCTCGTACATCGG Rev: TGGCAGTAGGTCTGGTGCTCAA
<i>MAPK3</i>	Fwd: TGGCAAGCACTACCTGGATCAG Rev: GCAGAGACTGTAGGTAGTTTCGG
<i>PCNA</i>	Fwd: CAAGTAATGTCGATAAAGAGGAGG Rev: GTGTCACCGTTGAAGAGAGTGG

## 5.2.6 Statistical analysis

Statistical analysis was performed as in 2.2.5. Statistical analysis for RNA sequencing is described in 5.2.3.2.5.

## 5.3 Results

### 5.3.1 Overview of RNA sequencing data

Whole transcriptomic sequencing was performed to investigate the differences in DPSCs gene expression upon M2 activation via its selective agonist APE (100  $\mu$ M) for 4 and 24 h. The conditions chosen for transcriptomic analysis were based on the observable effect of APE on DPSCs proliferation (See Chapter 3 for details), where 100  $\mu$ M APE was shown to inhibit DPSCs proliferation without affecting their viability, stemness, and ability to recover their growth upon withdrawal. Furthermore, the 100  $\mu$ M concentration maintained DPSCs in a quiescent state for up to 144 h. In addition, significant differential expression of genes investigated with targeted q-PCR were observed as early as 24 h after stimulation with APE. The acquired sequencing data were processed for differentially expressed genes (DEGs) in response to M2 activation via its selective agonist APE. The sequenced sample groups consisted of four biological repeats of untreated controls (Ctrl) and treated samples with the M2 agonist (APE) at each timepoint (4 and 24 h), where a degree of homogeneity is observable between biological replicates indicated by the correlation analysis that showed the  $R^2$  between the biological replicates was higher than 0.98 (Figure 5-3). All sequenced samples passed the quality control criteria (Sup 5-1) and scored more than 96% in mapping to the reference genome (Human Genome) (Sup 5-2). Multivariate analysis using principal component analysis (PCA) showed that the duration of stimulation (4 and 24 h) caused the highest variance in clustering by 52% (x-axis), followed by 11% due to nature of stimulation (untreated (Ctrl) vs treated (APE) at the y-axis) (Figure 5-4). At 24 h the separation along the y-axis of gene expression between untreated controls and cells treated with APE was the greatest, suggesting greater differences will be observed at this time point.

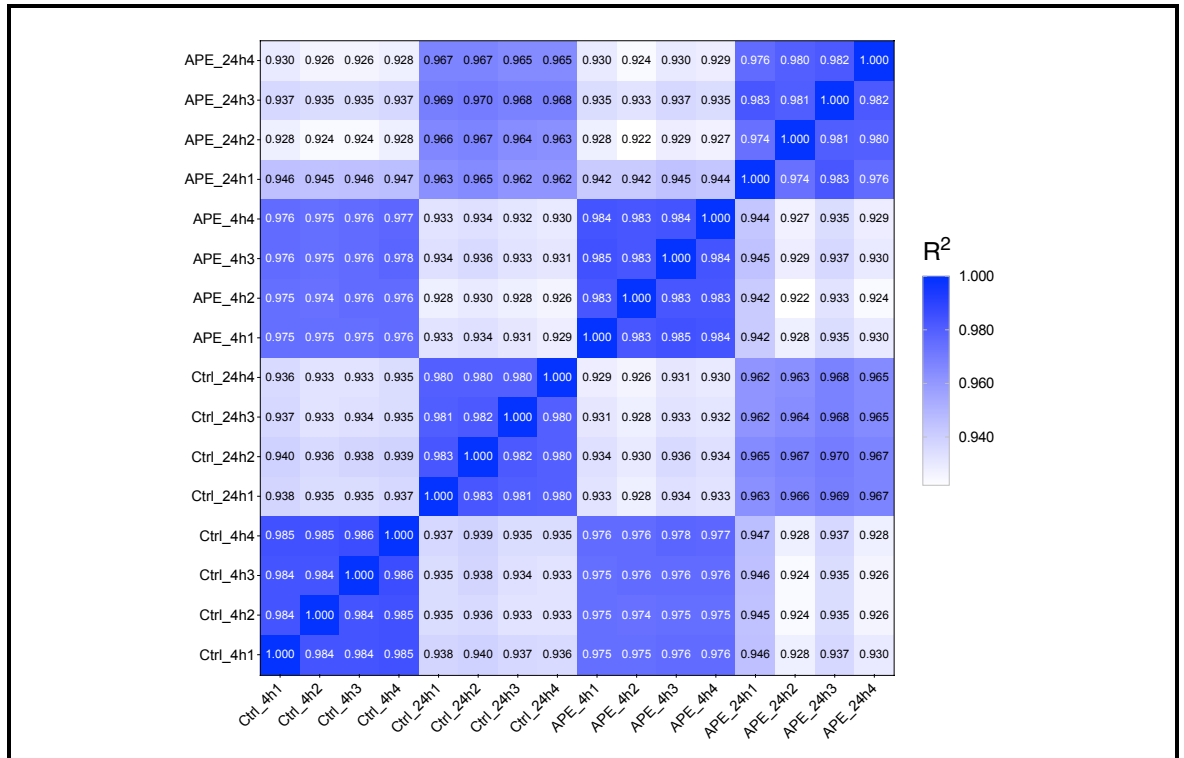


**Figure 5-3 Pearson correlation coefficients between samples.** The Pearson correlation coefficients between replicates of the same condition remained high, with an average coefficient of  $r = 0.988$  for replicates in the 4h untreated group (Ctrl\_4h1-4),  $r=0.985$  for replicates in the 24h untreated group (Ctrl\_24h1-4),  $r=0.987$  for replicates in the 4h treated group (APE\_4h1-4), and  $r=0.984$  for replicates in the 24h treated group (APE\_24h1-4), which indicated satisfactory reproducibility of the biological replicates.

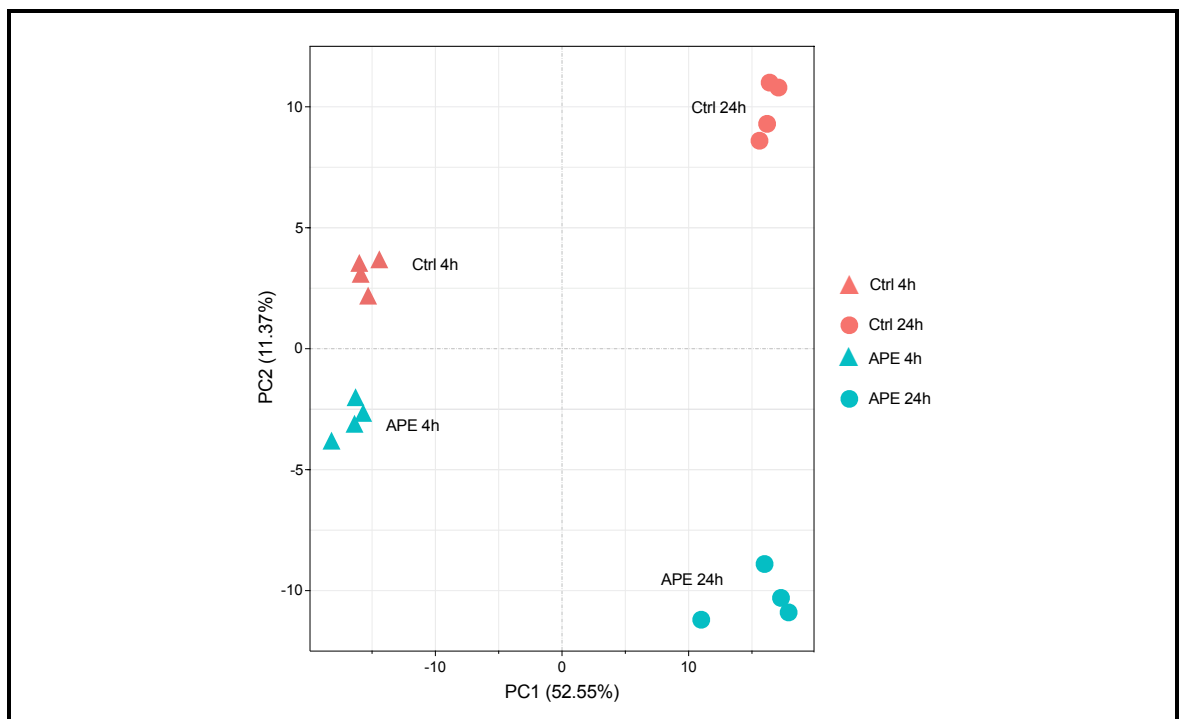


**Figure 5-4 Principal Component Analysis (PCA).** Grouping of samples was based on variance in expression. PCA analysis of differential gene expression in response to M2 activation via APE and the untreated controls (Ctrl). PC1 shows the largest variance (52%) along the x-axis and PC2 displays the second largest variance (11%) on the y-axis.

Gene expression and co-expression patterns presents an overview of the sequenced samples (Figure 5-5). The data indicates that the number of genes expressed in the treated group with the M2 agonist (APE) is less compared to the

untreated control (Ctrl) (Figure 5-5 A). The number of genes expressed across the duration of stimulation is higher in the untreated control at 24 h compared to 4 h (Ctrl 24h, Ctrl 4h, respectively), whereas relatively there is no difference in the treated group with the M2 agonist between 24 h and 4 h (APE 24h, APE 4h, respectively) (Figure 5-5 B). However, the number of DEGs between the untreated and treated samples is greater at 24 h compared to 4 h (Ctrl vs APE 24h, Ctrl vs APE 4h, respectively) (Figure 5-5 C). The data further showed 38 DEGs in both stimulation timepoints (overlapping region between Ctrl vs APE 4h and Ctrl vs APE 24h) (Figure 5-5 C).

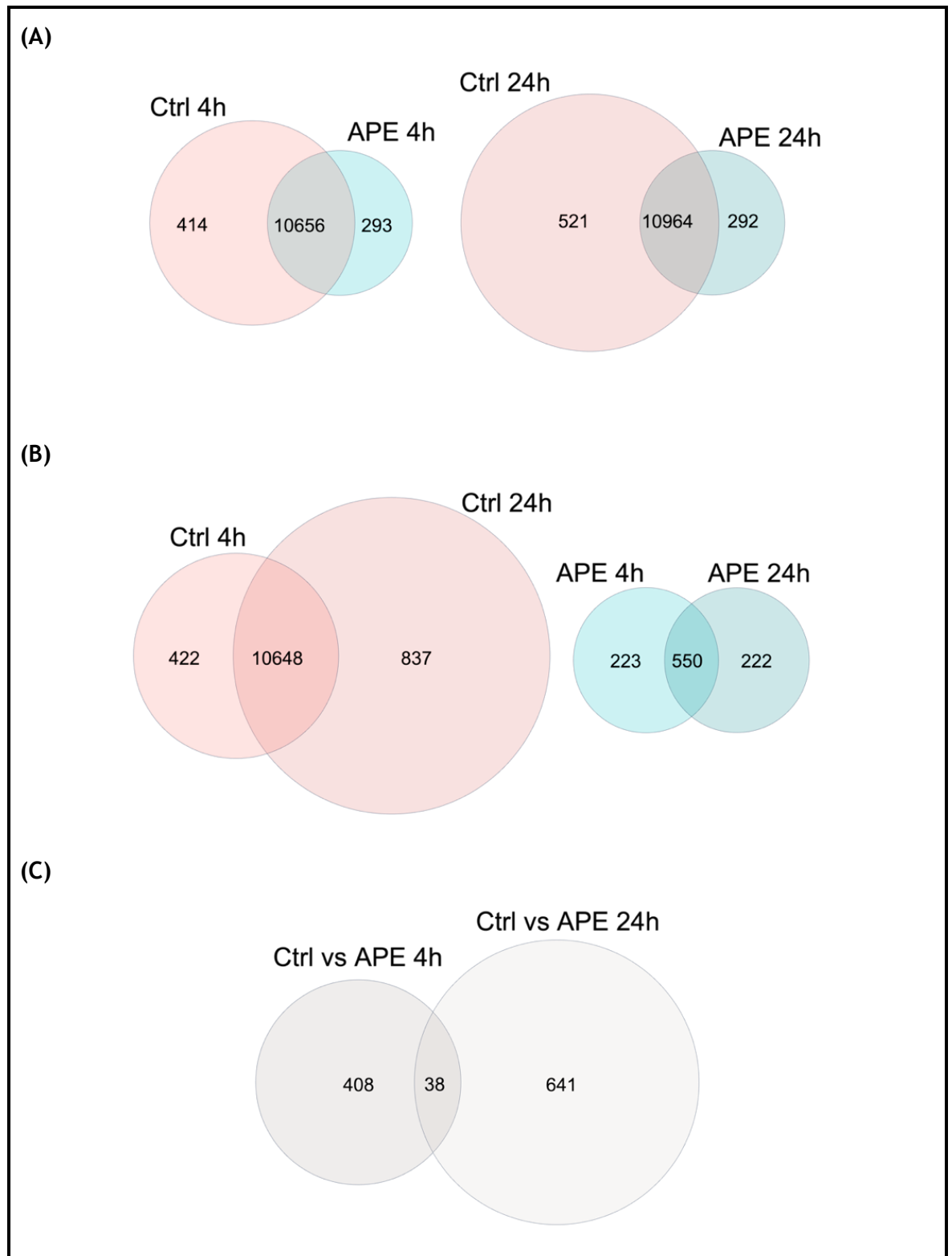


**Figure 5-5 Venn diagrams illustrating gene expression patterns and co-expression in each experimental group. Non-overlapping regions shows the number of genes that are detected in the experimental groups, while overlapping regions shows the number of genes that are shared between the two groups. (A) Gene expression patterns after 4 and 24 hours of stimulation between untreated (Ctrl) and treated (APE). (B) Gene expression patterns of the same experimental group across the duration of stimulation. (C) DEGs pattern between stimulation timepoints.**

### 5.3.2 Differentially expressed genes in response to M2 agonist stimulation

The DEGs analysis was then carried out to determine the effect of M2 agonist stimulation, via its selective agonist (APE), on DPSCs gene expression. Significant DEGs were determined as those genes that display a fold change greater than 1 and a padj of less than or equal to 0.05. Volcano plots were utilised to compare DEGs between untreated DPSCs and M2 agonist stimulated at 4 and 24 h (Figure 5-6). The data show 117 significantly upregulated genes and 329 significantly downregulated genes after 4 h of M2 stimulation compared with untreated control (Figure 5-6 A). For the 24 h stimulation, the data show 205 significantly upregulated genes and 474 significantly downregulated genes of M2 stimulation compared with untreated control (Figure 5-6 B).

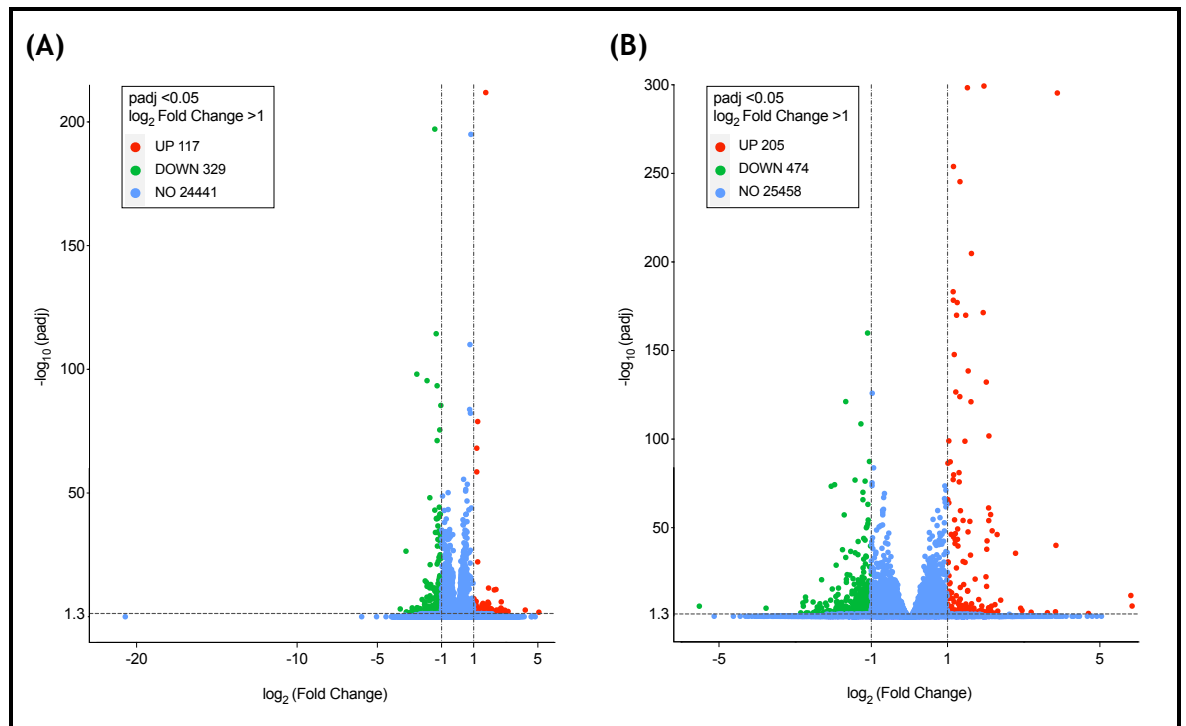


**Figure 5-6** Volcano plots for differentially expressed genes (DEGs). DPSCs stimulated with the M2 agonist (APE) vs untreated cells as controls after 4 hours (A) and 24 hours (B). Scattered points represent genes: the x-axis is the log<sub>2</sub> fold change for the ratio of treated vs untreated cells, whereas the y-axis is the -log<sub>10</sub> of the padj-value in which 1.3 represents a padj < 0.05. Red dots are thus genes significantly upregulated after stimulation with the M2 agonist (117 after 4h and 205 after 24h), green dots are genes significantly downregulated after stimulation (329 after 4h and 474 after 24h), blue dots indicate the remaining genes present in the array that were not significantly changed.

Heatmap analysis of normalised Log<sub>2</sub> fold change in gene expression was utilised to determine the top 50 DEGs (ranked by padj value) at each timepoint (Figure 5-7). Most of the genes in the treated group (APE) showed downregulated expression after 4 h (Figure 5-7 A), while most of the genes in the 24 h treated group (APE) showed upregulated expression (Figure 5-7 B).

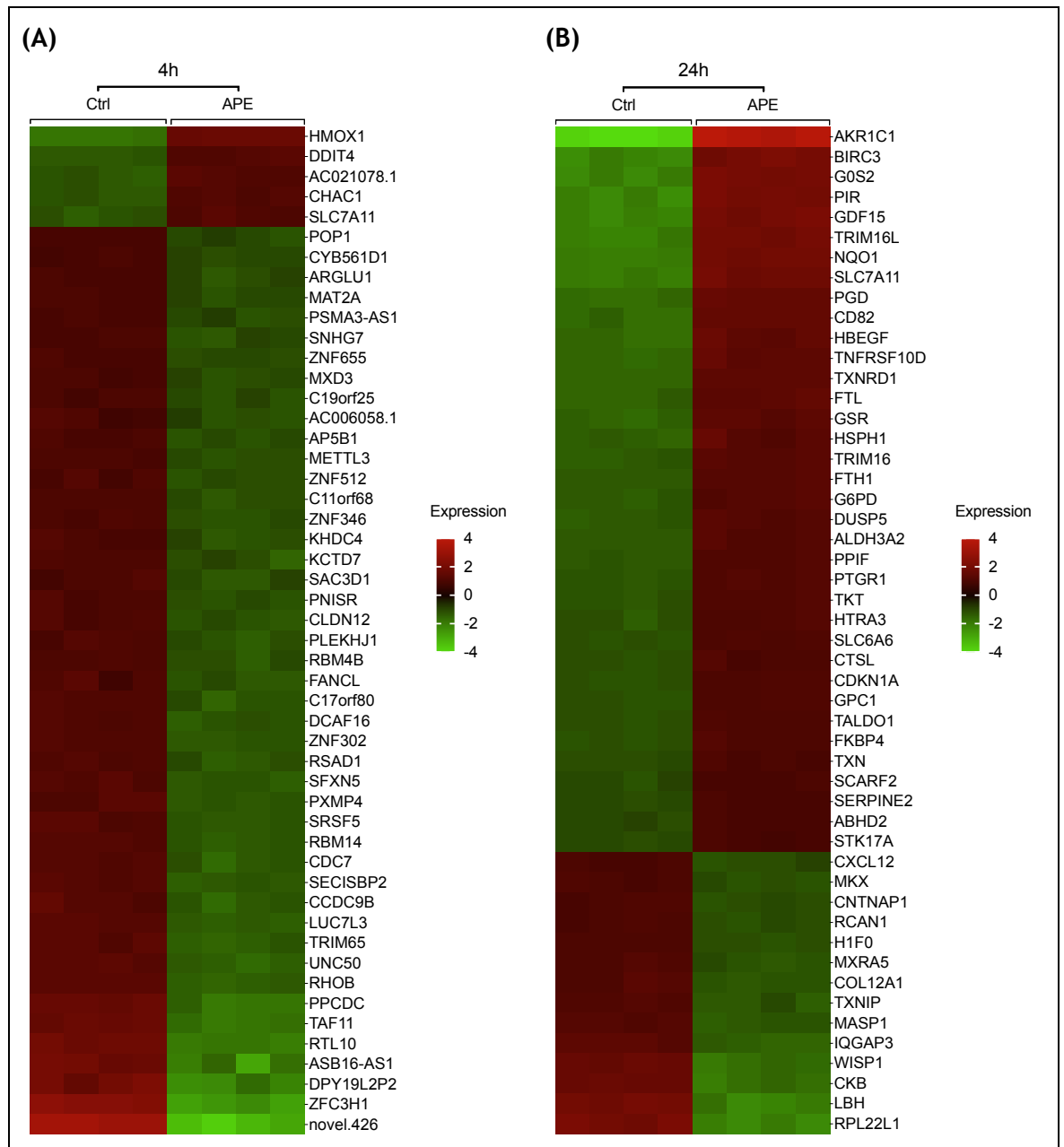


**Figure 5-7** Heatmaps of the top 50 significantly (DEGs) after stimulation with the M2 agonist. Top 50 for 4 hours shown in (A) and top 50 for 24 hours shown in (B). The genes are clustered based on the normalised Log<sub>2</sub> fold change in gene expression, where the red and green colour scale at the right of the heatmap represents higher and lower relative expression levels, respectively. Each row represents one gene, and each column represents a single sample of the experimental groups; untreated (Ctrl) and treated (APE). The gene symbols are shown on the right side of the rows.

Heatmap analysis of the 38 DEGs found to be significantly differentially expressed at both stimulation timepoints (4 and 24 h; Figure 5-5 C) showed most with a downregulated expression (Figure 5-8). Interestingly, a few DEGs showed a unique pattern of expression during the stimulation time course. For example, *STAG3L1* and *TRIM47* display downregulated expression after 4 h of stimulation, and then upregulated expression at 24 h (Figure 5-8).

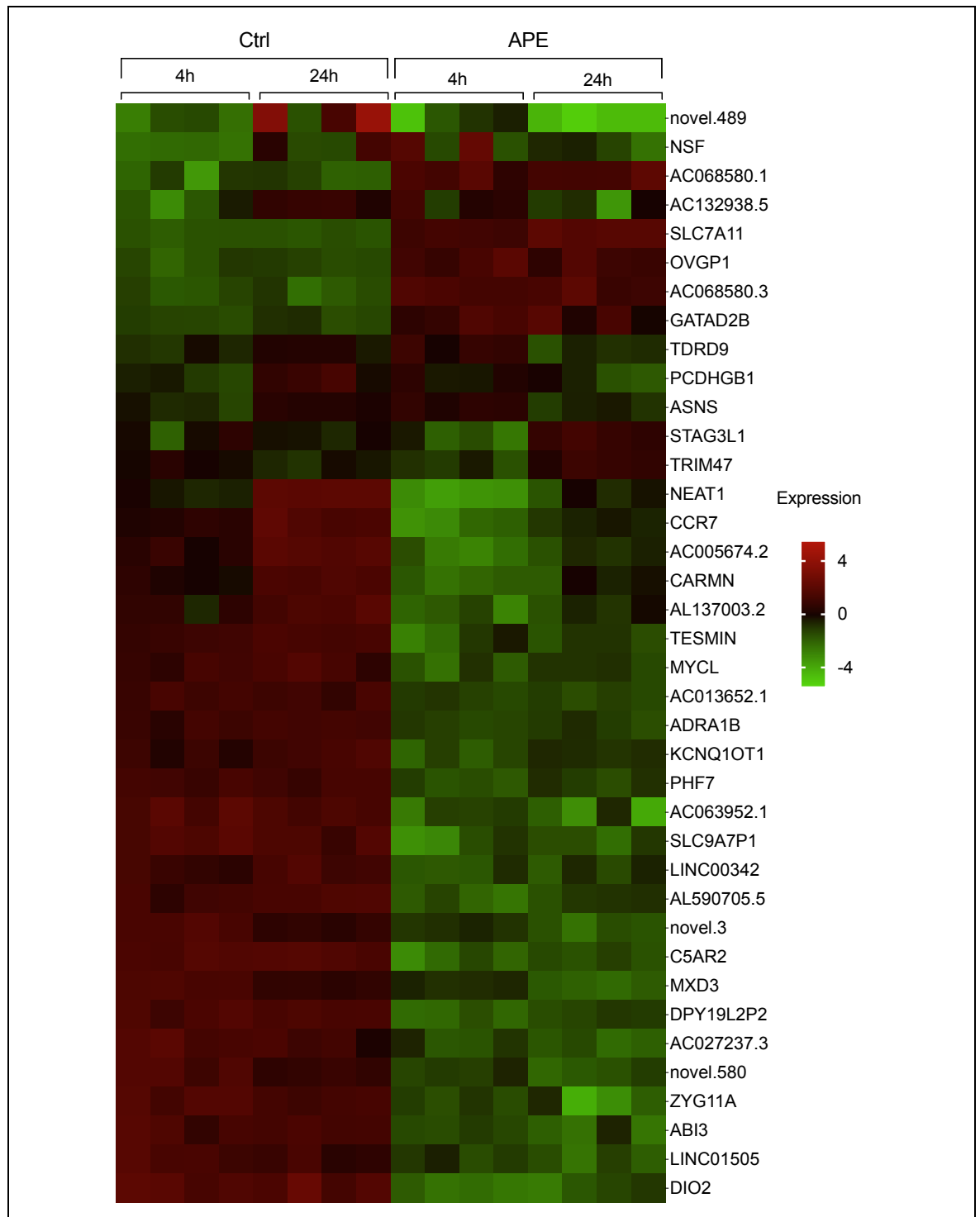


**Figure 5-8** Heatmap of the 38 significantly differentially expressed genes (DEGs) at both timepoints (4h and 24h). The genes are clustered based on the normalised Log2 fold change in gene expression, where the red and green colour scale at the right of the heatmap represents higher and lower relative expression levels, respectively. Each row represents one gene, and each column represents a single sample of the experimental groups; untreated (Ctrl) and treated (APE) after 4 and 24 hours. The gene symbols are shown on the right side of the rows.

### 5.3.3 Gene Ontology (GO) analysis

Gene ontology (GO) analysis was then carried out to investigate the biological functions of the DEGs in response to M2 stimulation via its selective agonist (APE). An overview of the analysis showed no significant enrichment in the 4 h stimulated group compared to the 24 h group that revealed a total of 29 significant enriched GO terms in the three categories of GO terms: Biological Process (BP), Cellular Component (CC), and Molecular Function (MF) (13 in BP, three in CC, and 13 in MF) (Figure 5-9 A). The sub-analysis of the upregulated and downregulated significantly enriched GO terms showed a similar pattern in regard to stimulation duration, however, with increased number of GO terms on account of the recalculated *p*adj (Figure 5-9 B). The 4 h stimulated group showed only eight significantly upregulated GO terms in MF, while the 24 h group showed 61 significantly upregulated GO terms in BP, 1 in CC, and 26 in MF (Figure 5-9 B). The 24 h stimulated group also showed two significantly downregulated GO terms in MF (Figure 5-9 B).

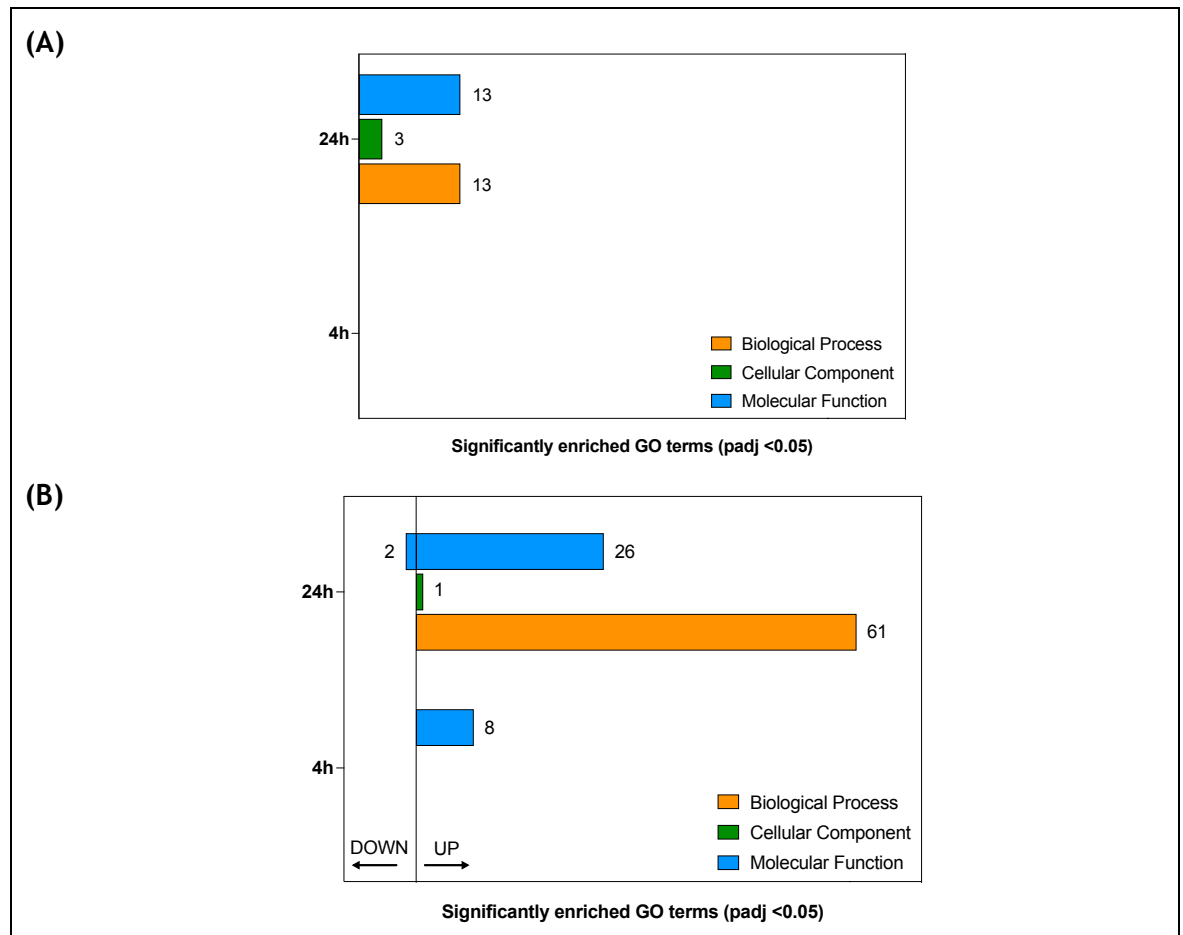


**Figure 5-9** GO enrichment analysis of significantly enriched GO terms. **(A)** Overview of significantly enriched GO terms in the three GO categories after 4 and 24 hours of stimulation with the M2 agonist (APE) relative to the corresponding controls (i.e., untreated at 4 and 24h). **(B)** Overview of significantly upregulated and downregulated enriched GO terms in the three GO categories after 4 and 24 hours of stimulation with the M2 agonist.

The analysis of the top ten in each GO category showed only significantly enriched GO terms in the 24 h stimulated group (Figure 5-10 B). The significantly enriched terms in BP generally describe cellular detoxification and regulation of cellular processes and homeostasis in response to environmental challenges. The significantly enriched terms in CC generally describe the extracellular matrix and its interaction with the cell surface in facilitating processes such as growth, differentiation, and migration. The significantly enriched terms in MF generally describe cellular signalling and metabolism involved in pathways associated with cell growth, differentiation, and the cell cycle.

The analysis of the top ten in each GO category of upregulated and downregulated DEGs between M2 stimulated cells and untreated ones was also carried out (Figure 5-11). The 4 h stimulated group showed eight significantly upregulated GO terms in MF that generally describe the function of helicases and ATPases in processes involved in RNA binding, transcription, and translation (Figure 5-11 B). The 24 h stimulated group showed two significantly downregulated GO terms in MF that

generally describe proteins involved kinase proteins involved in transmembrane signal transduction differentiation (Figure 5-11 C). Moreover, the 24 h stimulated group showed ten significantly upregulated GO terms in BP that generally describe cellular responses to oxidative stress and metabolic processes involved in production of antioxidants (Figure 5-11 D). Additionally, the 24 h stimulated group showed one significantly upregulated GO terms in CC that generally describe formation of secondary lysosomes involved in clearing foreign matter and antigen presentation for the immune system (Figure 5-11 D). Also, the 24 h stimulated group showed ten significantly upregulated GO terms in MF that generally describe mechanisms involved in cellular metabolism and reactions involved in oxidation of fatty acids and production of ATP (Figure 5-11 D).

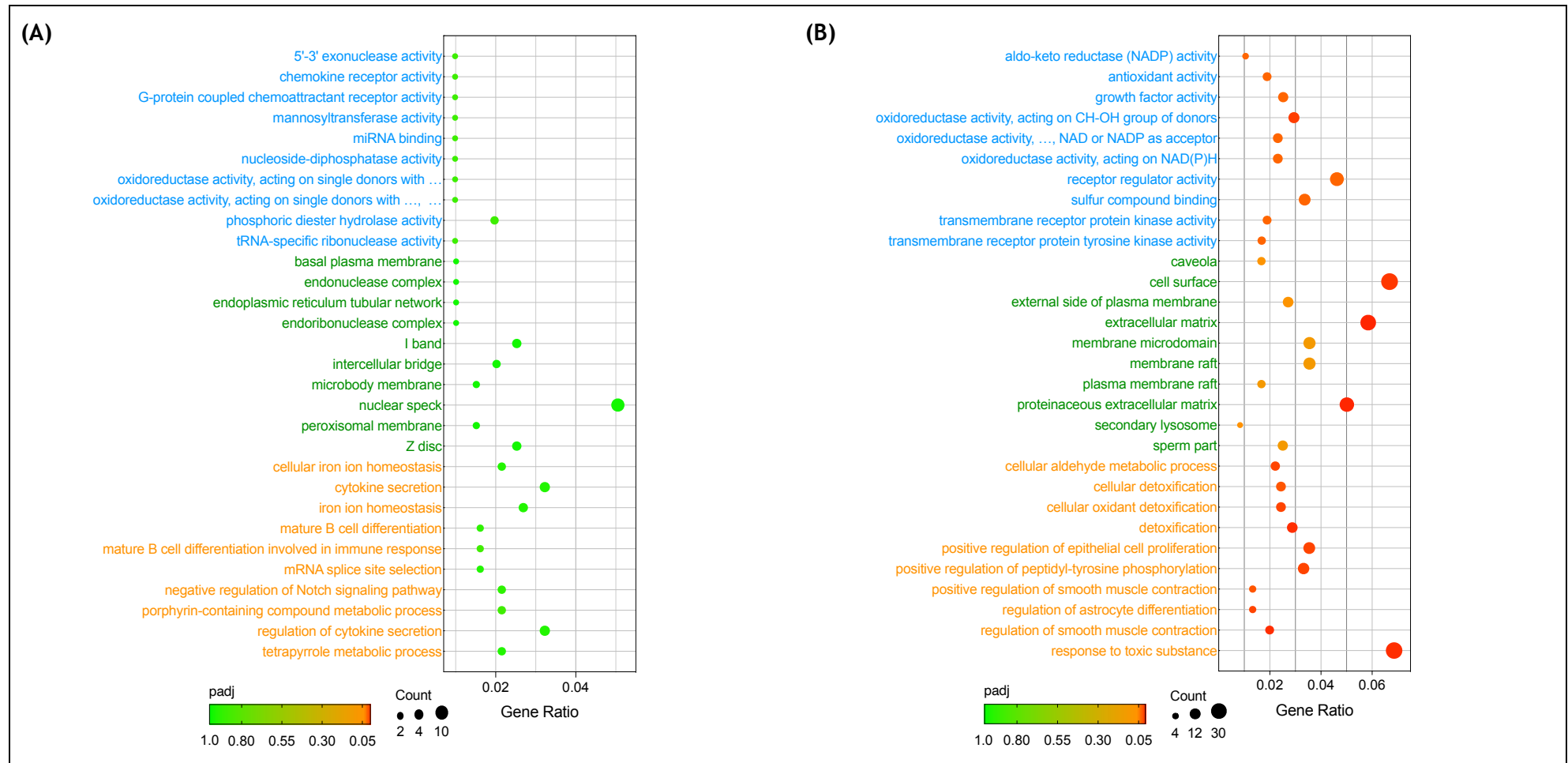
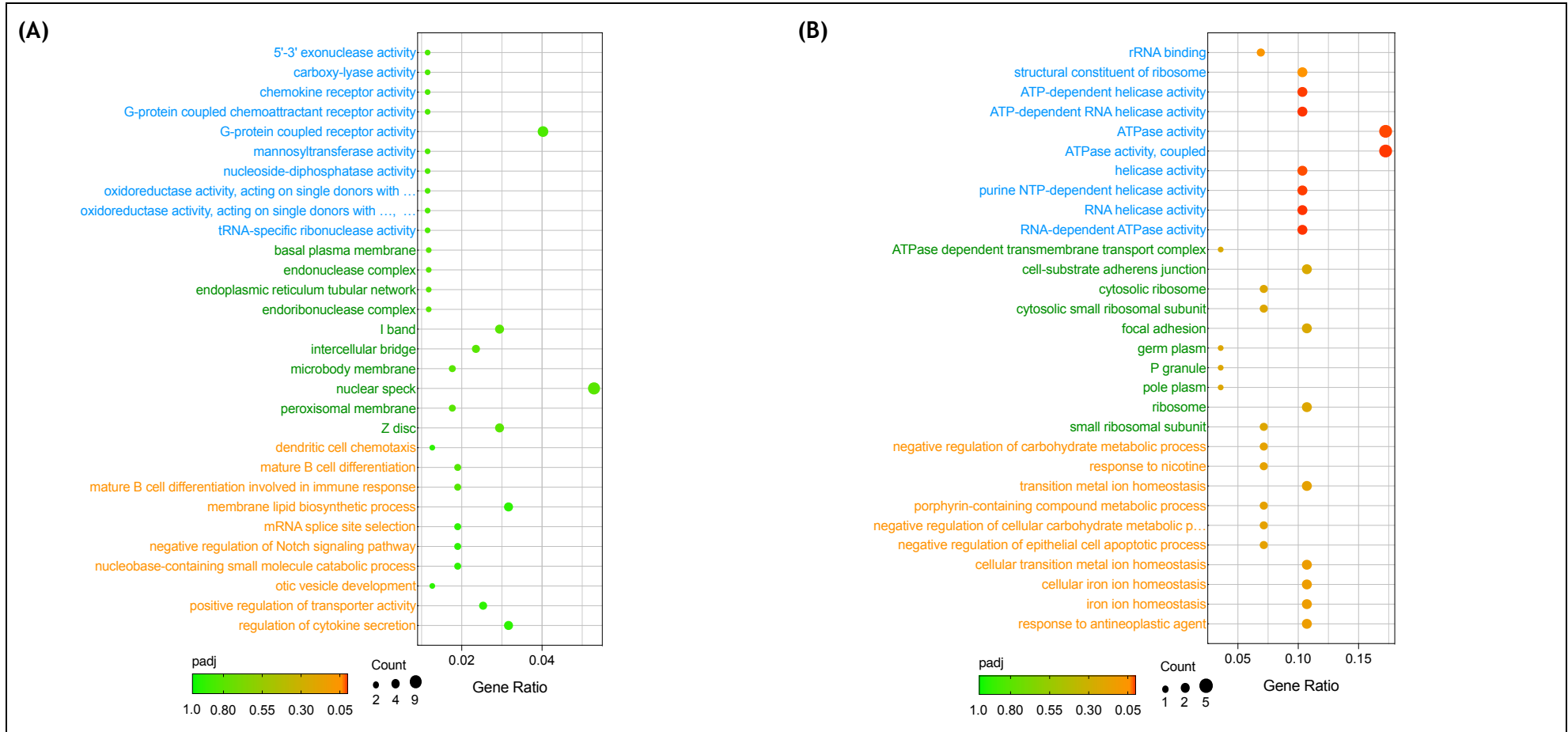


Figure 5-10 Top 30 GO terms (top ten in each category) after stimulation with the M2 agonist (APE). (A) shows the 4 hours data and (B) shows the 24 hours data. (A-B) shows the top ten GO terms of the three categories (Biological Process: orange font, Cellular Component: green font, Molecular function: blue font). Gene ratio (x-axis) is the percentage of genes present in this GO term over the total number of genes in this category. The size of the dot is based on gene count enriched in the pathway, and the colour of the dot shows the pathway enrichment significance where a red dot represents a padj <0.05. The description of GO terms is shown on the left side of each plot.

Chapter 5: Activated pathways in response to M2 muscarinic receptor activation.



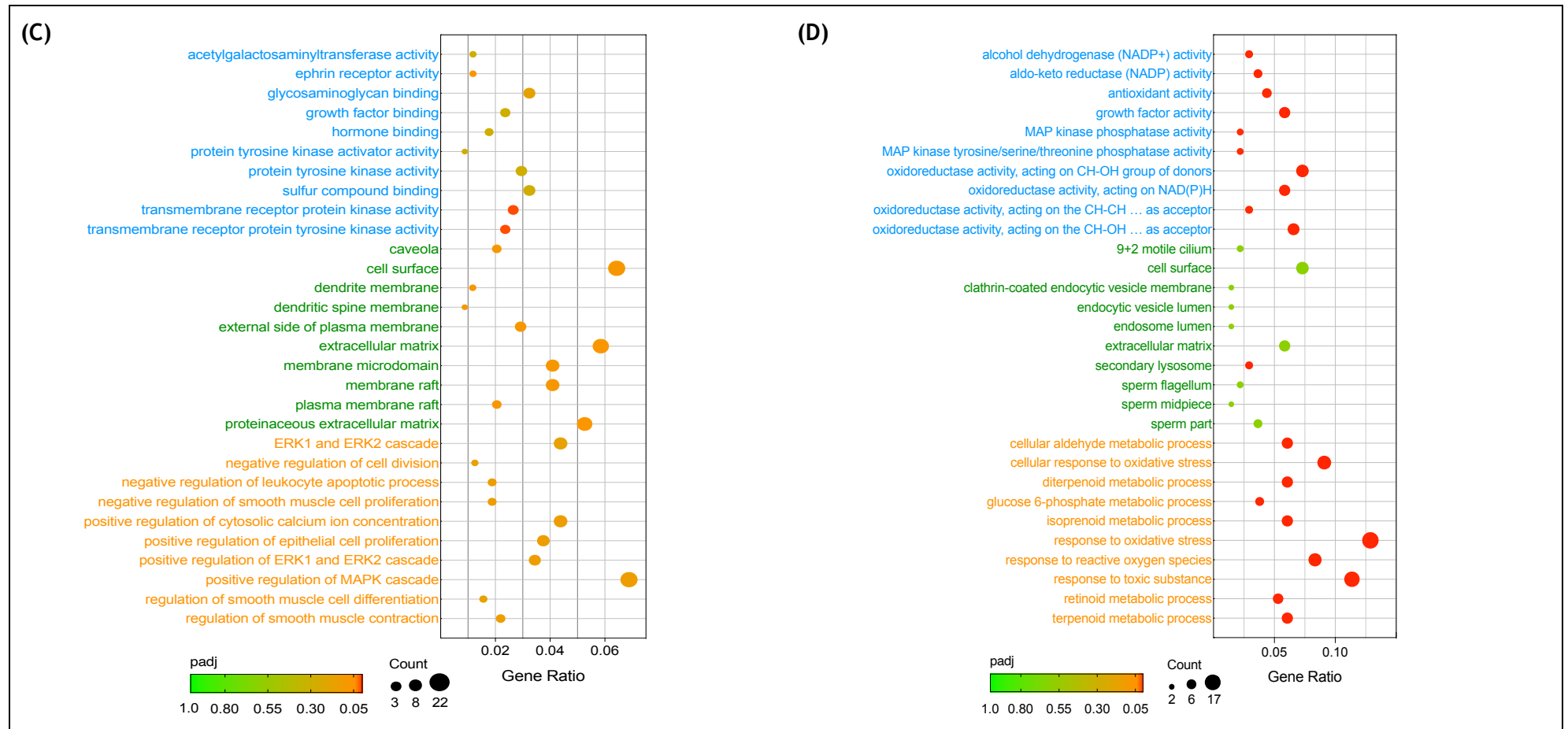
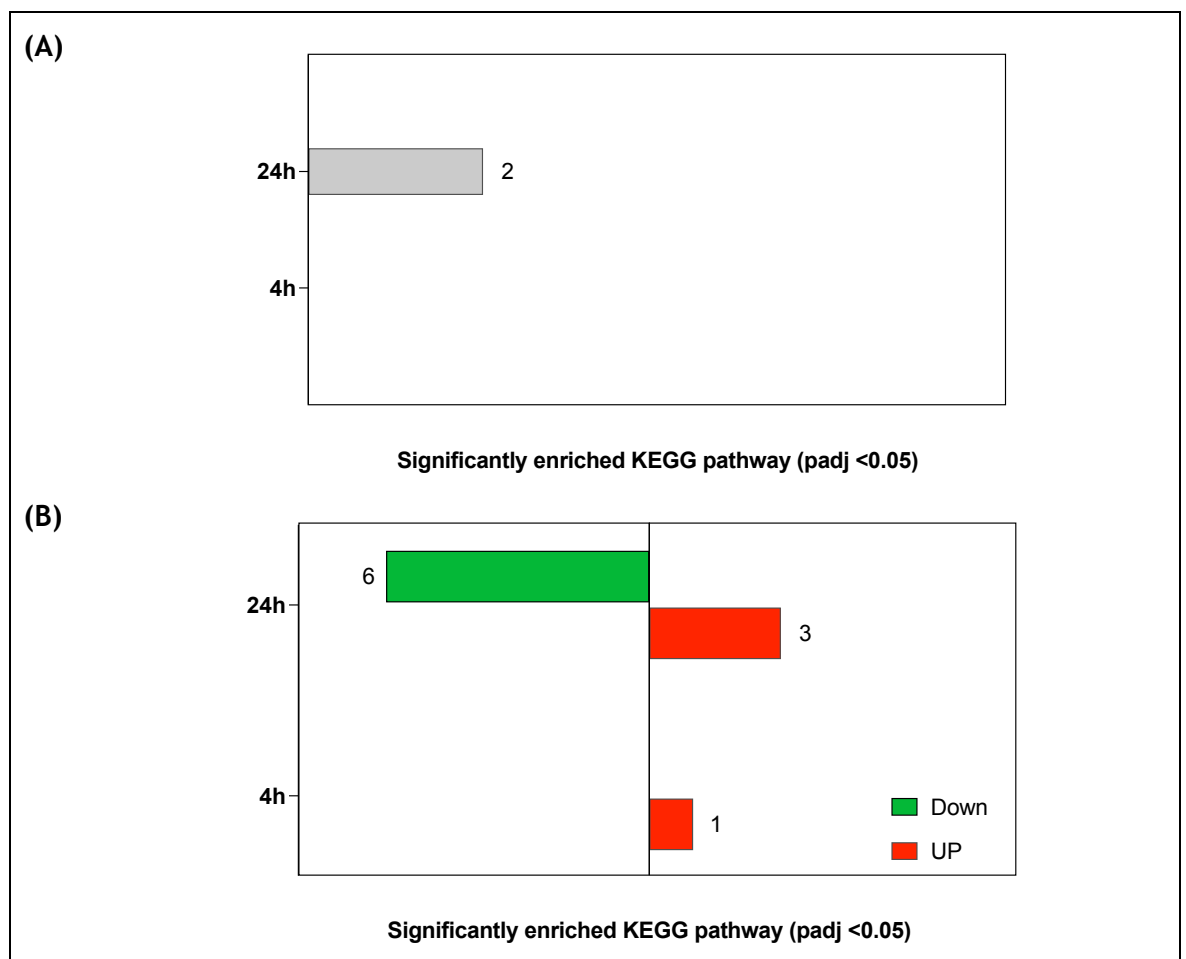


Figure 5-11 Top 30 GO terms (top ten in each category) of upregulated and downregulated DEGs. (A-D) shows the top ten GO terms of the three categories (Biological Process: orange font, Cellular Component: green font, Molecular function: blue font). Gene ratio (x-axis) is the percentage of genes present in this GO term over the total number of genes in this category. The size of the dot is based on gene count enriched in the pathway, and the colour of the dot shows the pathway enrichment significance where a red dot represents a padj < 0.05. The description of GO terms is shown on the left side of each plot. (A-B) Analysis after 4h of stimulations showing (A) downregulated and (B) upregulated enriched GO terms. (C-D) Analysis after 24h of stimulations showing (C) downregulated and (D) upregulated enriched GO terms.

### 5.3.4 KEGG enrichment analysis

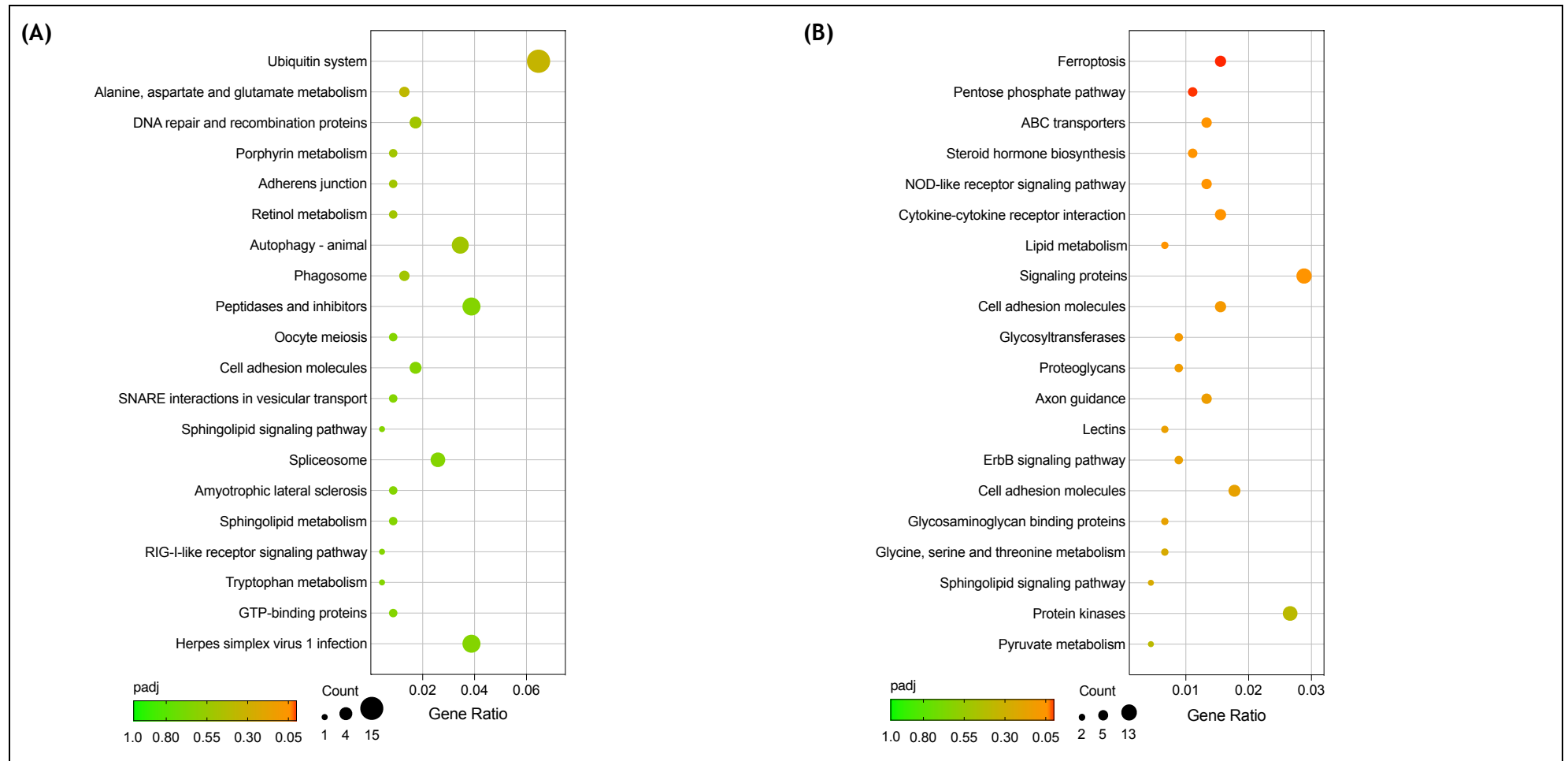
The KEGG pathway enrichment analysis was carried out on the DEGs to further understand the molecular details of biological processes based on curated lists of genes and proteins. An overview of the analysis showed no significant enrichment in the 4 h stimulated group compared to the 24 h group that showed two significantly enriched pathways (Figure 5-12 A). The sub-analysis of the significantly upregulated and downregulated enriched KEGG pathways showed the 4 h stimulated group displaying one significantly upregulated KEGG pathway, while the 24 h group showed three significantly upregulated and six significantly downregulated KEGG pathways (Figure 5-12 B). This increase in number of enriched KEGG pathways is due to the recalculated padj.



**Figure 5-12** KEGG enrichment analysis of significant enriched KEGG pathways. (A) Overview of significantly enriched KEGG pathways after 4 and 24 hours of stimulation with the M2 agonist (APE). (B) Overview of significantly upregulated and downregulated KEGG pathways after 4 and 24 hours of stimulation with the M2 agonist.

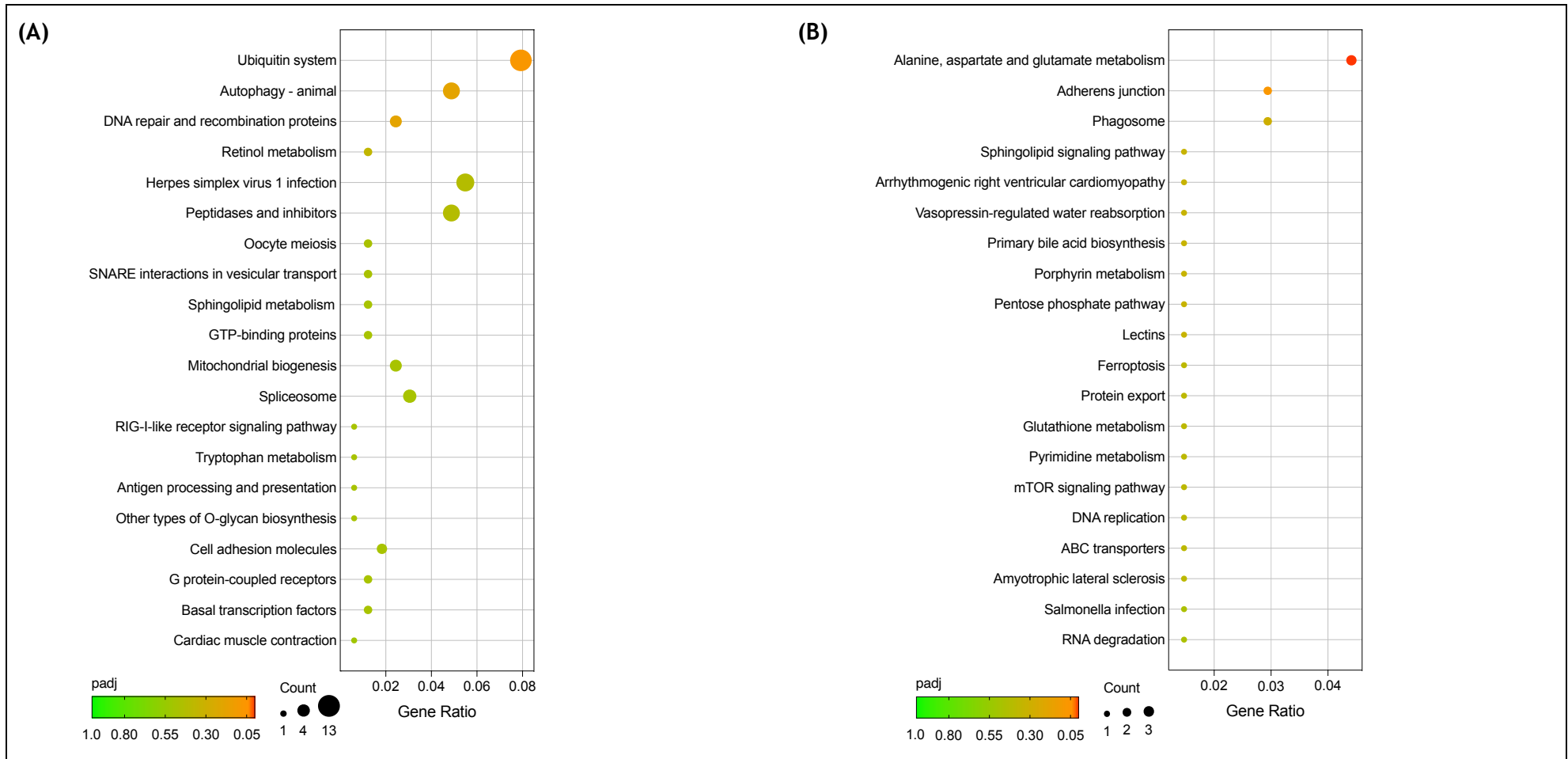
The analysis of the top 20 KEGG pathways showed only two significantly enriched pathways in the 24 h stimulated group that generally describe mechanisms that function in cellular metabolism (Figure 5-13 B).

The analysis of the top 20 GO KEGG pathways of upregulated and downregulated DEGs was also carried out (Figure 5-14). The 4 h stimulated group showed only one significantly upregulated KEGG pathway that generally describe a metabolic pathway involved in the production and degradation of alanine, aspartate, and glutamate (Figure 5-14 B). The 24 h stimulated group showed six significantly downregulated KEGG pathways that generally describe pathways involved in cell metabolism, adhesion, and migration (Figure 5-14 C). Moreover, the 24 h stimulated group showed three significantly upregulated KEGG pathways that generally describe mechanisms that function in cellular metabolism and hormone production (Figure 5-14 D).



**Figure 5-13 Top 20 KEGG pathways after stimulation with the M2 agonist (APE). (A) shows the 4 hours data and (B) shows the 24 hours data. (A-B) shows the top 20 KEGG pathways (ranked by p-value). Gene ratio (x-axis) is the percentage of significant genes over the total genes in a given pathway. The size of the dot is based on gene count enriched in the pathway, and the colour of the dot shows the pathway enrichment significance where a red dot represents a padj <0.05. The description of the pathway is shown on the left side of each plot.**

Chapter 5: Activated pathways in response to M2 muscarinic receptor activation.



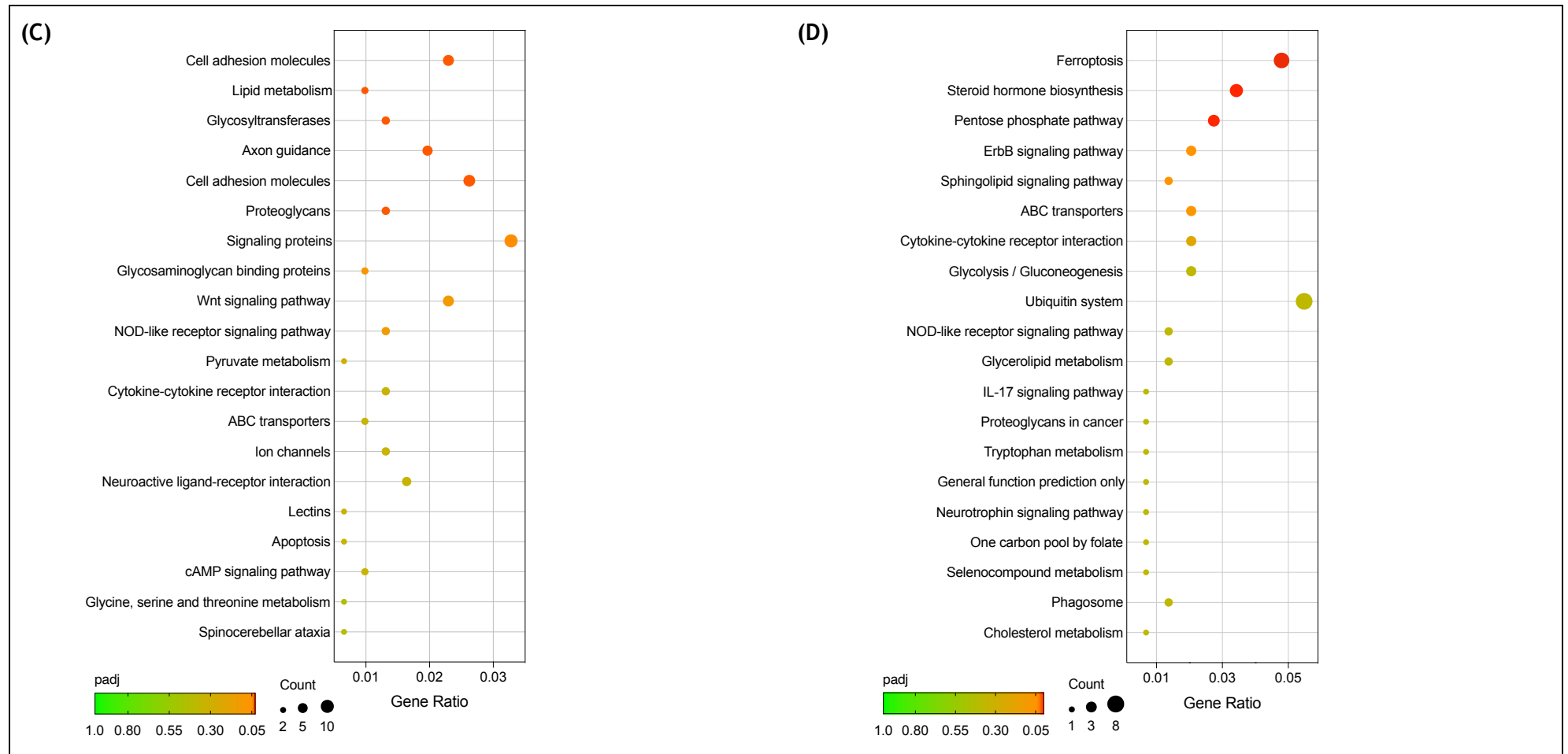


**Figure 5-14 Top 20 downregulated and upregulated KEGG pathways. (A-D) shows the top 20 KEGG pathways (ranked by p-value). Gene ratio (x-axis) is the percentage of significant genes over the total genes in a given pathway. The size of the dot is based on gene count enriched in the pathway, and the colour of the dot shows the pathway enrichment significance where a red dot represents a padj <0.05. The description of the pathway is shown on the left side of each plot. (A-B) Analysis after 4h of stimulations showing (A) downregulated and (B) upregulated enriched KEGG pathways. (C-D) Analysis after 24h of stimulations showing (C) downregulated and (D) upregulated KEGG pathways.**

### 5.3.5 Protein-protein interaction analysis

Protein-protein interaction (PPI) analysis was based on the STRING database (v11.5) (Szklarczyk *et al.*, 2015), and PPI network visualization was created with Cytoscape (v3.10.0) (Shannon *et al.*, 2003). The PPI network of the significant DEGs consists of 27 proteins in the 4h stimulation timepoint and 184 proteins in the 24h stimulation timepoint. The proteins in the 4 h stimulation timepoint produced 16 pairs of PPIs, while the proteins in the 24 h stimulation timepoint produced 269 pairs of PPIs (Figure 5-15).

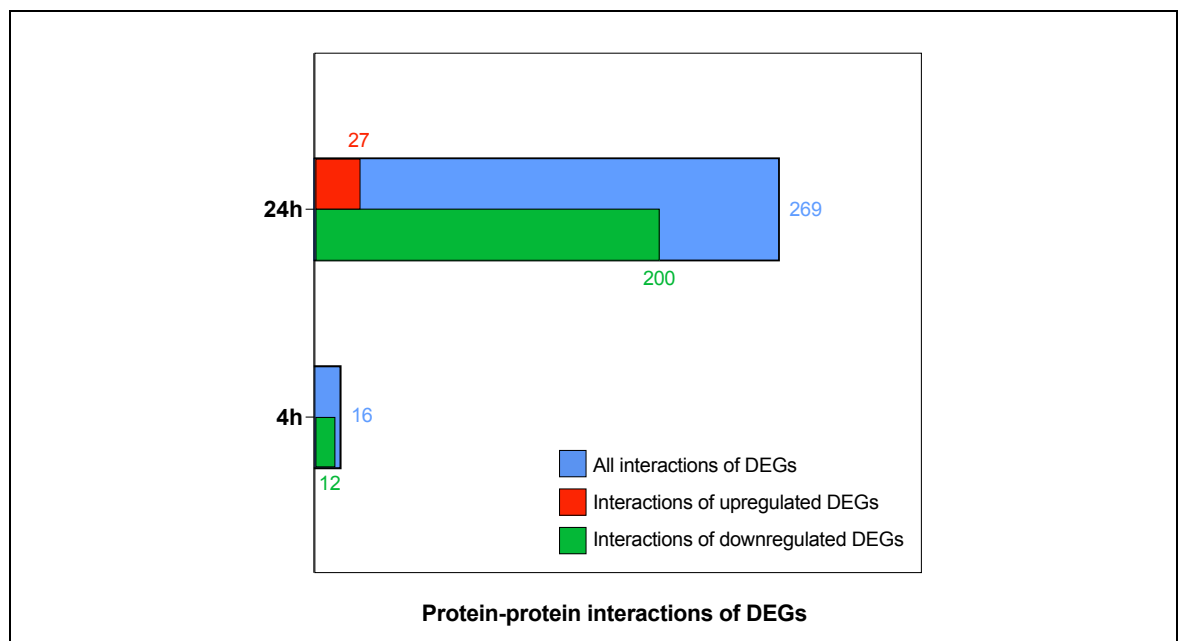
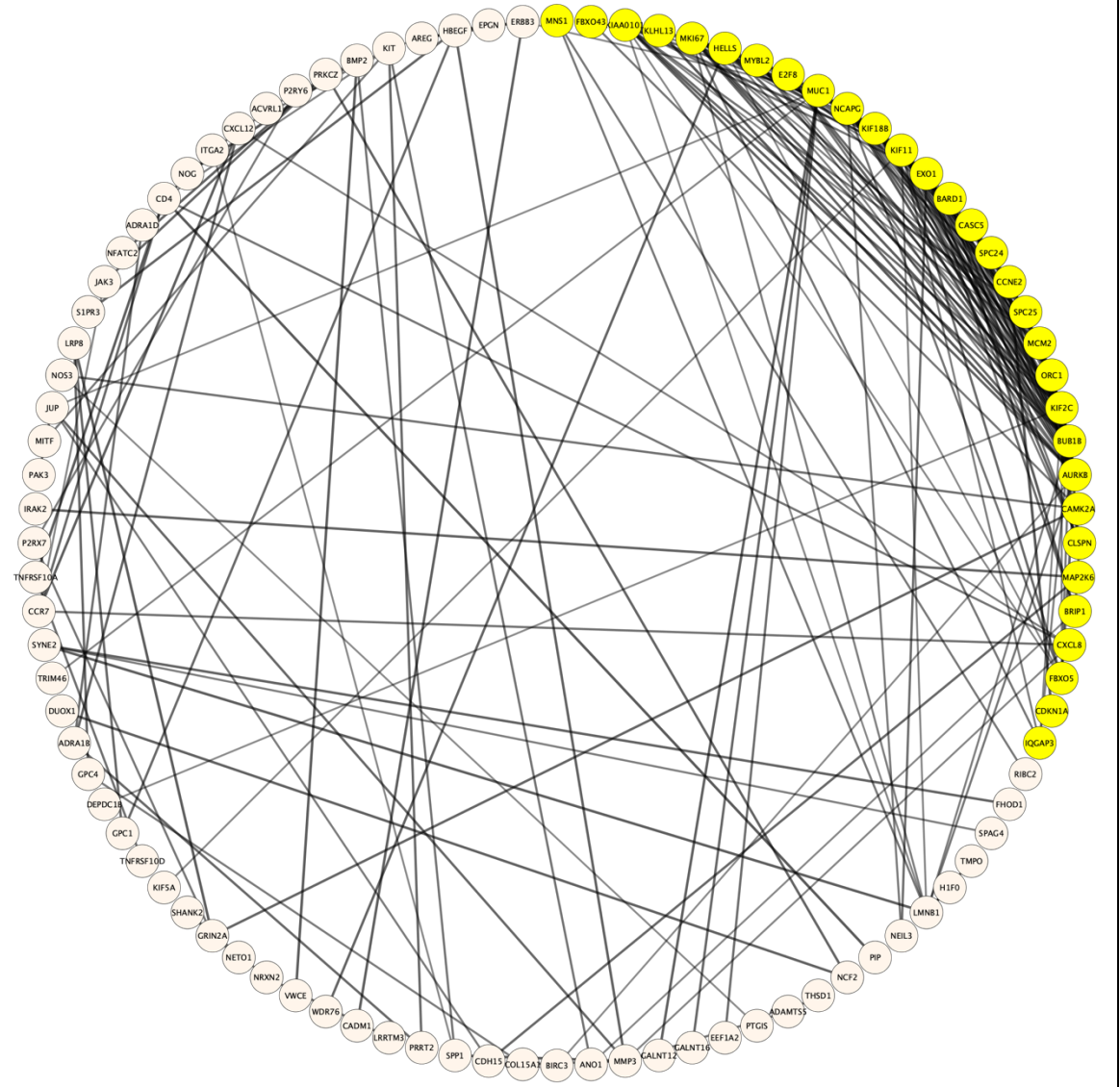


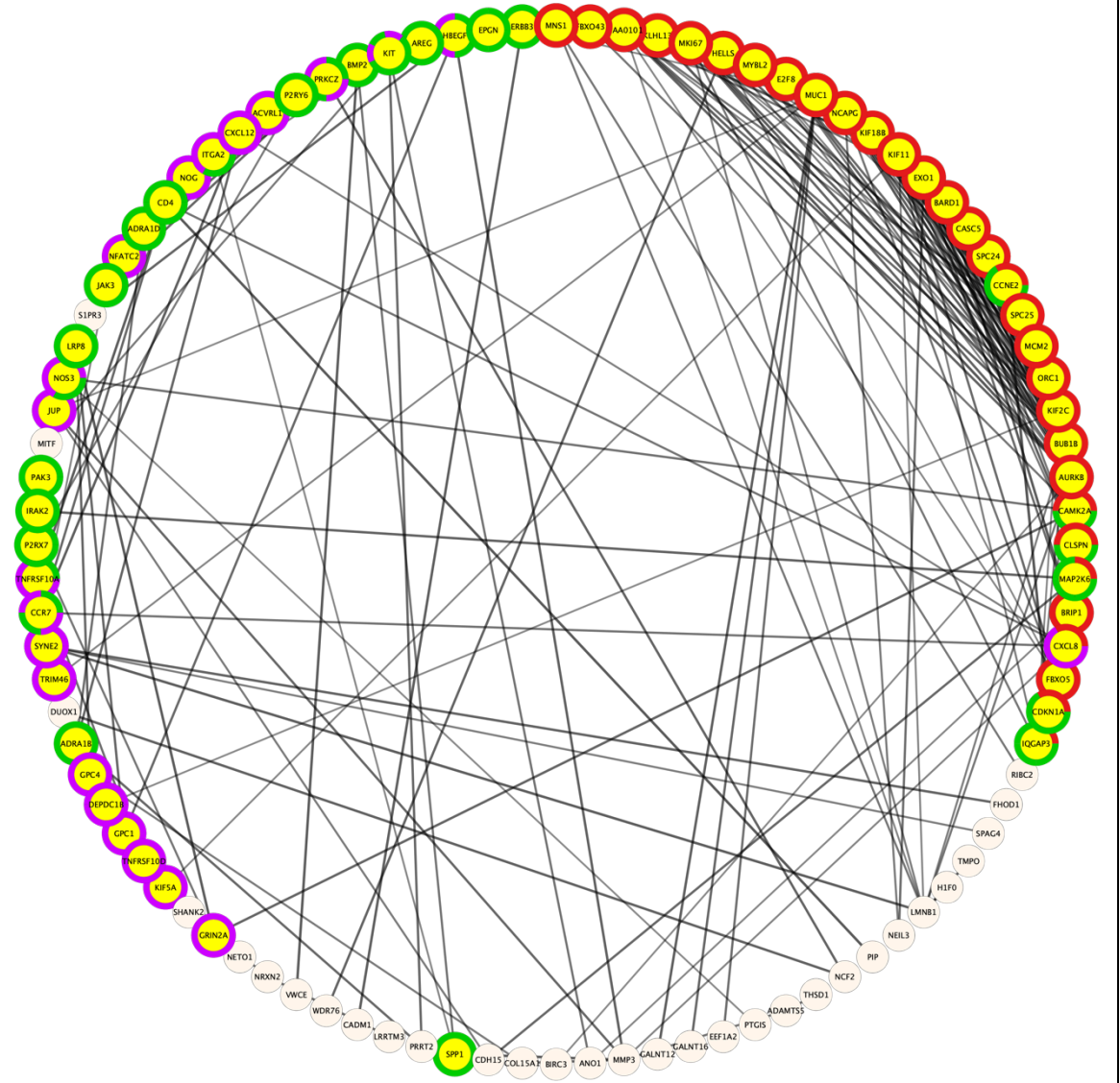
**Figure 5-15 Overview of protein-protein interaction analysis. Data represent the significant protein coding DEGs after 4 and 24 h of stimulation with the M2 agonist APE.**

The PPIs in the 4 h stimulation group do not produce enough interactions to generate a meaningful network of interaction (Sup 5-3), thus further analysis was only generated from the 24 h stimulation group. The main network of PPIs generated from the 24 h showed most interactions between genes involved in cell cycle, DNA replication, and chromosome segregation (Figure 5-16 A). The network also showed interactions between genes involved in cell migration, and highlights genes involved in the MAPK cascades and their interactions inside the network (Figure 5-16 B).

**Figure 5-16 Main network of protein-protein interaction after 24 h of stimulation with the M2 agonist APE. Data represents significant protein coding DEGs. (A) shows most interactions between highlighted genes which are involved in cell cycle.**



**(B)** shows interactions between highlighted genes **(B)** involved in cell cycle (red band), cell migration (purple band), and genes involved in the MAPK cascades (green band) and their interactions inside the network.



Sub analysis of PPIs generated from the 24 h stimulation group was done using the default criteria of the MCODE clustering algorithm (v2.0.2, Degree Cut off: 2, K-score: 2, Node Score Cut off: 0.2, Max. Depth: 100) (Bader and Hogue, 2003). Seven modules including 33 protein coding genes were obtained (Figure 5-17). Among these, the first module contained 12 genes with an average of ten interactions per protein coding gene, of which the AURKB, BUB1B, EXO1, KIAA0101, KIF11, KIF2C, MKI67, NCAPG, and ORC genes are involved in cell cycle and regulation of cell cycle process (Figure 5-17 A). The other six modules have lesser PPIs, however they produce noteworthy interconnectivity. For an example, the second module contained the GBP2, MX2, OAS3, and XAF1 genes which are involved in Interferon signalling and response to cytokine stimulus (Figure 5-17 B). The third module contained four genes involved in regulating cell adhesion, and of which CCR7, CXCL12, and CXCL8 are involved in chemokine-mediated signalling pathway (Figure 5-17 B). Moreover, the fourth module contained four genes that function in the ephrin receptor signalling pathway (Figure 5-17 B), which are involved in several downstream signalling pathways including the Ras-MAPK pathway and the PI3K-AKT pathway (Darling and Lamb, 2019). Module five describes genes involved in the Wnt signalling pathway, module six describes genes involved in the pentose phosphate pathway (PPP), and module seven describes genes involved in keratan sulphate biosynthesis (Figure 5-17 B).

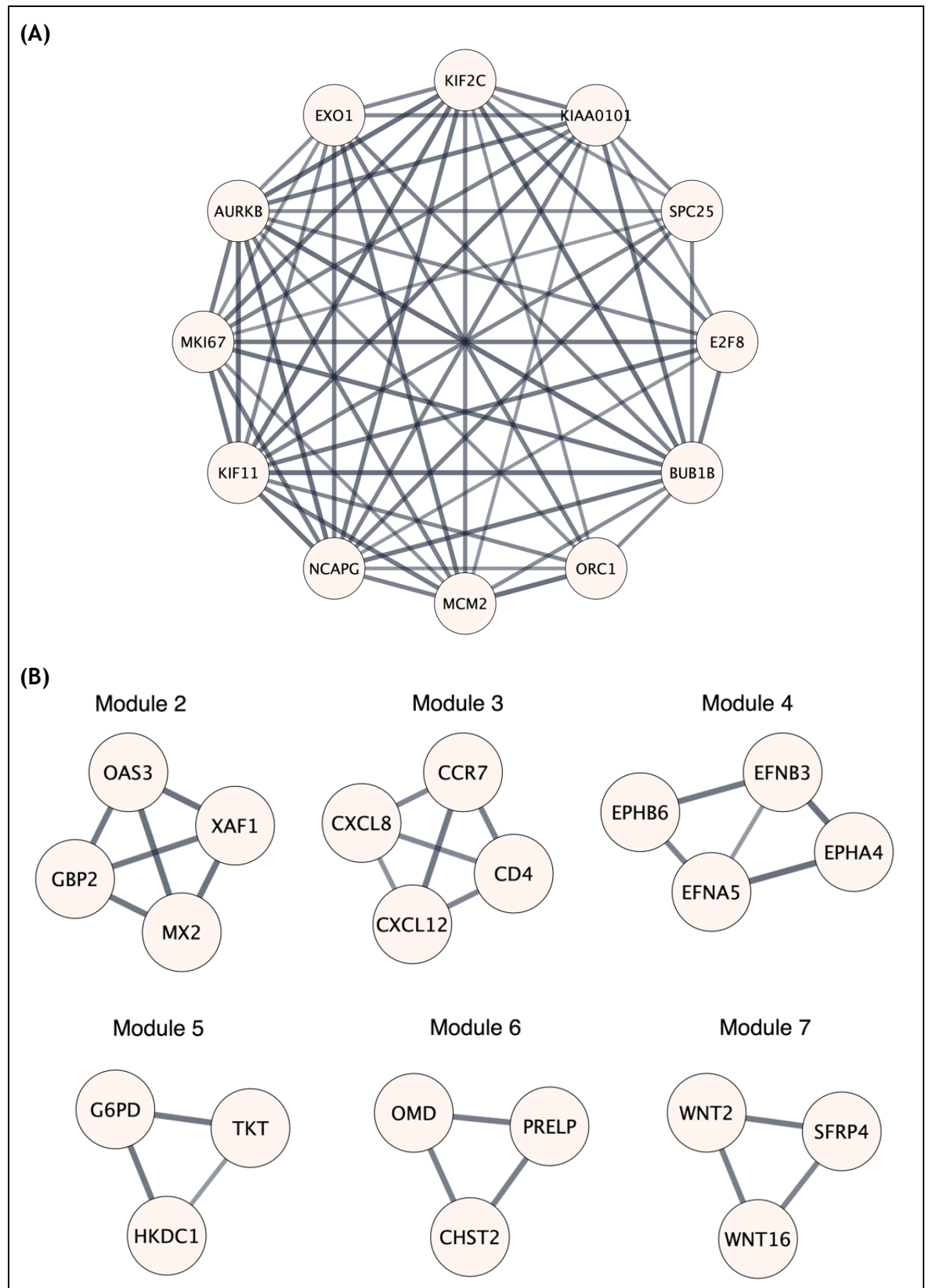


**Figure 5-17** Generated modules of the protein-protein interaction (PPI) network. Modules are ranked by MCODE clustering algorithm. (A) Shows the first module with a score of 10.3 and an average of ten interactions per node (gene). (B) Shows modules 2-7 where 2 and 3 score 4, while 4-7 score 3. Only the first module had a connection between nodes with a confidence interval greater than 0.7.

### 5.3.6 Involvement of MAPK/ERK in downstream signalling of the M2 receptor

As a means better to understand one of the pathways involved in the inhibitory effect on DPSCs proliferation post M2 stimulation via its selective agonist (APE), the mitogen-activated protein kinase (MAPK) pathway was investigated. Specifically, phosphorylation of extracellular signal-regulated kinases 1/2 (ERK 1/2), as these kinases (i.e., ERK 1/2) were reported to be central in MAPK signalling cascades and mediating extracellular signals to intracellular targets (Guo *et al.*, 2020). The notion to investigate these kinases is based on the MAPK pathway being associated with several of the reported DEGs in the RNA seq analysis (Figure 5-16 B), and the previous finding demonstrating a role for ERK 1/2 phosphorylation in relation to M2 signalling in BM-MSCs (Hoogduijn, Cheng and Genever, 2009). Herein, the results of the ERK 1/2 phosphorylation ELISA showed that the M2 agonist stimulation up-regulated the phosphorylated form of ERK 1/2 as early as five min post treatment when compared to untreated control (Figure 5-18 A). Moreover, expression of genes involved in ERK1/2 signalling such as *MAPK3*, *MAPK1* and *PCNA* were all upregulated (Figure 5-18 B).

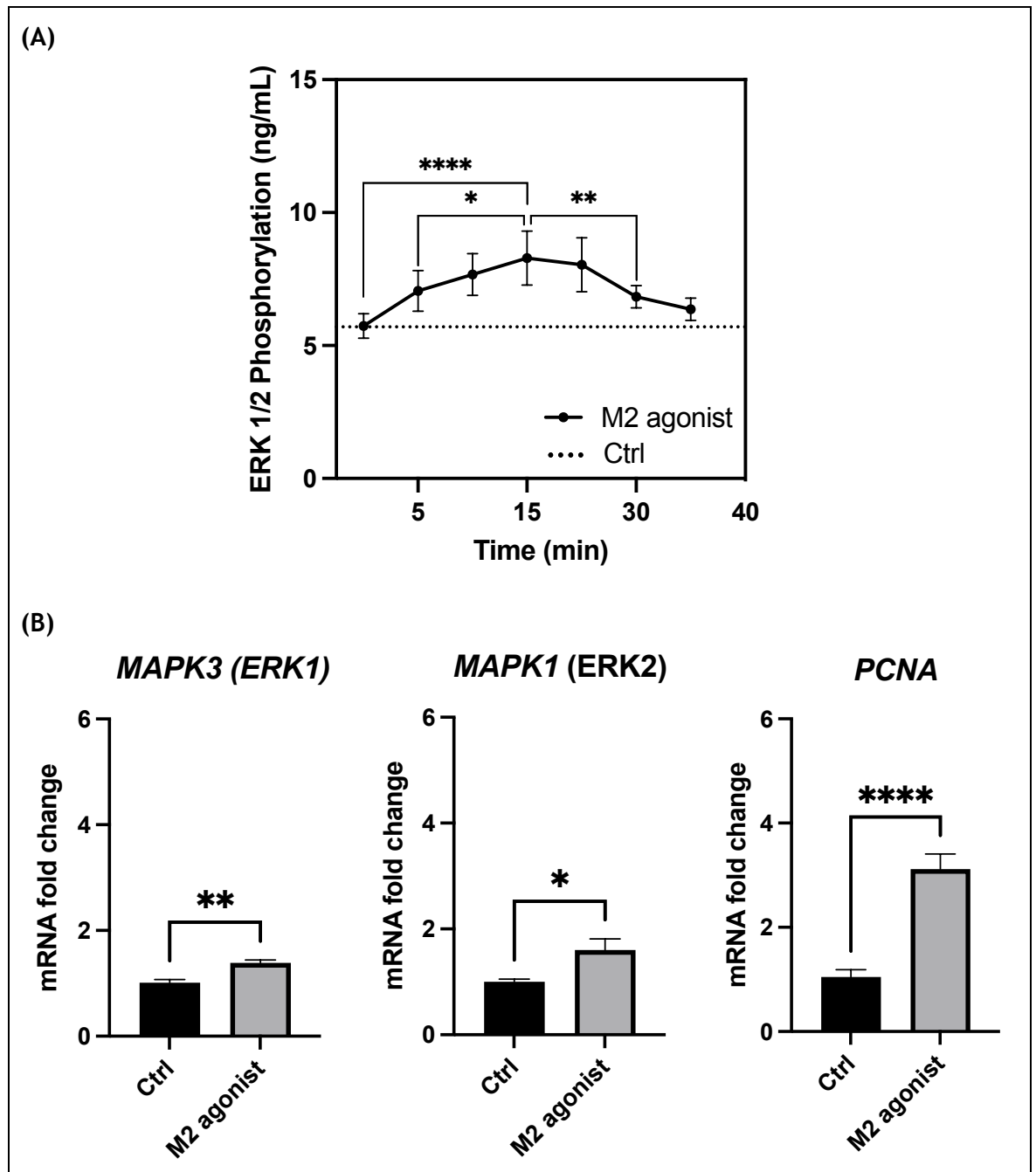


**Figure 5-18 Analysis of MAPK/ERK pathway. (A)** Phospho-ERK1/2 levels shows progressive increase in samples stimulated with the M2 agonist (APE) compared to the untreated control (Ctrl), most significantly after 15 min of treatment and up to 30 min post-treatment. **(B)** Expression of genes involved in ERK1/2 signalling shows significant upregulated expression presented as the mean fold change compared to the untreated control (Ctrl) using the  $2^{-\Delta\Delta Ct}$  method (Livak and Schmittgen, 2001). Gene expression is relative to the housekeeping gene (GAPDH). A difference of  $P < 0.05$  was considered statistically significant. (\* $p < 0.05$ , \*\* $p < 0.01$ , \*\*\*\*  $p < 0.0001$ ). Data for all are derived from duplicate wells of three independent experiments.

## 5.4 Discussion

In the previous chapters, the data showed that M2 activation, via its selective agonist (APE), inhibited DPSCs proliferation by inducing a cell cycle arrest. This inhibition in proliferation occurs in a reversible manner and was shown to not have an effect on DPSCs viability and survival. The data suggest that M2 activation places DPSCs in a quiescent state. Moreover, results showed that DPSCs maintain expression of stemness markers after stimulation with the M2 agonist. In addition to these results, data showed that M2 activation inhibited DPSCs migration and interfered with DPSCs commitment to an osteoblast lineage. All of which indicates the involvement of the M2 receptor in several pathways related to the basic activities of DPSCs. Therefore, this chapter set to explore this by investigating enriched pathways in the downstream signalling of the M2 receptor in DPSCs. This was largely done through whole transcriptomic sequencing of DPSCs after stimulation with the M2 receptor selective agonist (APE) and followed by investigating the involvement of the MAPK/ERK pathway.

The transcriptomic data revealed that duration of stimulation had the largest impact on the number of detected DEGs. Subsequently, pathway enrichment analysis follows this trend, showing that 24 h stimulation with the M2 agonist (APE) produced the most effect in terms of DEGs and enriched pathways. This arguably was expected, as previous result typically showed a phenotypic effect of M2 stimulation after 72 h. The rationale behind selecting the 24 h timepoint is to allow exploration of genes and pathways involved in producing the witnessed effect on DPSCs proliferation, migration, and cell cycle. While the rationale behind selecting the 4 h timepoint was to explore early changes in gene expression and how the witnessed effects are initiated. Although the data acquired after the 4 h timepoint revealed less DEGs (446) compared to 24 h (679), it provided information in terms of the differences in both the gene expression and enriched pathway patterns.

Focusing on the top 50 DEGs revealed that most are downregulated after 4 h of stimulation, while the opposite is happening after 24 h of stimulation with most of the DEGs showing upregulated expression. This suggests DPSCs response to M2 stimulation by arguably initiating a shutdown in normal biological process and then commencing a response through upregulation of genes that ultimately result in

the observed phenotypic effects of M2 activation in DPSCs. This is evident when looking at the number of DEGs co-expressed at both the 4 and 24 h timepoints. Only 38 DEGs are co-expressed in the two stimulation timepoints, which suggest that the DEGs are largely different between the 4 and 24 h stimulation timepoints. Furthermore, most of the co-expressed 38 DEGs showed a uniform downregulated expression across stimulation timepoints, and a few showed a unique pattern of expression. For an example, the *STAG3L1* and *TRIM47* genes display downregulated expression after 4 h of stimulation, and then upregulated expression at 24 h. Both genes are involved in cell signalling and response to stimulation. The *STAG3L1* gene encodes proteins of yet unknown function, however deletion of this gene has been implicated in Williams syndrome, characterised by developmental abnormalities including dental ones (such as malocclusion, hypodontia, and enamel hypoplasia) (Merla *et al.*, 2010; Wong, Ramachandra and Singh, 2015). On the other hand, the *TRIM47* gene is involved in several protein ubiquitination pathways (Liang *et al.*, 2019; Li *et al.*, 2021), namely E3 ubiquitin-protein ligase that mediates the ubiquitination and proteasomal degradation of Cyldromatosis (CYLD) (Ji *et al.*, 2018). CYLD is deubiquitinating enzyme that influence signal transduction involved in a variety of processes including immune response, cell cycle, and differentiation. Thus, TRIM47 acts as a regulatory enzyme that controls the levels of CYLD enzyme in the cell by targeting it for degradation. TRIM47 also regulates several downstream effectors such as nuclear factor kappa-B (NF- $\kappa$ B) via protein kinases C and D (PKC- $\epsilon$ /PKD3) (Azuma *et al.*, 2021), expression of STAT3 signalling targets (*MCL-1*, *MMP2*, and *c-MYC*) (Wang, Fu and Xing, 2022), and modulating the PI3K/Akt pathway via regulating phosphorylation of Akt and PI3K (Wang *et al.*, 2020). This showed involvement of genes responsible for several different pathways that can arguably explain the differences in DPSCs response between the 4 and 24 h stimulation timepoints. In fact, several genes among these 38 DEGs can be grouped based on their involvement in several different functions. These functions broadly include regulation of cell signalling, cell adhesion, cell cycle, and response to stimulus (Table 5-2). All of which provides insights into the molecular mechanisms that are involved in the response of DPSCs to M2 receptor activation.

**Table 5-2 Functional summary of protein coding DEGs co-expressed in stimulation timepoints. Stimulation timepoints involve the 4 and 24 hours. Description summary obtained from [NCBI](#) and [GeneCards](#) database.**

Function summary	Genes
Cell signalling	<i>ADRA1B</i> , <i>ASNS</i> , <i>NSF</i> , and <i>OVGP1</i> .
Cell adhesion	<i>ABI3</i> , <i>C5AR2</i> , and <i>PCDHGB1</i> .
Cell cycle	<i>ASNS</i> , <i>CARMN</i> , <i>GATAD2B</i> , <i>MXD3</i> , <i>MYCL</i> , <i>TDRD9</i> , <i>TESMIN</i> , and <i>ZYG11A</i> .
Immune response	<i>CCR7</i> , <i>PHF71</i> , <i>SLC7A11</i> , and <i>TRIM47</i> .

### 5.4.1 Transcriptomic data

Activation of the M2 receptor via its selective agonist (APE) revealed a total of 446 significant DEGs in DPSCs after 4 h of stimulation. The data showed that among the total significant DEGs, 329 were downregulated and 117 were upregulated compared to the unstimulated control. Among these DEGs, 188 are protein coding genes in the downregulated DEGs (57% out of 329), and 27 in the upregulated DEGs (23% of 117). This in part, and the lower number of DEGs, explains the very little significantly enriched pathways observed in the 4 h stimulation group. Surprisingly, the upregulated significant DEGs showed eight significantly enriched GO pathways, and one significantly enriched KEGG pathway.

The eight significantly upregulated GO pathways belong to the molecular function category. These GO terms generally describe functions relating to nucleic acid helicase and ATPase activities involved in RNA binding (Figure 5-11 B). These eight significantly upregulated GO pathways have three genes in common: *EIF4A1*, *DDX47* and *TDRD9*. The *EIF4A1* gene encodes eukaryotic initiation factor 4A-I protein which enables double-stranded RNA binding (Castello *et al.*, 2012), and is involved in downstream signalling of the MAPK and mTOR pathways (Boussemart *et al.*, 2014; Maracci *et al.*, 2022). The *DDX47* gene encodes a member of the DEAD box protein family which are involved in regulation of RNA translation and transcription (Schütz *et al.*, 2010). The *TDRD9* gene encodes a member of the Tudor domain-containing proteins which are involved in regulation of RNA binding, RNA helicase activity, and play a role in germ cell development (Babakhanzadeh *et al.*, 2020).

The upregulated KEGG pathway analysis identified a metabolic pathway involved in the production and degradation of alanine, aspartate, and glutamate (Figure 5-14 B). This KEGG pathway included the *ASNS* gene that encodes asparagine synthetase enzyme, which catalyses the synthesis of asparagine from glutamine and aspartate (Ruzzo *et al.*, 2013). This enzyme activity, arguably, is associated with response to cellular stress and may have a role in endothelial cell proliferation (Li, Kumar and Carmeliet, 2019). Furthermore, depletion of this enzyme has been reported to regulate the cell cycle and proliferation of cancer cell lines (Yang *et al.*, 2014; Xu *et al.*, 2016; Deng *et al.*, 2020).

Stimulation of DPSCs with the M2 receptor selective agonist (APE) revealed a total of 679 significant DEGs after 24 h. The data showed that among the total significant DEGs, 474 were downregulated in expression, and 205 were upregulated in expression compared to the unstimulated control. Among these DEGs, 368 are protein coding genes in the downregulated DEGs (78% out of 474), and 139 in the upregulated DEGs (67% of 205). Although the numbers of the upregulated protein coding DEGs are considerably less than the downregulated counterpart, they display a more significant padj value. This can be seen in the top 50 DEGs heatmap (Figure 5-7 B) and the number of significantly enriched GO pathways (88 upregulated vs two down downregulated) (Figure 5-9 B).

Indeed, looking at downregulated GO pathways, only two were significantly enriched and they belong to the molecular function category. These GO terms generally describe kinase proteins involved in transmembrane signal transduction (Figure 5-11 C). These significantly enriched GO pathways have the *KIT*, *FGFR2*, *EPHA4*, *EFNB3*, *TEK*, *ERBB3*, *EPHB6*, *NTRK3* genes in common. Collectively, tyrosine kinase proteins encoded by these genes are involved in a wide range of cellular processes, including cell growth, division, differentiation and migration (Table 5-3). Once activated, these proteins phosphorylate other proteins, initiating a cascade of downstream signalling such as MAPK, Akt/PI3-K, mTOR.

**Table 5-3 Function summary of DEGs involved in downregulated GO pathways. The summary is of DEGs in significantly downregulated GO pathways after 24 h stimulation with the M2 selective agonist (APE).**

Gene	Encoded protein	Function summary and involved pathways
<i>KIT</i>	Encodes tyrosine-protein kinase KIT (Also known as C-Kit).	The protein phosphorylates multiple intracellular proteins involved in regulating proliferation, differentiation, and migration. Involved in the signalling cascade of the MAPK pathway, Akt/PI3-K pathways, and activation of STAT (Linnekin, 1999; Fathi <i>et al.</i> , 2020; Pathania, Pentikäinen and Singh, 2021).
<i>FGFR2</i>	Encodes a member of the fibroblast growth factor receptor family.	The protein is involved in regulation of cell proliferation, differentiation, and migration. Involved in the signalling cascade of the MAPK pathway, AKT1 signalling and mTOR signalling (Eswarakumar, Lax and Schlessinger, 2005; Lau, So and Leung, 2013; Ornitz and Itoh, 2015).
<i>EPHA4</i>	Encodes a member the ephrin receptor subfamily A of the protein-tyrosine kinase family.	The protein is involved in regulation of cell morphology, cell adhesion and cell-cell signalling. Involved in the signalling cascade of the MAPK/ERK pathway (Wilkinson, 2014; Chen <i>et al.</i> , 2021).
<i>EPHB6</i>	Encodes a member the ephrin receptor subfamily B of the protein-tyrosine kinase family.	The protein is involved in regulation of cell adhesion. Involved in the signalling cascade of the MAPK/ERK pathway (Stokowski <i>et al.</i> , 2007).
<i>TEK</i>	Encodes a receptor that belongs to the protein tyrosine kinase Tie2 family (Also known as TIE-2).	The protein is involved in regulation of cell survival, proliferation, migration, and adhesion. Involved in the signalling cascade of the MAPK/ERK pathway and Akt/PI3-K pathways (Peters <i>et al.</i> , 2004; Echavarría and Hussain, 2013; Kook <i>et al.</i> , 2014).
<i>ERBB3</i>	Encodes a member of the epidermal growth factor receptor family of receptor tyrosine kinases (Also known as HER3)	The protein is involved in activation of pathways which lead to cell proliferation or differentiation. Involved in the signalling cascade of the MAPK Signalling, Akt signalling, and mTOR Signalling (Yasuda <i>et al.</i> , 2014; Liu <i>et al.</i> , 2022).
<i>NTRK3</i>	Encodes a member of the neurotrophic tyrosine receptor kinase family (Also known as TRKC)	The protein is involved in regulation of cell survival and differentiation. Involved in the signalling cascade of the MAPK pathway and Akt/PI3-K pathways (Curtis, Gomez and Schiller, 2012; Yan <i>et al.</i> , 2016; Yao <i>et al.</i> , 2017)

Looking at upregulated GO pathways, a total of 88 significantly GO terms were enriched. The biological processes category had the most with 61 upregulated GO terms, followed by 26 in the molecular function category, and one in the cellular component category (Figure 5-9 B). To give a comprehensive look at these upregulated GO pathways, the top ten of each category (ranked by *p*adj value) were presented (Figure 5-11 C). The top ten significantly upregulated GO terms in BP generally describe metabolic and cellular responses to stress and metabolite

processing (Figure 5-11 D). The involved metabolic processes produce reactive oxygen species (ROS), leading to oxidative stress that further influences cell cycle checkpoints and upregulation of antioxidant (Ghaffari, 2008; Testa *et al.*, 2016; Mu *et al.*, 2020). It should be noted that cellular response to oxidative stress varies depending on the cell type and degree of stress confronted and range from influencing proliferation to cell death (Tan and Suda, 2018). The remaining 51 significantly upregulated GO terms in the biological processes category describe several clusters of processes involved in cell response and metabolism, hence, they have been grouped accordingly (Table 5-4).

**Table 5-4 Clusters of the remaining significantly upregulated GO terms. The clusters belong to the biological processes category that are not shown in the results of the 24 h timepoint.**

Cluster	Biological processes significantly upregulated GO terms
Cellular Stress Responses and Detoxification	Response to heat Cellular response to heat Cellular response to temperature stimulus Detoxification Cellular oxidant detoxification Cellular detoxification Cellular response to reactive oxygen species Reactive oxygen species metabolic process
Metabolism of Small Molecules	Glycoside metabolic process Pentose metabolic process NADP metabolic process Pentose-phosphate shunt Glyceraldehyde-3-phosphate metabolic process Quinone metabolic process Organic acid transport Carboxylic acid transport Primary alcohol metabolic process Pyridine nucleotide metabolic process Nicotinamide nucleotide metabolic process Pyridine-containing compound metabolic process
Cellular Signalling Regulation	Regulation of signalling receptor activity Modulation of chemical synaptic transmission Regulation of trans-synaptic signalling Regulation of cellular response to heat Regulation of neuronal synaptic plasticity Regulation of cell activation Negative regulation of protein serine/threonine kinase activity
Metabolism of Lipids and Steroids	Response to lipid Steroid catabolic process Cellular ketone metabolic process Steroid metabolic process Acylglycerol homeostasis Triglyceride homeostasis Bile acid and bile salt transport

Immune Responses and Inflammation	Leukocyte migration Inflammatory response
Multicellular Organism Processes	Multi-multicellular organism process Antibiotic metabolic process Detection of mechanical stimulus involved in sensory perception

The top ten significantly upregulated GO terms in the molecular function category generally describe enzymatic activities in redox regulation and signalling (Figure 5-11 D). Collectively these terms highlight the diversity of enzymatic activities related to redox regulation (i.e., oxidoreductase activity terms), antioxidant defence, and signalling pathways involved in growth and metabolic processes. The remaining 16 significantly upregulated GO terms in the molecular function category describe several clusters of molecular interactions involved in enzymatic activities, cellular signalling, and protein transportation (Table 5-5). Looking at the upregulated GO terms in the cellular components category, only one significantly GO terms was found which describe formation of secondary lysosomes involved in clearing foreign matter and antigens presentation for the immune system (Figure 5-11 D).

**Table 5-5 Clusters of the remaining significantly upregulated GO terms. The clusters belong to the molecular function category that are not shown in the results of the 24 h timepoint.**

Cluster	Molecular function significantly upregulated GO terms
Oxidoreductase Activities and Metabolism	<p>Oxidoreductase activity, acting on the aldehyde or oxo group of donors, NAD or NADP as acceptor.</p> <p>Oxidoreductase activity, acting on a sulphur group of donors, NAD(P) as acceptor.</p> <p>Oxidoreductase activity, acting on the aldehyde or oxo group of donors.</p> <p>Steroid dehydrogenase activity, acting on the CH-OH group of donors, NAD or NADP as acceptor.</p> <p>Steroid dehydrogenase activity</p> <p>Oxidoreductase activity, acting on NAD(P)H, quinone or similar compound as acceptor.</p> <p>Oxidoreductase activity, acting on paired donors, with incorporation or reduction of molecular oxygen, NAD(P)H as one donor, and incorporation of one atom of oxygen.</p> <p>Oxidoreductase activity, acting on the CH-CH group of donors.</p> <p>Oxidoreductase activity, acting on a sulphur group of donors.</p> <p>Monooxygenase activity</p>
Receptor Functions	<p>Receptor ligand activity</p> <p>Receptor regulator activity</p> <p>Epidermal growth factor receptor binding</p>
Transporter Activities	<p>Organic acid transmembrane transporter activity</p> <p>Carboxylic acid transmembrane transporter activity</p>
Protein Interactions and Binding	<p>Proteoglycan binding</p>

These discussed results suggest that DPSCs response to M2 receptor stimulation has shifted after 24 h towards involving or initiating biological process that eventually results in the observed inhibition effect on proliferation, cell cycle, and migration. Indeed, at the 4 h timepoint most of the significant GO pathways are interactions at the molecular level. At this phase, it can be argued that DPSCs response to the stimulation is mainly through molecular interactions at a transcription level happening within the nucleus. As the stimulation progress to the 24 h timepoint, it can be observed that DPSCs started to mobilize biological events that trigger process ultimately producing the observed inhibition effect on DPSCs migration and proliferation. Taking a more holistic look at all the

upregulated GO pathways, several DEGs were found to be common between the enriched pathways. Indeed, the *AKR1C1*, *AKR1C3*, *TXNRD1*, *NQO1*, *G6PD*, *PGD*, *TALDO1*, *ALDH3A1*, and *AKR1B10* genes were involved in more than 15 GO pathways (Table 5-6).

**Table 5-6 Function summary of DEGs involved in more than 15 upregulated GO pathways. Summary is of significantly upregulated pathways after 24 h stimulation with the M2 selective agonist (APE). NO. Go pathways: number of upregulated pathways that involve the same gene.**

Gene	No. GO pathways	Encoded protein	Function summary and involved pathways
<i>AKR1C1</i> <i>AKR1C3</i>	29 26	Each encodes a member of the aldo -keto reductase AKR1 family (also known as HSDs)	Both enzymes are involved in the metabolic processing of diverse endogenous or exogenous substrates including steroids, fats, hormones, and drugs. They reduce endogenous substrates' ketosteroid to hydroxysteroid. Both utilise the nicotinamide adenine dinucleotide phosphate (NADPH) coenzymes to perform their oxidoreductases activity (Penning, 2015; Chu <i>et al.</i> , 2022). The genes are regulated by antioxidant response elements of the Nrf2-Keap1 pathway in response to oxidative stress and generated ROS (Jin and Penning, 2007). The protein encoded by <i>AKR1C3</i> is suggested to mediated prostaglandin metabolism via Akt/PI3-K signalling pathways (Wang <i>et al.</i> , 2008).
<i>TXNRD1</i>	23	encodes a member of the thioredoxin reductase family (also known as TrxR1)	The cytoplasmatic isozyme, the presence of NADPH, play a key role in redox homoeostasis. Regulate cellular redox reactions, growth and differentiation (Damdimopoulos <i>et al.</i> , 2004). It maintains the reduced state of proteins involved in DNA synthesis, repair, and transcriptional regulation, thus having a regulatory function of cell cycle (Muri <i>et al.</i> , 2018). Act as a modulator of the Nrf2-Keap1 response pathway to oxidative stress and ROS (Cebula, Schmidt and Arnér, 2015).
<i>NQO1</i>	22	encodes a member of the NAD(P)H dehydrogenase quinone family (also known as QR1)	Regulates cellular redox state primarily through quinone detoxification and suppress oxidative stress (Ross and Siegel, 2018). Involved in regulation of mRNA translation, enables proteins binding and stabilization against proteasomal degradation, generation of NAD <sup>+</sup> to protect DNA from oxidative stress damage (Ross and Siegel, 2021).

<i>G6PD</i>	19	encodes glucose-6-phosphate dehydrogenase	Mainly involved in the production of NADPH, play role in the defence against oxidizing agents and in reductive biosynthetic reactions. This enzyme acts on glucose-6-phosphate, which is the first and rate-limiting step of the oxidative phase of the PPP. By producing NADPH, G6PD arms the cell with reducing potential required for activates that suppress detrimental effects of oxidative stress (Cosentino, Grieco and Costanzo, 2011).
<i>PGD</i>	18	encodes 6-phosphogluconate dehydrogenase	Mainly involved in the production of NADPH, play role in the defence against oxidizing agents and in reductive biosynthetic reactions. This enzyme acts on 6-phosphogluconate at a later step in the oxidative phase of the PPP. Enables cells to counterbalance oxidative stress (Lin <i>et al.</i> , 2015).
<i>TALDO1</i>	17	encodes Transaldolase 1	Involved in the nonoxidative phase of the PPP activities by providing ribose-5-phosphate for nucleic acid synthesis and NADPH for lipid biosynthesis. The generation of NADPH by this enzyme, enables maintaining a reduced state of glutathione and, thus, protection from ROS (Banki <i>et al.</i> , 1996). TALDO1 involvement in nucleotides production infer its regulatory role in DNA replication and repair (Perl, 2007).
<i>ALDH3A1</i>	16	Encodes a member of Aldehyde Dehydrogenase 3 Family	Oxidize various aldehydes to the corresponding carboxylic acids using NADPH enzymes as a cofactor. Involved in the detoxification of alcohol-derived acetaldehyde and maintain cellular homeostasis during oxidative stress (Voulgaridou <i>et al.</i> , 2017). Besides its redox functions, ALDH3A1 play a functional role in the differentiation and proliferation of stem cells (Muzio <i>et al.</i> , 2012).
<i>AKR1B10</i>	15	encodes a member of the aldo -keto reductase AKR1 family	The enzyme is involved in the metabolic processing of diverse endogenous or exogenous substances including steroids, fats, hormones, and drugs. It reduces endogenous substrates' aldehyde to alcohol. Utilise NADPH coenzymes to perform its oxidoreductases activity such as reduction of oxidative stress products (Jin and Penning, 2007; Huang <i>et al.</i> , 2016). Involved in the downstream signalling of the Nrf2-Keap1 pathway that regulate redox homeostasis (Hayes <i>et al.</i> , 2015). Involved in regulating cell survival,

The six significantly downregulated KEGG pathways generally describe pathways involved in cell metabolism, adhesion, and migration (Figure 5-14 C). Most DEGs involved in these pathways such as *CADM1*, *CDH15*, *CDHR4*, *CNTN1*, *CNTN3*, *CNTNAP1*, *JAM2*, *NRXN3*, *PCDHB10*, *PCDHGB1*, *ROBO4*, *SDK1*, and *TMEM25* are protein coding genes for cell adhesion molecules. Besides their role in regulating cell adhesion, cell adhesion molecules can display adhesion-independent signalling that regulate cellular functions like migration, proliferation, survival and differentiation (Cavallaro and Dejana, 2011). The three significantly upregulated KEGG pathways generally describe mechanisms that function in cellular metabolism and hormone production (Figure 5-14 D). Ferroptosis regulates cell survival and is associated with regulation of iron metabolism, steroid hormone biosynthesis refers to the enzymatic processes involved in the production of steroid hormones, while the pentose phosphate pathway describes metabolic process involved in the generation of NADPH. To put these distinct cellular functions into context, the redox regulation and signalling discussed above should be considered. Based on that, one of the primordial responses that cells take to stimuli include oxidative stress. This is typically associated with an imbalance or increase in production of ROS and cellular antioxidant defence mechanisms. If this goes unchecked, it can cause cellular damage and death if their levels become excessive (Tan and Suda, 2018). In the enriched GO pathways, the *AKR1* encoding gene has been observed to be involved in 29 enriched pathways. In this scenario, AKR1 proteins are suggested to play a role in maintaining cellular redox balance and mitigating oxidative stress. In conjunction with NADPH enzymes, provided through the pentose phosphate pathway, these proteins minimise the detrimental effects of oxidative stress, ROS, and help regulate hormones imbalance. Furthermore, AKR1 proteins can suppresses the detrimental effects of ferroptosis, thus maintaining cell survival (Mura *et al.*, 2006; Chen *et al.*, 2023). All of which suggest that several yet to be proven, mechanisms may be operational and produce the observed inhibitory effects of the M2 receptor on DPSC function, in a balance, without affecting these cells survival and viability.

### 5.4.2 Protein interaction network

The protein interaction network of significant DEGs showed very little protein-protein interactions (PPIs) at the 4 h timepoint, thus the analysis was focused on the 24 h timepoint. Herein, protein coding DEGs were mapped to the search tool for retrieval of interacting genes (STRING) to acquire protein-protein interaction PPI networks. This was carried out as a mean applied to predict functional interactions of coded proteins (Szklarczyk *et al.*, 2015) and where presumably that interaction is happening in the context of the biological activity of the cell. The database aligns the nodes in correspondence to the proteins (i.e., protein coding DEGs) and the edges representing the interactions based on curated sources, including experimental repositories, computational prediction methods, and public text collections. While the data generated from this method bring value in predicting PPIs and associated cellular process, potential caveats and limitations should be noted. These include whether these PPIs are mediating or inhibiting the associated biological activity, and the fact that this methodology is a predication tool calls for experimental follow-up analysis. With this in mind, the PPI analysis here revealed several networks in the 24 h timepoint, where one had the greatest number of nodes and interactions and thus deemed the main network. Visualisation of this network, by using STRING annotation function, showed the abundance of interactions happening between nodes of gene coding proteins involved in regulating the processes of cell cycle, DNA replication, and chromosome segregation (Figure 5-16 A). This supports the discussion points above, finding several DEGs and enriched pathways to be involved directly and indirectly in influencing the cell cycle. Furthermore, the network also showed interactions between nodes representing gene coding proteins involved in cell migration (Figure 5-16 B). This also is in alignment with several DEGs and enriched pathways involved in cell migration, adhesion, and response to cytokine or stimuli. What is more, the network highlights nodes representing gene coding proteins that are involved in downstream signalling of the MAPK pathway (Figure 5-16 B). Indeed, the MAPK pathway has been witnessed as a recurring theme among the analysed DEGs and enriched pathways above.

In order to further examine the protein interactions at the 24 h timepoint, PPI module analysis was conducted. The analysis showed seven modules, among which, the first module involved core nodes from the main network that had an

average of ten interactions per node. This module, expectedly, support the findings of the main PPIs network by describing gene coding proteins involved in cell cycle and regulation of cell cycle process (Figure 5-17 A). The remaining modules display lesser degree of interactions, however, produce noteworthy interconnectivity. For instance, the second module showed interactions between gene coding proteins involved in Interferon signalling and response to cytokine stimulus (Figure 5-17 B). While the third showed interactions between gene coding proteins involved regulating cell adhesion and the chemokine-mediated signalling pathway (Figure 5-17 B). All of which support the evidence obtained above from the DEGs analysis and enriched pathways.

### 5.4.3 The MAPK/ERK pathway

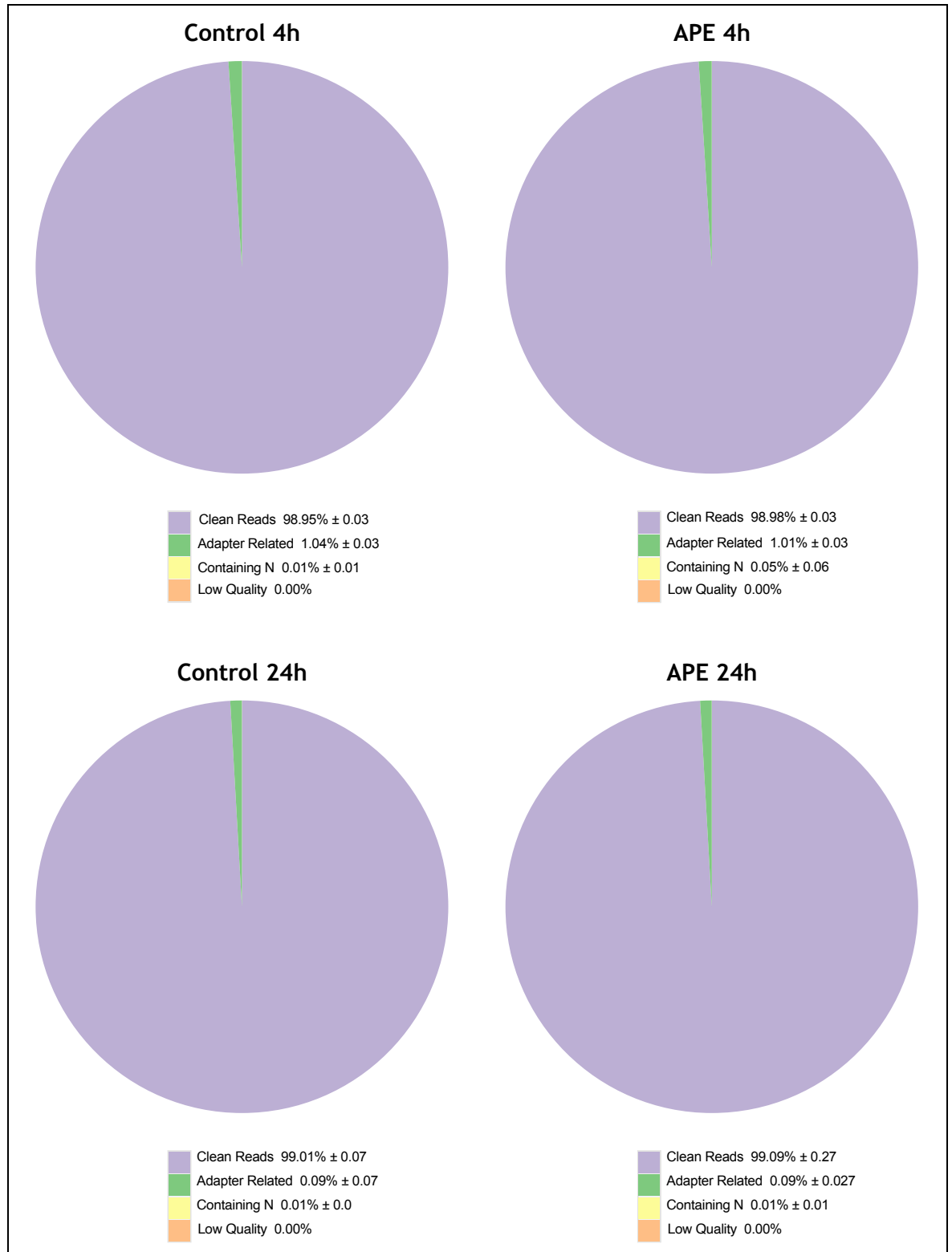
Intracellular signalling pathways involving epidermal growth factor (EGF) (Krampera *et al.*, 2005), MAPK (Hoogduijn, Cheng and Genever, 2009), Protein Kinase C (PKC) (Tang *et al.*, 2012) are major regulators of MSC proliferation and migration. In particular, the MAPK/ERK pathway, with phosphorylation of ERKs are known to regulate proliferation and differentiation of stem cells (Michailovici *et al.*, 2014), and which are also considered to be common pathways for all muscarinic receptors signalling as they are G protein coupled receptors. The transcriptomic data above showed a strong involvement of the MAPK pathway, besides Akt/PI3-K and mTOR, as common signalling pathway among the significant DEGs. In fact, there is cross-talk between these pathways in regulating each other via cross-inhibition and cross-activation (Mendoza, Er and Blenis, 2011). Here, the involvement of the MAPK/ERK pathways in translating the downstream effect of M2 activation has been demonstrated. Indeed, M2 activation upregulated phospho-ERK1/2 levels as early as five minutes (Figure 5-18 A). This will translate into the cell's nucleus and regulate transcription of multiple genes. Indeed, expression ERK1, ERK2, and PCNA mRNA were upregulated after M2 activation. All of which clearly suggests a role for M2 in modulating a major pathway that influence DPSCs proliferation, migration, and cell cycle.

### 5.4.4 Key summary points

- Transcriptomic data showed stimulation duration produced the greatest effect in the 24 h timepoint compared to 4 h.

- The nature and expression pattern of DEGs are significantly different between the 4 and 24 h timepoints, suggesting different response of DPSC as the stimulation progress.
- The transcriptomic data support the observed effect studied in the previous chapter, strengthening the notion of the inhibitory effect of the M2 receptor.
- The enriched pathways analysis describes molecular interactions and biological process that are involved in producing the observed inhibitory effects of M2 activation in DPSCs.
- The transcriptomic data, specifically enriched pathways, provide terms consolidated from several sources, thus it need to be considered in context of the sequenced cell type, nature of stimulus, and accomplished experimental work.

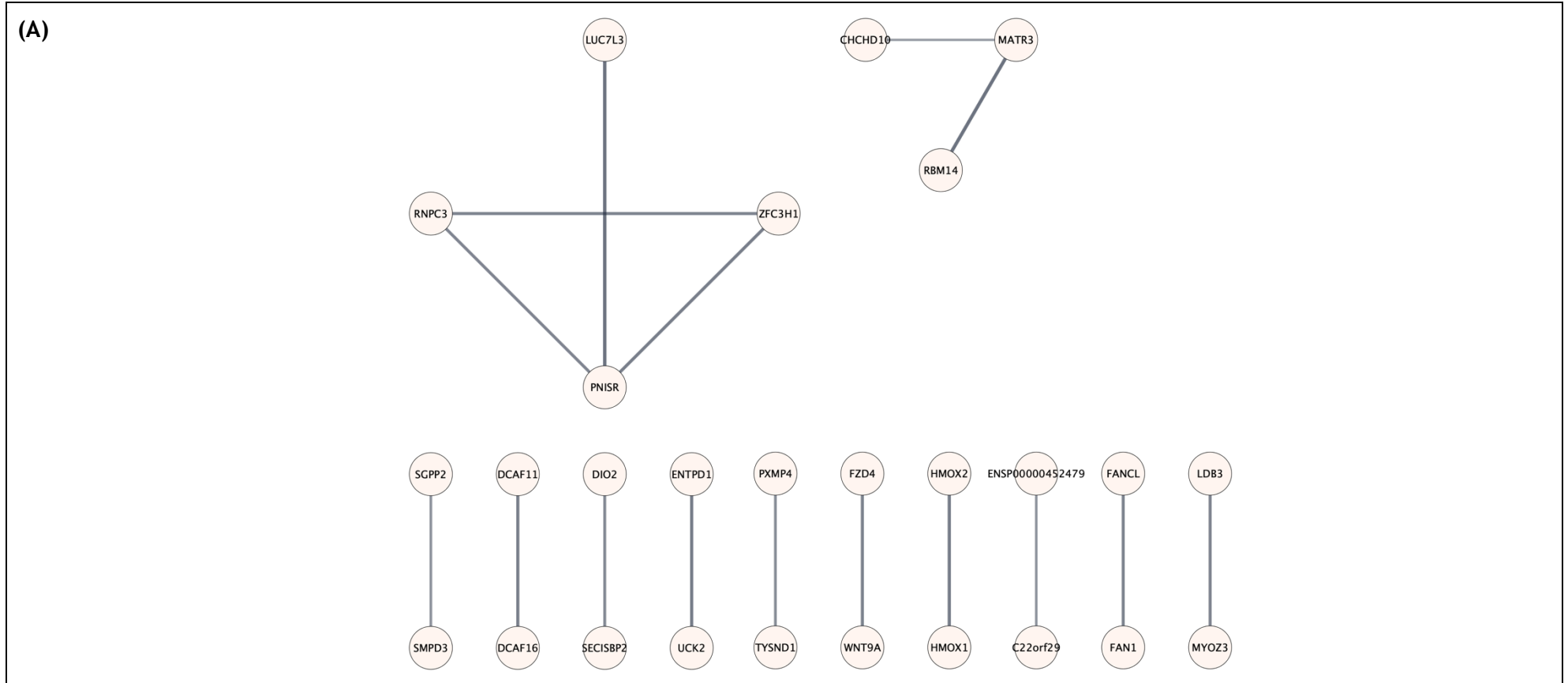
## 5.5 Supplementary



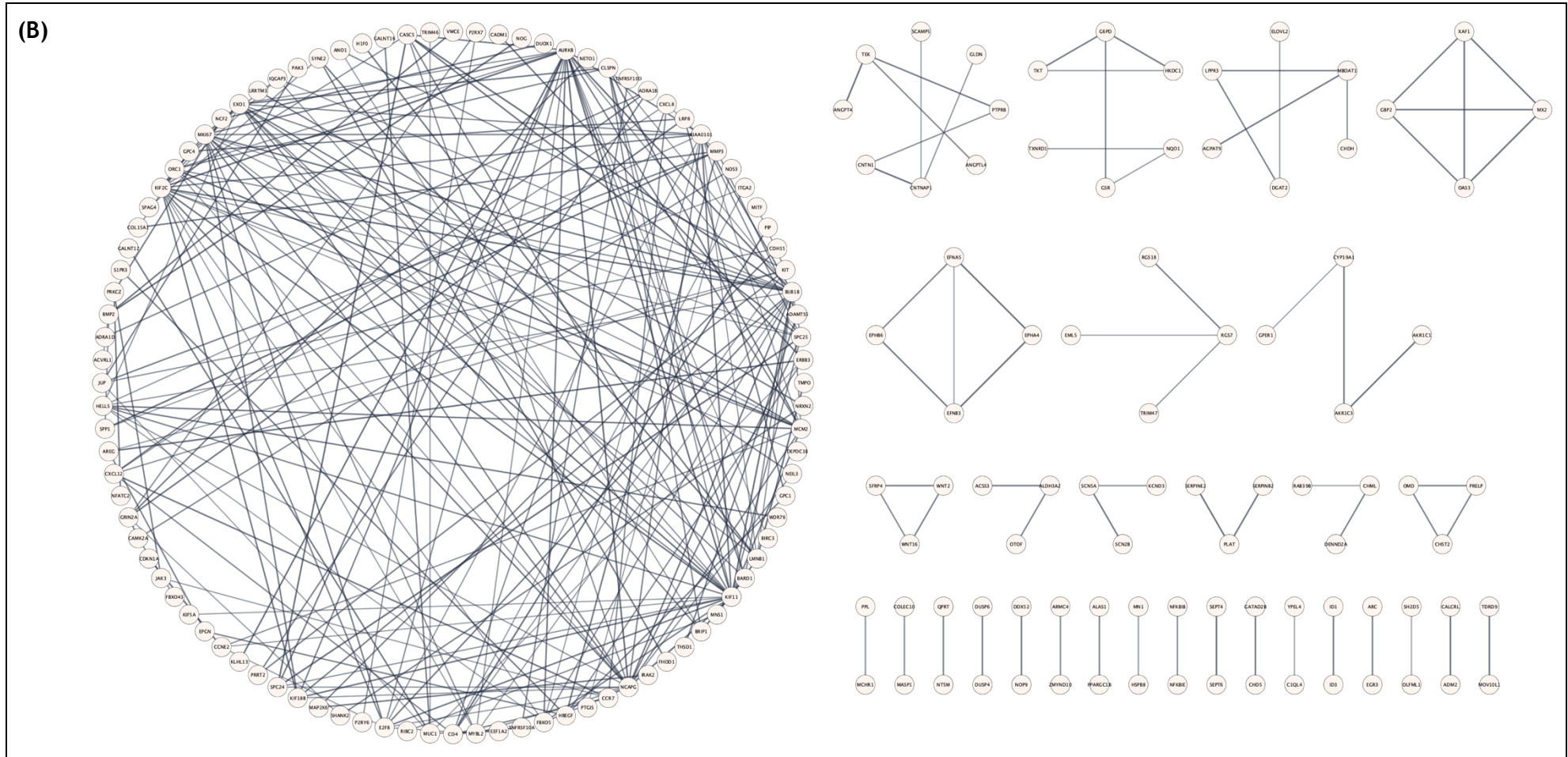
**Sup 5-1 Quality control criteria for all sequenced samples (n= 16). Data for each group is presented as the mean ± SEM. All samples showed above 98% of clean reads which are used for all subsequent bioinformatics analysis.**

Sample	Raw Reads	Clean Reads	Q20 (%)	Q30 (%)	Error (%)	Total Mapped (% of Clean Data)
Ctrl_4h1	41910710	41467144	98.26	94.98	0.02	40016129(96.5%)
Ctrl_4h2	39519882	39122028	98.08	94.56	0.02	37605468(96.12%)
Ctrl_4h3	45827876	45354712	98.2	94.88	0.02	43669806(96.29%)
Ctrl_4h4	56111190	55503728	98.3	95.11	0.02	53480809(96.36%)
Ctrl_24h1	46862402	46357828	98.22	94.92	0.02	44682293(96.39%)
Ctrl_24h2	51892280	51406134	98.07	94.48	0.02	49667223(96.62%)
Ctrl_24h3	41788154	41403140	98.2	94.89	0.02	40032722(96.69%)
Ctrl_24h4	39396898	38995902	98.14	94.69	0.02	37672481(96.61%)
APE_4h1	49806768	49279110	98.16	94.78	0.02	47556745(96.5%)
APE_4h2	42446076	42030922	98.1	94.51	0.02	40565540(96.51%)
APE_4h3	44411448	43960832	98.18	94.75	0.02	42381916(96.41%)
APE_4h4	39510182	39112722	98.07	94.52	0.02	37656332(96.28%)
APE_24h1	47190568	46896060	98.02	94.37	0.02	45204511(96.39%)
APE_24h2	46179680	45640650	98.09	94.61	0.02	44114592(96.66%)
APE_24h3	48140224	47787202	98.2	94.79	0.02	46194627(96.67%)
APE_24h4	40063010	39622240	98.17	94.78	0.02	38257084(96.55%)

**Sup 5-2 Quality check and mapping statistics.** For sequenced samples, the high-throughput RNA sequencing obtained 39–56 million single-ended raw reads. After filtering for low quality reads and adapter sequences, 38–55 million clean reads (98–99% from raw data) were generated. Among the clean data of the 16 libraries, about 96% of clean sequences was successfully mapped to the entire reference transcriptome. The Phred-like quality scores (Q20 and Q30) are used to measure the accuracy of nucleotide identity data from a sequencing run. A higher quality score indicates a lower probability that an individual base is called incorrectly, where Q20 indicates the probability of an incorrect base call is 1 in 100; Q30, 1 in 1000. Higher Q scores indicate a smaller probability of error as shown in error %



Chapter 5: Activated pathways in response to M2 muscarinic receptor activation.



Sup 5-3 Unprocessed protein-protein interaction (PPI) networks. (A) PPI network of the 4 h stimulation with the M2 agonist showing negligible interactions. (B) PPI network of the 24 h stimulation with the M2 agonist showing one main network with abundance of interactions and several smaller networks with lesser interactions

## **6 General discussion**

The work in this thesis aimed to characterise non-neuronal cholinergic signalling in DPSCs. In humans, the function of ACh goes beyond that of a neurotransmitter, and it is now established that it plays a key role in non-neuronal cell signalling (Wessler, Kirkpatrick and Racké, 1998). In fact, the near-ubiquitous expression of ACh in all life forms changes the perspective of ACh signalling and highlights its important functions in cellular homeostasis. Cholinergic signalling occurs through two major classes of AChRs, the mAChRs and nAChRs. These AChRs are also divided into subtypes and subunits, and their expression varies across different non-neuronal cell types and is influenced by cell state and environmental factors (Wessler and Kirkpatrick, 2008). This adds a significant challenge when evaluating a particular role of ACh and AChRs in non-neuronal cells. Nevertheless, there is extensive literature providing evidence of a role for ACh in modulating a diversity of cellular events in non-neuronal cells (Shirvan, Pollard and Heldman, 1991; Grando, 1997; Wessler, Kirkpatrick and Racké, 1998; Albuquerque *et al.*, 2009). In particular, it has previously been demonstrated that ACh signalling in MSCs influences their functions and, thus, their regenerative potential (Hoogduijn, Cheng and Genever, 2009; Piovesana *et al.*, 2018).

The expression of AChRs in MSCs has been reviewed early on in this thesis (See 1.2 for details). The aim of the review was to focus on the role of these receptors and ACh signalling from a regenerative standpoint. The review summarised the expression of both m and n-AChRs in several different MSCs. Several studies showed the involvement of AChRs in modulating MSCs' function. Moreover, AChR expression in MSCs appeared dynamic, dependent on the type of MSCs, donor, and differentiation status (See 1.2 for details). Only a few studies describe the expression of functional AChRs in MSCs, and even less showed a direct influence on classical MSCs functions (i.e., growth, migration, and differentiation) (Danielyan *et al.*, 2009; Hoogduijn, Cheng and Genever, 2009; Schraufstatter, DiScipio and Khaldoyanidi, 2010; Piovesana *et al.*, 2018; Tie *et al.*, 2018) Thus, a complete characterisation of the role of AChRs and ACh signalling on MSCs functions, particularly regenerative potential, remains to be conducted. Thus, the aim of this thesis was to perform a robust investigation into the role of specific AChRs in DPSCs. While the work here commenced by confirming the presence of several AChRs in DPSCs, it subsequently focused on one. The following will discuss the findings and narrative that led to dissecting the role of the M2 mAChR in influencing DPSCs proliferation, migration, and differentiation potential.

This thesis starts by developing methodologies for the culture of commercially available primary human DPSCs and their differentiation. The rationale behind culture media change was to have control over supplementation, thus, ensuring reproducibility. DMEM-KO is a well-established medium for DPSCs culture based on the breadth of literature (see 2.4 for details). The work here ensured that this media switch did not affect DPSCs stemness. DPSCs grown in DMEM-KO retained gene expression of stemness markers and could commit to an osteogenic lineage upon endorsement. The developed osteogenic protocol stands as a good measure to investigate DPSCs differentiation. Osteogenic differentiation is considered one of the most studied differentiation protocols in DPSCs. (Seong *et al.*, 2010; Brar and Toor, 2012; Langenbach and Handschel, 2013; Liu *et al.*, 2015; Aydin and Şahin, 2019). Based on this, and the plethora of protocols to initiate osteogenic differentiation, this thesis had to establish a methodology that ensures a working osteogenic differentiation procedure. Consequently, the initial work here describes the successful osteogenic differentiation of DPSCs, which was validated by phenotypic staining and gene expression of key osteogenesis markers.

The project then proceeded to detect the gene expression of AChRs, and transcripts of genes involved in ACh synthesis, transportation, and degradation in DPSCs. Gel-based RT-PCR provided an efficient but informative result when no prior data was available on the expression of the genes investigated in DPSCs. The q-PCR data confirmed the expression of the detected genes and allowed relative quantification of the most abundant transcripts. The melt curves added validity by demonstrating the specificity of the primers employed in the gene analysis. Collectively, these three methods showed that DPSCs expressed transcripts for the M2, M3, and M5 mAChRs, transcripts that make  $\alpha 7$  and  $\alpha 4\beta 2$  nAChRs, and transcripts encoding ACHE, which functions by hydrolysing ACh. In other words, DPSCs are equipped with machinery to bind and terminate ACh, thus the existence of ACh signalling in DPSCs. To confirm that this existence is functional, this thesis investigated the functionality of stimulated AChRs on DPSCs growth and proliferation.

The expression of functional AChRs was investigated using ACh and several agonists that serve as analogues of ACh. These commercially available cholinergic agonists have been validated in the literature, and some are even used as therapeutics. The intention behind using these agonists was to detect the

functionality of AChRs, observe the effect on DPSCs proliferation, and screen for the optimal concentration within the range of the reported inhibition constant ( $K_i$ ). This work involved the use of universal cholinergic agonists that stimulate both m and n- AChRs, non-selective agonists that can stimulate all mAChRs or all nAChRs, and selective agonists that only stimulate one subtype of mAChRs or one conformation of nAChRs. Based on the latter and the commercial availability of used agonists, DPSCs were shown to express functional M2 mAChR,  $\alpha 7$ nAChR, and  $\alpha 4\beta 2$ nAChR. This was further validated using selective antagonists to determine the agonists' specificity to bind their receptors selectively. This thesis then focused on mAChRs for several reasons. Firstly, mAChR downstream signalling occurs through the coupled G proteins and involves several phases of effectors and secondary messengers implicated in various cellular events. Secondly, the predominate expression of the M2 mAChR gene and, finally, the profound inhibitory effect of this receptor on DPSCs proliferation. This thesis then narrowed the focus to the M2 mAChR mainly for two reasons. The reliability of protein expression data and the fact that this receptor had a selective agonist that enabled investigations of the active state of this receptor. Based on this, all subsequent work in this thesis was carried out using the selective M2 mAChR agonist (APE) to mimic ACh in activating M2 in nature.

The initial data generated showed that M2 activation inhibits DPSCs proliferation. This was expected as the M2 mAChR belongs to the inhibitory group of mAChRs. The following work aimed to characterise the nature of this proliferation inhibition in DPSCs. The proliferation inhibition concerning M2 activation, via its selective agonist, was examined extensively. The data via several metabolic assays showed that the 100  $\mu$ M of the M2 selective agonist was the optimal concentration in producing consistent yet un-detrimental effects on DPSCs. This aligns with the range of the reported inhibition constant ( $K_i$ ) in the literature and is comparable to the studies that used the same M2 selective agonist (i.e., APE) (see 3.4 for details). Hence, the subsequent work was based on using this concentration to activate the M2 mAChR. Secondly, DPSCs survival was investigated since the witnessed effect of this stimulation was inhibitory. The assays designed to measure cell death by means of necrosis or apoptosis collectively report that M2 activation, via its selective agonist (100  $\mu$ M APE), did not affect DPSCs viability or survival. In fact, one of the simplest yet solid indications for this was the ability of DPSCs to resume their proliferation rate upon agonist withdrawal. Finally, the

cell cycle analysis confirmed the nature of this proliferation inhibition to be a cell cycle arrest. Based on expression analysis of genes involved in cell cycle progression, it is believed that the CDK inhibitor P21 (encoded by the *CDKN1A* gene) is the primary influencer of DPSCs cycle arrest in response to M2 activation. Putting all these results in context, the conclusion of DPSCs quiescence in response to M2 mAChR activation was likely (see 3.4 for details).

At this point of the project, other properties of DPSCs, such as stemness, migration, and differentiation potential, were investigated. This was to determine if the M2-induced effect is causing the cells to stop proliferating in order to differentiate. The results showed that DPSCs maintained gene expression of investigated stemness and pluripotency markers after stimulation with the M2 agonist. This further supports the notion that M2 activation places DPSCs in a 'quiescent state', preserving their stemness properties and self-renewal potential. This viable but inactive state of DPSCs stimulated with M2 agonist was seen in other functions such as migration and willingness to undergo osteogenic differentiation. The ability of DPSCs to migrate and close the created wound *in vitro* was inhibited. This investigation was carried out in the presence of Mitomycin C in stimulated and unstimulated DPSCs to rule out influence of proliferation on wound closure. The ability of DPSCs to commit to an osteogenic lineage was hindered in the presence of the M2 agonist. Both the phenotypic staining and gene expression analysis of osteogenesis key markers showed an overall reduction in the presence of the M2 agonist. Some interesting observations were the continued elevated expression of *RUNX2* in differentiated DPSCs stimulated with the M2 agonist and the upregulated expression of the M2 mAChR during osteogenic differentiation of cells that was not stimulated with the M2 agonist. All suggest mechanisms in play outside the scope of the investigated differentiation; hence, the direction to take a holistic approach and investigate enriched pathways involved in the downstream signalling of the M2 mAChR in DPSCs.

RNA sequencing (RNA-seq) was used to investigate the transcriptomic changes in DPSCs in response to M2 mAChR activation. DPSCs were stimulated with the M2 agonist for 4 and 24 hours, which are timepoints ahead of the phenotypic effects observed in this thesis. The rationale was to capture the transcriptomic changes that led to the inhibitory effects of M2 activation in DPSCs. The RNA-seq data

showed a temporal response of DPSCs to stimulation, with different numbers of significant differentially expressed genes (DEGs) and patterns of DEG expression at 4 and 24 hours. After 4 hours of stimulation, DPSCs responded by shutting down normal biological processes, as evidenced by the expression pattern of significantly downregulated DEGs (Figure 5-7). Most of the activity at this timepoint occurred at the transcription level and involved molecular interactions that function in RNA binding, translation, and transcription. After 24 hours of stimulation, the DPSC response began to evolve, as evidenced by the expression pattern of significantly upregulated DEGs (Figure 5-7) and the increased involvement of biological processes that eventually led to the observed phenotypic inhibitory effect. Pathway enrichment analysis was used to put the significantly DEGs into context. The analysis revealed a wealth of information about enriched pathways after M2 activation in DPSCs. The common theme of this analysis was the involvement of several metabolic pathways in regulating cellular processes. These pathways are also associated with cell response to stimuli and oxidative stress. The cellular processes involved in this analysis were growth, proliferation, migration, and cell cycle. The RNA-seq data also showed several significant DEGs' involvement in various signalling pathways, most notably the MAPK pathway. Therefore, the subsequent work investigated the involvement of the MAPK pathway in the downstream signalling of M2 in DPSCs. The results showed upregulation of ERK1 and ERK2 phosphorylation and transcripts, major downstream effectors of the MAPK pathway.

One of the main limitations of this study is the heterogeneity of the investigated DPSCs. The supplied cells were isolated for a third molar of a 17 year old male during routine tooth extraction. Lonza only advertise expression of the typical CD markers used to characterise MSCs and report the cells to express CD105, CD166, CD29, CD90, and CD73, and to not express CD34, CD45, and CD133. Therefore, It remains unclear how much of the population are multipotent stem cells and how much are limited potency progenitors. This raises questions about which proportion expressed the functional AChRs and the effects witnessed on proliferation, cell cycle, and differentiation. It is fair to say that these investigations were on dental pulp stromal cells until reproducibility can be performed on distinct isolated subpopulations of known characteristics. In light of this, the presented findings are reported on a heterogeneous DPSCs population.

## 6.1 Findings in the context of therapeutic applications

The work presented here exploited a cholinergic pharmacological agonist - APE, to elucidate the role of M2 mAChR in DPSCs. Many more cholinergic agents are commercially available and some have now been used as therapeutic agents in treatment of various systemic diseases (Pakala, Brown and Preuss, 2019). The current work demonstrates the ability to manipulate DPSCs behaviour and regenerative potential through the use of a specific muscarinic agonist. This modulation of DPSCs behaviour gives insight into potential drug targets that may be used in regenerative based therapies centred around the use of DPSCs, but also highlights the need for further studies in MSCs. One could imagine, the modulation of DPSCs cell cycle via the use of the M2 selective agonist to finely control stem cell niches and their behaviour, or the proliferative activities of harvested stem cell populations in culture prior to clinical application or indeed following delivery at the therapeutic site. What is more, cholinergic pharmaceutical agents are also available as selective antagonists and allosteric modulators (Decker, Meyer and Sullivan, 2001; Birdsall and Lazareno, 2005; Kruse *et al.*, 2014; Sriram and Insel, 2018; Verma *et al.*, 2018) This opens up possibilities of controlling or shutting off the downstream effects of a given AChR. The work here demonstrated the ability of the M2 selective antagonist to abort the inhibitory effect of the activated M2 mAChR. This highlights the prospect of using cholinergic pharmaceutical agents to modulate stem cells behaviour mechanistically via two means and the potential for cholinergic licensed medications in controlling stem cells *in vitro* and ultimately *in vivo*.

While the work here largely investigates the role of M2 mAChR in DPSCs, it offers a glimpse into the potential role of ACh signalling in dental pulp tissue more widely. AChRs may serve to modulate DPSCs behaviour during pulpal insult and offer potential avenues in managing pulpal therapies. Indeed, it has been reported that mAChRs expression pattern differ based on the status of the pulp, with changes identified between health and disease (Sterin-Borda *et al.*, 2011). The authors suggested that inflamed pulps express more of the M3 mAChR, compared to the M1 mAChR in healthy pulps, based on the ability of the M3 mAChR antagonist to displace the general mAChR agonist. Additionally, the presence of functional mAChRs have been reported in dental pulp tissue (Yu *et al.*, 2001; Borda *et al.*, 2007; De Couto *et al.*, 2009; De Couto Pita *et al.*, 2009). However, scarce evidence

exists about the role of these receptors in modulating tissue repair or proliferation and differentiation of the pulp tissue or cells. With confirmation of expression of both functional m and n-AChRs and the dissection of M2 mAChR role in modulating DPSCs proliferation, migration, and differentiation, potential exists to modulate DPSCs behaviour during pulpal-tissue repair. This potentially unlocks opportunities to enhance outcomes of vital pulp therapies and develop biologically based endodontic treatment strategies.

The work here extensively investigated one out of five potentially functional AChRs in DPSCs. The remaining detected AChRs are yet to be investigated comprehensively. The implications for the existence of an AChRs signalling network are thrilling when the range of licensed AChRs agonists and antagonists are considered. The re-purposing of these compounds will allow us to understand the role of AChRs in DPSCs and potentially MSCs and improve the therapeutic output of stem cell-based applications.

## 6.2 Future work

The work reported in this thesis constitutes a starting point for characterising ACh signalling in DPSCs. It showed the presence of several AChRs in DPSCs and it extensively examined the functional role of the M2 mAChR in modulating DPSCs behaviour. Moving forwards, it would be compelling to investigate the presence of functional AChRs in the reported subpopulations of DPSCs. Single-cell RNA sequencing (scRNA-seq) is a method suggested to quantify and characterise cellular heterogeneity (Choi and Kim, 2019). Additionally, several techniques can be exploited to identify and characterise the remaining AChRs in DPSCs. Besides stimulation with selective agonists, gene knockout via small interfering RNAs (siRNAs), short hairpin RNAs (shRNAs) could be useful to further elucidate the role of detected AChRs in DPSCs.

Regarding the findings of M2 mAChR activation in DPSCs, there remain areas worthy of exploration. For example, the cell cycle analysis concluded a cell cycle arrest in the G2/M phase. Investigations to narrow the exact phase of which this arrest takes place could be explored using Ki67 antibody to stain the cells during mitosis (i.e. M phase) (Sun and Kaufman, 2018). This could provide an understanding of the impact of M2 signalling in influencing activities such chromosome spindle attachment and separation. Furthermore, the gene

expression analysis points to the P21 CDK inhibitor as the main influencer of DPSCs cycle arrest in response to M2 activation. There is a cascade of events between M2 activation and the elevated expression of the P21 gene worthy of investigation. This could potentially show the involvement of several pathways such as the mTOR pathway, STAT signalling, and the p53 pathway. This, besides the MAPK pathway, can further enhance the knowledge about the downstream effectors involved in M2 mAChR signalling in DPSCs.

Furthermore, investigations into the potential role of M2 mAChR role in osteogenic differentiation is worthy of exploration. The upregulated expression of *RUNX2* despite the hindered osteogenic differentiation of DPSCs stimulated with the M2 agonist is an interesting finding. This suggests that *RUNX2* might be involved in M2 mAChR downstream signalling outside the scope of differentiation. After all, *RUNX2* is a transcription factor that could be implicated in several activities besides regulating osteogenic differentiation. Considering the differentiation data, expression of the M2 mAChR gene and protein are upregulated in DPSCs that underwent osteogenic differentiation without even stimulating with the M2 agonist. This suggest that M2 mAChR might have a role, yet to be explored in the osteogenic differentiation of DPSCs.

The transcriptomic data provide a wealth of key target genes involved in many signalling mechanisms. Beside genes involved in cell cycle, genes involved in migration and chemokine responses are abundant. This suggests a role for M2 mAChR signalling in regulating immunomodulatory processes. This is worthy of further exploration, since the transcriptomic data highlight DPSCs response to be associated with stimulus induced stress and oxidative stress.

### **6.3 Concluding remarks**

This body of work represents a comprehensive investigation into the existence of ACh signalling in a heterogeneous DPSC population. It brings novelty by identifying the presence of functional AChRs in DPSCs and characterises the role of the M2 mAChR in modulating the behaviour of this cell type.

It adds to the body of knowledge pertaining to both the regenerative potential of DPSCs and the role of the M2 mAChR in this. It is clear from this work that ACh signalling is functional in DPSCs and should be considered to have a role in regulating cell function. This work paves the way for further work that aims to understand and control the regenerative output of DPSCs via a cholinergic route. Ultimately, this has the potential to help manipulate DPSCs behaviour during regenerative medicinal applications.

## References

- Adler, M. *et al.* (1991) 'Regulation of acetylcholine hydrolysis in canine tracheal smooth muscle', *European journal of pharmacology*, 205(1), pp. 73-79.
- Ahmed, N. E.-M. B. *et al.* (2016) 'The effects of hypoxia on the stemness properties of human dental pulp stem cells (DPSCs)', *Scientific reports*, 6(1), pp. 1-10.
- Akpinar, G. *et al.* (2014) 'Phenotypic and proteomic characteristics of human dental pulp derived mesenchymal stem cells from a natal, an exfoliated deciduous, and an impacted third molar tooth', *Stem Cells International*, 2014.
- Aktas, H., Cai, H. and Cooper, G. M. (1997) 'Ras links growth factor signaling to the cell cycle machinery via regulation of cyclin D1 and the Cdk inhibitor p27KIP1', *Molecular and cellular biology*, 17(7), pp. 3850-3857.
- Alaidaroos, N. Y. A. *et al.* (2021) 'Differential SOD2 and GSTZ1 profiles contribute to contrasting dental pulp stem cell susceptibilities to oxidative damage and premature senescence', *Stem Cell Research & Therapy*, 12(1), pp. 1-19.
- El Alami, M. *et al.* (2014) 'Activation of p38, p21, and NRF-2 mediates decreased proliferation of human dental pulp stem cells cultured under 21% O<sub>2</sub>', *Stem cell reports*, 3(4), pp. 566-573.
- Alberts, B. *et al.* (2008) *The Cell Cycle, Molecular Biology of the Cell. 5th edition*. New York: Garland Science, pp. 1053-1060. doi: 10.1201/9781315735368.
- Albuquerque, E. X. *et al.* (2009) 'Mammalian nicotinic acetylcholine receptors: from structure to function', *Physiological reviews*, 89(1), pp. 73-120.
- Alessandrini, F. *et al.* (2015) 'The activation of M2 muscarinic receptor inhibits cell growth and survival in human glioblastoma cancer stem cells', *International Immunopharmacology*, 29(1), pp. 105-109. doi: 10.1016/j.intimp.2015.05.032.
- Alge, D. L. *et al.* (2010) 'Donor-matched comparison of dental pulp stem cells and bone marrow-derived mesenchymal stem cells in a rat model', *Journal of tissue engineering and regenerative medicine*, 4(1), pp. 73-81.
- Alqahtani, S. *et al.* (2023) 'Acetylcholine Receptors in Mesenchymal Stem Cells', *Stem Cells and Development*, 32(3-4), pp. 47-59.
- Alraies, A. *et al.* (2017) 'Variation in human dental pulp stem cell ageing profiles reflect contrasting proliferative and regenerative capabilities', *BMC cell biology*, 18, pp. 1-14.
- Alraies, A. *et al.* (2019) 'Discrimination of dental pulp stem cell regenerative heterogeneity by single-cell Raman spectroscopy', *Tissue Engineering Part C: Methods*, 25(8), pp. 489-499.
- Alvarez, R. *et al.* (2015) 'Single CD271 marker isolates mesenchymal stem cells from human dental pulp', *International journal of oral science*, 7(4), pp. 205-212.
- Anderson, R. G. W., Goldstein, J. L. and Brown, M. S. (1977) 'A mutation that impairs the ability of lipoprotein receptors to localise in coated pits on the cell surface of

## References

- human fibroblasts', *Nature*, 270(5639), pp. 695-699.
- De Angelis, F. *et al.* (2012) 'Muscarinic receptor subtypes as potential targets to modulate oligodendrocyte progenitor survival, proliferation, and differentiation', *Developmental Neurobiology*, 72(5), pp. 713-728. doi: 10.1002/dneu.20976.
- Armiñán, A. *et al.* (2009) 'Cardiac differentiation is driven by NKX2. 5 and GATA4 nuclear translocation in tissue-specific mesenchymal stem cells', *Stem Cells and Development*, 18(6), pp. 907-918.
- Arora, M. *et al.* (2017) 'Endogenous replication stress in mother cells leads to quiescence of daughter cells', *Cell reports*, 19(7), pp. 1351-1364.
- Arthur, A. *et al.* (2008) 'Adult human dental pulp stem cells differentiate toward functionally active neurons under appropriate environmental cues', *Stem cells*, 26(7), pp. 1787-1795.
- Arthur, A. *et al.* (2009) 'Implanted adult human dental pulp stem cells induce endogenous axon guidance', *Stem cells*, 27(9), pp. 2229-2237.
- Asrican, B. *et al.* (2016) 'Cholinergic circuit control of postnatal neurogenesis', *Neurogenesis*, 3(1), p. e1127310. doi: 10.1080/23262133.2015.1127310.
- Atari, M. *et al.* (2012) 'Dental pulp of the third molar: a new source of pluripotent-like stem cells', *Journal of cell science*, 125(14), pp. 3343-3356.
- Aubin, J. E. (2001) 'Regulation of osteoblast formation and function', *Reviews in Endocrine and Metabolic Disorders*, 2(1), pp. 81-94.
- Aure, M. H., Arany, S. and Ovitt, C. (2015) 'Salivary glands: stem cells, self-duplication, or both?', *Journal of dental research*, 94(11), pp. 1502-1507.
- Aydin, S. and Şahin, F. (2019) 'Stem Cells Derived from Dental Tissues', in *Cell Biology and Translational Medicine, Volume 5*. Springer, pp. 123-132. doi: 10.1007/5584\_2018\_333.
- Azuma, K. *et al.* (2021) 'TRIM47 activates NF-κB signaling via PKC-ε/PKD3 stabilization and contributes to endocrine therapy resistance in breast cancer', *Proceedings of the National Academy of Sciences*, 118(35), p. e2100784118.
- Babakhanzadeh, E. *et al.* (2020) 'Testicular expression of TDRD1, TDRD5, TDRD9 and TDRD12 in azoospermia', *BMC Medical Genetics*, 21, pp. 1-7.
- Bacakova, L. *et al.* (2018) 'Stem cells: their source, potency and use in regenerative therapies with focus on adipose-derived stem cells-a review', *Biotechnology advances*, 36(4), pp. 1111-1126.
- Bader, G. D. and Hogue, C. W. V (2003) 'An automated method for finding molecular complexes in large protein interaction networks', *BMC bioinformatics*, 4(1), pp. 1-27.
- von Bahr, L. *et al.* (2012) 'Long-term complications, immunologic effects, and role of passage for outcome in mesenchymal stromal cell therapy', *Biology of Blood and Marrow Transplantation*, 18(4), pp. 557-564.

## References

- Bakopoulou, A. *et al.* (2011) 'Assessment of the impact of two different isolation methods on the osteo/odontogenic differentiation potential of human dental stem cells derived from deciduous teeth', *Calcified Tissue International*, 88(2), pp. 130-141.
- Ball, K. L. (1997) 'p21: structure and functions associated with cyclin-CDK binding', *Progress in cell cycle research*, pp. 125-134.
- Banki, K. *et al.* (1996) 'Glutathione levels and sensitivity to apoptosis are regulated by changes in transaldolase expression', *Journal of Biological Chemistry*, 271(51), pp. 32994-33001.
- Barathi, V. A., Weon, S. R. and Beuerman, R. W. (2009) 'Expression of muscarinic receptors in human and mouse sclera and their role in the regulation of scleral fibroblasts proliferation.', *Molecular vision*, 15, pp. 1277-93.
- Di Bari, M. *et al.* (2015) 'Cytotoxic and genotoxic effects mediated by M2 muscarinic receptor activation in human glioblastoma cells', *Neurochemistry International*, 90, pp. 261-270. doi: 10.1016/j.neuint.2015.09.008.
- Barr, A. R. *et al.* (2017) 'DNA damage during S-phase mediates the proliferation-quiescence decision in the subsequent G1 via p21 expression', *Nature communications*, 8(1), p. 14728.
- Barros, M. A. *et al.* (2015) 'Immature dental pulp stem cells showed renotropic and pericyte-like properties in acute renal failure in rats', *Cell medicine*, 7(3), pp. 95-108.
- Bartek, J. and Lukas, J. (2001) 'Pathways governing G1/S transition and their response to DNA damage', *FEBS letters*, 490(3), pp. 117-122.
- Basu, K. *et al.* (2019) 'Why recombinant antibodies—Benefits and applications', *Current opinion in biotechnology*, 60, pp. 153-158.
- Batouli, S. *et al.* (2003) 'Comparison of stem-cell-mediated osteogenesis and dentinogenesis', *Journal of dental research*, 82(12), pp. 976-981.
- Benavente, C. A. *et al.* (2003) 'Subcellular distribution and mitogenic effect of basic fibroblast growth factor in mesenchymal uncommitted stem cells', *Growth Factors*, 21(2), pp. 87-94.
- Bencherif, M. and Lukas, R. J. (1993) 'Cytochalasin modulation of nicotinic cholinergic receptor expression and muscarinic receptor function in human TE671/RD cells: a possible functional role of the cytoskeleton', *Journal of neurochemistry*, 61(3), pp. 852-864.
- Bernardo, M. E. and Fibbe, W. E. (2013) 'Mesenchymal stromal cells: sensors and switchers of inflammation', *Cell stem cell*, 13(4), pp. 392-402.
- De Biasio, A. and Blanco, F. J. (2013) 'Proliferating cell nuclear antigen structure and interactions: too many partners for one dancer?', *Advances in protein chemistry and structural biology*, 91, pp. 1-36.
- Birdsall, N. J. and Lazareno, S. (2005) 'Allosterism at muscarinic receptors: ligands and mechanisms.', *Mini reviews in medicinal chemistry*, 5(6), p. 523.

## References

- Boehm, E. M., Gildenberg, M. S. and Washington, M. T. (2016) 'The many roles of PCNA in eukaryotic DNA replication', *The Enzymes*, 39, pp. 231-254.
- Te Boekhorst, V., Preziosi, L. and Friedl, P. (2016) 'Plasticity of cell migration in vivo and in silico', *Annual review of cell and developmental biology*, 32, pp. 491-526.
- Boland, G. M. *et al.* (2004) 'Wnt 3a promotes proliferation and suppresses osteogenic differentiation of adult human mesenchymal stem cells', *Journal of cellular biochemistry*, 93(6), pp. 1210-1230.
- Borda, E. *et al.* (2007) 'Nitric oxide synthase and PGE2 reciprocal interactions in rat dental pulp: cholinergic modulation', *Journal of endodontics*, 33(2), pp. 142-147.
- Boskey, A. L. (1995) 'Osteopontin and related phosphorylated sialoproteins: effects on mineralization.', *Annals of the New York Academy of Sciences*, 760, pp. 249-256.
- Botticelli, E. *et al.* (2022) 'Analysis of Signal Transduction Pathways Downstream M2 Receptor Activation: Effects on Schwann Cell Migration and Morphology', *Life*, 12(2), p. 211.
- Boufker, H. I. *et al.* (2011) 'Role of farnesoid X receptor (FXR) in the process of differentiation of bone marrow stromal cells into osteoblasts', *Bone*, 49(6), pp. 1219-1231.
- Boussemart, L. *et al.* (2014) 'eIF4F is a nexus of resistance to anti-BRAF and anti-MEK cancer therapies', *Nature*, 513(7516), pp. 105-109.
- Brar, G. S. and Toor, R. S. S. (2012) 'Dental stem cells: dentinogenic, osteogenic, and neurogenic differentiation and its clinical cell based therapies', *Indian Journal of Dental Research*, 23(3), p. 393.
- Bray, A. F. *et al.* (2014) 'Human dental pulp stem cells respond to cues from the rat retina and differentiate to express the retinal neuronal marker rhodopsin', *Neuroscience*, 280, pp. 142-155.
- Bruderer, M. *et al.* (2014) 'Role and regulation of RUNX2 in osteogenesis', *Eur Cell Mater*, 28(28), pp. 269-286.
- Bühling, F. *et al.* (2007) 'Tiotropium suppresses acetylcholine-induced release of chemotactic mediators in vitro', *Respiratory medicine*, 101(11), pp. 2386-2394.
- Burry, R. W. (2011) 'Controls for immunocytochemistry: an update', *Journal of Histochemistry & Cytochemistry*, 59(1), pp. 6-12.
- Cai, J. *et al.* (2013) 'Generation of tooth-like structures from integration-free human urine induced pluripotent stem cells', *Cell regeneration*, 2(1), p. 6.
- Calabrese, G. *et al.* (2016) 'Collagen-hydroxyapatite scaffolds induce human adipose derived stem cells osteogenic differentiation in vitro', *PLoS one*, 11(3), p. e0151181.
- Calaf, G. M. *et al.* (2022) 'Muscarinic receptors associated with cancer', *Cancers*, 14(9), p. 2322.

## References

- Campisi, J. and d'Adda di Fagagna, F. (2007) 'Cellular senescence: when bad things happen to good cells', *Nature reviews Molecular cell biology*, 8(9), pp. 729-740.
- Carballosa, C. M., Greenberg, J. M. and Cheung, H. S. (2016) 'Expression and function of nicotinic acetylcholine receptors in stem cells', *AIMS BIOENGINEERING*, 3(3), pp. 245-263. doi: 10.3934/bioeng.2016.3.245.
- Carinci, F. *et al.* (2008) 'Comparison between genetic portraits of osteoblasts derived from primary cultures and osteoblasts obtained from human pulpar stem cells', *Journal of Craniofacial Surgery*, 19(3), pp. 616-625.
- Carnevale, G. *et al.* (2013) 'In vitro differentiation into insulin-producing  $\beta$ -cells of stem cells isolated from human amniotic fluid and dental pulp', *Digestive and Liver Disease*, 45(8), pp. 669-676.
- Carvalho, M. S. *et al.* (2019) 'Synergistic effect of extracellularly supplemented osteopontin and osteocalcin on stem cell proliferation, osteogenic differentiation, and angiogenic properties', *Journal of Cellular Biochemistry*, 120(4), pp. 6555-6569.
- Carvalho, M. S. *et al.* (2021) 'Bone matrix non-collagenous proteins in tissue engineering: Creating new bone by mimicking the extracellular matrix', *Polymers*, 13(7), p. 1095.
- Castello, A. *et al.* (2012) 'Insights into RNA biology from an atlas of mammalian mRNA-binding proteins', *Cell*, 149(6), pp. 1393-1406.
- Castillo-González, A. C. *et al.* (2015) 'Dysregulated cholinergic network as a novel biomarker of poor prognostic in patients with head and neck squamous cell carcinoma', *BMC cancer*, 15, pp. 1-13.
- Caulfield, M. P. (1993) 'Muscarinic receptors—characterization, coupling and function', *Pharmacology & therapeutics*, 58(3), pp. 319-379.
- Cavallaro, U. and Dejana, E. (2011) 'Adhesion molecule signalling: not always a sticky business', *Nature reviews Molecular cell biology*, 12(3), pp. 189-197.
- Cayrol, C., Knibiehler, M. and Ducommun, B. (1998) 'p21 binding to PCNA causes G1 and G2 cell cycle arrest in p53-deficient cells', *Oncogene*, 16(3), pp. 311-320.
- Cazzalini, O. *et al.* (2003) 'p21CDKN1A does not interfere with loading of PCNA at DNA replication sites, but inhibits subsequent binding of DNA polymerase  $\delta$  at the G1/S phase transition', *Cell Cycle*, 2(6), pp. 595-602.
- Cebula, M., Schmidt, E. E. and Arnér, E. S. J. (2015) 'TrxR1 as a potent regulator of the Nrf2-Keap1 response system', *Antioxidants & redox signaling*, 23(10), pp. 823-853.
- Cecchini, M. J., Amiri, M. and Dick, F. A. (2012) 'Analysis of cell cycle position in mammalian cells', *JoVE (Journal of Visualized Experiments)*, (59), p. e3491.
- Cen, L. *et al.* (2008) 'Collagen tissue engineering: development of novel biomaterials and applications', *Pediatric research*, 63(5), pp. 492-496.
- Chai, Y. *et al.* (2000) 'Fate of the mammalian cranial neural crest during tooth and

## References

- mandibular morphogenesis', *Development*, 127(8), pp. 1671-1679.
- Chamieh, F. *et al.* (2016) 'Accelerated craniofacial bone regeneration through dense collagen gel scaffolds seeded with dental pulp stem cells', *Scientific reports*, 6, p. 38814.
- Chan, A. H. P. and Huang, N. F. (2020) 'Effects of nicotine on the translation of stem cell therapy', *REGENERATIVE MEDICINE*, 15(5), pp. 1679-1688. doi: 10.2217/rme-2020-0032.
- Chang, W. *et al.* (2012) 'Phorbol myristate acetate differentiates human adipose-derived mesenchymal stem cells into functional cardiogenic cells', *Biochemical and Biophysical Research Communications*, 424(4), pp. 740-746. doi: 10.1016/j.bbrc.2012.07.022.
- Chassot, A.-A. *et al.* (2008) 'Confluence-induced cell cycle exit involves pre-mitotic CDK inhibition by p27Kip1 and cyclin D1 downregulation', *Cell cycle*, 7(13), pp. 2038-2046.
- Chen, F.-M. *et al.* (2012) 'Stem cell-delivery therapeutics for periodontal tissue regeneration', *Biomaterials*, 33(27), pp. 6320-6344.
- Chen, J. *et al.* (2023) 'AKR1C3 suppresses ferroptosis in hepatocellular carcinoma through regulation of YAP/SLC7A11 signaling pathway', *Molecular Carcinogenesis*, 62(6), pp. 833-844.
- Chen, S. *et al.* (2009) 'Runx2, osx, and dspp in tooth development', *Journal of dental research*, 88(10), pp. 904-909.
- Chen, Y.-L. *et al.* (2021) 'Ephrin A4-ephrin receptor A10 signaling promotes cell migration and spheroid formation by upregulating NANOG expression in oral squamous cell carcinoma cells', *Scientific reports*, 11(1), p. 644.
- Cheng, H. *et al.* (2010) 'Transient receptor potential melastatin type 7 channel is critical for the survival of bone marrow derived mesenchymal stem cells', *Stem cells and development*, 19(9), pp. 1393-1403.
- Cheng, M. *et al.* (1999) 'The p21Cip1 and p27Kip1 CDK "inhibitors" are essential activators of cyclin D-dependent kinases in murine fibroblasts', *The EMBO journal*, 18(6), pp. 1571-1583.
- Cheng, P.-H. *et al.* (2008) 'Postnatal stem/progenitor cells derived from the dental pulp of adult chimpanzee', *BMC cell biology*, 9(1), pp. 1-11.
- Cheung, T. H. and Rando, T. A. (2013) 'Molecular regulation of stem cell quiescence', *Nature reviews Molecular cell biology*, 14(6), pp. 329-340.
- Childs, B. G. *et al.* (2015) 'Cellular senescence in aging and age-related disease: from mechanisms to therapy', *Nature medicine*, 21(12), pp. 1424-1435.
- Choe, K. N. and Moldovan, G.-L. (2017) 'Forging ahead through darkness: PCNA, still the principal conductor at the replication fork', *Molecular cell*, 65(3), pp. 380-392.
- Choi, M. R. *et al.* (2010) 'Selection of optimal passage of bone marrow-derived mesenchymal stem cells for stem cell therapy in patients with amyotrophic lateral

## References

- sclerosis', *Neuroscience letters*, 472(2), pp. 94-98.
- Choi, Y. H. and Kim, J. K. (2019) 'Dissecting cellular heterogeneity using single-cell RNA sequencing', *Molecules and cells*, 42(3), p. 189.
- Chong, P. *et al.* (2012) 'Human peripheral blood derived mesenchymal stem cells demonstrate similar characteristics and chondrogenic differentiation potential to bone marrow derived mesenchymal stem cells', *Journal of Orthopaedic Research*, 30(4), pp. 634-642.
- Chu, M.-S. *et al.* (2006) 'Signalling pathway in the induction of neurite outgrowth in human mesenchymal stem cells', *Cellular Signalling*, 18(4), pp. 519-530. doi: 10.1016/j.cellsig.2005.05.018.
- Chu, X. *et al.* (2022) 'Overview of human 20 alpha-hydroxysteroid dehydrogenase (AKR1C1): Functions, regulation, and structural insights of inhibitors', *Chemico-Biological Interactions*, 351, p. 109746.
- Chun, S. Y. *et al.* (2010) 'Analysis of the soluble human tooth proteome and its ability to induce dentin/tooth regeneration', *Tissue Engineering Part A*, 17(1-2), pp. 181-191.
- Cohen, P. and Frame, S. (2001) 'The renaissance of GSK3', *Nature reviews Molecular cell biology*, 2(10), pp. 769-776.
- Coller, H. A., Sang, L. and Roberts, J. M. (2006) 'A new description of cellular quiescence', *PLoS biology*, 4(3), p. e83.
- Coronado, D. *et al.* (2013) 'A short G1 phase is an intrinsic determinant of naive embryonic stem cell pluripotency', *Stem cell research*, 10(1), pp. 118-131.
- Cosentino, C., Grieco, D. and Costanzo, V. (2011) 'ATM activates the pentose phosphate pathway promoting anti-oxidant defence and DNA repair', *The EMBO journal*, 30(3), pp. 546-555.
- De Couto, P. A. *et al.* (2009) 'Cholinoceptor modulation on nitric oxide regulates prostaglandin E (2) and metalloproteinase-3 production in experimentally induced inflammation of rat dental pulp.', *Journal of endodontics*, 35(4), p. 529.
- De Couto Pita, A. *et al.* (2009) 'Differential cholinoceptor modulation of nitric oxide isoforms in experimentally-induced inflammation of dental pulp tissue', *International endodontic journal*, 42(6), pp. 525-533.
- Cristofaro, I. *et al.* (2018) 'Activation of M2 muscarinic acetylcholine receptors by a hybrid agonist enhances cytotoxic effects in GB7 glioblastoma cancer stem cells', *Neurochemistry International*, 118(February), pp. 52-60. doi: 10.1016/j.neuint.2018.04.010.
- Cristofaro, I., Alessandrini, F., *et al.* (2020) 'Cross Interaction between M2 Muscarinic Receptor and Notch1/EGFR Pathway in Human Glioblastoma Cancer Stem Cells: Effects on Cell Cycle Progression and Survival', *Cells*, 9(3), p. 657. doi: 10.3390/cells9030657.
- Cristofaro, I., Limongi, C., *et al.* (2020) 'M2 Receptor Activation Counteracts the Glioblastoma Cancer Stem Cell Response to Hypoxia Condition', *International*

*journal of molecular sciences*, 21(5), p. 1700. doi: 10.3390/ijms21051700.

- Cummings, B. S. and Schnellmann, R. G. (2004) 'Measurement of cell death in mammalian cells.', *Current protocols in pharmacology*, Chapter 12(1), p. Unit 12.8. doi: 10.1002/0471141755.ph1208s25.
- Curtis, K. M., Gomez, L. A. and Schiller, P. C. (2012) 'Rac1b regulates NT3-stimulated Mek-Erk signaling, directing marrow-isolated adult multilineage inducible (MIAMI) cells toward an early neuronal phenotype', *Molecular and Cellular Neuroscience*, 49(2), pp. 138-148.
- Czechowski, T. *et al.* (2004) 'Real-time RT-PCR profiling of over 1400 Arabidopsis transcription factors: unprecedented sensitivity reveals novel root-and shoot-specific genes', *The Plant Journal*, 38(2), pp. 366-379.
- d'Aquino, R. *et al.* (2007) 'Human postnatal dental pulp cells co-differentiate into osteoblasts and endotheliocytes: A pivotal synergy leading to adult bone tissue formation', *Cell Death and Differentiation*, 14(6), pp. 1162-1171. doi: 10.1038/sj.cdd.4402121.
- d'Aquino, R. *et al.* (2009) 'Human mandible bone defect repair by the grafting of dental pulp stem/progenitor cells and collagen sponge biocomplexes', *Eur Cell Mater*, 18(7), pp. 75-83.
- Dalby, M. J., García, A. J. and Salmeron-Sanchez, M. (2018) 'Receptor control in mesenchymal stem cell engineering', *Nature Reviews Materials*, 3(3), pp. 1-14.
- Damdimopoulos, A. E. *et al.* (2004) 'An alternative splicing variant of the selenoprotein thioredoxin reductase is a modulator of estrogen signaling', *Journal of Biological Chemistry*, 279(37), pp. 38721-38729.
- Dani, J. A. and Bertrand, D. (2007) 'Nicotinic acetylcholine receptors and nicotinic cholinergic mechanisms of the central nervous system', *Annu. Rev. Pharmacol. Toxicol.*, 47, pp. 699-729.
- Danielyan, L. *et al.* (2009) 'Survival, neuron-like differentiation and functionality of mesenchymal stem cells in neurotoxic environment: the critical role of erythropoietin.', *Cell death and differentiation*, 16(12), pp. 1599-1614. doi: 10.1038/cdd.2009.95.
- Darling, T. K. and Lamb, T. J. (2019) 'Emerging roles for Eph receptors and ephrin ligands in immunity', *Frontiers in immunology*, 10, p. 1473.
- Datta, N. *et al.* (2006) 'In vitro generated extracellular matrix and fluid shear stress synergistically enhance 3D osteoblastic differentiation', *Proceedings of the National Academy of Sciences*, 103(8), pp. 2488-2493.
- Decaestecker, C. *et al.* (2007) 'Can anti-migratory drugs be screened in vitro? A review of 2D and 3D assays for the quantitative analysis of cell migration', *Medicinal research reviews*, 27(2), pp. 149-176.
- Decker, M. W., Meyer, M. D. and Sullivan, J. P. (2001) 'The therapeutic potential of nicotinic acetylcholine receptor agonists for pain control', *Expert opinion on investigational drugs*, 10(10), pp. 1819-1830.

## References

- Demarco, F. F. *et al.* (2010) 'Effects of morphogen and scaffold porogen on the differentiation of dental pulp stem cells', *Journal of endodontics*, 36(11), pp. 1805-1811.
- Demircan, P. C. *et al.* (2011) 'Immunoregulatory effects of human dental pulp-derived stem cells on T cells: comparison of transwell co-culture and mixed lymphocyte reaction systems', *Cytotherapy*, 13(10), pp. 1205-1220.
- Deng, L. *et al.* (2020) 'p53-mediated control of aspartate-asparagine homeostasis dictates LKB1 activity and modulates cell survival', *Nature communications*, 11(1), p. 1755.
- Dicker, A. *et al.* (2005) 'Differential function of the  $\alpha$ 2A-adrenoceptor and phosphodiesterase-3B in human adipocytes of different origin', *International journal of obesity*, 29(12), p. 1413.
- Diefenderfer, D. L. *et al.* (2003) 'BMP responsiveness in human mesenchymal stem cells', *Connective tissue research*, 44(1), pp. 305-311.
- Ding, L. *et al.* (2020) 'The roles of cyclin-dependent kinases in cell-cycle progression and therapeutic strategies in human breast cancer', *International journal of molecular sciences*, 21(6), p. 1960.
- Dissanayaka, W. L. *et al.* (2011) 'Characterization of dental pulp stem cells isolated from canine premolars', *Journal of endodontics*, 37(8), pp. 1074-1080.
- Dong, J. *et al.* (2018) 'Protein kinase A mediates scopolamine-induced mTOR activation and an antidepressant response', *Journal of Affective Disorders*, 227, pp. 633-642.
- Ducoux, M. *et al.* (2001) 'Mediation of proliferating cell nuclear antigen (PCNA)-dependent DNA replication through a conserved p21Cip1-like PCNA-binding motif present in the third subunit of human DNA polymerase  $\delta$ ', *Journal of Biological Chemistry*, 276(52), pp. 49258-49266.
- Dumic-Cule, I. *et al.* (2018) 'Bone morphogenetic proteins in fracture repair', *International orthopaedics*, 42(11), pp. 2619-2626.
- Dzantiev, L. *et al.* (2004) 'A defined human system that supports bidirectional mismatch-provoked excision', *Molecular cell*, 15(1), pp. 31-41.
- Echavarria, R. and Hussain, S. N. A. (2013) 'Regulation of angiopoietin-1/Tie-2 receptor signaling in endothelial cells by dual-specificity phosphatases 1, 4, and 5', *Journal of the American Heart Association*, 2(6), p. e000571.
- Eglen, R. M. (2005) 'Muscarinic receptor subtype pharmacology and physiology', *Progress in medicinal chemistry*, 43, pp. 105-136.
- Eglen, R. M. (2006) 'Muscarinic receptor subtypes in neuronal and non-neuronal cholinergic function', *Autonomic and Autacoid Pharmacology*, 26(3), pp. 219-233.
- Eglen, R. M. (2012) 'Overview of muscarinic receptor subtypes', *Handbook of Experimental Pharmacology*. Springer, pp. 3-28. doi: 10.1007/978-3-642-23274-9\_1.

## References

- Eglen, R. M., Choppin, A. and Watson, N. (2001) 'Therapeutic opportunities from muscarinic receptor research', *Trends in pharmacological sciences*, 22(8), pp. 409-414.
- Ekholm, S. V and Reed, S. I. (2000) 'Regulation of G1 cyclin-dependent kinases in the mammalian cell cycle', *Current opinion in cell biology*, 12(6), pp. 676-684.
- El-Fakahany, E. E. and Jakubik, J. (2016) 'Radioligand binding at muscarinic receptors', in *Muscarinic Receptor: From Structure to Animal Models*. Springer, pp. 37-68.
- El-Habta, R., Kingham, P. J. and Backman, L. J. (2018) 'Adipose stem cells enhance myoblast proliferation via acetylcholine and extracellular signal-regulated kinase 1/2 signaling.', *Muscle & nerve*, 57(2), pp. 305-311. doi: 10.1002/mus.25741.
- El-Sayed, K. M. F., Klingebiel, P. and Dörfer, C. E. (2016) 'Toll-like receptor expression profile of human dental pulp stem/progenitor cells', *Journal of Endodontics*, 42(3), pp. 413-417.
- Elwary, S. M. A., Chavan, B. and Schallreuter, K. U. (2006) 'The vesicular acetylcholine transporter is present in melanocytes and keratinocytes in the human epidermis', *Journal of investigative dermatology*, 126(8), pp. 1879-1884.
- Erices, A. *et al.* (2002) 'Gp130 activation by soluble interleukin-6 receptor/interleukin-6 enhances osteoblastic differentiation of human bone marrow-derived mesenchymal stem cells', *Experimental cell research*, 280(1), pp. 24-32.
- Espagnolle, N. *et al.* (2014) 'CD 146 expression on mesenchymal stem cells is associated with their vascular smooth muscle commitment', *Journal of cellular and molecular medicine*, 18(1), pp. 104-114.
- Eswarakumar, V. P., Lax, I. and Schlessinger, J. (2005) 'Cellular signaling by fibroblast growth factor receptors', *Cytokine & growth factor reviews*, 16(2), pp. 139-149.
- Evinger, M. J. *et al.* (1994) 'A single transmitter regulates gene expression through two separate mechanisms: cholinergic regulation of phenylethanolamine N-methyltransferase mRNA via nicotinic and muscarinic pathways', *Journal of Neuroscience*, 14(4), pp. 2106-2116.
- Fathi, E. *et al.* (2020) 'An overview of the myocardial regeneration potential of cardiac c-Kit+ progenitor cells via PI3K and MAPK signaling pathways', *Future Cardiology*, 16(3), pp. 199-209.
- Fedarko, N. S. *et al.* (2004) 'Three small integrin-binding ligand N-linked glycoproteins (SIBLINGs) bind and activate specific matrix metalloproteinases', *The FASEB Journal*, 18(6), pp. 734-736.
- Felder, C. C. *et al.* (2000) 'Therapeutic opportunities for muscarinic receptors in the central nervous system', *Journal of medicinal chemistry*, 43(23), pp. 4333-4353.
- Ferreira, J. N. *et al.* (2019) 'A magnetic three-dimensional levitated primary cell culture system for the development of secretory salivary gland-like organoids', *Journal of Tissue Engineering and Regenerative Medicine*, 13(3), pp. 495-508. doi: 10.1002/term.2809.
- Ferretti, M. *et al.* (2012) 'M2 muscarinic receptors inhibit cell proliferation in human

## References

- glioblastoma cell lines', *Life Sciences*, 91(21-22), pp. 1134-1137. doi: 10.1016/j.lfs.2012.04.033.
- Ferretti, M. *et al.* (2013) 'M2 receptor activation inhibits cell cycle progression and survival in human glioblastoma cells', *Journal of cellular and molecular medicine*, 17(4), pp. 552-566. doi: 10.1111/jcmm.12038.
- Ferrier, J. *et al.* (2015) 'Cholinergic neurotransmission in the posterior insular cortex is altered in preclinical models of neuropathic pain: key role of muscarinic M2 receptors in donepezil-induced antinociception', *Journal of Neuroscience*, 35(50), pp. 16418-16430.
- Forsgren, S. *et al.* (2009) 'Novel information on the non-neuronal cholinergic system in orthopedics provides new possible treatment strategies for inflammatory and degenerative diseases', *Orthopedic Reviews*, 1(1), p. 11. doi: 10.4081/or.2009.e11.
- Frank, O. *et al.* (2002) 'Real-time quantitative RT-PCR analysis of human bone marrow stromal cells during osteogenic differentiation in vitro', *Journal of cellular biochemistry*, 85(4), pp. 737-746.
- Fredriksson, R. *et al.* (2003) 'The G-protein-coupled receptors in the human genome form five main families. Phylogenetic analysis, paralogon groups, and fingerprints', *Molecular pharmacology*, 63(6), pp. 1256-1272.
- Friedenstein, A. J. *et al.* (1974) 'Precursors for fibroblasts in different populations of hematopoietic cells as detected by the in vitro colony assay method', *Experimental hematology*, 2(2), pp. 83-92.
- Frouin, I. *et al.* (2003) 'Human proliferating cell nuclear antigen, poly (ADP-ribose) polymerase-1, and p21 waf1/cip1: a dynamic exchange of partners', *Journal of Biological Chemistry*, 278(41), pp. 39265-39268.
- Fukada, S. *et al.* (2007) 'Molecular signature of quiescent satellite cells in adult skeletal muscle', *Stem cells*, 25(10), pp. 2448-2459.
- Fukami-Kobayashi, J. and Mitsui, Y. (1999) 'Cyclin D1 inhibits cell proliferation through binding to PCNA and cdk2', *Experimental cell research*, 246(2), pp. 338-347.
- Furumatsu, T. *et al.* (2005) 'Smad3 Induces Chondrogenesis through the Activation of SOX9 via CREB-binding Protein/p300 Recruitment\*[boxes]', *Journal of Biological Chemistry*, 280(9), pp. 8343-8350.
- Gahring, L. C. and Rogers, S. W. (2005) 'Neuronal nicotinic acetylcholine receptor expression and function on nonneuronal cells', *The AAPS Journal*, 7(4), pp. E885-E894. doi: 10.1208/aapsj070486.
- Gandia, C. *et al.* (2008) 'Human dental pulp stem cells improve left ventricular function, induce angiogenesis, and reduce infarct size in rats with acute myocardial infarction', *Stem cells*, 26(3), pp. 638-645.
- Ganss, B., Kim, R. H. and Sodek, J. (1999) 'Bone sialoprotein', *Critical Reviews in Oral Biology & Medicine*, 10(1), pp. 79-98.
- Gao, Y., Yi, X. and Ding, Y. (2017) 'Combined transcriptomic analysis revealed AKR1B10

## References

played an important role in psoriasis through the dysregulated lipid pathway and overproliferation of keratinocyte', *BioMed research international*, 2017.

- Gauthier, P. *et al.* (2017) 'Cementogenic genes in human periodontal ligament stem cells are downregulated in response to osteogenic stimulation while upregulated by vitamin C treatment', *Cell and tissue research*, 368(1), pp. 79-92.
- Ge, C. *et al.* (2007) 'Critical role of the extracellular signal-regulated kinase-MAPK pathway in osteoblast differentiation and skeletal development', *The Journal of cell biology*, 176(5), pp. 709-718.
- Ge, C. *et al.* (2016) 'Reciprocal control of osteogenic and adipogenic differentiation by ERK/MAP kinase phosphorylation of Runx2 and PPAR $\gamma$  transcription factors', *Journal of cellular physiology*, 231(3), pp. 587-596.
- Gether, U. (2000) 'Uncovering molecular mechanisms involved in activation of G protein-coupled receptors', *Endocrine reviews*, 21(1), pp. 90-113.
- Ghaffari, S. (2008) 'Oxidative stress in the regulation of normal and neoplastic hematopoiesis', *Antioxidants & redox signaling*, 10(11), pp. 1923-1940.
- Gire, V. and Dulić, V. (2015) 'Senescence from G2 arrest, revisited', *Cell cycle*, 14(3), pp. 297-304.
- Giuliani, A. *et al.* (2013) 'Three years after transplants in human mandibles, histological and in-line holotomography revealed that stem cells regenerated a compact rather than a spongy bone: Biological and clinical implications', *Stem cells translational medicine*, 2(4), pp. 316-324.
- Gnanasegaran, N. *et al.* (2017) 'Effect of dental pulp stem cells in MPTP-induced old-aged mice model', *European journal of clinical investigation*, 47(6), pp. 403-414.
- Golub, E. E. and Boesze-Battaglia, K. (2007) 'The role of alkaline phosphatase in mineralization', *Current opinion in Orthopaedics*, 18(5), pp. 444-448.
- Gong, D. and Ferrell Jr, J. E. (2010) 'The roles of cyclin A2, B1, and B2 in early and late mitotic events', *Molecular biology of the cell*, 21(18), pp. 3149-3161.
- Gonzales, K. A. U. *et al.* (2015) 'Deterministic restriction on pluripotent state dissolution by cell-cycle pathways', *Cell*, 162(3), pp. 564-579.
- Gorgoulis, V. *et al.* (2019) 'Cellular senescence: defining a path forward', *Cell*, 179(4), pp. 813-827.
- Govindasamy, V., Abdullah, A. N., *et al.* (2010) 'Inherent differential propensity of dental pulp stem cells derived from human deciduous and permanent teeth', *Journal of Endodontics*, 36(9), pp. 1504-1515.
- Govindasamy, V., Ronald, V. S., *et al.* (2010) 'Micromanipulation of culture niche permits long-term expansion of dental pulp stem cells--an economic and commercial angle.', *In vitro cellular & developmental biology. Animal*, 46(9), pp. 764-773. doi: 10.1007/s11626-010-9332-0.
- Govindasamy, V *et al.* (2011) 'Differentiation of dental pulp stem cells into islet-like aggregates', *Journal of dental research*, 90(5), pp. 646-652.

## References

- Govindasamy, Vijayendran *et al.* (2011) 'Human platelet lysate permits scale-up of dental pulp stromal cells for clinical applications', *Cytotherapy*, 13(10), pp. 1221-1233.
- Graham, E. S. *et al.* (2013) 'M1 muscarinic receptor activation mediates cell death in M1-HEK293 cells', *PloS one*, 8(9), p. e72011.
- Grando, S. A. (1997) 'Biological Functions of Keratinocyte Cholinergic Receptors', *Journal of Investigative Dermatology Symposium Proceedings*, 2(1), pp. 41-48. doi: 10.1038/jidsymp.1997.10.
- Grando, S. A. *et al.* (2007) 'Recent progress in understanding the non-neuronal cholinergic system in humans.', *Life sciences*, 80(24-25), pp. 2181-5. doi: 10.1016/j.lfs.2007.03.015.
- Grassi, F. *et al.* (2004) 'Fusion-independent expression of functional ACh receptors in mouse mesoangioblast stem cells contacting muscle cells', *JOURNAL OF PHYSIOLOGY-LONDON*, 560(2), pp. 479-489. doi: 10.1113/jphysiol.2004.070607.
- Graziano, A. *et al.* (2008) 'Human CD34+ stem cells produce bone nodules in vivo', *Cell proliferation*, 41(1), pp. 1-11.
- Gregory, C. A. *et al.* (2004) 'An Alizarin red-based assay of mineralization by adherent cells in culture: Comparison with cetylpyridinium chloride extraction', *Analytical Biochemistry*, 329(1), pp. 77-84. doi: 10.1016/j.ab.2004.02.002.
- Grimes, C. A. and Jope, R. S. (2001) 'The multifaceted roles of glycogen synthase kinase 3 $\beta$  in cellular signaling', *Progress in neurobiology*, 65(4), pp. 391-426.
- Gromolak, S. *et al.* (2020) 'Biological characteristics and osteogenic differentiation of ovine bone marrow derived mesenchymal stem cells stimulated with FGF-2 and BMP-2', *International journal of molecular sciences*, 21(24), p. 9726.
- Gronthos, S. *et al.* (2000) 'Postnatal human dental pulp stem cells (DPSCs) in vitro and in vivo', *Proceedings of the National Academy of Sciences*, 97(25), pp. 13625-13630.
- Gronthos, S. *et al.* (2002) 'Stem cell properties of human dental pulp stem cells', *Journal of dental research*, 81(8), pp. 531-535.
- Gulseren, G. *et al.* (2015) 'Alkaline phosphatase-mimicking peptide nanofibers for osteogenic differentiation', *Biomacromolecules*, 16(7), pp. 2198-2208.
- Guo, Y. *et al.* (2013) 'Large scale comparison of gene expression levels by microarrays and RNAseq using TCGA data', *PloS one*, 8(8), p. e71462.
- Guo, Y. *et al.* (2020) 'ERK/MAPK signalling pathway and tumorigenesis', *Experimental and therapeutic medicine*, 19(3), pp. 1997-2007.
- Haberberger, R. V. *et al.* (2002) 'Expression of the high-affinity choline transporter, CHT1, in the neuronal and non-neuronal cholinergic system of human and rat skin', *Journal of investigative dermatology*, 119(4), pp. 943-948.
- Haga, K. *et al.* (2012) 'Structure of the human M2 muscarinic acetylcholine receptor bound to an antagonist', *Nature*, 482(7386), pp. 547-551.

## References

- Hanna-Mitchell, A. T. *et al.* (2007) 'Non-neuronal acetylcholine and urinary bladder urothelium', *Life sciences*, 80(24-25), pp. 2298-2302.
- Hanna, H., Mir, L. M. and Andre, F. M. (2018) 'In vitro osteoblastic differentiation of mesenchymal stem cells generates cell layers with distinct properties', *Stem cell research & therapy*, 9(1), pp. 1-11.
- Harper, J. W. *et al.* (1993) 'The p21 Cdk-interacting protein Cip1 is a potent inhibitor of G1 cyclin-dependent kinases', *Cell*, 75(4), pp. 805-816.
- Harper, J. W. *et al.* (1995) 'Inhibition of cyclin-dependent kinases by p21.', *Molecular biology of the cell*, 6(4), pp. 387-400.
- Hatakeyama, W. *et al.* (2013) 'Effects of apatite particle size in two apatite/collagen composites on the osteogenic differentiation profile of osteoblastic cells', *International journal of molecular medicine*, 32(6), pp. 1255-1261.
- Hayes, A. J. *et al.* (2015) 'Keap1-Nrf2 signalling in pancreatic cancer', *The International Journal of Biochemistry & Cell Biology*, 65, pp. 288-299.
- Heller, R. C. *et al.* (2011) 'Eukaryotic origin-dependent DNA replication in vitro reveals sequential action of DDK and S-CDK kinases', *Cell*, 146(1), pp. 80-91.
- Hessle, L. *et al.* (2002) 'Tissue-nonspecific alkaline phosphatase and plasma cell membrane glycoprotein-1 are central antagonistic regulators of bone mineralization', *Proceedings of the National Academy of Sciences*, 99(14), pp. 9445-9449.
- Heubach, J. F. *et al.* (2004) 'Electrophysiological properties of human mesenchymal stem cells', *The Journal of physiology*, 554(3), pp. 659-672.
- Hidalgo San Jose, L. *et al.* (2018) 'Microfluidic Encapsulation Supports Stem Cell Viability, Proliferation, and Neuronal Differentiation.', *Tissue engineering. Part C, Methods*, 24(3), pp. 158-170. doi: 10.1089/ten.TEC.2017.0368.
- Holmes, J. M. *et al.* (2003) 'Impact of patching and atropine treatment on the child and family in the amblyopia treatment study.', *Archives of Ophthalmology (Chicago, Ill.: 1960)*, 121(11), pp. 1625-1632.
- Hong, F. *et al.* (2020) 'TRPM7 upregulate the activity of SMAD1 through PLC signaling way to promote osteogenesis of hBMSCs', *BioMed research international*, 2020.
- Hoogduijn, M. J., Cheng, A. and Genever, P. G. (2009) 'Functional nicotinic and muscarinic receptors on mesenchymal stem cells', *Stem Cells and Development*, 18(1), pp. 103-112. doi: 10.1089/scd.2008.0032.
- Horwitz, E. M. *et al.* (2005) 'Clarification of the nomenclature for MSC: The International Society for Cellular Therapy position statement', *Cytotherapy*, 7(5), pp. 393-395.
- Howard, C., Murray, P. E. and Namerow, K. N. (2010) 'Dental pulp stem cell migration', *Journal of endodontics*, 36(12), pp. 1963-1966.
- Hu, J. *et al.* (2016) 'Periodontal regeneration in swine after cell injection and cell sheet transplantation of human dental pulp stem cells following good manufacturing practice', *Stem cell research & therapy*, 7(1), p. 130.

## References

- Hu, L., Liu, Y. and Wang, S. (2018) 'Stem cell-based tooth and periodontal regeneration', *Oral Diseases*, 24(5), pp. 696-705. doi: 10.1111/odi.12703.
- Huang, A. H. *et al.* (2008) 'Isolation and characterization of dental pulp stem cells from a supernumerary tooth', *Journal of Oral Pathology & Medicine*, 37(9), pp. 571-574.
- Huang, G.-J., Gronthos, S. and Shi, S. (2009) 'Mesenchymal stem cells derived from dental tissues vs. those from other sources: their biology and role in regenerative medicine', *Journal of dental research*, 88(9), pp. 792-806.
- Huang, L. *et al.* (2016) 'Aldo-keto reductase family 1 member B10 inhibitors: potential drugs for cancer treatment', *Recent patents on anti-cancer drug discovery*, 11(2), pp. 184-196.
- Hulme, E. C. *et al.* (2003) 'Structure and activation of muscarinic acetylcholine receptors'. Portland Press Ltd.
- Hulme, E. C., Birdsall, N. J. M. and Buckley, N. J. (1990) 'Muscarinic receptor subtypes', *Annual review of pharmacology and toxicology*, 30(1), pp. 633-673.
- Hur, E.-M. and Kim, K.-T. (2002) 'G protein-coupled receptor signalling and cross-talk: achieving rapidity and specificity', *Cellular signalling*, 14(5), pp. 397-405.
- Ikeda, E. *et al.* (2009) 'Fully functional bioengineered tooth replacement as an organ replacement therapy', *Proceedings of the National Academy of Sciences*, 106(32), pp. 13475-13480. doi: 10.1073/pnas.0902944106.
- Ishii, M. and Kurachi, Y. (2006) 'Muscarinic Acetylcholine Receptors', *Current Pharmaceutical Design*, 12(28), pp. 3573-3581. doi: 10.2174/138161206778522056.
- Ishikawa, Y. *et al.* (2010) 'Mapping of BrdU label-retaining dental pulp cells in growing teeth and their regenerative capacity after injuries', *Histochemistry and cell biology*, 134, pp. 227-241.
- Ishiyama, M. *et al.* (1997) 'A highly water-soluble disulfonated tetrazolium salt as a chromogenic indicator for NADH as well as cell viability', *Talanta*, 44(7), pp. 1299-1305.
- Ishizaka, R. *et al.* (2013) 'Stimulation of angiogenesis, neurogenesis and regeneration by side population cells from dental pulp', *Biomaterials*, 34(8), pp. 1888-1897.
- Ishizuka, T. *et al.* (2018) 'Effects of muscarinic acetylcholine receptor stimulation on the differentiation of mouse induced pluripotent stem cells into neural progenitor cells', *Clinical and Experimental Pharmacology and Physiology*, 45(11), pp. 1198-1205.
- Ishkitiev, N. *et al.* (2010) 'Deciduous and permanent dental pulp mesenchymal cells acquire hepatic morphologic and functional features in vitro', *Journal of endodontics*, 36(3), pp. 469-474.
- Ishkitiev, N. *et al.* (2012) 'High-purity hepatic lineage differentiated from dental pulp stem cells in serum-free medium', *Journal of Endodontics*, 38(4), pp. 475-480.

## References

- Jacoby, E. *et al.* (2006) 'The 7 TM G-protein-coupled receptor target family', *ChemMedChem: Chemistry Enabling Drug Discovery*, 1(8), pp. 760-782.
- Jakubik, J. and El-Fakahany, E. E. (2016) 'Allosteric modulation of muscarinic receptors', in *Muscarinic Receptor: From Structure to Animal Models*. Springer, pp. 95-130.
- Janebodin, K. *et al.* (2013) 'VEGFR2-dependent angiogenic capacity of pericyte-like dental pulp stem cells', *Journal of dental research*, 92(6), pp. 524-531.
- Jensen, K. *et al.* (2013) 'Chronic nicotine exposure stimulates biliary growth and fibrosis in normal rats', *Digestive and Liver Disease*, 45(9), pp. 754-761.
- Ji, Y.-X. *et al.* (2018) 'The deubiquitinating enzyme cylindromatosis mitigates nonalcoholic steatohepatitis', *Nature medicine*, 24(2), pp. 213-223.
- Jin, Y. and Penning, T. M. (2007) 'Aldo-keto reductases and bioactivation/detoxication', *Annu. Rev. Pharmacol. Toxicol.*, 47, pp. 263-292.
- Jo, Y.-Y. *et al.* (2007) 'Isolation and characterization of postnatal stem cells from human dental tissues', *Tissue engineering*, 13(4), pp. 767-773.
- Jöhren, K. and Höltje, H.-D. (2002) 'A model of the human M<sub>2</sub> muscarinic acetylcholine receptor', *Journal of computer-aided molecular design*, 16(11), pp. 795-801.
- Jositsch, G. *et al.* (2009) 'Suitability of muscarinic acetylcholine receptor antibodies for immunohistochemistry evaluated on tissue sections of receptor gene-deficient mice', *Naunyn-Schmiedeberg's archives of pharmacology*, 379(4), pp. 389-395.
- Jung, S. *et al.* (2012) 'Ex vivo expansion of human mesenchymal stem cells in defined serum-free media', *Stem Cells International*. Hindawi. doi: 10.1155/2012/123030.
- Kamal, N. S. M. *et al.* (2020) 'Aging of the cells: Insight into cellular senescence and detection Methods', *European journal of cell biology*, 99(6), p. 151108.
- Karbanová, J. *et al.* (2011) 'Characterization of dental pulp stem cells from impacted third molars cultured in low serum-containing medium', *Cells Tissues Organs*, 193(6), pp. 344-365.
- Kärner, E. *et al.* (2007) 'Bone matrix formation in osteogenic cultures derived from human embryonic stem cells in vitro', *Stem cells and development*, 16(1), pp. 39-52.
- Kastenhuber, E. R. and Lowe, S. W. (2017) 'Putting p53 in context', *Cell*, 170(6), pp. 1062-1078.
- Kasteri, J. *et al.* (2018) 'Translation control by p53', *Cancers*, 10(5), p. 133.
- Kawashima, K. and Fujii, T. (2000) 'Extraneuronal cholinergic system in lymphocytes', *Pharmacology & therapeutics*, 86(1), pp. 29-48.
- Kawashima, K. and Fujii, T. (2008) 'Basic and clinical aspects of non-neuronal acetylcholine: overview of non-neuronal cholinergic systems and their biological significance', *Journal of pharmacological sciences*, 106(2), pp. 167-173.

## References

- Kawashima, N. (2012) 'Characterisation of dental pulp stem cells: a new horizon for tissue regeneration?', *Archives of oral biology*, 57(11), pp. 1439-1458.
- Kebig, A. *et al.* (2009) 'An optical dynamic mass redistribution assay reveals biased signaling of dualsteric GPCR activators', *Journal of Receptors and Signal Transduction*, 29(3-4), pp. 140-145.
- Kenakin, T. (2002) 'Drug efficacy at G protein-coupled receptors', *Annual review of pharmacology and toxicology*, 42(1), pp. 349-379.
- Kenakin, T. (2007) 'Functional selectivity through protean and biased agonism: who steers the ship?', *Molecular pharmacology*, 72(6), pp. 1393-1401.
- Kerkis, I. *et al.* (2006) 'Isolation and characterization of a population of immature dental pulp stem cells expressing OCT-4 and other embryonic stem cell markers', *Cells Tissues Organs*, 184(3-4), pp. 105-116.
- Kerkis, I. and Caplan, A. I. (2011) 'Stem cells in dental pulp of deciduous teeth', *Tissue Engineering Part B: Reviews*, 18(2), pp. 129-138.
- Khorsand, A. *et al.* (2013) 'Autologous dental pulp stem cells in regeneration of defect created in canine periodontal tissue', *Journal of oral implantology*, 39(4), pp. 433-443.
- Kim, D., Langmead, B. and Salzberg, S. L. (2015) 'HISAT: a fast spliced aligner with low memory requirements', *Nature methods*, 12(4), pp. 357-360.
- Kim, S. Y. *et al.* (2012) 'Nicotinic acetylcholine receptor  $\alpha 7$  and  $\beta 4$  subunits contribute nicotine-induced apoptosis in periodontal ligament stem cells', *Molecules and Cells*, 33(4), pp. 343-350. doi: 10.1007/s10059-012-2172-x.
- Kiraly, M. *et al.* (2009) 'Simultaneous PKC and cAMP activation induces differentiation of human dental pulp stem cells into functionally active neurons', *Neurochemistry international*, 55(5), pp. 323-332.
- Király, M. *et al.* (2011) 'Integration of neuronally predifferentiated human dental pulp stem cells into rat brain in vivo', *Neurochemistry international*, 59(3), pp. 371-381.
- Kobayashi, T. *et al.* (2020) 'Characterization of proliferation, differentiation potential, and gene expression among clonal cultures of human dental pulp cells', *Human Cell*, 33, pp. 490-501.
- Kok, Z. Y. *et al.* (2022) 'Dental pulp stem cell heterogeneity: Finding superior quality "needles" in a dental pulpal "haystack" for regenerative medicine-based applications', *Stem Cells International*, 2022.
- Kolf, C. M., Cho, E. and Tuan, R. S. (2007) 'Mesenchymal stromal cells: biology of adult mesenchymal stem cells: regulation of niche, self-renewal and differentiation', *Arthritis research & therapy*, 9(1), pp. 1-10.
- Kolios, G. and Moodley, Y. (2013) 'Introduction to stem cells and regenerative medicine', *Respiration*, 85(1), pp. 3-10.
- Komori, T. (2010a) 'Regulation of bone development and extracellular matrix protein

## References

- genes by RUNX2', *Cell and tissue research*, 339, pp. 189-195.
- Komori, T. (2010b) 'Regulation of osteoblast and odontoblast differentiation by runx2', *Journal of Oral Biosciences*, 52(1), pp. 22-25.
- Kook, S.-H. *et al.* (2014) 'COMP-angiopoietin 1 increases proliferation, differentiation, and migration of stem-like cells through Tie-2-mediated activation of p38 MAPK and PI3K/Akt signal transduction pathways', *Biochemical and Biophysical Research Communications*, 455(3-4), pp. 371-377.
- Van Koppen, C. J. (2001) 'Multiple pathways for the dynamin-regulated internalization of muscarinic acetylcholine receptors', *Biochemical Society Transactions*, 29(4), pp. 505-508.
- van Koppen, C. J. and Kaiser, B. (2003) 'Regulation of muscarinic acetylcholine receptor signaling', *Pharmacology & therapeutics*, 98(2), pp. 197-220.
- Korotchikina, L. G. *et al.* (2010) 'The choice between p53-induced senescence and quiescence is determined in part by the mTOR pathway', *Aging (Albany NY)*, 2(6), p. 344.
- Korzeniewski, C. and Callewaert, D. M. (1983) 'An enzyme-release assay for natural cytotoxicity', *Journal of immunological methods*, 64(3), pp. 313-320.
- Kotova, P. D. *et al.* (2020) 'Calcium signaling mediated by aminergic GPCRs is impaired by the PI3K inhibitor LY294002 and its analog LY303511 in a PI3K-independent manner.', *European journal of pharmacology*, 880, p. 173182. doi: 10.1016/j.ejphar.2020.173182.
- Krampera, M. *et al.* (2005) 'HB-EGF/HER-1 signaling in bone marrow mesenchymal stem cells: inducing cell expansion and reversibly preventing multilineage differentiation', *Blood*, 106(1), pp. 59-66.
- Krishna, T. S. R. *et al.* (1994) 'Crystal structure of the eukaryotic DNA polymerase processivity factor PCNA', *Cell*, 79(7), pp. 1233-1243.
- Kruse, A. C. *et al.* (2012) 'Structure and dynamics of the M3 muscarinic acetylcholine receptor', *Nature*, 482(7386), p. 552.
- Kruse, A. C. *et al.* (2013) 'Muscarinic receptors as model targets and antitargets for structure-based ligand discovery', *Molecular pharmacology*, 84(4), pp. 528-540.
- Kruse, A. C. *et al.* (2014) 'Muscarinic acetylcholine receptors: novel opportunities for drug development', *Nature reviews Drug discovery*, 13(7), pp. 549-560.
- Kumar, P., Nagarajan, A. and Uchil, P. D. (2018) 'Analysis of cell viability by the lactate dehydrogenase assay', *Cold Spring Harbor Protocols*, 2018(6), p. pdb-prot095497.
- Kumari, R. and Jat, P. (2021) 'Mechanisms of cellular senescence: cell cycle arrest and senescence associated secretory phenotype', *Frontiers in cell and developmental biology*, 9, p. 645593.
- Kummer, W. *et al.* (2006) 'Role of acetylcholine and muscarinic receptors in serotonin-induced bronchoconstriction in the mouse', *Journal of Molecular Neuroscience*, 30(1-2), p. 67.

## References

- Kushnerev, E. *et al.* (2016) 'Regeneration of corneal epithelium with dental pulp stem cells using a contact lens delivery system', *Investigative ophthalmology & visual science*, 57(13), pp. 5192-5199.
- LaBaer, J. *et al.* (1997) 'New functional activities for the p21 family of CDK inhibitors.', *Genes & development*, 11(7), pp. 847-862.
- Laino, G. *et al.* (2005) 'Dental pulp stem cells can be detected in aged humans: an useful source for living autologous fibrous bone tissue (LAB)', *Journal of Bone and Mineral Research*, 20(8), pp. 1394-1402.
- Lan, X. *et al.* (2019) 'Dental pulp stem cells: an attractive alternative for cell therapy in ischemic stroke', *Frontiers in neurology*, 10, p. 824.
- Langenbach, F. and Handschel, J. (2013) 'Effects of dexamethasone, ascorbic acid and  $\beta$ -glycerophosphate on the osteogenic differentiation of stem cells in vitro', *Stem Cell Research & Therapy*, 4(5), p. 117. doi: 10.1186/scrt328.
- Lappano, R. and Maggiolini, M. (2011) 'G protein-coupled receptors: novel targets for drug discovery in cancer', *Nature reviews Drug discovery*, 10(1), pp. 47-60.
- Laptenko, O. *et al.* (2011) 'p53 binding to nucleosomes within the p21 promoter in vivo leads to nucleosome loss and transcriptional activation', *Proceedings of the National Academy of Sciences*, 108(26), pp. 10385-10390.
- Lasne, F. (2001) 'Double-blotting: a solution to the problem of non-specific binding of secondary antibodies in immunoblotting procedures', *Journal of immunological methods*, 253(1-2), pp. 125-131.
- Lau, M.-T., So, W.-K. and Leung, P. C. K. (2013) 'Fibroblast growth factor 2 induces E-cadherin down-regulation via PI3K/Akt/mTOR and MAPK/ERK signaling in ovarian cancer cells', *PloS one*, 8(3), p. e59083.
- Leach, K. *et al.* (2012) 'Structure-function studies of muscarinic acetylcholine receptors', in *Muscarinic Receptors*. Springer, pp. 29-48.
- Ledesma-Martínez, E., Mendoza-Núñez, V. M. and Santiago-Osorio, E. (2016) 'Mesenchymal stem cells derived from dental pulp: a review', *Stem cells international*, 2016.
- Lee, J.-H. *et al.* (2011) 'Odontogenic differentiation of human dental pulp stem cells induced by preameloblast-derived factors', *Biomaterials*, 32(36), pp. 9696-9706.
- Lei, M. *et al.* (2014) 'Mesenchymal stem cell characteristics of dental pulp and periodontal ligament stem cells after in vivo transplantation', *Biomaterials*, 35(24), pp. 6332-6343.
- Leong, W. K. *et al.* (2012) 'Human adult dental pulp stem cells enhance poststroke functional recovery through non-neural replacement mechanisms', *Stem cells translational medicine*, 1(3), pp. 177-187.
- Li, Houwei *et al.* (2006) 'Jagged1 protein enhances the differentiation of mesenchymal stem cells into cardiomyocytes', *Biochemical and biophysical research communications*, 341(2), pp. 320-325.

## References

- Li, L. *et al.* (2021) 'TRIM47 accelerates aerobic glycolysis and tumor progression through regulating ubiquitination of FBP1 in pancreatic cancer', *Pharmacological Research*, 166, p. 105429.
- Li, X., Kumar, A. and Carmeliet, P. (2019) 'Metabolic pathways fueling the endothelial cell drive', *Annual Review of Physiology*, 81, pp. 483-503.
- Li, Z. *et al.* (2014) 'Immunomodulatory properties of dental tissue-derived mesenchymal stem cells', *Oral Diseases*, 20(1), pp. 25-34. doi: 10.1111/odi.12086.
- Lian, J. B. and Stein, G. S. (2003) 'Runx2/Cbfa1: a multifunctional regulator of bone formation', *Current pharmaceutical design*, 9(32), pp. 2677-2685.
- Liang, C.-C., Park, A. Y. and Guan, J.-L. (2007) 'In vitro scratch assay: a convenient and inexpensive method for analysis of cell migration in vitro.', *Nature protocols*, 2(2), pp. 329-33. doi: 10.1038/nprot.2007.30.
- Liang, Q. *et al.* (2019) 'TRIM47 is up-regulated in colorectal cancer, promoting ubiquitination and degradation of SMAD4', *Journal of Experimental & Clinical Cancer Research*, 38(1), pp. 1-14.
- Liao, Y., Smyth, G. K. and Shi, W. (2014) 'featureCounts: an efficient general purpose program for assigning sequence reads to genomic features', *Bioinformatics*, 30(7), pp. 923-930.
- Lin, J. *et al.* (2020) 'GSK-3B in DNA repair, apoptosis, and resistance of chemotherapy, radiotherapy of cancer', *Biochimica et Biophysica Acta (BBA)-Molecular Cell Research*, 1867(5), p. 118659.
- Lin, R. *et al.* (2015) '6-Phosphogluconate dehydrogenase links oxidative PPP, lipogenesis and tumour growth by inhibiting LKB1-AMPK signalling', *Nature cell biology*, 17(11), pp. 1484-1496.
- Linardou, H. *et al.* (2012) 'The prognostic and predictive value of mRNA expression of vascular endothelial growth factor family members in breast cancer: a study in primary tumors of high-risk early breast cancer patients participating in a randomized Hellenic Cooperative Oncology G', *Breast Cancer Research*, 14(6), pp. 1-16.
- Lindemann, D. *et al.* (2014) 'Effects of cryopreservation on the characteristics of dental pulp stem cells of intact deciduous teeth', *Archives of oral biology*, 59(9), pp. 970-976.
- Lindroos, B. *et al.* (2008) 'Characterisation of human dental stem cells and buccal mucosa fibroblasts', *Biochemical and biophysical research communications*, 368(2), pp. 329-335.
- Linnekin, D. (1999) 'Early signaling pathways activated by c-Kit in hematopoietic cells', *The international journal of biochemistry & cell biology*, 31(10), pp. 1053-1074.
- Lips, K. S. *et al.* (2005) 'Polyspecific cation transporters mediate luminal release of acetylcholine from bronchial epithelium', *American journal of respiratory cell and molecular biology*, 33(1), pp. 79-88.
- Lips, K. S., Wunsch, J., *et al.* (2007) 'Acetylcholine and molecular components of its

## References

- synthesis and release machinery in the urothelium', *European urology*, 51(4), pp. 1042-1053.
- Lips, K. S., Lührmann, A., *et al.* (2007) 'Down-regulation of the non-neuronal acetylcholine synthesis and release machinery in acute allergic airway inflammation of rat and mouse', *Life sciences*, 80(24-25), pp. 2263-2269.
- Liu, F. *et al.* (2008) 'Changes in the expression of CD106, osteogenic genes, and transcription factors involved in the osteogenic differentiation of human bone marrow mesenchymal stem cells', *Journal of bone and mineral metabolism*, 26, pp. 312-320.
- Liu, J. *et al.* (2015) 'Concise reviews: characteristics and potential applications of human dental tissue-derived mesenchymal stem cells', *Stem cells*, 33(3), pp. 627-638.
- Liu, L. *et al.* (2009) 'Stem cell regulatory gene expression in human adult dental pulp and periodontal ligament cells undergoing odontogenic/osteogenic differentiation', *Journal of Endodontics*, 35(10), pp. 1368-1376.
- Liu, Na *et al.* (2011) 'High levels of  $\beta$ -catenin signaling reduce osteogenic differentiation of stem cells in inflammatory microenvironments through inhibition of the noncanonical Wnt pathway', *Journal of Bone and Mineral Research*, 26(9), pp. 2082-2095.
- Liu, Y. *et al.* (2022) 'Human umbilical cord-derived mesenchymal stem cells not only ameliorate blood glucose but also protect vascular endothelium from diabetic damage through a paracrine mechanism mediated by MAPK/ERK signaling', *Stem Cell Research & Therapy*, 13(1), p. 258.
- Liu, Z., Zhuge, Y. and Velazquez, O. C. (2009) 'Trafficking and differentiation of mesenchymal stem cells', *Journal of cellular biochemistry*, 106(6), pp. 984-991.
- Livak, K. J. and Schmittgen, T. D. (2001) 'Analysis of relative gene expression data using real-time quantitative PCR and the  $2^{-\Delta\Delta CT}$  method', *methods*, 25(4), pp. 402-408.
- Loewi, O. (1921) 'Über humorale übertragbarkeit der Herznervenwirkung', *Pflüger's Archiv für die gesamte Physiologie des Menschen und der Tiere*, 189(1), pp. 239-242.
- Loreti, S. *et al.* (2006) 'Rat Schwann cells express M1-M4 muscarinic receptor subtypes', *Journal of Neuroscience Research*, 84(1), pp. 97-105. doi: 10.1002/jnr.20874.
- Loreti, S. *et al.* (2007) 'Acetylcholine inhibits cell cycle progression in rat Schwann cells by activation of the M2 receptor subtype', *Neuron Glia Biology*, 3(4), pp. 269-279. doi: 10.1017/S1740925X08000045.
- Louvrier, A. *et al.* (2018) 'Odontoblastic differentiation of dental pulp stem cells from healthy and carious teeth on an original PCL-based 3D scaffold', *International endodontic journal*, 51, pp. e252-e263.
- Love, M. I., Huber, W. and Anders, S. (2014) 'Moderated estimation of fold change and dispersion for RNA-seq data with DESeq2', *Genome biology*, 15(12), pp. 1-21.
- Luo, J. (2009) 'Glycogen synthase kinase 3 $\beta$  (GSK3 $\beta$ ) in tumorigenesis and cancer

## References

- chemotherapy', *Cancer letters*, 273(2), pp. 194-200.
- Luo, L. *et al.* (2020) 'Group II muscarinic acetylcholine receptors attenuate hepatic injury via Nrf2/ARE pathway', *Toxicology and Applied Pharmacology*, 395, p. 114978.
- Lykhmus, O. *et al.* (2019) 'Mesenchymal Stem Cells or Interleukin-6 Improve Episodic Memory of Mice Lacking alpha 7 Nicotinic Acetylcholine Receptors', *NEUROSCIENCE*, 413, pp. 31-44. doi: 10.1016/j.neuroscience.2019.06.004.
- Ma, D. *et al.* (2018) 'Stathmin inhibits proliferation and differentiation of dental pulp stem cells via sonic hedgehog/Gli', *Journal of cellular and molecular medicine*, 22(7), pp. 3442-3451.
- Ma, W. *et al.* (2000) 'Acetylcholine stimulates cortical precursor cell proliferation in vitro via muscarinic receptor activation and MAP kinase phosphorylation', *European Journal of Neuroscience*, 12(4), pp. 1227-1240. doi: 10.1046/j.1460-9568.2000.00010.x.
- Maeda, S. *et al.* (2019) 'Structures of the M1 and M2 muscarinic acetylcholine receptor/G-protein complexes', *Science*, 364(6440), pp. 552-557. doi: 10.1126/science.aaw5188.
- Mafi, P. *et al.* (2011) 'Suppl 2: Adult Mesenchymal Stem Cells and Cell Surface Characterization-A Systematic Review of the Literature', *The open orthopaedics journal*, 5, p. 253.
- Manoukian, A. S. and Woodgett, J. R. (2002) 'Role of glycogen synthase kinase-3 in cancer: regulation by Wnts and other signaling pathways'.
- Mansilla, S. F. *et al.* (2020) 'CDK-independent and PCNA-dependent functions of p21 in DNA replication', *Genes*, 11(6), p. 593.
- Maracci, C. *et al.* (2022) 'The mTOR/4E-BP1/eIF4E signalling pathway as a source of cancer drug targets', *Current Medicinal Chemistry*, 29(20), pp. 3501-3529.
- Marescal, O. and Cheeseman, I. M. (2020) 'Cellular mechanisms and regulation of quiescence', *Developmental cell*, 55(3), pp. 259-271.
- Marrs, T. T., Maynard, R. L. and Sidell, F. (2007) 'Chemical warfare agents: toxicology and treatment'.
- Martens, W. *et al.* (2012) 'Expression pattern of basal markers in human dental pulp stem cells and tissue', *Cells Tissues Organs*, 196(6), pp. 490-500.
- Martens, W. *et al.* (2013) 'Dental stem cells and their promising role in neural regeneration: an update', *Clinical Oral Investigations*, 17(9), pp. 1969-1983.
- Martínez-Alonso, D. and Malumbres, M. (2020) 'Mammalian cell cycle cyclins', in *Seminars in Cell & Developmental Biology*. Elsevier, pp. 28-35.
- Massoulié, J. *et al.* (1993) 'Molecular and cellular biology of cholinesterases', *Progress in neurobiology*, 41(1), pp. 31-91.
- Matuskova, M. *et al.* (2018) 'Genetically engineered mesenchymal stromal cells in cancer

## References

- gene therapy', *Bratisl Lek Listy*, 119(4), pp. 221-223.
- McGee-Russell, S. M. (1958) 'Histochemical methods for calcium', *Journal of Histochemistry & Cytochemistry*, 6(1), pp. 22-42.
- McKee, M. D. and Nanci, A. (1996) 'Osteopontin at mineralized tissue interfaces in bone, teeth, and osseointegrated implants: ultrastructural distribution and implications for mineralized tissue formation, turnover, and repair', *Microscopy research and technique*, 33(2), pp. 141-164.
- Mead, T. J. and Lefebvre, V. (2014) 'Proliferation assays (BrdU and EdU) on skeletal tissue sections', *Skeletal Development and Repair: Methods and Protocols*, pp. 233-243.
- de Mendonça Costa, A. *et al.* (2008) 'Reconstruction of large cranial defects in nonimmunosuppressed experimental design with human dental pulp stem cells', *Journal of Craniofacial Surgery*, 19(1), pp. 204-210.
- Mendoza, M. C., Er, E. E. and Blenis, J. (2011) 'The Ras-ERK and PI3K-mTOR pathways: cross-talk and compensation', *Trends in biochemical sciences*, 36(6), pp. 320-328.
- Merla, G. *et al.* (2010) 'Copy number variants at Williams-Beuren syndrome 7q11. 23 region', *Human genetics*, 128, pp. 3-26.
- Michailovici, I. *et al.* (2014) 'Nuclear to cytoplasmic shuttling of ERK promotes differentiation of muscle stem/progenitor cells', *Development*, 141(13), pp. 2611-2620.
- Michel, A. D. and Whiting, R. L. (1987) 'Direct binding studies on ileal and cardiac muscarinic receptors', *British journal of pharmacology*, 92(4), pp. 755-767.
- Miletich, I. and Sharpe, P. T. (2004) 'Neural crest contribution to mammalian tooth formation', *Birth Defects Research Part C: Embryo Today: Reviews*, 72(2), pp. 200-212.
- Min, T.-J. *et al.* (2021) '3D spheroid formation using BMP-loaded microparticles enhances odontoblastic differentiation of human dental pulp stem cells', *Stem Cells International*, 2021.
- Miyazawa, A., Fujiyoshi, Y. and Unwin, N. (2003) 'Structure and gating mechanism of the acetylcholine receptor pore', *Nature*, 423(6943), p. 949.
- Mocciaro, A. *et al.* (2010) 'Vertebrate cells genetically deficient for Cdc14A or Cdc14B retain DNA damage checkpoint proficiency but are impaired in DNA repair', *Journal of cell biology*, 189(4), pp. 631-639.
- Mohr, K., Tränkle, C. and Holzgrabe, U. (2003) 'Structure/activity relationships of M 2 muscarinic allosteric modulators', *Receptors and Channels*, 9(4), pp. 229-240.
- Mohyeldin, A., Garzón-Muvdi, T. and Quiñones-Hinojosa, A. (2010) 'Oxygen in stem cell biology: a critical component of the stem cell niche', *Cell stem cell*, 7(2), pp. 150-161.
- Moldovan, G.-L., Pfander, B. and Jentsch, S. (2006) 'PCNA controls establishment of sister chromatid cohesion during S phase', *Molecular cell*, 23(5), pp. 723-732.

## References

- Moldovan, G.-L., Pfander, B. and Jentsch, S. (2007) 'PCNA, the maestro of the replication fork', *Cell*, 129(4), pp. 665-679.
- Molinari, M. *et al.* (2000) 'Human Cdc25 A inactivation in response to S phase inhibition and its role in preventing premature mitosis', *EMBO reports*, 1(1), pp. 71-79.
- Mona, M. *et al.* (2019) 'MIST1, an inductive signal for salivary amylase in mesenchymal stem cells', *International Journal of Molecular Sciences*, 20(3). doi: 10.3390/ijms20030767.
- Mousawi, F. *et al.* (2020) 'Chemical activation of the Piezo1 channel drives mesenchymal stem cell migration via inducing ATP release and activation of P2 receptor purinergic signaling', *Stem Cells*, 38(3), pp. 410-421.
- Mu, W.-C. *et al.* (2020) 'The mitochondrial metabolic checkpoint in stem cell aging and rejuvenation', *Mechanisms of ageing and development*, 188, p. 111254.
- Mura, C. V *et al.* (2006) 'Quiescence induced by iron challenge protects neuroblastoma cells from oxidative stress', *Journal of neurochemistry*, 98(1), pp. 11-19.
- Muramatsu, I. *et al.* (2016) 'Binding Method for Detection of Muscarinic Acetylcholine Receptors in Receptor's Natural Environment', in *Muscarinic Receptor: From Structure to Animal Models*. Springer, pp. 69-81.
- Muri, J. *et al.* (2018) 'The thioredoxin-1 system is essential for fueling DNA synthesis during T-cell metabolic reprogramming and proliferation', *Nature communications*, 9(1), p. 1851.
- Muzio, G. *et al.* (2012) 'Aldehyde dehydrogenases and cell proliferation', *Free Radical Biology and Medicine*, 52(4), pp. 735-746.
- Nakashima, M. *et al.* (2017) 'Pulp regeneration by transplantation of dental pulp stem cells in pulpitis: a pilot clinical study', *Stem cell research & therapy*, 8, pp. 1-13.
- Nakashima, M., Iohara, K. and Sugiyama, M. (2009) 'Human dental pulp stem cells with highly angiogenic and neurogenic potential for possible use in pulp regeneration', *Cytokine & growth factor reviews*, 20(5-6), pp. 435-440.
- NCBI Bethesda (MD) (1988) *National Center for Biotechnology Information, National Library of Medicine (US), National Center for Biotechnology Information, Genome*. Available at: <https://www.ncbi.nlm.nih.gov/genome/> (Accessed: 1 July 2023).
- Nel, S. *et al.* (2022) 'Determinants of dental pulp stem cell heterogeneity', *Journal of Endodontics*, 48(10), pp. 1232-1240.
- Neri, D., Petrucci, H. and Roncucci, G. (1995) 'Engineering recombinant antibodies for immunotherapy', *Cell biophysics*, 27(1), pp. 47-61.
- Nery, A. A. *et al.* (2019) 'Combination of Chemical and Neurotrophin Stimulation Modulates Neurotransmitter Receptor Expression and Activity in Transdifferentiating Human Adipose Stromal Cells.', *Stem cell reviews and reports*, 15(6), pp. 851-863. doi: 10.1007/s12015-019-09915-1.
- Neve, A., Corrado, A. and Cantatore, F. P. (2013) 'Osteocalcin: skeletal and extra-

## References

- skeletal effects', *Journal of cellular physiology*, 228(6), pp. 1149-1153.
- Nguyen, S. T., Nguyen, H. T.-L. and Truong, K. D. (2020) 'Comparative cytotoxic effects of methanol, ethanol and DMSO on human cancer cell lines', *Biomedical Research and Therapy*, 7(7), pp. 3855-3859.
- Ni, P. *et al.* (2011) 'Preparation of poly (ethylene glycol)/polylactide hybrid fibrous scaffolds for bone tissue engineering', *International Journal of Nanomedicine*, 6, p. 3065.
- Nicola, F. do C. *et al.* (2016) 'Human dental pulp stem cells transplantation combined with treadmill training in rats after traumatic spinal cord injury', *Brazilian Journal of Medical and Biological Research*, 49(9).
- Nishimura, H. *et al.* (2016) 'GSK-3 inhibitor inhibits cell proliferation and induces apoptosis in human osteosarcoma cells', *Oncology Reports*, 35(4), pp. 2348-2354.
- Niu, L. *et al.* (2016) 'Mineralogenic characteristics of osteogenic lineage-committed human dental pulp stem cells following their exposure to a discoloration-free calcium aluminosilicate cement', *Dental Materials*, 32(10), pp. 1235-1247.
- Noda, S. *et al.* (2019) 'Effect of cell culture density on dental pulp-derived mesenchymal stem cells with reference to osteogenic differentiation', *Scientific Reports*, 9(1), p. 5430.
- Nombela-Arrieta, C., Ritz, J. and Silberstein, L. E. (2011) 'The elusive nature and function of mesenchymal stem cells', *Nature Reviews Molecular Cell Biology*, 12(2), pp. 126-131. doi: 10.1038/nrm3049.
- Oddo, S. and LaFerla, F. M. (2006) 'The role of nicotinic acetylcholine receptors in Alzheimer's disease', in *Journal of Physiology Paris*, pp. 172-179. doi: 10.1016/j.jphysparis.2005.12.080.
- Ogata, Y. (2008) 'Bone sialoprotein and its transcriptional regulatory mechanism', *Journal of periodontal research*, 43(2), pp. 127-135.
- Okajcekova, T. *et al.* (2020) 'A comparative in vitro analysis of the osteogenic potential of human dental pulp stem cells using various differentiation conditions', *International journal of molecular sciences*, 21(7), p. 2280.
- Onishi, T. *et al.* (1998) 'Distinct and overlapping patterns of localization of bone morphogenetic protein (BMP) family members and a BMP type II receptor during fracture healing in rats', *Bone*, 22(6), pp. 605-612.
- Orapiriyakul, W. *et al.* (2020) 'Nanovibrational stimulation of mesenchymal stem cells induces therapeutic reactive oxygen species and inflammation for three-dimensional bone tissue engineering', *ACS nano*, 14(8), pp. 10027-10044.
- Orbay, H., Tobita, M. and Mizuno, H. (2012) 'Mesenchymal Stem Cells Isolated from Adipose and Other Tissues: Basic Biological Properties and Clinical Applications', *Stem Cells International*, 2012, pp. 1-9. doi: 10.1155/2012/461718.
- Ornitz, D. M. and Itoh, N. (2015) 'The fibroblast growth factor signaling pathway', *Wiley Interdisciplinary Reviews: Developmental Biology*, 4(3), pp. 215-266.

## References

- Owen, T. A. *et al.* (1990) 'Progressive development of the rat osteoblast phenotype in vitro: reciprocal relationships in expression of genes associated with osteoblast proliferation and differentiation during formation of the bone extracellular matrix', *Journal of cellular physiology*, 143(3), pp. 420-430.
- P De Miguel, M., Fuentes-Julián, S. and Alcaina, Y. (2010) 'Pluripotent stem cells: origin, maintenance and induction', *Stem cell reviews and reports*, 6(4), pp. 633-649.
- Pacini, L. *et al.* (2014) 'M2muscarinic receptors inhibit cell proliferation and migration in urothelial bladder cancer cells', *Cancer biology & therapy*, 15(11), pp. 1489-1498. doi: 10.4161/15384047.2014.955740.
- Pagella, P. *et al.* (2021) 'A single-cell atlas of human teeth', *Isience*, 24(5).
- Pahl, A. *et al.* (2006) 'Synergistic effects of the anti-cholinergic R, R-glycopyrrolate with anti-inflammatory drugs', *Biochemical pharmacology*, 72(12), pp. 1690-1696.
- Pakala, R. S., Brown, K. N. and Preuss, C. V (2019) 'Cholinergic medications'.
- Palczewski, K. *et al.* (2000) 'Crystal structure of rhodopsin: AG protein-coupled receptor', *science*, 289(5480), pp. 739-745.
- Papaccio, G. *et al.* (2006) 'Long-term cryopreservation of dental pulp stem cells (SBP-DPSCs) and their differentiated osteoblasts: a cell source for tissue repair', *Journal of cellular physiology*, 208(2), pp. 319-325.
- Paraoanu, L. E. *et al.* (2007) 'Expression and possible functions of the cholinergic system in a murine embryonic stem cell line', *Life sciences*, 80(24-25), pp. 2375-2379.
- Park, J. Y. *et al.* (2015) '3D printing technology to control BMP-2 and VEGF delivery spatially and temporally to promote large-volume bone regeneration', *Journal of Materials Chemistry B*, 3(27), pp. 5415-5425.
- Parkinson Study Group (2006) 'Randomized placebo-controlled study of the nicotinic agonist SIB-1508Y in Parkinson disease', *Neurology*, 66(3), pp. 408-410.
- Patel, M. *et al.* (2009) 'Phenotype and behaviour of dental pulp cells during expansion culture', *Archives of Oral Biology*, 54(10), pp. 898-908.
- Pathania, S., Pentikäinen, O. T. and Singh, P. K. (2021) 'A holistic view on c-Kit in cancer: Structure, signaling, pathophysiology and its inhibitors', *Biochimica et Biophysica Acta (BBA)-Reviews on Cancer*, 1876(2), p. 188631.
- Patravale, V. *et al.* (2012) 'Nanotoxicology: evaluating toxicity potential of drug-nanoparticles', *Nanoparticulate Drug Delivery*, pp. 123-155. doi: 10.1533/9781908818195.123.
- Pavletich, N. P. (1999) 'Mechanisms of cyclin-dependent kinase regulation: structures of Cdk, their cyclin activators, and Cip and INK4 inhibitors', *Journal of molecular biology*, 287(5), pp. 821-828.
- Penning, T. M. (2015) 'The aldo-keto reductases (AKRs): Overview', *Chemico-biological interactions*, 234, pp. 236-246.
- Perl, A. (2007) 'The pathogenesis of transaldolase deficiency', *IUBMB life*, 59(6), pp.

## References

365-373.

- Pernarella, M. *et al.* (2020) 'Effects mediated by the alpha 7 nicotinic acetylcholine receptor on cell proliferation and migration in rat adipose-derived stem cells', *EUROPEAN JOURNAL OF HISTOCHEMISTRY*, 64. doi: 10.4081/ejh.2020.3159.
- Perry, B. C. *et al.* (2008) 'Collection, cryopreservation, and characterization of human dental pulp-derived mesenchymal stem cells for banking and clinical use', *Tissue Engineering Part C: Methods*, 14(2), pp. 149-156.
- Pertea, M. *et al.* (2015) 'StringTie enables improved reconstruction of a transcriptome from RNA-seq reads', *Nature biotechnology*, 33(3), pp. 290-295.
- Peters, K. G. *et al.* (2004) 'Functional significance of Tie2 signaling in the adult vasculature', *Recent progress in hormone research*, 59(1), pp. 51-71.
- Petrie, R. J., Doyle, A. D. and Yamada, K. M. (2009) 'Random versus directionally persistent cell migration', *Nature reviews Molecular cell biology*, 10(8), pp. 538-549.
- Pierdomenico, L. *et al.* (2005) 'Multipotent mesenchymal stem cells with immunosuppressive activity can be easily isolated from dental pulp', *Transplantation*, 80(6), pp. 836-842.
- Piovesana, R. *et al.* (2018) 'M2 muscarinic receptor activation inhibits cell proliferation and migration of rat adipose-mesenchymal stem cells', *Journal of Cellular Physiology*, 233(7), pp. 5348-5360. doi: 10.1002/jcp.26350.
- Piovesana, R. *et al.* (2019) 'M2 receptors activation modulates cell growth, migration and differentiation of rat Schwann-like adipose-derived stem cells', *Cell Death Discovery*, 5(1), p. 92.
- Piovesana, R. *et al.* (2022) 'Notch signal mediates the cross-interaction between M2 muscarinic acetylcholine receptor and neuregulin/ErbB pathway: Effects on Schwann cell proliferation', *Biomolecules*, 12(2), p. 239.
- Pisciotta, A., Carnevale, G., *et al.* (2015) 'Human dental pulp stem cells (hDPSCs): isolation, enrichment and comparative differentiation of two sub-populations', *BMC developmental biology*, 15, pp. 1-16.
- Pisciotta, A., Riccio, M., *et al.* (2015) 'Stem cells isolated from human dental pulp and amniotic fluid improve skeletal muscle histopathology in mdx/SCID mice', *Stem cell research & therapy*, 6(1), p. 156.
- Pittenger, M. F. *et al.* (1999) 'Multilineage potential of adult human mesenchymal stem cells', *science*, 284(5411), pp. 143-147.
- Pivoriūnas, A. *et al.* (2009) 'Proteomic analysis of stromal cells derived from the dental pulp of human exfoliated deciduous teeth', *Stem cells and development*, 19(7), pp. 1081-1093.
- Pradidarcheep, W. and Michel, M. C. (2016) 'Use of antibodies in the research on muscarinic receptor subtypes', in *Muscarinic Receptor: From Structure to Animal Models*. Springer, pp. 83-94.

## References

- Prilla, S. *et al.* (2006) 'Allosteric interactions with muscarinic acetylcholine receptors: complex role of the conserved tryptophan M2422Trp in a critical cluster of amino acids for baseline affinity, subtype selectivity, and cooperativity', *Molecular pharmacology*, 70(1), pp. 181-193.
- Profita, M. *et al.* (2005) 'Muscarinic receptors, leukotriene B4 production and neutrophilic inflammation in COPD patients', *Allergy*, 60(11), pp. 1361-1369.
- Qu, C. *et al.* (2020) 'Evaluation of growth, stemness, and angiogenic properties of dental pulp stem cells cultured in cGMP xeno-/serum-free medium', *Cell and tissue research*, 380, pp. 93-105.
- Ragheb, F. *et al.* (2001) 'Pharmacological and functional characterization of muscarinic receptor subtypes in developing oligodendrocytes.', *Journal of neurochemistry*, 77(5), pp. 1396-406. doi: 10.1046/j.1471-4159.2001.00356.x.
- Ratajczak, M. Z. *et al.* (2012) 'Pluripotent and multipotent stem cells in adult tissues', *Advances in medical sciences*, 57(1), pp. 1-17.
- Reiner, C. and Nathanson, N. M. (2012) 'Muscarinic receptor trafficking', *Muscarinic receptors*, pp. 61-78.
- Reinhardt, J., Stühler, A. and Blümel, J. (2011) 'Safety of bovine sera for production of mesenchymal stem cells for therapeutic use', *Human gene therapy*, 22(6), p. 775.
- Reinheimer, T. *et al.* (1998) 'Non-neuronal acetylcholine is increased in chronic inflammation like atopic dermatitis', in *NAUNYN-SCHMIEDEBERGS ARCHIVES OF PHARMACOLOGY*. SPRINGER VERLAG 175 FIFTH AVE, NEW YORK, NY 10010 USA, pp. R87-R87.
- Resende, R. R. and Adhikari, A. (2009) 'Cholinergic receptor pathways involved in apoptosis, cell proliferation and neuronal differentiation', *Cell Communication and Signaling*, 7(1), p. 20.
- Rodas-Junco, B. A. and Villicaña, C. (2017) 'Dental Pulp Stem Cells: Current Advances in Isolation, Expansion and Preservation', *Tissue Engineering and Regenerative Medicine*, 14(4), pp. 333-347. doi: 10.1007/s13770-017-0036-3.
- Rogers, I. and Casper, R. F. (2004) 'Umbilical cord blood stem cells', *Best practice & research Clinical obstetrics & gynaecology*, 18(6), pp. 893-908.
- Rogers, S. W. and Gahring, L. C. (2012) 'Nicotinic receptor Alpha7 expression during tooth morphogenesis reveals functional pleiotropy', *PLoS One*. Edited by J. Najbauer, 7(5), p. e36467. doi: 10.1371/journal.pone.0036467.
- Roseberry, A. G. and Hosey, M. M. (2001) 'Internalization of the M2 muscarinic acetylcholine receptor proceeds through an atypical pathway in HEK293 cells that is independent of clathrin and caveolae', *Journal of cell science*, 114(4), pp. 739-746.
- Rosemond, E. *et al.* (2011) 'Regulation of M3 muscarinic receptor expression and function by transmembrane protein 147', *Molecular pharmacology*, 79(2), pp. 251-261.
- Ross, D. and Siegel, D. (2018) 'NQO1 in protection against oxidative stress', *Current Opinion in Toxicology*, 7, pp. 67-72.

## References

- Ross, D. and Siegel, D. (2021) 'The diverse functionality of NQO1 and its roles in redox control', *Redox Biology*, 41, p. 101950.
- Rubanyi, G. M. (1991) 'Endothelium-derived relaxing and contracting factors', *Journal of cellular biochemistry*, 46(1), pp. 27-36.
- Ruzzo, E. K. *et al.* (2013) 'Deficiency of asparagine synthetase causes congenital microcephaly and a progressive form of encephalopathy', *Neuron*, 80(2), pp. 429-441.
- Sakai, K. *et al.* (2012) 'Human dental pulp-derived stem cells promote locomotor recovery after complete transection of the rat spinal cord by multiple neuro-regenerative mechanisms', *The Journal of clinical investigation*, 122(1), pp. 80-90.
- Sasaki, R. *et al.* (2011) 'PLGA artificial nerve conduits with dental pulp cells promote facial nerve regeneration', *Journal of tissue engineering and regenerative medicine*, 5(10), pp. 823-830.
- Sastry, B. V and Sadavongvivad, C. (1978) 'Cholinergic systems in non-nervous tissues.', *Pharmacological reviews*, 30(1), pp. 65-132.
- Satyanarayana, A. and Kaldis, P. (2009) 'Mammalian cell-cycle regulation: several Cdks, numerous cyclins and diverse compensatory mechanisms', *Oncogene*, 28(33), pp. 2925-2939.
- Scheinman, M. M., Thorburn, D. and Abbott, J. A. (1975) 'Use of atropine in patients with acute myocardial infarction and sinus bradycardia.', *Circulation*, 52(4), pp. 627-633.
- Schlador, M. L., Grubbs, R. D. and Nathanson, N. M. (2000) 'Multiple topological domains mediate subtype-specific internalization of the M2 muscarinic acetylcholine receptor', *Journal of Biological Chemistry*, 275(30), pp. 23295-23302.
- Schlereth, T. *et al.* (2006) 'In vivo release of non-neuronal acetylcholine from the human skin as measured by dermal microdialysis: effect of botulinum toxin', *British journal of pharmacology*, 147(2), pp. 183-187.
- Schneider, C. A., Rasband, W. S. and Eliceiri, K. W. (2012) 'NIH Image to ImageJ: 25 years of image analysis', *Nature methods*, 9(7), pp. 671-675.
- Schraufstatter, I. U., DiScipio, R. G. and Khaldoyanidi, S. K. (2010) 'Alpha 7 Subunit of nAChR Regulates Migration of Human Mesenchymal Stem Cells', *Journal of stem cells*, 4(4), p. 203. Available at: /pmc/articles/PMC2925301/ (Accessed: 22 July 2021).
- Schütz, P. *et al.* (2010) 'Comparative structural analysis of human DEAD-box RNA helicases', *PloS one*, 5(9), p. e12791.
- Sellheyer, K. and Krahl, D. (2010) 'Skin mesenchymal stem cells: prospects for clinical dermatology', *Journal of the American Academy of Dermatology*, 63(5), pp. 859-865.
- Seong, J. M. *et al.* (2010) 'Stem cells in bone tissue engineering', *Biomedical materials*, 5(6), p. 62001.

## References

- Serobyán, N. *et al.* (2007) 'The cholinergic system is involved in regulation of the development of the hematopoietic system.', *Life sciences*, 80(24-25), pp. 2352-2360. doi: 10.1016/j.lfs.2007.04.017.
- Serrano, M., Hannon, G. J. and Beach, D. (1993) 'A new regulatory motif in cell-cycle control causing specific inhibition of cyclin D/CDK4', *nature*, 366(6456), pp. 704-707.
- Shang, L., Shao, J. and Ge, S. (2021) 'Immunomodulatory functions of oral mesenchymal stem cells: Novel force for tissue regeneration and disease therapy', *Journal of Leukocyte Biology*, 110(3), pp. 539-552.
- Shannon, P. *et al.* (2003) 'Cytoscape: a software environment for integrated models of biomolecular interaction networks', *Genome research*, 13(11), pp. 2498-2504.
- Sharma, A. K. *et al.* (2009) 'Defined populations of bone marrow derived mesenchymal stem and endothelial progenitor cells for bladder regeneration', *The Journal of urology*, 182(4S), pp. 1898-1905.
- Sherr, C. J. (1994) 'Growth factor-regulated G1 cyclins.', *Stem cells (Dayton, Ohio)*, 12, pp. 47-55.
- Shi, X. *et al.* (2009) 'In-vitro osteogenesis of synovium stem cells induced by controlled release of bisphosphate additives from microspherical mesoporous silica composite', *Biomaterials*, 30(23-24), pp. 3996-4005.
- Shimizu, T. *et al.* (2014) 'Vitamin K-dependent carboxylation of osteocalcin affects the efficacy of teriparatide (PTH1-34) for skeletal repair', *Bone*, 64, pp. 95-101.
- Shirvan, M. H., Pollard, H. B. and Heldman, E. (1991) 'Mixed nicotinic and muscarinic features of cholinergic receptor coupled to secretion in bovine chromaffin cells', *Proceedings of the National Academy of Sciences*, 88(11), pp. 4860-4864.
- Shlomovitz, I., Speir, M. and Gerlic, M. (2019) 'Flipping the dogma-phosphatidylserine in non-apoptotic cell death', *Cell Communication and Signaling*, 17(1), pp. 1-12.
- Shoi, K. *et al.* (2014) 'Characterization of pulp and follicle stem cells from impacted supernumerary maxillary incisors', *Pediatric dentistry*, 36(3), pp. 79E-84E.
- Da Silva-Álvarez, S. *et al.* (2019) 'The development of cell senescence', *Experimental gerontology*, 128, p. 110742.
- Sipp, D., Robey, P. G. and Turner, L. (2018) 'Clear up this stem-cell mess'. Nature Publishing Group UK London.
- Smith, A. (2006) 'A glossary for stem-cell biology', *Nature*, 441(7097), p. 1060.
- Sodek, J., Ganss, B. and McKee, M. D. (2000) 'Osteopontin', *Critical Reviews in Oral Biology & Medicine*, 11(3), pp. 279-303.
- Sonnemann, K. J. and Bement, W. M. (2011) 'Wound repair: toward understanding and integration of single-cell and multicellular wound responses', *Annual review of cell and developmental biology*, 27, pp. 237-263.
- Sonoyama, W. *et al.* (2006) 'Mesenchymal stem cell-mediated functional tooth

## References

- regeneration in swine', *PloS one*, 1(1), p. e79.
- Spath, L. *et al.* (2010) 'Explant-derived human dental pulp stem cells enhance differentiation and proliferation potentials', *Journal of cellular and molecular medicine*, 14(6b), pp. 1635-1644.
- Spencer, S. L. *et al.* (2013) 'The proliferation-quiescence decision is controlled by a bifurcation in CDK2 activity at mitotic exit', *Cell*, 155(2), pp. 369-383.
- Spieker, J. *et al.* (2016) 'Acetylcholinesterase regulates skeletal in ovo development of chicken limbs by ACh-dependent and-independent mechanisms', *PLOS one*, 11(8), p. e0161675.
- Spieker, J. *et al.* (2017) 'Endochondral ossification is accelerated in cholinesterase-deficient mice and in avian mesenchymal micromass cultures', *PloS one*, 12(1), p. e0170252.
- Spyridopoulos, I. *et al.* (2001) 'Alcohol enhances oxysterol-induced apoptosis in human endothelial cells by a calcium-dependent mechanism', *Arteriosclerosis, thrombosis, and vascular biology*, 21(3), pp. 439-444.
- Sriram, K. and Insel, P. A. (2018) 'G protein-coupled receptors as targets for approved drugs: how many targets and how many drugs?', *Molecular pharmacology*, 93(4), pp. 251-258.
- Staines, K. A., MacRae, V. E. and Farquharson, C. (2012) 'The importance of the SIBLING family of proteins on skeletal mineralisation and bone remodelling', *Journal of Endocrinology*, 214(3), pp. 241-255.
- Stein, G. S. and Lian, J. B. (1993) 'MOLECULAR MECHANISMS MEDIATING DEVELOPMENTAL AND HORMONE-REGULATED EXPRESSION OF GENES IN OSTEOBLASTS', in Noda, M. (ed.) *Cellular and Molecular Biology of Bone*. San Diego: Elsevier, pp. 47-95. doi: 10.1016/B978-0-08-092500-4.50006-1.
- Sterin-Borda, L. *et al.* (2011) 'Inflammation Triggers Constitutive Activity and Agonist-induced Negative Responses at M3 Muscarinic Receptor in Dental Pulp', *Journal of endodontics*, 37(2), pp. 185-190.
- Stokowski, A. *et al.* (2007) 'EphB/ephrin-B interaction mediates adult stem cell attachment, spreading, and migration: implications for dental tissue repair', *Stem cells*, 25(1), pp. 156-164.
- Strober, W. (1997) 'Trypan blue exclusion test of cell viability', *Current protocols in immunology*, 21(1), p. A-3B.
- Suchánek, J. *et al.* (2010) 'Stem cells from human exfoliated deciduous teeth-isolation, long term cultivation and phenotypical analysis', *Acta Medica (Hradec Kralove)*, 53(2), pp. 93-99.
- Sugiyama, M. *et al.* (2011) 'Dental pulp-derived CD31-/CD146- side population stem/progenitor cells enhance recovery of focal cerebral ischemia in rats', *Tissue Engineering Part A*, 17(9-10), pp. 1303-1311.
- Sun, F. *et al.* (2019) 'Acacetin-induced cell apoptosis in head and neck squamous cell carcinoma cells: Evidence for the role of muscarinic M3 receptor', *Phytotherapy*

## References

- Research*, 33(5), pp. 1551-1561.
- Sun, H.-H. *et al.* (2014) 'Investigation of dental pulp stem cells isolated from discarded human teeth extracted due to aggressive periodontitis', *Biomaterials*, 35(35), pp. 9459-9472.
- Sun, J. *et al.* (2015) 'Role of bone morphogenetic protein-2 in osteogenic differentiation of mesenchymal stem cells', *Molecular medicine reports*, 12(3), pp. 4230-4237.
- Sun, X. and Kaufman, P. D. (2018) 'Ki-67: more than a proliferation marker', *Chromosoma*, 127, pp. 175-186.
- Sun, Y. *et al.* (2017) 'Effect of iRoot Fast Set root repair material on the proliferation, migration and differentiation of human dental pulp stem cells in vitro', *PLoS ONE*, 12(10), pp. 1-15. doi: 10.1371/journal.pone.0186848.
- Suno, R., Asada, H. and Kobayashi, T. (2016) 'Towards the Crystal Structure Determination of Muscarinic Acetylcholine Receptors', in *Muscarinic Receptor: From Structure to Animal Models*. Springer, pp. 1-13.
- Syed-Picard, F. N. *et al.* (2015) 'Dental pulp stem cells: a new cellular resource for corneal stromal regeneration', *Stem cells translational medicine*, 4(3), pp. 276-285.
- Szabó, A. and Mayor, R. (2016) 'Modelling collective cell migration of neural crest', *Current opinion in cell biology*, 42, pp. 22-28.
- Szklarczyk, D. *et al.* (2015) 'STRING v10: protein-protein interaction networks, integrated over the tree of life', *Nucleic acids research*, 43(D1), pp. D447-D452.
- TAIRA, M. *et al.* (2012) 'Quantitative analyses of osteogenic-differentiation-related gene expressions in human osteoblast-like cells (SaOS-2) cultured on hydroxyapatite and titanium', *Journal of Oral Tissue Engineering*, 10(1), pp. 34-41.
- Takahashi, K. and Yamanaka, S. (2006) 'Induction of pluripotent stem cells from mouse embryonic and adult fibroblast cultures by defined factors', *cell*, 126(4), pp. 663-676.
- Takeda-Kawaguchi, T. *et al.* (2014) 'Derivation of iPSCs after culture of human dental pulp cells under defined conditions', *PLoS One*, 9(12), p. e115392.
- Takeda, T. *et al.* (2008) 'Characterization of dental pulp stem cells of human tooth germs', *Journal of dental research*, 87(7), pp. 676-681.
- Tan, D. Q. and Suda, T. (2018) 'Reactive oxygen species and mitochondrial homeostasis as regulators of stem cell fate and function', *Antioxidants & redox signaling*, 29(2), pp. 149-168.
- Tang, J.-M. M. *et al.* (2012) 'Acetylcholine induces mesenchymal stem cell migration via Ca<sup>2+</sup>/PKC/ERK1/2 signal pathway', *Journal of Cellular Biochemistry*, 113(8), pp. 2704-2713. doi: 10.1002/jcb.24148.
- Testa, U. *et al.* (2016) 'Oxidative stress and hypoxia in normal and leukemic stem cells', *Experimental hematology*, 44(7), pp. 540-560.

## References

- Thangaraj, G. *et al.* (2016) 'Inflammatory effects of TNF $\alpha$  are counteracted by X-ray irradiation and AChE inhibition in mouse micromass cultures', *Chemico-Biological Interactions*, 259, pp. 313-318. doi: 10.1016/j.cbi.2016.03.027.
- Thomson, J. A. *et al.* (1998) 'Embryonic stem cell lines derived from human blastocysts', *science*, 282(5391), pp. 1145-1147.
- Thuong Nguyen, V. *et al.* (2000) 'Choline Acetyltransferase, Acetylcholinesterase, and Nicotinic Acetylcholine Receptors of Human Gingival and Esophageal Epithelia', *Journal of Dental Research*, 79(4), pp. 939-949. doi: 10.1177/00220345000790040901.
- Turner, P. J. *et al.* (2010) 'Osteopontin deficiency increases bone fragility but preserves bone mass', *Bone*, 46(6), pp. 1564-1573.
- Tie, K. *et al.* (2018) 'Histone hypo-acetylation of Sox9 mediates nicotine-induced weak cartilage repair by suppressing BMSC chondrogenic differentiation', *Stem Cell Research and Therapy*, 9(1), p. 98. doi: 10.1186/s13287-018-0853-x.
- Tomic, S. *et al.* (2011) 'Immunomodulatory properties of mesenchymal stem cells derived from dental pulp and dental follicle are susceptible to activation by toll-like receptor agonists', *Stem cells and development*, 20(4), pp. 695-708.
- Tracey, K. J. (2007) 'Physiology and immunology of the cholinergic antiinflammatory pathway', *The Journal of clinical investigation*, 117(2), pp. 289-296.
- Tran, H. L. B. and Doan, V. N. (2015) 'Human dental pulp stem cells cultured onto dentin derived scaffold can regenerate dentin-like tissue in vivo', *Cell and tissue banking*, 16(4), pp. 559-568.
- Tremel, A. *et al.* (2009) 'Cell migration and proliferation during monolayer formation and wound healing', *Chemical Engineering Science*, 64(2), pp. 247-253.
- Troyer, D. L. and Weiss, M. L. (2008) 'Concise review: Wharton's Jelly-derived cells are a primitive stromal cell population', *Stem cells*, 26(3), pp. 591-599.
- Tsimbouri, P. M. *et al.* (2017) 'Stimulation of 3D osteogenesis by mesenchymal stem cells using a nanovibrational bioreactor', *Nature Biomedical Engineering*, 1(9), pp. 758-770.
- Tuček, S. (1982) 'The synthesis of acetylcholine in skeletal muscles of the rat', *The Journal of physiology*, 322(1), pp. 53-69.
- Uggenti, C. *et al.* (2014) 'M2 muscarinic receptor activation regulates schwann cell differentiation and myelin organization', *Developmental Neurobiology*, 74(7), pp. 676-691. doi: 10.1002/dneu.22161.
- Ullah, I. *et al.* (2017) 'Transplantation of human dental pulp-derived stem cells or differentiated neuronal cells from human dental pulp-derived stem cells identically enhances regeneration of the injured peripheral nerve', *Stem cells and development*, 26(17), pp. 1247-1257.
- Unger, V. M. *et al.* (1997) 'Arrangement of rhodopsin transmembrane  $\alpha$ -helices', *Nature*, 389(6647), pp. 203-206.

## References

- Urkasemsin, G. *et al.* (2019) 'Strategies for Developing Functional Secretory Epithelia from Porcine Salivary Gland Explant Outgrowth Culture Models.', *Biomolecules*, 9(11). doi: 10.3390/biom9110657.
- Verma, S. *et al.* (2018) 'Muscarinic and nicotinic acetylcholine receptor agonists: current scenario in Alzheimer's disease therapy', *Journal of Pharmacy and Pharmacology*, 70(8), pp. 985-993.
- Vermeulen, K., Berneman, Z. N. and Van Bockstaele, D. R. (2003) 'Cell cycle and apoptosis', *Cell proliferation*, 36(3), pp. 165-175.
- Viswanathan, S. *et al.* (2019) 'Mesenchymal stem versus stromal cells: International Society for Cell & Gene Therapy (ISCT®) Mesenchymal Stromal Cell committee position statement on nomenclature', *Cytotherapy*, 21(10), pp. 1019-1024.
- Vivino, F. B. *et al.* (1999) 'Pilocarpine tablets for the treatment of dry mouth and dry eye symptoms in patients with Sjögren syndrome: a randomized, placebo-controlled, fixed-dose, multicenter trial', *Archives of internal medicine*, 159(2), pp. 174-181.
- Voigt, V. *et al.* (2013) 'Transport of the areca nut alkaloid arecaidine by the human proton-coupled amino acid transporter 1 (hPAT1)', *Journal of Pharmacy and Pharmacology*, 65(4), pp. 582-590. doi: 10.1111/jphp.12006.
- Voulgaridou, G.-P. *et al.* (2017) 'Human aldehyde dehydrogenase 3A1 (ALDH3A1) exhibits chaperone-like function', *The International Journal of Biochemistry & Cell Biology*, 89, pp. 16-24.
- Vousden, K. H. and Prives, C. (2009) 'Blinded by the light: the growing complexity of p53', *Cell*, 137(3), pp. 413-431.
- Wang, C. *et al.* (2009) 'Aldo-keto reductase family 1 member B10 promotes cell survival by regulating lipid synthesis and eliminating carbonyls', *Journal of Biological Chemistry*, 284(39), pp. 26742-26748.
- Wang, J. *et al.* (2010) 'The odontogenic differentiation of human dental pulp stem cells on nanofibrous poly (L-lactic acid) scaffolds in vitro and in vivo', *Acta biomaterialia*, 6(10), pp. 3856-3863.
- Wang, L. *et al.* (2017) 'The Alpha 7 Nicotinic Acetylcholine Receptor of Deciduous Dental Pulp Stem Cells Regulates Osteoclastogenesis During Physiological Root Resorption', *Stem Cells and Development*, 26(16), pp. 1186-1198. doi: 10.1089/scd.2017.0033.
- Wang, S. *et al.* (2008) 'AKR1C2 and AKR1C3 mediated prostaglandin D2 metabolism augments the PI3K/Akt proliferative signaling pathway in human prostate cancer cells', *Molecular and cellular endocrinology*, 289(1-2), pp. 60-66.
- Wang, S. *et al.* (2012) 'Insulin-like growth factor 1 can promote the osteogenic differentiation and osteogenesis of stem cells from apical papilla', *Stem cell research*, 8(3), pp. 346-356.
- Wang, S., Qu, X. and Zhao, R. C. (2012) 'Clinical applications of mesenchymal stem cells', *Journal of hematology & oncology*, 5(1), pp. 1-9.

## References

- Wang, X., Fu, Y. and Xing, Y. (2022) 'TRIM47 promotes ovarian cancer cell proliferation, migration, and invasion by activating STAT3 signaling', *Clinics*, 77.
- Wang, Y.-H. *et al.* (2006) 'Examination of Mineralized Nodule Formation in Living Osteoblastic Cultures Using Fluorescent Dyes', *Biotechnology Progress*, 22(6), pp. 1697-1701. doi: 10.1021/bp060274b.
- Wang, Y. *et al.* (2020) 'Knockdown of TRIM47 inhibits breast cancer tumorigenesis and progression through the inactivation of PI3K/Akt pathway', *Chemico-biological interactions*, 317, p. 108960.
- Warbrick, E. *et al.* (1995) 'A small peptide inhibitor of DNA replication defines the site of interaction between the cyclin-dependent kinase inhibitor p21WAF1 and proliferating cell nuclear antigen', *Current Biology*, 5(3), pp. 275-282.
- Weist, R. *et al.* (2018) 'Differential Expression of Cholinergic System Components in Human Induced Pluripotent Stem Cells, Bone Marrow-Derived Multipotent Stromal Cells, and Induced Pluripotent Stem Cell-Derived Multipotent Stromal Cells', *Stem Cells and Development*, 27(3), pp. 166-183. doi: 10.1089/scd.2017.0162.
- Welcker, M. *et al.* (1998) 'p21WAF1/CIP1 mutants deficient in inhibiting cyclin-dependent kinases (CDKs) can promote assembly of active cyclin D/CDK4 (6) complexes in human tumor cells', *Cancer research*, 58(22), pp. 5053-5056.
- Werle, S. B. *et al.* (2016) 'Carious deciduous teeth are a potential source for dental pulp stem cells', *Clinical oral investigations*, 20(1), pp. 75-81.
- Wess, J., Eglen, R. M. and Gautam, D. (2007) 'Muscarinic acetylcholine receptors: mutant mice provide new insights for drug development', *Nature reviews Drug discovery*, 6(9), pp. 721-733.
- Wessler, I., Roth, E., *et al.* (2001) 'Release of non-neuronal acetylcholine from the isolated human placenta is mediated by organic cation transporters', *British journal of pharmacology*, 134(5), p. 951.
- Wessler, I., Kilbinger, H., *et al.* (2001) 'The Non-neuronal Cholinergic System The Biological Role of Non-neuronal Acetylcholine in Plants and Humans', *The Japanese Journal of Pharmacology*, 85(1), pp. 2-10.
- Wessler, I. *et al.* (2003) 'The non-neuronal cholinergic system in humans: expression, function and pathophysiology', *Life sciences*, 72(18-19), pp. 2055-2061.
- Wessler, I. K. and Kirkpatrick, C. J. (2012) 'Activation of muscarinic receptors by non-neuronal acetylcholine', in *Muscarinic Receptors*. Springer, pp. 469-491.
- Wessler, I. K. and Kirkpatrick, C. J. (2016) 'Detection of non-neuronal acetylcholine', in *Muscarinic Receptor: From Structure to Animal Models*. Springer, pp. 205-220.
- Wessler, I. K. and Kirkpatrick, C. J. (2017) 'Non-neuronal acetylcholine involved in reproduction in mammals and honeybees', *Journal of Neurochemistry*, 142, pp. 144-150.
- Wessler, I. and Kirkpatrick, C. J. (2008) 'Acetylcholine beyond neurons: The non-neuronal cholinergic system in humans', *British Journal of Pharmacology*. Wiley Online Library, pp. 1558-1571. doi: 10.1038/bjp.2008.185.

## References

- Wessler, I., Kirkpatrick, C. J. and Racke, K. (1999) 'The cholinergic "pitfall": acetylcholine, a universal cell molecule in biological systems, including humans', *Clinical and Experimental Pharmacology and Physiology*, 26(3), pp. 198-205.
- Wessler, I., Kirkpatrick, C. J. and Racké, K. (1998) 'Non-neuronal acetylcholine, a locally acting molecule, widely distributed in biological systems: expression and function in humans', *Pharmacology & therapeutics*, 77(1), pp. 59-79.
- White, H. L. and Wu, J. C. (1973) 'Choline and carnitine acetyltransferases of heart', *Biochemistry*, 12(5), pp. 841-846.
- Wilkinson, D. G. (2014) 'Regulation of cell differentiation by Eph receptor and ephrin signaling', *Cell adhesion & migration*, 8(4), pp. 339-348.
- Williams, C. L. (2003) 'Muscarinic signaling in carcinoma cells', *Life sciences*, 72(18-19), pp. 2173-2182.
- Wiseman, L. R. and Faulds, D. (1995) 'Oral pilocarpine: a review of its pharmacological properties and clinical potential in xerostomia', *Drugs*, 49(1), pp. 143-155.
- Wong, D., Ramachandra, S. S. and Singh, A. K. (2015) 'Dental management of patient with Williams Syndrome-A case report', *Contemporary Clinical Dentistry*, 6(3), p. 418.
- Wu, T. *et al.* (2021) 'clusterProfiler 4.0: A universal enrichment tool for interpreting omics data', *The innovation*, 2(3).
- Wu, W. *et al.* (2015) 'Derivation and growth characteristics of dental pulp stem cells from patients of different ages', *Molecular Medicine Reports*, 12(4), pp. 5127-5134.
- Xiao, H. *et al.* (2019) 'Nicotine exposure during pregnancy programs osteopenia in male offspring rats via  $\alpha 4\beta 2$ -nAChR-p300-ACE pathway', *The FASEB Journal*, 33(11), pp. 12972-12982. doi: 10.1096/fj.201901145RR.
- Xu, H. *et al.* (2001) 'A novel PCNA-binding motif identified by the panning of a random peptide display library', *Biochemistry*, 40(14), pp. 4512-4520.
- Xu, J. *et al.* (2015) 'Potential mechanisms underlying the Runx2 induced osteogenesis of bone marrow mesenchymal stem cells', *American journal of translational research*, 7(12), p. 2527.
- Xu, Y. *et al.* (2016) 'Loss of asparagine synthetase suppresses the growth of human lung cancer cells by arresting cell cycle at G0/G1 phase', *Cancer gene therapy*, 23(9), pp. 287-294.
- Yamaguchi, A. *et al.* (2008) 'Regulation of osteoblast differentiation mediated by BMP, Notch, and CCN3/NOV', *Japanese Dental Science Review*, 44(1), pp. 48-56.
- Yamasaki, M., Matsui, M. and Watanabe, M. (2010) 'Preferential localization of muscarinic M1 receptor on dendritic shaft and spine of cortical pyramidal cells and its anatomical evidence for volume transmission', *Journal of Neuroscience*, 30(12), pp. 4408-4418.
- Yan, X. *et al.* (2010) 'iPS cells reprogrammed from human mesenchymal-like

## References

- stem/progenitor cells of dental tissue origin', *Stem cells and development*, 19(4), pp. 469-480.
- Yan, Y. *et al.* (2016) 'Neurotrophin-3 promotes proliferation and cholinergic neuronal differentiation of bone marrow-derived neural stem cells via notch signaling pathway', *Life sciences*, 166, pp. 131-138.
- Yanagita, M. *et al.* (2008) 'Nicotine inhibits mineralization of human dental pulp cells', *Journal of endodontics*, 34(9), pp. 1061-1065.
- Yang, C. *et al.* (2017) 'Potential of human dental stem cells in repairing the complete transection of rat spinal cord', *Journal of neural engineering*, 14(2), p. 26005.
- Yang, H. *et al.* (2014) 'Down-regulation of asparagine synthetase induces cell cycle arrest and inhibits cell proliferation of breast cancer', *Chemical biology & drug design*, 84(5), pp. 578-584.
- Yang, K.-L. *et al.* (2009) 'A simple and efficient method for generating Nurr1-positive neuronal stem cells from human wisdom teeth (tNSC) and the potential of tNSC for stroke therapy', *Cytotherapy*, 11(5), pp. 606-617.
- Yang, X. *et al.* (2017) 'Effect of nicotine on the proliferation and chondrogenic differentiation of the human Wharton's jelly mesenchymal stem cells', *Bio-Medical Materials and Engineering*, 28(s1), pp. S217-S228. doi: 10.3233/BME-171644.
- Yao, Q. *et al.* (2017) 'Neurotrophin 3 upregulates proliferation and collagen production in human aortic valve interstitial cells: a potential role in aortic valve sclerosis', *American Journal of Physiology-Cell Physiology*, 312(6), pp. C697-C706.
- Yasuda, K. *et al.* (2014) 'Nuclear envelope localization of R an-binding protein 2 and R an-GTP ase-activating protein 1 in psoriatic epidermal keratinocytes', *Experimental dermatology*, 23(2), pp. 119-124.
- Yeeles, J. T. P. *et al.* (2015) 'Regulated eukaryotic DNA replication origin firing with purified proteins', *Nature*, 519(7544), pp. 431-435.
- Yegani, A. A. *et al.* (2020) 'Biological behaviors of muscarinic receptors in mesenchymal stem cells derived from human placenta and bone marrow', *Iranian Journal of Basic Medical Sciences*, 23(1), pp. 124-132. doi: 10.22038/IJBMS.2019.38582.9151.
- Yu, C. Y. *et al.* (2001) 'Acetylcholine-induced vasodilation of isolated pulpal arterioles', *Journal of dental research*, 80(11), pp. 1995-1999.
- Yu, Y., Kovacevic, Z. and Richardson, D. R. (2007) 'Tuning cell cycle regulation with an iron key', *Cell cycle*, 6(16), pp. 1982-1994.
- Zablotni, A. *et al.* (2015) 'Regulation of acetylcholine receptors during differentiation of bone mesenchymal stem cells harvested from human reaming debris', *International Immunopharmacology*, 29(1), pp. 119-126. doi: 10.1016/j.intimp.2015.07.021.
- Zhang, W. *et al.* (2006) 'Multilineage differentiation potential of stem cells derived from human dental pulp after cryopreservation', *Tissue engineering*, 12(10), pp. 2813-2823.

## References

- Zhao, Y. *et al.* (2012) 'Fas ligand regulates the immunomodulatory properties of dental pulp stem cells', *Journal of Dental Research*, 91(10), pp. 948-954.
- Zholos, A. V, Zholos, A. A. and Bolton, T. B. (2004) 'G-protein-gated TRP-like cationic channel activated by muscarinic receptors: effect of potential on single-channel gating', *The journal of general physiology*, 123(5), pp. 581-598.
- Zhou, P. *et al.* (2021) 'Establishing a deeper understanding of the osteogenic differentiation of monolayer cultured human pluripotent stem cells using novel and detailed analyses', *Stem cell research & therapy*, 12(1), pp. 1-16.
- Zhou, Z. *et al.* (2013) 'Nicotine Deteriorates the Osteogenic Differentiation of Periodontal Ligament Stem Cells through alpha 7 Nicotinic Acetylcholine Receptor Regulating wnt Pathway', *PLOS ONE*, 8(12). doi: 10.1371/journal.pone.0083102.
- Zhu, L., Dissanayaka, W. L. and Zhang, C. (2019) 'Dental pulp stem cells overexpressing stromal-derived factor-1 $\alpha$  and vascular endothelial growth factor in dental pulp regeneration', *Clinical Oral Investigations*, 23(5), pp. 2497-2509.
- Zhu, X. and Birnbaumer, L. (1996) 'G protein subunits and the stimulation of phospholipase C by Gs-and Gi-coupled receptors: Lack of receptor selectivity of Galpha (16) and evidence for a synergic interaction between Gbeta gamma and the alpha subunit of a receptor activated G protein', *Proceedings of the National Academy of Sciences*, 93(7), pp. 2827-2831.
- Zuk, P. A. *et al.* (2002) 'Human adipose tissue is a source of multipotent stem cells', *Molecular biology of the cell*, 13(12), pp. 4279-4295.
- Van Zwieten, P. A. and Doods, H. N. (1995) 'Muscarinic receptors and drugs in cardiovascular medicine', *Cardiovascular Drugs and Therapy*, 9(1), pp. 159-167.